

KARLSRUHE INSTITUTE OF TECHNOLOGY (KIT)

**Collective Communications  
and Computation Mechanisms  
on the RF Channel  
for Organic Printed Smart Labels  
and Resource-limited IoT Nodes**

For obtaining the academic degree of  
Doctor of Engineering

Department of Informatics  
Karlsruhe Institute of Technology (KIT)  
Karlsruhe, Germany

Approved

Dissertation

by

Predrag Jakimovski

From Kumanovo, Macedonia

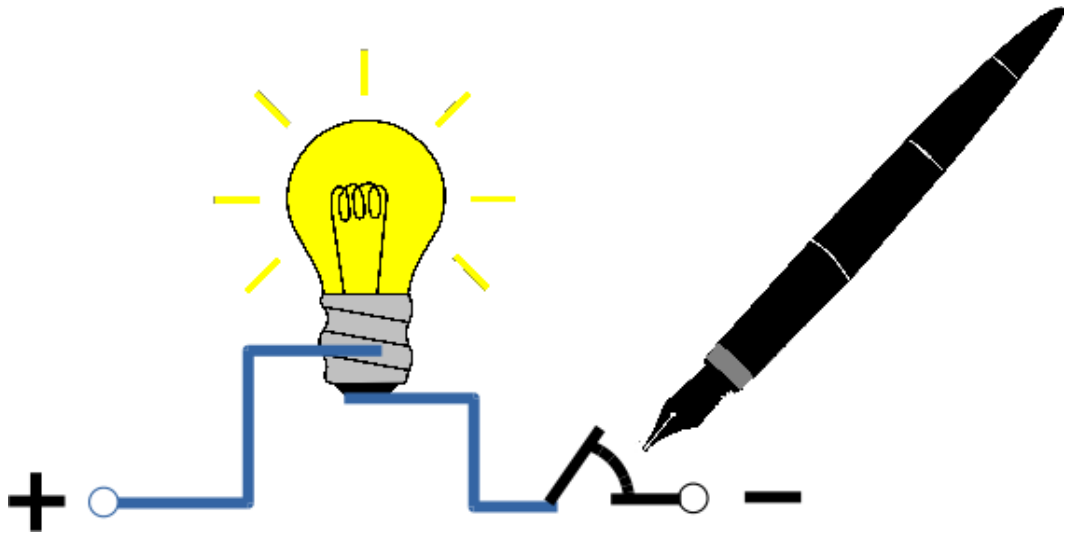
Date of Examination: 9 May 2019

Supervisor: Prof. Dr. Michael Beigl

Co-supervisor: Prof. Dr. Hedda R. Schmidtke



This document is licensed under a Creative Commons Attribution-NonCommercial-NoDerivatives 4.0 International License (CC BY-NC-ND 4.0):  
<https://creativecommons.org/licenses/by-nc-nd/4.0/deed.en>



*"The pen is mightier than the sword."*

Edward George Bulwer-Lytton, (\* May 25, 1803; † January 18, 1873)

## *Abstract*

Faculty of Informatics

Pervasive Computing Systems – TecO

Doctor of Engineering

by Predrag Jakimovski

Radio Frequency IDentification (RFID) and Wireless Sensor Networks (WSN) are seen as enabler technologies for realizing the Internet of Things (IoT). Organic and printed Electronics (OE) has the potential to provide low cost and all-printable smart RFID labels in high volumes. With regard to WSN, power harvesting techniques and resource-efficient communications are promising key technologies to create sustainable and for the environment friendly sensing devices. However, the implementation of OE smart labels is only allowing printable devices of ultra-low hardware complexity, that cannot employ standard RFID communications. And, the deployment of current WSN technology is far away from offering battery-free and low-cost sensing technology. To this end, the steady growth of IoT is increasing the demand for more network capacity and computational power. With respect to wireless communications research, the state-of-the-art employs superimposed radio transmission in form of physical layer network coding and computation over the MAC to increase information flow and computational power, but lacks on practicability and robustness so far. With regard to these research challenges we developed in particular two approaches, i.e., code-based Collective Communications for dense sensing environments, and time-based Collective Communications (CC) for resource-limited WSNs. In respect to the code-based CC approach we exploit the principle of superimposed radio transmission to acquire highly scalable and robust communications obtaining with it at the same time as well minimalistic smart RFID labels, that can be manufactured in high volume with present-day OE. The implementation of our code-based CC relies on collaborative and simultaneous transmission of randomly drawn burst sequences encoding the data. Based on the framework of hyper-dimensional computing, statistical laws and the superposition principle of radio waves we obtained the communication of so called ensemble information, meaning the concurrent bulk reading of sensed values, ranges, quality rating, identifiers (IDs), and so on. With 21 transducers on a small-scale reader platform we tested the performance of our approach successfully proving the scalability and reliability.

To this end, we implemented our code-based CC mechanism into an all-printable passive RFID label down to the logic gate level, indicating a circuit complexity of about 500 transistors. In respect to time-based CC approach we utilize the superimposed radio transmission to obtain resource-limited WSNs, that can be deployed in wide areas for establishing, e.g., smart environments. In our application scenario for resource-limited WSN, we utilize the superimposed radio transmission to calculate functions of interest, i.e., to accomplish data processing directly on the radio channel. To prove our concept in a case study, we created a WSN with 15 simple nodes measuring the environmental mean temperature. Based on our analysis about the wireless computation error we were able to minimize the stochastic error arbitrarily, and to remove the systematic error completely.

KARLSRUHE INSTITUT FÜR TECHNOLOGIE (KIT)

## *Zusammenfassung*

Fakultät für Informatik

am Lehrstuhl für Pervasive Computing Systems - TecO

zur Erlangung des akademischen Grades Doktoringenieur (Dr.-Ing.)

von Predrag Jakimovski (Dipl.-Inform. )

Elektronische Funketiketten (RFID) und drahtlose Sensornetzwerke (WSN) haben das Potenzial das Internet der Dinge (IoT) zu verwirklichen. Die Polymer-Elektronik (OE) bietet die Möglichkeit RFID Smartlabels massenhaft und günstig zu drucken. Mit Technologien wie dem Power Harvesting und ressourceneffiziente Kommunikation könnten in naher Zukunft nachhaltige und umweltfreundliche WSN realisiert werden. Die Umsetzung dieser Technologien in praktischer Anwendung gestaltet sich jedoch schwierig. Man kann zwar Elektronik auf Papier oder Folie drucken, jedoch lassen sich aufgrund der zu geringen Schaltungskomplexität kaum Standard Kommunikationsprotokolle integrieren. Ein weiteres Problem stellt die traditionelle Form der Kommunikation und Verarbeitung von Daten dar, da das schnelle Wachstum des Internets von "Things" immer größere Kapazitäten erfordert. Im Bereich der drahtlosen Kommunikation bietet der aktuelle Stand der Technik erhebliche Verbesserungen mit Hilfe des Überlagerungsprinzips von Funkwellen, die sind jedoch in der Praxis empfindlich und kaum einsetzbar, oder in deren Fähigkeit stark eingeschränkt. Im Hinblick auf diese Problemstellung werden in dieser Dissertation insgesamt zwei unterschiedliche Lösungsansätze beschrieben, die sich das Prinzip der Überlagerung von Funkwellen zu Nutze machen. Der eine Lösungsansatz wird Code-basiertes Collective Communication genannt, welcher für die hoch skalierbare und robuste Kommunikation konzipiert wurde, und zugleich einen minimalistischen Polymer-Tag ermöglicht. Der andere Lösungsansatz wird Zeit-basiertes Collective Communication (CC) genannt, welcher für die Realisierung von ressourcenarme WSN entwickelt wurde. Das Code-basierte CC beruht auf die kollektive und gleichzeitige Übertragung von Daten, welches die Daten durch randomisierte Burstfolgen kodiert. Basierend auf die Ausnutzung von stochastischen Gesetzen und dem Überlagerungsprinzip von elektromagnetischen Wellen wird die Übertragung von sogenannten Ensemble-Informationen ermöglicht, welche die Eigenschaft haben Zustandsinformationen zum Pulk von Tags zuzuordnen.

Mit Hilfe einer Auslese-Plattform aus 21 Ersatztranspondern und einem Lesegerät wird die Robustheit und Skalierbarkeit des Verfahrens nachgewiesen. Zusätzlich ist bis zur Transistorebene ein druckbarer passiver 64-bit Tag implementiert, welcher den Code-basierten CC Mechanismus integriert und, eine minimale Hardware-Komplexität von um die 500 Transistoren aufweist. Das Zeit-basierte CC ist für die Verarbeitung von gleichzeitig gesendete Daten auf dem Funkkanal im WSN konzipiert. Insbesondere kann eine Datenverarbeitung auf dem Kanal realisiert werden, die beispielsweise in Smart Environments eingesetzt werden kann. In einer Fallstudie mit 15 Sensorknoten wurde beispielhaft die mittlere Temperatur der Umgebung während der Übertragung berechnet. In der Analyse des Rechenfehlers wurden die stochastischen und systematischen Fehler identifiziert, die dann durch eine analytische Lösung vollständig korrigiert werden konnten.

## *Acknowledgements*

At first, I would like to express my sincere gratitude to my mentor Prof. Dr. Michael Beigl for allowing me to pursue this research work under his supervision within the research project Polytos. The ideas, techniques and approaches proposed in this thesis are the results of countless number of discussions and brainstormings we had on many meetings and occasions. I am particularly thankful to Prof. Dr. Hedda R. Schmidtke for her insights and innovative thinking which have given a solid shape to this thesis. She has shown a lot of care and concern on the progress of my research work and been an excellent co-mentor throughout the period of my research. Also, I am very much grateful to my friend and college Dr. Stephan Sigg for his supervision, motivations and support. He has been very cooperative and open to make research together, so that many of the scientific publications resulted from our joint research activities. Concerning the chair for Pervasive Computing Systems, the TecO group has been a truly inspiring and friendly place to conduct project work and carry out the research and, I am very glad to have had support from so many friends, colleagues and student staff, so that here I wish to thank them all. In no particular order: Ali Hadda, Florian Becker, Michael Zangl, Dr. Behnam Banitalebi, Dr. Takashi Miyaki, Dr. Christian Decker, Dr. Leonardo Weiss Ferreira Chaves, Nina Oertel, ... and Dhafar Rifat.

Further on, I am in particular very thankful to my very good friend and supporter Dr. Matthias Eck for taking his time to read the draft and look over the chapters of this thesis. His invaluable comments and suggestions have greatly improved the writing and presentation of the thesis. The path to this long journey has been the true test of my abilities and self determinations. The first milestone of the journey has now completed and I have now reached to the stage where I can contemplate my past and acknowledge the relentless support I received from my family. It is been the desire of my parents Mr. Trajko Jakimovski and Mrs. Milevka Jakimovska to see me succeed and achieve this very important goal of completing the PhD. The words in this thesis will be very little to express my gratitude and love to their everlasting support.

# Contents

<b>Abstract</b>	<b>iii</b>
<b>Zusammenfassung</b>	<b>v</b>
<b>Acknowledgements</b>	<b>vii</b>
<b>List of Publications</b>	<b>xi</b>
<b>List of Figures</b>	<b>xii</b>
<b>List of Tables</b>	<b>xvi</b>
<b>Abbreviations</b>	<b>xvii</b>
<b>1 Introduction</b>	<b>1</b>
1.1 Internet of Things (IoT) . . . . .	1
1.2 Printed Electronics and Sensor-Based IoT Devices . . . . .	2
1.3 Application Scenario: Supply Chain Management . . . . .	4
1.4 Problem Statement and Motivation . . . . .	6
1.5 Summary of Contributions . . . . .	7
1.6 Outline . . . . .	10
<b>2 Background and Related Work</b>	<b>11</b>
2.1 Intelligent Environments . . . . .	11
2.2 Printed Electronics for RFID and Smart Labels . . . . .	14
2.3 Wireless Communications for Printed Electronics . . . . .	21
2.4 Special Case: Code Division Multiple Access (CDMA) . . . . .	21
2.5 Classical Networking and Beyond for IoT . . . . .	24
2.5.1 Design Architectures and Management . . . . .	25
2.5.2 Computation versus Communication . . . . .	26
2.6 Beyond the IoT Standard: Function Calculation over Wireless Channels . . . . .	28
2.6.1 Linear Network Coding on the Physical Layer . . . . .	33
2.6.2 Analog Computing over Wireless Channels . . . . .	37
2.6.3 Jam Signaling . . . . .	40
2.6.4 Critical Discourse Analysis . . . . .	43

2.7	Summary . . . . .	45
<b>3</b>	<b>Code-Based Collective Communications for Dense Sensing Environments</b>	<b>47</b>
3.1	Introduction . . . . .	48
3.2	Smart Supply Chain Management: An Example . . . . .	49
3.3	General Approach . . . . .	52
3.4	Collective Transmission . . . . .	54
	3.4.1 Binary Query . . . . .	57
	3.4.2 Proportion Query . . . . .	58
3.5	Evaluation . . . . .	60
	3.5.1 Organic Electronics Testbed . . . . .	60
	3.5.2 Testbed Experiment . . . . .	61
	3.5.2.1 Experiment Design . . . . .	61
	3.5.2.2 Results . . . . .	62
	3.5.3 Discussion . . . . .	62
3.6	Summary . . . . .	63
<b>4</b>	<b>Experimental Platform for Simultaneous Wireless Transmission</b>	<b>64</b>
4.1	Introduction . . . . .	64
4.2	Reader System Testbed . . . . .	65
	4.2.1 OE Testbed Setup . . . . .	66
	4.2.2 Transducer Device . . . . .	67
	4.2.3 Schematics . . . . .	68
4.3	Software-defined Radio (SDR) . . . . .	70
4.4	Broadcast Tests . . . . .	72
4.5	Summary . . . . .	75
<b>5</b>	<b>An Implementation Example of a Printable Passive Smart Label</b>	<b>76</b>
5.1	Introduction . . . . .	77
5.2	Collective Communications for Printed Smart Labels . . . . .	78
5.3	Circuit Design . . . . .	80
5.4	Collective Synchronization Strategy . . . . .	82
	5.4.1 Synchronized Tags Based on External Clock Recognition . . . . .	85
	5.4.2 Clock Recognition Unit (CRU) . . . . .	87
5.5	Simulation Results . . . . .	88
5.6	Feasibility Assessment . . . . .	90
5.7	Discussion . . . . .	93
5.8	Summary . . . . .	94
<b>6</b>	<b>Time-Based Collective Communications for Resource-limited IoT</b>	<b>96</b>
6.1	Introduction . . . . .	96
6.2	Approach for Function Computation via RF Channel . . . . .	99
	6.2.1 Basic Operations on the Wireless Channel . . . . .	102
	6.2.1.1 Scenario 1: Counting . . . . .	102
	6.2.1.2 Scenario 2: Summation . . . . .	104
	6.2.1.3 Scenario 3: Multiplication . . . . .	107
	6.2.1.4 Scenario 4: Division and Subtraction . . . . .	109

6.2.2	Functions of Interest Calculable on the RF Channel . . . . .	109
6.3	Case Study . . . . .	110
6.3.1	Wireless Sensor Network Platform . . . . .	111
6.3.2	Calculation of Mean Temperature Using the WSN Platform . . . .	113
6.3.3	Results . . . . .	114
6.4	Summary . . . . .	116
<b>7</b>	<b>Analysis of Superimposed Computing and Circuit Design</b>	<b>117</b>
7.1	Introduction . . . . .	117
7.2	Error Analysis of Wireless Superimposed Computing . . . . .	118
7.2.1	Computation Scheme . . . . .	118
7.2.2	Estimation of Errors Induced by Collisions . . . . .	121
7.3	Simulations . . . . .	124
7.3.1	Experiment1: Error Tracking . . . . .	125
7.3.2	Experiment 2: Computation Accuracy . . . . .	125
7.3.3	Experiment 3: Large-scaled WSN . . . . .	128
7.4	Design of a Resource-limited Sensor Node . . . . .	132
7.4.1	Operation Mode . . . . .	133
7.4.2	Control Logic . . . . .	133
7.4.3	Random Burst Sequence Generation . . . . .	134
7.4.4	Circuit Core Design . . . . .	135
7.4.5	Computation on the RF Channel . . . . .	139
7.5	Summary . . . . .	139
<b>8</b>	<b>Conclusion and Outlook</b>	<b>141</b>
8.1	Conclusion . . . . .	141
8.2	Future Work . . . . .	143
<b>A</b>	<b>Printed RFID in a Nutshell</b>	<b>145</b>
A.1	Introduction . . . . .	145
A.2	Some Printed Electronics Foundations . . . . .	147
A.3	Some Review on RFID-Related Printed Electronics . . . . .	152
A.4	Some Mass-Printing Techniques for Printed Electronics . . . . .	157
A.5	Some Technical Key Issues in Printed Electronics . . . . .	159
	<b>Bibliography</b>	<b>161</b>

# List of Publications

1. Predrag Jakimovski, Ali Hadda, Michael Zangl, and Nina Oertel: **Fully Functional Passive RFID Tag with Integrated Sensor Based on Collective Communication and Organic Printed Electronics**, at the 10th International Conference on Wireless and Mobile Communications (ICWMC), 2014.
2. Stephan Sigg, Predrag Jakimovski, Yusheng Ji, and Michael Beigl: **Utilising Convolutions of Random Functions to Realise Function Calculation via a Physical Channel**, at the IEEE 14th Workshop on Signal Processing Advances in Wireless Communications (SPAWC), 2013.
3. Stephan Sigg, Predrag Jakimovski, and Michael Beigl: **Calculation of Functions on the RF-channel for IoT**. In Proceedings of the 3rd international conference on the Internet of Things (IoT2012), October 2012.
4. Predrag Jakimovski, Hedda R. Schmidtke, Stephan Sigg, Leonardo Weiss Ferreira Chaves, and Michael Beigl: **Collective Communication for Dense Sensing Environments**. In Journal of Ambient Intelligence and Smart Environments (JAISE), March 2012.
5. Predrag Jakimovski, Till Riedel, Ali Hadda, and Michael Beigl: **Design of a Printed Organic RFID Circuit with an Integrated Sensor for Smart Labels**. 9th International Multi-conference on Systems, Signals and Devices (SSD) 2012, IEEE Xplore.
6. Stephan Sigg, Predrag Jakimovski, Florian Becker, Hedda R. Schmidtke, Alexander Neumann, Yusheng Ji, and Michael Beigl: **Neuron Inspired Collaborative Transmission in Wireless Sensor Networks**. The 8th Annual International Conference on Mobile and Ubiquitous Systems: MobiQuitous 2011, Copenhagen, Denmark, December 6-8, 2011.
7. Predrag Jakimovski and Hedda R. Schmidtke: **Delayed Synapses: An LSM Model for Studying Aspects of Temporal Context in Memory**. Modeling and Using Context, 7th International and Interdisciplinary Conference, CONTEXT 2011, Germany, September 26-30, 2011, Lecture Notes in Computer Science, Volume 6967/2011, pages 138-144.
8. Predrag Jakimovski, Florian Becker, Stephan Sigg, Hedda R. Schmidtke, and Michael Beigl: **Collective Communication for Dense Sensing Environments**. In The 7th International Conference on Intelligent Environments - IE'11, Nottingham Trent University, United Kingdom, July 2011, pages 157-164. *(Best Paper Award)*

# List of Figures

1.1	The vision of printed RFID smart label on packaging material. . . . .	3
1.2	Compliance and violation checks at item-level along a supply chain. In case of detecting a violation escalation is initiated, meaning goods are either disposed or returned. . . . .	5
1.3	Thesis problem statement and motivation. . . . .	8
2.1	Showcasing the CDMA scheme: data signal is spread and XOR'ed with special code sequence. . . . .	22
2.2	Illustration of a WSN employing superimposed radio transmission. . . . .	30
2.3	Function computation using the natural analog wireless channel. . . . .	31
2.4	The subfigures (a), (b) and (c) show three different routing strategies for the two-way relay channel illustrating the evolution of different communication paradigms. The classical way of communication shown in subfigure (a) requires 4 time slots. The use of network coding at relay shown in subfigure (b) reduces communication complexity to 3 time slots. And, letting Alice and Bob transmit their messages simultaneously as shown in subfigure (c), where the relay sends a function of it back to the senders, the communication complexity is even reduced to 2 time slots. . . . .	34
2.5	Showcasing the scheme for analog computation over the wireless channel.	39
2.6	Showcasing of the SDJS scheme with 32 time slots and 27 active nodes transmitting a jam signal in a randomly drawn time slot. The receiver $Rx$ estimates the number of transmitters based on the received number of jammed time slots using the SDJS approach [1] . . . . .	42
3.1	A typical application scenario for item level tagging in supply chain management: pallets are investigated by a screening device. . . . .	51
3.2	A model of a simple tag using a destructive, physical temperature sensor (gray and white bar): the start/stop pointer is shifted forward along the fixed random vector $z_0$ as increasing temperatures permanently alter the material of the sensor (grey). When a readout signal is received the correspondingly shifted vector would be transmitted. . . . .	55
3.3	Principle of collective transmission. Each sensor node reached by an external trigger signal is transmitting its binary sequence at the same time. Based on the different number of '1's in each time slot different maximal amplitudes are generated. On the receiver side, the superimposed binary sequence is captured. . . . .	55

3.4	The superposition principle: $s(t)$ is a superimposed signal generated by three sine signals $s_1(t)$ , $s_2(t)$ and $s_3(t)$ . The sine signals are chosen slightly different from each other in frequency, phase and amplitude strength, i.e., $f_{s_1} = 16$ Hz, $f_{s_2} = 18$ Hz and $f_{s_3} = 20$ Hz. Thus, when two or more waves traverse the same space, the amplitude at each point is the sum of the amplitudes of the individual waves. . . . .	56
3.5	Raw data of a superimposed signal caused by 21 transducers transmitting different binary sequences simultaneously. The signal length is set to 100 time slots. . . . .	57
3.6	Quantification of the superimposed signal shown in Figure 3.5. In each time slot the maximal amplitude is detected and visualized by a single bar. . . . .	57
4.1	This figure depicts our OE testbed for reading smart sensing devices, that simulate printed polymer tags. . . . .	66
4.2	The picture above (A) shows our Si-based transponder device. The circuit layouts below (B,C) depict the top and bottom side of the circuit board. The bottom layout (C) indicates the planar antenna, which harvests the power from 2D power sheet [2]. Circuit design and implementation is made by Ali Hadda [3]. . . . .	68
4.3	Shows the Hartley-Oscillator circuit [4] used as signal generator for ON-OFF Keying in our transducer device. . . . .	70
4.4	Schematic of our Si-based transponder. . . . .	71
4.5	Shows the flow-graph of the implemented Software-defined Radio (SDR). . . . .	72
4.6	The four histograms illustrate the distributions of amplitudes which are generated by 5, 10, 15 and 30 transducers sending a sinusoidal signal simultaneously. . . . .	73
4.7	The four distributions indicate various Rice PDFs obtained by fitting data of 5, 10, 15 and 30 transducers which sent a sinusoidal signal simultaneously. . . . .	73
4.8	Raw data of a superimposed signal is shown caused by 12 simultaneously sending transducer devices, whereby 6 of them each sent the same random burst sequence. . . . .	74
5.1	A passive tag reader system illustrates simultaneous transmission of bit streams sent by a set of 64-bit smart labels. . . . .	79
5.2	This block diagram is an example of a circuitry implementing the basic principle of Collective Communications. CRU stands for Clock Recognition Unit, recognizing and conveying externally induced clocking, i.e., by a reader device. The sensor and counter value determine the line select of the ROM, which together enable to output to a sensed value the corresponding bit sequence. . . . .	80
5.3	The circuit block diagram shows the holistic printable passive tag. . . . .	82
5.4	Four different patterns of reader signaling illustrate four alternatives of commands signaling with respect to a collective and simultaneous communication, when tags have to start and subsequently transmit their data back to the reader device. . . . .	84
5.5	The schematic shows partially the circuit logic in connection with the tag rectifier for interpreting signaling coming from reader device. . . . .	85

5.6 The schematic presents the Clock Recognition Unit (CRU) consisting mainly by two circuit functionalities, namely by (1) the circuitry for external clock recognition induced by a reader device, and (2) the circuit function for a counter to determine global bit index. The bit index determines and indicates current bit position for all simultaneously queried tags, that need to be send out in the following cycle. . . . . 87

5.7 The overall signal analysis indicates the maximal amplitude difference between different trails with up to 16 simulated passive tags transmitting simultaneously. . . . . 89

5.8 The schematic of this circuit arrangement implements with respect to our 64-bit polymer tag the remaining part of the tag’s circuit logic. . . . . 91

6.1 Burst-sequences encoding the sensor values of the sensor nodes superimpose on the RF channel. The reader device receives the outcome of a function computation. . . . . 98

6.2 The sum of Poisson processes with mean value  $\mu_i$  yields again a Poisson distribution with  $\mu = \mu_1 + \mu_2 + \mu_3 + \dots$  and  $p(k; \mu t) = e^{-\mu t} \frac{(\mu t)^k}{k!}$ . . . . . 99

6.3 A burst signal superimposed by 15 transmit nodes as observed by the receiver. . . . . 101

6.4 Three sensor nodes transmit simultaneously random burst sequences encoding a constant value  $\mu_{s_i} = v_{s_i} = 1$ . A reader device captures the superimposition and calculates  $\mu_R \approx 3$ . A short time frame and the collision of bursts observed in second sub-interval the function computation results into a bias calculation of  $\mu_R = \mu_{s_1} + \mu_{s_2} + \mu_{s_3}$ . . . . . 103

6.5 These two histograms H1 and H2 show the results of 1000 trials each calculating  $v_{s_1} + v_{s_2} + v_{s_3} = 4 + 10 + 17 = 31$  via RF channel. H1 is obtained by using  $10^3$  time slots for a sub-interval and 5000 sub-intervals for a time frame. H2 is obtained by using  $10^4$  time slots for a sub-interval and 5000 sub-intervals for a time frame. . . . . 104

6.6 The function computation over the wireless channel using  $10^4$  time slots per sub-interval shows clearly an improved calculation accuracy in contrast to a chosen sub-interval length of  $10^3$  slots. The use of differently large time frames show scarcely an impact on the calculation accuracy. . 106

6.7 With respect to a chosen sub-interval length of  $10^3$  slots and the application of equation (6.4) the resulting curve (solid line) shows in comparison to the results in Figure 6.6 a significantly improved calculation accuracy approaching the true value (dashed line). The effort for decreasing the calculation uncertainty is exponential shown by error bars. . . . . 107

6.8 By applying Eq. 6.4 this plot shows results of rectified calculations for using  $10^3$  and  $10^4$  time slots per sub-interval. . . . . 108

6.9 Block diagram showing our simple sensor node. . . . . 111

6.10 The sensor node consists of a 2.4 GHz sinusoid signal generator (A) connected to an Arduino Uno micro-controller (B) interfacing with a sensor device. . . . . 112

6.11 Schematic of our 2.4 GHz oscillator circuit adapted from John Wright’s signal generator [5] by permission. . . . . 112

6.12 Wireless sensor network of the Intel Berkeley Lab [6]. The formation of nodes in the encircled area is used to position our 15 nodes in our lab. . . 113

6.13 Deviation error between computation accuracy and the ground truth. . . 114

6.14	On-the-channel computed mean temperature of 15 nodes in comparison to the averaged measurement series gained from the Intel lab data when $10^3$ time slots are used. The standard deviation error is $\sigma = 0.2293^\circ C$ . . .	115
6.15	On-the-channel computed mean temperature of 15 nodes in comparison to the averaged measurement series gained from the Intel lab data when $10^6$ time slots are used. The standard deviation error is $\sigma = 0.0378^\circ C$ . . .	115
7.1	A sketch of our scheme for the computation of mathematical function via communication channel . . . . .	119
7.2	A binary reception vector of a receiver indicates a bit-sequence representing a concatenated burst sequence . . . . .	120
7.3	Probability tree . . . . .	121
7.4	Plot (a) shows averaged values of absolute calculation error of calculating the mathematical task $10 + 5 + 3 + 2 + 1 = 21$ over wireless channel using different sub-interval lengths. Plot (b) shows nonlinear fits to data presented in plot (a). . . . .	126
7.5	The subplots here show simulation results of wireless superimposed computing performed by a WSN with 5 sensor nodes. The left and right column present statistics for the calculation error experienced during calculating $95 \times 1000$ mathematical tasks such as $v_{s_1} + v_{s_2} + v_{s_3} + v_{s_4} + v_{s_5}$ , and $v_{s_1}, v_{s_2}, v_{s_3}, v_{s_4}, v_{s_5} \in [1, 20]$ . . . . .	127
7.6	The 3D bar-chart presents error mean of wireless superimposed computing for various WSN sizes and different lengths of time frame experienced each time by calculating 1000 mathematical tasks. . . . .	130
7.7	System architecture of the resource restricted IoT sensor node. The Random Number Generator (RNG) is an inherent part of the circuit logic. . .	133
A.1	Depicted is an organic transistor printed on a plastic substrate. The source and drain are separated by a semiconductor polymer. An insulating polymer forms the dielectric layer between gate and the other layers. .	148
A.2	The diode (left) and capacitor (right) together form a half-wave rectifier with a reservoir capacitor. . . . .	149
A.3	Half-wave rectifier circuit with a reservoir capacitor. . . . .	150
A.4	Circuit diagram of a 5-stage ring oscillator realized with five logic inverter gates. The capacitor between two inverter gates serves to delay the input signal of the following inverter. . . . .	150
A.5	The circuit diagrams (A), . . . , (D) illustrate four different architectures realizing the logic inverter gate 'NOT'. The configurations (A) and (B) are characterized as unipolar, that are realized with p-only semiconductor material, whereby (A) is an inverter with load resistor, and (B) integrates a depletion load transistor. The configurations (C) and (D) are denoted as complementary CMOS-like inverter architectures. A distinctive feature indicates configuration (D), because its complementary circuit architecture is realized by a single ambipolar semiconductor material underlaid with a grayed out rectangle in subfigure (D). . . . .	150
A.6	Flexography. . . . .	158
A.7	Gravure printing. . . . .	158
A.8	Offset lithography. . . . .	159

# List of Tables

2.1	The acronym <b>NA</b> means 'Not Available'. . . . .	16
2.2	Some performance characteristics of common printing technologies obtained from Mandal et al. [7] and Baeg et al. [8]. . . . .	17
2.3	Deployed silicon microchips and ASICs for current RFID standards. . . . .	20
3.1	Results . . . . .	62
4.1	This Table lists all electronic devices used to assemble the reader hardware infrastructure. . . . .	67
6.1	Elementary functions for data processing over the wireless channel. . . . .	109
6.2	An excerpt of common functions being calculable on the RF channel and applied in data analysis. . . . .	110
7.1	Errors experienced by calculation of valued during simultaneous transmission ( $t = 10^6$ and $\kappa = 10^3$ ) . . . . .	129
7.2	Errors experienced by calculation of valued during simultaneous transmission ( $t = 10^7$ and $\kappa = 10^4$ ) . . . . .	130
7.3	Errors experienced by calculation of valued during simultaneous transmission ( $t = 10^6$ and $\kappa = 10^2$ ) . . . . .	130
7.4	Errors experienced by calculation of valued during simultaneous transmission ( $t = 10^7$ and $\kappa = 10^3$ ) . . . . .	131
A.1	Printed devices:state of the art. . . . .	153

# Abbreviations

<b>a-IGZO</b>	<b>amorphous-Indium-Gallium-Zinc-Oxide</b>
<b>ADC</b>	<b>Analog-to-Digital-Converter</b>
<b>AmI</b>	<b>Ambient Intelligence</b>
<b>ASIC</b>	<b>Application Specific Integrated Circuit</b>
<b>AWGN</b>	<b>Additive White Gaussian Noise</b>
<b>BER</b>	<b>Bit Error Rate</b>
<b>BPSK</b>	<b>Binary Phase Shift Keying</b>
<b>CC</b>	<b>Collective Communications</b>
<b>CDMA</b>	<b>Code Division Multiple Access</b>
<b>CMOS</b>	<b>Complementary Metal-Oxide-Semiconductor</b>
<b>CDF</b>	<b>Cumulative Distribution Function</b>
<b>CMU</b>	<b>Central Management Unit</b>
<b>CoMAC</b>	<b>Computation over MAC</b>
<b>CORDIC</b>	<b>Coordinate Rotation Digital Computer</b>
<b>CRU</b>	<b>Clock Recognition Unit</b>
<b>CSI</b>	<b>Channel State Information</b>
<b>D</b>	<b>Drain</b>
<b>DAC</b>	<b>Digital Analog Converter</b>
<b>DC</b>	<b>Direct Current</b>
<b>ERP</b>	<b>Enterprise Resource Planning</b>
<b>FDMA</b>	<b>Frequency Division Multiple Access</b>
<b>FDS</b>	<b>Frequency Domain Signature</b>
<b>FM</b>	<b>Frequency Modulator</b>
<b>FSM</b>	<b>Finite State Machine</b>
<b>FSRG</b>	<b>Feedback Shift Register Generator</b>

<b>G</b>	<b>G</b> ate
<b>GE</b>	<b>G</b> ate <b>E</b> quivalent
<b>GF</b>	<b>G</b> alois <b>F</b> ield
<b>GLFSR</b>	<b>G</b> eneralized <b>L</b> inear <b>F</b> eedback <b>S</b> hift <b>R</b> egister
<b>GRC</b>	<b>G</b> NU <b>R</b> adio <b>C</b> ompanion
<b>HF</b>	<b>H</b> igh <b>F</b> requency
<b>IC</b>	<b>I</b> ntegrated <b>C</b> ircuit
<b>IE</b>	<b>I</b> ntelligent <b>E</b> nvironments
<b>ID</b>	<b>I</b> Dentification
<b>IoT</b>	<b>I</b> nternet of <b>T</b> hings
<b>ISO</b>	<b>I</b> nternational <b>O</b> rganization for <b>S</b> tandardization
<b>ISM</b>	<b>I</b> ndustrial, <b>S</b> cientific and <b>M</b> edical band
<b>ITM</b>	<b>I</b> nverse <b>T</b> ransform <b>M</b> ethod
<b>L</b>	channel <b>L</b> ength
<b>LCG</b>	<b>L</b> inear <b>C</b> ongruential <b>G</b> enerator
<b>LF</b>	<b>L</b> ow <b>F</b> requency
<b>LFG</b>	<b>L</b> agged <b>F</b> ibonacci <b>G</b> enerator
<b>LSE</b>	<b>L</b> east <b>S</b> quares <b>E</b> stimation
<b>LUT</b>	<b>L</b> ook-Up <b>T</b> able
<b>MAC</b>	<b>M</b> edia <b>A</b> ccess <b>C</b> ontrol
<b>MOSFET</b>	<b>M</b> etal- <b>O</b> xide- <b>S</b> emiconductor <b>F</b> ield- <b>E</b> ffect <b>T</b> ransistor
<b>MSK</b>	<b>M</b> inimum <b>S</b> hift <b>K</b> eying
<b>NFC</b>	<b>N</b> ear <b>F</b> ield <b>C</b> ommunication
<b>OE</b>	<b>O</b> rganic and printed <b>E</b> lectronics
<b>OECT</b>	<b>O</b> rganic <b>E</b> lectro <b>C</b> hemical <b>T</b> ransistors
<b>OFET</b>	<b>O</b> rganic <b>F</b> ield <b>E</b> ffect <b>T</b> ransistor
<b>OLED</b>	<b>O</b> rganic <b>L</b> ight <b>E</b> mitting <b>D</b> iode
<b>OOK</b>	<b>O</b> N- <b>O</b> FF- <b>K</b> eying
<b>OPV</b>	<b>O</b> rganic <b>P</b> hoto <b>V</b> oltaics
<b>OSC</b>	<b>O</b> rganic <b>S</b> emi <b>C</b> onductor
<b>OTFT</b>	<b>O</b> rganic <b>T</b> hin- <b>F</b> ilm <b>T</b> ransistor
<b>PCB</b>	<b>P</b> rinted <b>C</b> ircuit <b>B</b> oard
<b>PDF</b>	<b>P</b> robability <b>D</b> ensity <b>F</b> unction

<b>PE</b>	<b>Printed Electronics</b>
<b>PRISMA</b>	<b>PRI SMARt</b> label
<b>PRNG</b>	<b>Pseudo-Random Number Generator</b>
<b>PROLOG</b>	<b>PR</b> inted <b>O</b> rganic <b>LOG</b> ic circuits
<b>PS</b>	<b>Parabolic Synthesis</b>
<b>PSK</b>	<b>Phase Shift Keying</b>
<b>R2R</b>	<b>Roll-to-Roll</b>
<b>RC</b>	<b>Resistor - Capacitor</b>
<b>REST</b>	<b>RE</b> presentational <b>S</b> tate <b>T</b> ransfer
<b>RFID</b>	<b>R</b> adio <b>F</b> requency <b>ID</b> entification
<b>RF</b>	<b>R</b> adio <b>F</b> requency
<b>RNG</b>	<b>R</b> andom <b>N</b> umber <b>G</b> enerator
<b>ROM</b>	<b>R</b> ead- <b>O</b> nly- <b>M</b> emory
<b>RSS</b>	<b>R</b> eceived <b>S</b> ignal <b>S</b> trength
<b>S</b>	<b>S</b> ource
<b>SAR</b>	<b>S</b> uccessive- <b>A</b> pproximation- <b>R</b> egister
<b>SDJS</b>	<b>S</b> ynchronous <b>D</b> istributed <b>J</b> am <b>S</b> ignaling
<b>SDR</b>	<b>S</b> oftware <b>D</b> efined <b>R</b> adio
<b>SIMO</b>	<b>S</b> ingle <b>I</b> ntput, <b>M</b> ultiple <b>O</b> utput
<b>SME</b>	<b>S</b> Mart <b>E</b> nvironments
<b>SNR</b>	<b>S</b> ignal-to- <b>N</b> oise- <b>R</b> atio
<b>TDMA</b>	<b>T</b> ime <b>D</b> ivision <b>M</b> ultiple <b>A</b> ccess
<b>TDR</b>	<b>T</b> ime <b>D</b> omain <b>R</b> eflect
<b>TDS</b>	<b>E</b> PCglobal <b>T</b> ag <b>D</b> ata <b>S</b> tandard
<b>TRNG</b>	<b>T</b> rue <b>R</b> andom <b>N</b> umber <b>G</b> enerator
<b>USRP</b>	<b>U</b> niversal <b>S</b> oftware <b>R</b> adio <b>P</b> eripheral
<b>VCO</b>	<b>V</b> oltage- <b>C</b> ontrolled <b>O</b> scillator
<b>VSA</b>	<b>V</b> ector <b>S</b> ymbolic <b>A</b> rchitecture
<b>W</b>	channel <b>W</b> idth
<b>WISP</b>	<b>W</b> ireless <b>I</b> dentification <b>S</b> ensor <b>P</b> latform
<b>WORM</b>	<b>W</b> rite <b>O</b> nce <b>R</b> ead <b>M</b> any
<b>WSN</b>	<b>W</b> ireless <b>S</b> ensor <b>N</b> etworks
<b>XOR</b>	<b>e</b> Xclusive <b>O</b> R

*To my Mom and Dad*

# Chapter 1

## Introduction

### 1.1 Internet of Things (IoT)

The Internet of Things (IoT) describes an advanced worldwide network of intercommunicating electronic devices, where everything is linked with everything else [9, 10]. Thereby, everyday objects are equipped with electronic devices embedding sensors, actuators, microchips and antennas, which are enabled to sense continuously the environment and provide the sensory, as well as status or context-based information to the world wide web. In the application layer of the Internet the uploaded data is evaluated and shared [11]. The things equipped with actuators and displays are enabled to give feedback to their environment, become intelligent, responsive, to anticipate what to do next and interact with other things or people [10, 12, 13]. In such scenarios very often the objective is to establish living spaces, so called SMart Environments (SME) and Ambient Intelligence (AmI) [14, 15]. Furthermore, the physical object itself is promoted to act as a 'living being' implementing an intelligent software agent [14]. The advancement in hardware technology and steady economic growth is allowing to create billions of smart 'things' connected virtually with the real world deployed in any conceivable use case scenarios [12–14]. As an application scenario, one can think of a supply chain, where each merchandise is tagged with an electronic device at item-level [16–18]. Thus, an Internet-enabled single object, e.g., a perishable item such as a package of frozen fish sticks, can be connected with different business and technical domains [18], such as the production place, food control, logistics, warehouses, retail and stock market. Hence, the cross-linkage of the single object over different stake holders opens a new horizon in terms of novel business opportunities and lifestyles [16–18]. IoT creates here a greater value and provides diverse services, such as checking and localizing inventory

with one click [17]. It would be too expensive to equip every item with powerful electronic devices [17], though, so that in the last decades the research and industry focused on developing of various technologies concerning identification, communication, sensing and computation, to realize IoT [10, 12, 17, 19].

While high priced objects, such as phones, cars, TV's or fridges can be equipped with any communication and sensing technology, because the final price for the object increases in relation to value-for-money insignificantly [10, 20], in contrast, the embedding of electronics on low priced objects requires low cost identification and communication technology [21, 22]. Apart from optically readable barcodes printed on each commercial product for identification [23], respectively, using derivative technologies, a push technology towards IoT became the Radio Frequency IDentification (RFID) technology, which in principle allows to realize item-level tagging [17, 23]. However, the deployment of silicon RFID chips for item-level tagging is still limited [22, 24], because the manufacturing costs for microchips exceed the economic reasonable threshold [25] despite steady hardware improvement and declining prices. Thus, current stage of IoT is incomplete, because the set of things being not in the Internet is by far greater, than the things being made smart through electronics [17]. Further, besides economic constraints [25, 26], the IoT is facing the following major technical issues [27]:

- handling massive amounts of data acquired through item-level tagging and sensing
- storage capacity and information processing
- maintenance of large IoT infrastructures
- power consumption and sustainability of sensing devices

According to the IoT vision, billions or even trillions of tags and sensors will be connected to physical objects uploading information to the Internet, tracking objects, monitoring of movements, and providing rich context information [9, 10, 28, 29]. However, gathering and storing information continuously from each electronic device will not only produce a big knowledge base about the world, but also to a huge search space for information retrieval and context recognition [27, 29], such that identifying relevant data is going to become a daunting task [14].

## 1.2 Printed Electronics and Sensor-Based IoT Devices

The IoT is going to change our daily life [9], considering that everyday objects are equipped with intelligent electronic devices, such as smart cards, smart labels, smart

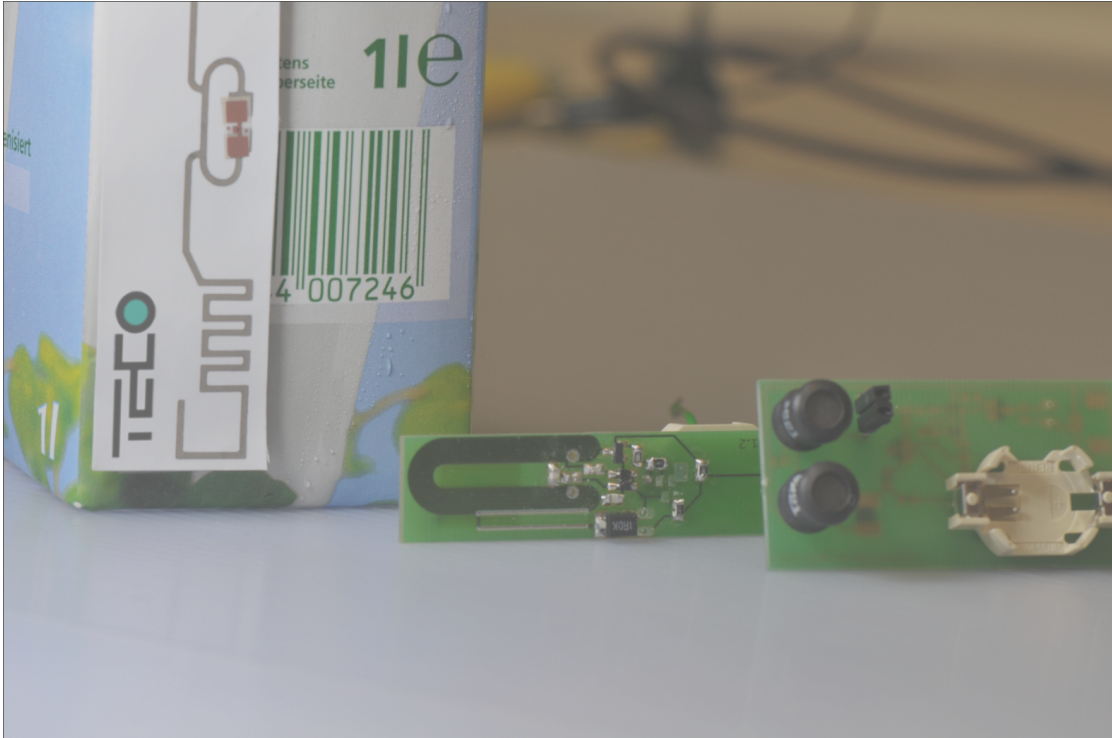


FIGURE 1.1: The vision of printed RFID smart label on packaging material.

objects or, employing smart packaging technology [30]. All these kinds of smart devices rely mainly on RFID technology providing identification and wireless communication capabilities [17, 30]. In practice, a reader system connected to the Internet is interrogating the smart things requesting their identification (ID), status and location for monitoring and tracking purposes [10, 27, 29]. The communication between reader device and the RFID-enabled objects relies on using, e.g., the EPCglobal Class 1 Generation 2 protocol (ISO 18000-6C) [31]. To establish a wireless communication each smart device requires a microprocessor, which is costly in comparison to item-level tagging [30].

An alternative of using conventional silicon-based microchip technology for manufacturing RFID labels and sensing electronic devices is the emergent polymer electronics technology, known as Organic and printed Electronics (OE) [32]. The idea behind OE is to print electronic circuits directly on substrates, such as plastic foils and paper [32]. In this way, an electronic device can be printed as graphics onto a large area or packaging material of a commercial product, shown as a vision in Figure 1.1. The Figure showcases an envisioned printed smart label on a milk package possessing capabilities of a silicon-based electronic device. Furthermore, the printing of electronics is going to enable manufacturing of low cost electronics in high volumes [22, 32], because the printing process itself is in principle almost the same as the printing of newspaper, magazines, books, graphics and text [32–34]. Thus, printed electronics can be seen as an enabler technology for IoT [35, 36]. Further, printed electronics is offering features, such

as being thin, light-weighted and flexible, such that IoT can be enriched by novel applications and possibilities [35]. For instance, key applications in OE [32, 37] are Organic Photovoltaic (OPV) the printing of solar cells, flexible displays, Organic Light Emitting Diode (OLED) lighting, printed RFID, smart textiles and smart objects integrating functions such as printed display, printed sensors, printed memory and printed battery. However, OE is still in its early stage of development, despite recent advances in the last decade [7, 8].

To bring up an example of OE research, the work in [38] describes a printed microprocessor with 3504 thin-film transistors printed on a  $1.20\text{ cm} \times 1.88\text{ cm}$  plastic film using inkjet printer and photolithography. The operational clocking runs at a maximum of 2.1 kHz. The electronic structure of a thin-film transistor measures a channel width of  $W = 140\text{ }\mu\text{m}$ , and length  $L = 5\text{ }\mu\text{m}$ . The 8-bit microprocessor can execute addition, subtraction and bit-shift. Considering the technical requirements to implement standard RFID technology with OE, then the printing of a microchip comprising all required RFID functionalities is going to occupy a large size of area, such that the resulting printed RFID tag will be of no practical use [39]. To this end, the electrical performance of such large sized RFID circuit can suffer [7, 8]. With regard to current state of OE technology [32], it has to be acknowledged, that there are limitations in terms of printing the number of transistors required to perform advanced functionalities, such as computation and communication capabilities. Thus, the key issues of OE can be summarized as follows [7, 8, 35, 36]

- low hardware complexity
- low electro mobility, i.e., switching speed of printed transistors
- low printing resolution of electronic structures
- device reliability and lifetime
- yield of printed devices in a mass production process

### 1.3 Application Scenario: Supply Chain Management

Despite technical issues, that are still unresolved with OE [7, 8], the prospect of low cost electronics and novel features in terms of merging electronic devices with physical objects, is motivating to continue with the development of OE for IoT [32]. A typical application scenario with respect to IoT describes the field of supply chain management, where manufactured goods and products of low value, such as milk and milk products

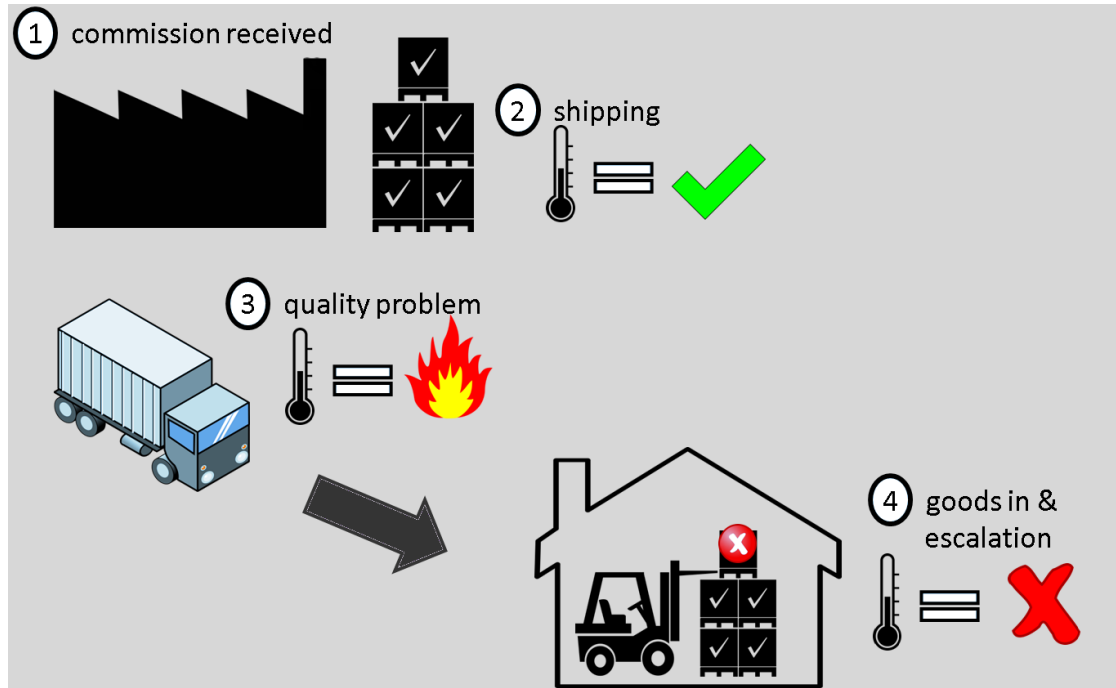


FIGURE 1.2: Compliance and violation checks at item-level along a supply chain. In case of detecting a violation escalation is initiated, meaning goods are either disposed or returned.

need to be monitored along the entire value chain, traced during transportation and maintained in retail stores [16, 18, 19, 40, 41]. Implementing the Internet of Things here provides business advantages [17, 19]. For instance, RFID-enabled items can be tracked in real time [17, 19]. A retailer can optimize his applications [42], such as automatically checking of goods receipt, monitoring and tracking of stocks in real time, or the detection of shoplifting. Furthermore, the data from retail stores obtained by smart shelves doing periodic checks can be used to optimize the entire supply chain [19, 41]. Here, the manufacturers can use the stock and sales data from retailers to produce and ship the right amount of products. In this way, over and underproduction can be avoided [17, 42, 43]. An example of a specific application scenario represents the surveillance of temperature sensitive goods and products in a cool chain illustrated in Figure 1.2. At the production place, during transportation and destination compliance and completeness checks are performed, such that product quality is kept and losses in terms of expiration and spoilage is reduced [44]. For this case, each item is tagged with an sensor-based OE smart label [45], thus, enabling the checking at item-level [46]. Based on the product quality threshold, e.g., the item is 'OK', if the smart label measurement indicates a temperature value below  $8^{\circ}\text{C}$ , the quality status is uploaded to the company's software system. Right after all items of a pallet are checked the software system is making the following decisions [44–46]

- reject the delivery, if a critical number of items has failed the compliance check

- sort out of corrupted goods, if the majority of items has status 'OK'
- continue with processing of the pallet, if no compliance violation is detected

In our application scenario in Figure 1.2, the factory receives an order for some pallets with perishables. In accordance with the terms of commission the perishables are put together and made ready for shipping. But, before the delivery goes to customer the perishables of each pallet are checked by item-level [46]. During transportation from factory to customer, case-related a problem occurs, e.g., some perishables of a pallet sustain damages through overheating. At the destination, e.g., a warehouse, the corrupted pallet is detected through repeated interrogation, and immediately discarded.

## 1.4 Problem Statement and Motivation

In the IoT a huge amount of RFID-like electronic devices and sensors is going to be deployed [9, 19, 45], for instance, in dense sensing environments and over wide areas. With regard to data collection the communication is going to face a technical challenge [10], because conventional communication schemes are limited with respect to scalability and power efficiency [30], so that the more devices share the same wireless channel the higher the communication load and, the longer the transmission range the higher the power consumption [30]. To this end, the idea of creating low cost OE smart devices is posing an inviolable barrier, because the technical evolution of OE indicates rather a random leap forward of development than a foreseeable progress [32], such that electronic devices of low hardware complexity can only be designed [35, 45]. However, the prospect of mapping the real-world space and time into a virtual world with high-resolution is enabling a high level of monitoring, controlling and management over an application scenario [44, 46]. This thesis is dealing with providing strategies and solutions regarding the following issues.

1. The large-scale and high volume deployment of electronic devices and sensors in dense environments generates a high communication load, that can lead to overload using conventional communications [19, 41]. Thus, preprocessing of data and simplification of communication is required to achieve high scalability and power efficient IoT devices [41].
2. The low hardware performance of OE is constraining the design of fully functional and all-printable OE smart devices including their communication capability [7, 8, 32].

3. The computation capabilities of resource-limited IoT devices are constrained with regard to interpreting, evaluating and forwarding sensory data [47–50]. Therefore, computation mechanisms for communicating of desired functions over the RF channel is required to adopt, for instance, resource-limited IoT nodes for Wireless Sensor Networks (WSN).

The issue of OE being weak in terms of printing an arbitrary but required circuit with high complexity is aggravating the problem of implementing standard communication protocols on organic and printed IoT devices [7, 35]. However, using conventional communications is in terms of efficacy and scalability inefficient in the scenario, so that novel forms of communication are needed to satisfy on the one hand OE constraints, and on the other hand an efficient information transmission over wireless channels. On the contrary, the implementation of item-level tagging is going to provide beside economic benefits [45], such as reduction of waste and loss, a sustainable technology in terms of resource conservation. In this thesis we are going to provide approaches for the issues described above which will rely on the concept of *superimposed radio transmission*. Figure 1.3 presents a concise block diagram of the thesis problem statement and motivation. The concept of superimposed radio transmission describes a communication form, where several senders transmit signals simultaneously over the same wireless channel to one or more receivers [51–54]. In the classic view this describes an interference, that is strictly to be avoided in the design of communications [55], where orthogonal communication in frequency, space, code and time division is allowed. However, the advantage of allowing superimposed radio transmission is the simplification of communication yielding a minimalistic circuit design for electronic devices [52], but catches the problem of unlocking the superimposed transmission. However, in this thesis we are going to show how a superimposed radio transmission can be exploited for various applications in communications and data processing. Further, how superimposed radio transmission enables a minimalistic circuit design for all-printable smart RFID labels and resource-limited IoT nodes needed in the domain of WSN. However, we also are going to show the limits of superimposed radio transmission.

## 1.5 Summary of Contributions

In particular, the main objective of this thesis is to provide practical strategies, data coding schemes and solutions for short-ranged RFID systems reading out minimalistic polymer tags, and long-ranged resource-limited wireless sensor networks relevant to the Internet of Things (IoT). The focus lies in designing and implementing novel communications and data processing mechanisms for organic and printed smart labels and

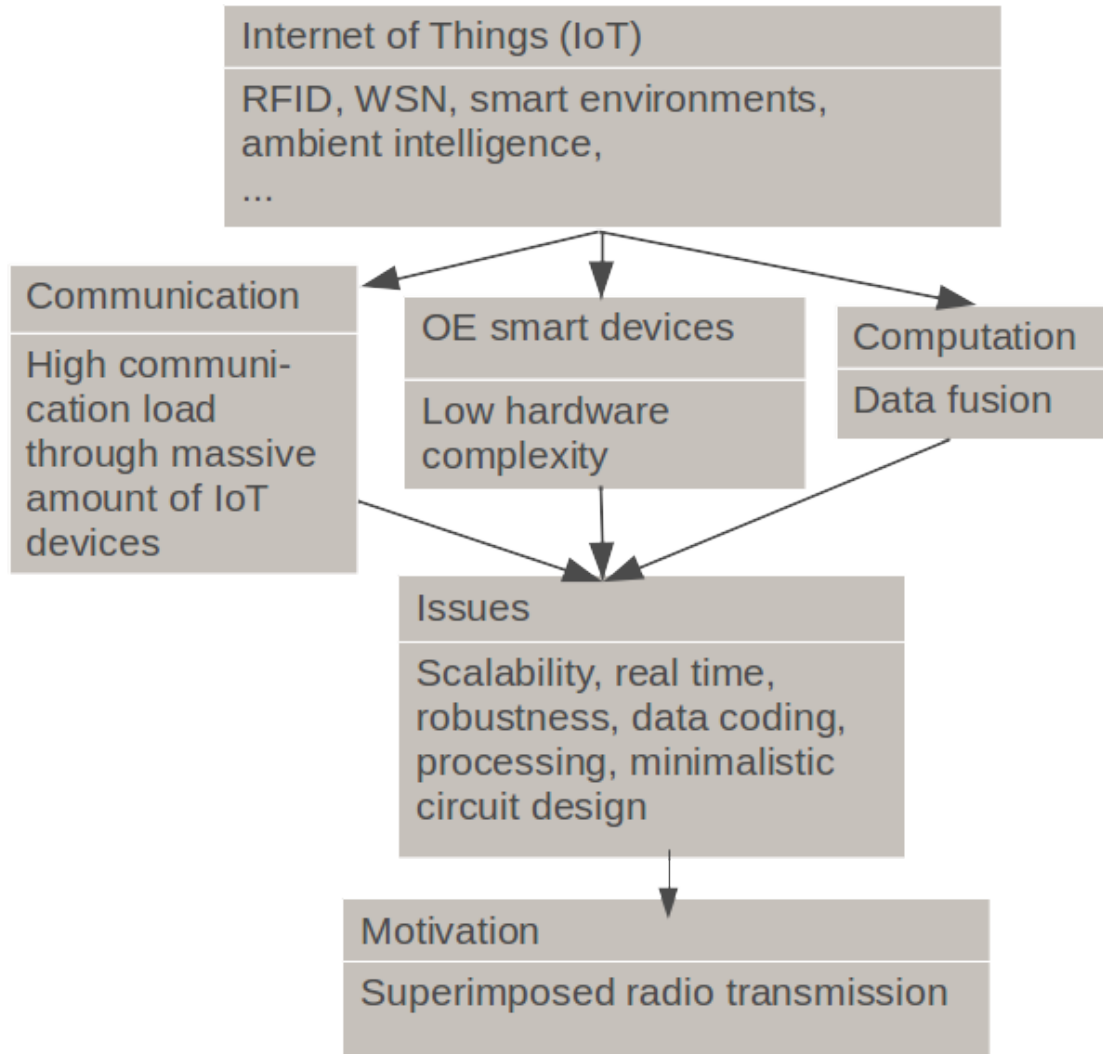


FIGURE 1.3: Thesis problem statement and motivation.

resource-limited IoT nodes. The communications and sensory processing mechanisms developed in this work are based on collaboratively and simultaneously transmitted information transfer exploiting the linear superposition principle of electromagnetic waves and the principle of randomness. Strictly speaking, simultaneously transmitted signals are considered in traditional way as interference that is to be avoided [55, 56], but in our new perspective a superimposed radio transmission provides inference, which represents a paradigm shift towards simultaneous communication and processing of data over the RF channel. The idea is to give up the peer-to-peer communication manner by waiving the request for IDentification (ID) of each device for the benefit of achieving a light-weighted circuit design regarding resource-limited sensing devices, that can be implemented in polymer electronics [51, 52]. Further on, this PhD thesis investigates two additional research questions, in particular, how to

(i) regain sensory information from a superimposed radio transmission and,

- (ii) calculate mathematical functions of interest during RF transmission on the wireless channel.

The elaboration of the listed questions into technical solutions is grounded on the following principles:

1. communication is based on ON-OFF-Keying (OOK),
2. coding scheme for data is based on randomly drawn bit sequences,
3. transmission of data starts at the same time and takes place simultaneously and collectively.

The superimposition of the signals on the RF channel is considered as an operational mechanism on simultaneously sent data [54, 57]. With regard to case (i) the thesis proposes the collective communication mechanism determined for dense environments, in order to establish intelligent environments deploying massive amounts of sensing devices.

The application scenario of a cool chain in a supply chain is chosen, to investigate the requirements and business opportunities. The goal of this endeavour was to achieve an economic reasonable communication technology that can be applied in the IoT to realize in conclusion ambient and intelligent environments. The idea of *collective information transmission* is developed to establish communication not between single senders and single receivers, but between collectives of senders and receivers, by making use of constructive interference of simultaneously sent signals. This PhD thesis details how the collective transmission approach can be realized for a concrete application scenario: item-level tagging using printed organic electronics [32, 45, 46]. It describes an approach that can be realized on very simple tags. With a test-bed implementation, we show prototypically that this approach can realize robust, collective, approximate read-out of more than 20 simultaneously sent signals. Further, we apply the approach *collective communications* to design and implement a sensor-based and all-printable 64-bit polymer tag tailored for a passive RFID reader system. In cooperation with the company PolyIC, well-known for printed electronics and printing technology, the feasibility of printing the here proposed smart label circuitry into OE has been investigated and confirmed by the project partner, that we published in work [58].

Regarding the issue (ii) the processing of sensed data is carried out over the wireless communication channel and not at the sink node. The use case scenario is designated for wireless sensor networks with resource-limited IoT nodes. In this approach the IoT devices are considered as heavily resource-limited, possibly parasitic or passively powered nodes. Although restricted in their computational capabilities, such nodes can draw on

a virtually unlimited power source. This property is exploited by trading computational load for communication load. In particular, this PhD thesis presents a communication scheme by which mathematical computations, i.e., mathematical functions of interest can be executed at the time of wireless transmission. This transmission scheme enables the execution of complex computations by a network of resource restricted, cooperating nodes at a computational load below the operation's computational complexity. The transmission scheme is derived analytically, and its feasibility for dense sensor networks explored in mathematical simulations. Further, its practicability is demonstrated in a case study with 15 simple sensor nodes deployed in our lab.

## 1.6 Outline

The thesis is organized as follows. After this chapter, in chapter 2 we provide the background and related work relevant to this thesis. That is, a comprehensive and thorough introduction/analysis to Intelligent Environments (IE) and its implementation with Internet of Things (IoT) technologies is given. Further, we investigate state-of-the-art wireless communications in connection with polymer electronics indicating a solution and research challenge at once, which targets to realize the vision of IoT. In this context, we analyze the related work in terms of minimalistic circuit design and practicability, which in particular deploy the novel paradigm of superimposed radio transmission. With the insights we gained out of the related work analysis, in chapter 3 we develop a code-based Collective Communications (CC) suited for minimalistic and printable polymer tags with respect to item-level tagging in dense sensing environments. In chapter 4 we unveil our reader system testbed for concurrent and superimposed wireless transmission, that we used in chapter 3 to test our collective communication approach with more than 20 transducers. Since we investigated our code-based CC approach with the help of Si-based technology thus far, in chapter 5 we implement an example of an organic printed and fully functional smart RFID label for a passive reader system, which integrates our CC at the logic gate level. After that, in chapter 6 we develop a time-based Collective Communications, designed for resource-limited WSNs and the implementation of wireless superimposed computing, i.e., to perform data processing during transmission on the RF channel. In a follow-up, in chapter 7 we provide a solution for removing the systematic computation error, that we experienced in our case study described in chapter 6. Further, for general purpose we provide design recommendations for implementing the minimalistic sensor node into a mixed-signal ASIC device. In the last chapter we draw conclusion and give outlook for future work.

## Chapter 2

# Background and Related Work

### 2.1 Intelligent Environments

*“The emergence of intelligence has its origin in perception of the physical world and communication between different participants”* [59]. And, since Mark Weiser [60] predicted that the use of everyday electronic devices with communication capabilities will be disappearing from active human awareness, since then successful progression is made in advancing various and versatile hard- and software technologies to emerge as a result into so called Intelligent Environments (IE) [14]. However, to realize the vision of Intelligent Environments in combination with the Internet of Things (IoT), massive amounts of sensor data need to be processed in a spatially distributed way [12, 27, 29, 61, 62]. Communication in Intelligent Environments is mostly implemented using RFID and WSN technologies with conventional connection-based communications. But, connection-based communications may be unsuitable for IE scenarios involving massive amounts of relatively simple sensing devices. While point-to-point communication within the Internet of Things is commonly used to communicate sensor readings, status and IDentification (ID), established in design defacto as a general rule to solve any kind of application task, very often a function of the sensed data and status within a collocated environment can be more appropriate to communicate [63] than the mere dissemination and collection of all generated data such as who, when and what is sensed, and where it is to be send in the designated area. Although there do not exist a specific standard architecture for the IoT [11], rather a set of different communication technologies (such as Bluetooth, ZigBee, WirelessHART, WLAN, RFID communication protocols and others, that are tailored for specific application scenarios and hardware), the communication between Things is mostly based on Shannon’s seminal work [64]: information is encoded by a bit and communication between participants is performed in separated bit-pipes. That

means, the communication channel is orthogonalized and accessed in the manner of multiplexing Time (TDMA), Frequency (FDMA) or Code (CDMA). Further, all existing communication technologies share/apply the same principle from Shannon to communicate, that is implemented at the lowest layer of a communication protocol the Physical and Media Access Channels (PHY/MAC) layer.

While in IoT research the urge exist to bring different communication technologies together [11, 29] such that Everything can be connected with anything (open issue [11], but not primarily subject of this thesis), Shannon's principle for modeling the PHY/MAC layer remains mostly the same and untouched. Why should one even try it, when Shannon's principle historically proved itself in communication design again and again (cf. wireless communications by reference [65], and reference [56]). Over the last few decades the hard- and software technology in communications achieved maturity such that Everything and Everyone can be connected to the worldwide Internet. For example, current research in cellular networks is in its 5-th Generation (5G) focusing to enable IoT [66]. Considering this technology development the improvement will be relying in essence on the hardware-side featuring large range communications, low energy consumption and being able to cope with different IoT technologies, i.e., to utilize for communication a much more wider frequency spectrum allowing a higher data throughput, flexibility and low latency between IoT devices [66, 67].

However, the modeling of communications into layers (e.g., consider the common Open Systems Interconnection (OSI) reference model, or any other communication protocol) allows seamless simplification of a connection-based and reliable communications [56]. But, these advantages come mostly at the cost of device complexity and its power consumption, and as we are going to show later, these will be the Achilles' heel for realizing the IoT vision.

To answer our rather provocative question from before, in advance there are following key issues to be considered:

- (i) economic reasons,
- (ii) power consumption, device complexity and
- (iii) computational power of electronic devices,
- (iv) scale-size of a device even down to the molecular level,
- (v) latency, scalability and throughput in terms of communications,
- (vi) communication complexity in terms of collocated, random planar and other than wireless networks.

With regard to the Things (or everyday objects) being connected to the Internet, and the above enlisted issues (i)–(vi), the most challenging hardware technologies represent RFID and WSNs. While causally economic constraints hinders a widespread deployment of RFID at item-level [16, 40], the embedding of battery-powered WSNs face a series danger to the environment [68]. In addition, the maintenance of conventional WSN infrastructure is cost-intensive [69].

However, despite experienced economic and technical challenges, the continuous improvement and deployment of current wireless sensor network technologies, as well as the RFID technology in various application scenarios is bringing the vision of the Internet of Things closer to its realization [10]. For instance, the RFID technology is successfully deployed in the area of object identification, surveillance and tracking goods in logistics [30]. The WSN technology is applied, e.g., in monitoring of environments, production lines in factories, or security zones [69]. The basis of these technologies, however, relies on the application of high-performance silicon chips. Based on continuous miniaturization and improvement of high-integrated chip circuits in periodic time [70] more functionalities and features can be integrated in the chip circuitry for almost the same chip production costs [71]. In fact, one can say that the hardware technology already exists in order to realize the vision of the IoT, but unfortunately this is failing, because the deployment of silicon-based technology in the area of, e.g., item-level tagging is not sufficiently cost effective [40]. Currently, for instance, it is not possible to fabricate silicon-based RFID chips below 2 euro cents per device [25]. To enable economical, large-scale and high-volume RFID deployment at item-level, it is required to reduce the manufacturing costs for RFID tags below 1 euro cent per device [25, 40]. Despite continued progress in developing microchip technology, the production costs of silicon-based chips remain unchanged, because the manufacturing processes in production lines are cost intensive, including infrastructure and clean room facilities maintenance costs [25, 71].

With regard to IoT an alternative for silicon-based technology is offered by the emergent Printed Electronics (PE) [45]. This technology deals with printing electronic devices directly on large area surfaces, such as packaging material. With respect to the printing process, organic or inorganic materials are used as inks. In the case of using carbon-based inks the printing of electronic devices is called polymer electronics, known as Organic Electronics (OE) [35, 36]. The idea is to enable high-volume and cost effective printing of electronic devices on substrates, such as plastic foils and paper. Current success of OE is illustrated by the Organic Photovoltaic (OPV), i.e., the printing of solar cells, or Organic Light Emitted Diodes (OLED) for illumination purposes and displays (cf. reference [36], or reference [35]). Moreover, the research and industry are focusing on enabling large-scale printing of RFID tags the so-called organic printed smart labels [45]. However, the realization of printing RFID circuits poses serious limitations

with respect to reliability and achievable hardware complexity. At the current state-of-the-art, printed circuits with few hundreds of transistors have been demonstrated, that can be even printed in mass production [72, 73]. But, as we are going to show in the next section, the printing of microchips for producing all-printable standard RFID tags is far away from its realization, because polymer electronics in general cannot meet the technical requirements.

The remaining part of this chapter is structured as follows. In section 2.2 we discuss the state-of-the-art, opportunities and issues of Printed Electronics (PE) relating to the Internet of Things, and derive out of it constraints for hardware parameters needed to realize all-printable and economically viable sensing devices such as RFID-like printed tags and smart labels. In section 2.3 and section 2.4 we turn to review about wireless communication mechanisms that can be implemented in such economically viable IoT devices with low hardware complexity. In our findings, we identify that the implementation of standard wireless communication strategies into organic smart labels and resource-restricted IoT nodes is a daunting task. As a result, and with respect to reviewing related work, in section 2.6 we resume to investigate beyond the standard wireless communications to further communication approaches that rely on exploiting superimposed radio transmission. And, since likewise our work is based on utilizing superimposed radio transmission schemes, we are going to provide a rigorous related work analysis in this matter, revealing that the reviewed approaches with regard to IoT hard- and software constraints lack on practicability or, being restricted in their applicability and versatility. In the final section 2.7 we summarize the presented background and related work providing with it the basis and boundary conditions for our upcoming work.

## **2.2 Printed Electronics for RFID and Smart Labels**

In our previous background introduction to Intelligent Environments we pointed out that RFID-based applications and WSN scenarios will be mostly implemented by low-cost and simple sensing devices. Depending on their economic viability the vision of IoT can be realized. Current Barcode technology is already such one enabling of identification at item-level, but this technology lacks on handling and processing of massive amounts of items, e.g., a mass check-in of pallets and containers at item-level [23]. In contrast, RFID technology is in comparison to Barcode in terms of memory capacity, readability, speed, being re-programmable, robustness and scalability vastly superior [17, 23], but the high fabrication costs for Si-based RFID chips impede their wide deployment in item-level-based applications, thus failing to realize the IoT [40]. However, the emergence of

Organic and printed Electronics (OE) arises the opportunity to create affordable all-printed RFID tags [45], which can compete with the well established Barcode system.

**Definition 2.1.** In contrast to **low-cost**, we define **ultra-low cost** to be less than the lowest price for a comparable technology, but not yet viable.

Apart from the advantages of OE being thin, light-weighted, flexible and presumably ultra-low cost in the near future [32, 36], the realization of this technology into printable smart labels is rather challenging, because the printing process itself is still an issue of current research [7]. Further on, the created conductive inks indicate low electro-mobility which result into slow-switched transistors, i.e., yielding 627 Hz at 10 V electricity supply [74]. In addition, the printing of circuits on substrates, such as paper and plastic foils, consumes large areas, so that yet complex integrated circuits, such as a microchip cannot be printed in the near and midterm future [32].

However, an all-printed 1-bit RFID tag based on carbon nano-tubes and gravure printing process has been reported from the Sunchon University [75] in 2010. More recently, the research group presented an improved version of 16-bit RFID tag at the IDTechEx RFID Europe event [76]. The RFID circuit is printed entirely on a polyester film, where nano-silver is used to print the antenna, because of the better interconnectivity. The all-printed rectifier of the tag provides a 10 V Direct Current (DC) from the 13.56 MHz reader signal. The all-printed ring oscillator can generate a clock signal of 102.8 Hz, which enables the transmission of a 96-bit transponder IDentification number (ID) in a second. In collaboration with the company Paru their goal is to achieve the printing of 96-bit RFID tags that conform to the ISO 14443 (International Organization for Standardization).

The first roll-to-roll printed 13.56 MHz RFID products [77] have already been presented by the company PolyIC [78] in 2007 (cf. reference [79]): a printed RFID tag with 4-bit memory, named PolyID<sup>®</sup>, and a smart object with a display function, named PolyLogo<sup>®</sup>. In their research in 2007, PolyIC introduced the first inductively coupled 64-bit printed RFID tag [80], fabricated in a lab with clean-room conditions. Apart from RFID antenna and the electrodes on it printed with a metallic ink, they used only plastic materials to manufacture the RFID tag [80]. However, since this time, PolyIC is working on their mass printing technology and OE to enable roll-to-roll manufacturing for high-volume and high-speed production [35, 79, 81].

In 2013, the company ThinFilm Electronics and its partner companies PARC developing addressable memory, and Polyera developing printed displays, presented a smart sensor label, which can be printed at high volumes on roll-to-roll printing process [82–84]. Their smart label system consists of a writable memory, sensing capability and a printed

TABLE 2.1: The acronym **NA** means 'Not Available'.

Printed device	Printing process	Substrate	Ink	TFT count	Reference
1-bit RFID tag	Gravure, inkjet	Polyester	Carbon, silver	5	[75]
64-bit RFID	Roll-to-roll	Plastic	Organic	> 200	[79, 80]
128-bit RFID	Inkjet	Metal	Silicon	1000	[85]
128-bit RFID	Inkjet	Plastic	Organic	1286	[86]
Hybrid RFID	Inkjet	Plastic	Organic/oxide	365/ 368	[87]
8-bit RFID	Inkjet	Plastic	Organic	300	[88]
16-bit RFID	Laser	Glass	Indium, gallium	222	[89]
Sensor label	Roll-to-roll	Plastic	Silicon	NA	[82, 84, 90]
Chipless RFID	Inkjet	Paper	Metal	0	[91, 92]

display which indicates visually the information when, for instance, the temperature of the product has exceeded the maximum threshold. This system is based on line-of-sight reading, and thus less applicable for mass-reading scenarios, such as monitoring of pallets in a cool chain, where items are highly dense stacked and invisible for inspection. However, it offers an additional support in supply chains, such as picking out of the damaged and expired products in a super market. In this way, options for improving supply chain management are extended.

Another fully functional printed RFID tag based on silicon ink has been introduced by the company Kivio [85, 93] in 2008. In comparison to others its distinctive feature is the use of a non-organic ink to print the RFID circuit, i.e., in the printing process, amorphous and polycrystalline silicon is used [94], that is in terms of charge carrier mobility superior to polymer electronics. The internal circuit logic of the tag consists of about 1000 printed transistors, and has the capability to radio its stored data from a 128-bit printed Read-Only-Memory (ROM) to an interrogator. The transmission is based on High Frequency (HF) (13.56 MHz) and synchronous tag-talks-first protocol. The entire RFID circuit is printed by inkjet on a thin metal foil substrate. The application area focuses on Near Field Communication (NFC), such as the NFC Barcode [85]. An implementation of long range communication is not available. The printing process uses inorganic silicon-based technology that can reduce the cost advantage the polymer electronics is offering.

The research group Holst Centre and their partners in the EU FP7 project ORICLA created a fully functional RFID tag based on polymer electronics and complementary hybrid organic-oxide thin-film technology [87, 95]. The RFID prototype is made on plastic foil with organic and oxide thin-film semiconductors, and features the world's first printed RFID tag that realizes reader-talks-first principle [95], i.e., it implements bidirectional communication between reader and tags. In contrast, the above presented

TABLE 2.2: Some performance characteristics of common printing technologies obtained from Mandal et al. [7] and Baeg et al. [8].

Printing technique	Feature size ( $\mu m$ )	Throughput ( $m^2 s^{-1}$ )
Inkjet	20-50	0.01-0.5
Offset	10-50	3-30
Gravure	75	3-60
Flexography	80	3-30
Screen	20-100	2-3

approaches toward printed RFID tags are based on tag-talks-first principle<sup>1</sup>. The problem here occurs when many tags try to contact the reader at the same time<sup>2</sup>. With respect to the enabling of a bidirectional communication in combination with reader-talks-first principle and the use of complementary hybrid organic-oxide semiconductor technology [87], it allows in comparison to the tag-talks-first principle to implement an effective anti-collision mechanism (i.e., the reader device can communicate its clock and identification data to the RFID tags, and the RFID tags in turn can decide on their own when to send data back). However, the use of inorganic semiconductors and inkjet printed devices can leverage the idea of mass printing in high volumes and the fabrication of cost-effective printed RFID tags.

In further research of the Holst Centre group an 8-bit RFID transponder chip is manufactured [88], where they deployed in the printing process improved Organic Semiconductor (OSC) and Thin-Film Technology (OTFT). Thereby, the electro-mobility of the OTFTs is enhanced up to  $0.5 \text{ cm}^2 \text{ V}^{-1} \text{ s}^{-1}$ . The RFID circuit is inkjet printed integrating about 300 OTFT transistors. It realizes basic circuit building blocks such as inverters, logic NANDs and 19-stage ring-oscillators printed on a surface area of  $34 \text{ mm}^2$  [88].

Since the ink's electro-mobility is a key parameter for creating complex digital circuits, others apply different conductive ink compounds and printing techniques, such as amorphous Indium-Gallium-Zinc-Oxide (a-IGZO) in application with a laser annealing process described in work [89]. In this work a 16-bit RFID tag is shown, which consists of 222 a-IGZO transistors printed on glass and a chip area of  $5.85 \text{ mm}^2$ . The field effect mobility of the a-IGZO TFTs is specified by  $> 10 \text{ cm}^2 \text{ V}^{-1} \text{ s}^{-1}$ . Despite of the impressive circuit speed in comparison to the related research, the mass printing capability of this

---

<sup>1</sup>As soon as the RFID tag gets powered from the RF field of the RFID reader, it transmits its data to the reader.

<sup>2</sup>In fact, current generation of p-type only printed thin-film RFID tags are enabled with a rudimentary ALOHA protocol, but the implementation of the anti-collision scheme is limited to about maximum 4 tags, and come at the cost of a slow reading [86, 95, 96]. The anti-collision scheme here is constructed in a manner, where tags send their data to an arbitrarily chosen time point.

technology is an open issue [89], and the use of rare metals [97] such as indium and gallium to create high-performance conductive inks, can aggravate the economic viability issue further.

Driven by lowering the costs for fabricating RFID tags, further techniques are promoted to realize item level tagging, such as printable and chipless RFID technology [91, 92, 98, 99]. In contrast to printed RFID tags including an Integrated Circuit (IC) chip, printed chipless RFID tags are characterized mainly by encoding the product ID by using Time Domain Reflectometry-based (TDR) and Frequency Domain Signature-based (FDS) techniques (cf. references [91, 99]). While TDR-RFID tags are based on microwave circulators and capacitors to generate RF wave transmission-lines in order to transmit the binary ID code, the FDS-RFID tags consist of resonators with different resonant frequencies which encode, i.e., the binary data. The coding capacity of TDR-based tags is currently limited by up to 8 bits [91], whereby FDS-based tags can contain theoretically unlimited capacity depending on frequency band and tag size [100]. For example, Islam and Karmakar describe in their work [100] a 16-bit chipless RFID tag printed on a  $1.65 \times 1.65 \text{ cm}^2$  substrate area, which operates in the 6 – 13 GHz frequency band. The first type of fully printed chipless RFID tags suffer from limited encoding capacity, whereas the second type requires large-scale size and wide frequency bands, which can be scarcely deployed for applications operating in the Industrial, Scientific and Medical (ISM) radio bands. An overview about recent advances in printable chipless RFID technology is given by references [91, 98] and reference [99].

To reflect the related research the aim of almost all described approaches is focusing on implementing common RFID standards such as the EPCglobal Tag Data Standard (TDS) [17] and Near Field Communication (ISO 14443) [30] into printable and low cost RFID tags on foil (cf. reference [35] and references above), which in essence pursue to enable same capabilities as the conventional Si-based RFID technology is already offering. For instance, bi-directional communication between reader and tags, anti-collision protocol for avoiding interference, and large data storage capacity on tag. The implementation of these features into a polymer tag, that can be even printed on roll-to-roll process in high volumes, is currently rather challenging [7, 35]. The lack of printing integrated circuits with large numbers of transistors into small area and, the lack of mass production accuracy and reliability, is suspending the realization of fully functional organic and all-printed RFID tags into the far-distant future. An exception of the PE approaches presented above represents the development of all-printable and chipless RFID tags. However, a chipless RFID tag is limited in terms of versatility and functionality, which has no own 'intelligence' (cf. discussion above, and references therein). But, the vision of IoT in combination with IEs demands from its participants

besides the storage capacity functionality further capabilities, such as sensing, displaying, computation and communication [14].

**Definition 2.2.** We declare an electronic device such as one RFID tag is indicating a circuitry of **low hardware complexity**, if its functionality is being implemented by approximately the lowest possible number of transistors. We define an electronic device to indicate an **ultra-low hardware complexity**, if its functionality or a comparable of it can be realized by even less circuit complexity.

As we can infer from related research towards all-printable and economically viable RFID technology the development of OE is focusing twofold:

- (i) design of low cost IoT by exploiting a presumably cost-effective OE and OE properties, such as the mechanical flexibility, lightweight and large area integration on thin substrates, and the
- (ii) integration of standard RFID communications into digital circuitry. Further, in the case of developing chipless RFID tags the focus is set at least to the enabling of functionalities, such as the reading of EPC code and featuring of large data carrier storage.

However, while OE is offering novel properties in IoT design and presumably ultra-low cost, the implementation of conventional connection-based communications into integrated printed RFID tags is rather ambitious. For example, the implementation of the EPC Class-1 Generation-2 protocol (EPC C-1 Gen-2) into an Integrated Circuit (IC) requires about 40k-50k transistors [101, chapter 5.5]. An implementation of a lightweight 64-bit ASIC for a minimalistic EPC C-1 Gen-2 RFID tag integrating a basic anti-collision protocol in combination with a simple cryptography functionality requires about 4k logic gates [102], which corresponds in transistor count to indicate about 16k transistors<sup>3</sup>. In Table 2.3 we compiled some references that implement standard RFID communications such as the NFC and EPC C-1 Gen-2 protocols into Si-based circuitry. Hence, the silicon hardware implementations range from deployed conventional microchips to ASICs with 8 – 256 bit architectures. To the best of our knowledge, the most minimalistic hardware implementation of the EPC C-1 Gen-2 protocol into silicon circuitry is provided by reference [102]. Similar works tackling the same issue are provided, e.g., by the references [104, 105]. However, according to Dobkin [101, chapter 5] the price for one RFID tag is determined apart from assembling the tag, also from the chip size, whereby the digital part of the chip can be minimized the analog part of the mixed-signal circuit design is mostly fixed. This, however, leads, that the

---

<sup>3</sup>The measuring unit 1 Gate Equivalent (GE) equals to 4 deployed transistors [103].

TABLE 2.3: Deployed silicon microchips and ASICs for current RFID standards.

RFID standard	Circuitry	Reference	Price
ISO 14443 (NFC)	Microprocessors > 50k Transistors	[30]	Around 1 and more Euros
EPC C-1 Gen-2	Microprocessors 35k-70k	[22, 101, 106]	Between 0.03 and 0.10 Euro
	64-bit ASICs $\approx$ 4k Gates	[102]	

total number of yield chips, that can be gained out of one silicon wafer manufactured in a chip foundry, cannot be increased further. As a result, the price for a single tag is languishing, such that the current price per tag cannot be undercut (cf. Table 2.3). As a consequence of it, the deployment of silicon chips for item-level tagging and IoT is not economically viable.

In contrast, OE technology is progressing to become ultra-low cost, but continue to be failing on meeting the hardware requirements needed to implement standards of traditional wireless communications (cf. our survey above and discussion in appendix A). In Table 2.1, we compiled references of PE research, which in particular develop all-printable RFID tags with various kinds of printing technologies, conductive inks, substrates and approaches showing the state-of-the-art. In addition, in Table 2.2 we enlisted some commonly applied printing techniques with their performance parameters in terms of print resolution and speed, providing with it the distinction between lab-scale manufacturing and mass-printing techniques. In comparison, inkjet and screen printing methods achieve manufacturing of OE circuit devices with much more higher hardware complexity than gravure, offset and flexography printing, but they lack mostly on production speed, that is owing additionally to the deployment of clean-room manufacturing techniques, such as photolithography (cf. references [7, 8]). In our opinion, however, the success of realizing the IoT vision will be essentially dependent on enabling the capability of mass-printing, which currently supports the printing of digital circuits with few hundreds of transistors (cf. Table 2.1). However, even if a mass-printing technology achieves the same state-of-the-art reliability, high print density and accuracy of manufacturing OE with clean-room techniques, which indicate hardware complexities of few thousands of transistors (cf. appendix A), the gap between OE and conventional Si-based RFID technology is still huge (cf. comparison between Table 2.1 and Table 2.3).

In our discourse for realizing the vision of IoT and IEs, thus far, we focused on analyzing the deployment of IoT enabling hardware technologies, such as the Organic and printed Electronics (OE) in comparison with the conventional Si-based technology. In essence, the success of it depends on the enabling of an ultra-low cost hardware technology. In

the following, we focus on analyzing the software side, for instance, the deployment of common wireless communications, which in essence determines the required hardware complexity for an IoT-enabled electronic device.

## 2.3 Wireless Communications for Printed Electronics

In the previous section we surveyed in essence the Organic and printed Electronics (OE) with respect to all-printable and fully functional RFID tags and smart labels. We acquired that OE is a promising technology to promote the Internet of Things (IoT), but the lack of hardware performance fails to implement conventional RFID communications with OE efficiently. Further on, with regard to wireless communications for OE smart label technology, the implementation of traditional multiple access channel strategies, such as Time Division Multiple Access (TDMA), Frequency Division Multiple Access (FDMA) or Code Division Multiple Access (CDMA), is currently rather a challenging task, because polymer electronics indicate low hardware performance, large surface occupation and high power consumption (cf. appendix A), that insufficiently fulfills to transfer the well-established methods [65] into OE circuitry. In the case of TDMA [107] timing is crucial, that needs a high precision clock generator. For instance, in a TDMA-based communication for every participant a separate time slot is provided, so that no interference can occur. Due to synchronization and communication overhead the hardware complexity and requirements for radio devices are considerably increased. In the case of FDMA [108] the implementation requires wide ranged and stable frequency generators. The participants share for communication the frequency spectrum, so that communication is separated in different frequency bands. Building accurate and stable oscillators regarding signal generators is commonly a daunting task [109]. Polymer electronics is thus far from achieving yet these hard requirements (cf. previous section, and appendix A). Further, these drawbacks also applies to an implementation of CDMA-based communications with OE technology. However, since conventional CDMA [110] features similarity to our work allowing multiple participants to communicate simultaneously, but distinguishes totally in communication design, in the following we proceed to describe and review the conventional CDMA scheme in more detail.

## 2.4 Special Case: Code Division Multiple Access (CDMA)

As we brought up in the previous section, CDMA radio communication allows a simultaneous channel access, where several transmitters send information simultaneously over a single communication channel [110]. Before data transmission is conducted the

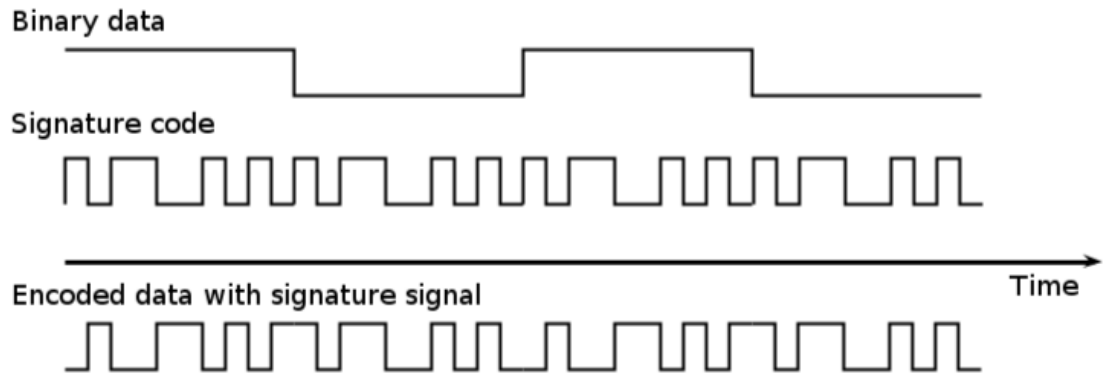


FIGURE 2.1: Showcasing the CDMA scheme: data signal is spread and XOR'ed with special code sequence.

multiple access channel method employs spread spectrum technology and special coding schemes [110]. Hence, before transmission the CDMA signal is generated by spreading the binary data uniformly with signature codes, whereby the codes were a priori created with pseudo-randomly drawn bit sequences (Gold codes), or by utilizing so-called orthogonal Walsh codes (cf. reference [110], and references therein). Upon the binary data stream the eXclusive OR (XOR) operation is applied bitwise in combination with a signature code. Figure 2.1 showcases the mechanism of a general CDMA encoding. In the CDMA system each transmitter uses an individual signature code to modulate its data for transmission. At the receiver side the separation of the signals is done by correlating the received signal with the commonly known signature codes assigned to the transmitters. The receiver can extract the data stream, if the received signal matches, i.e., is cross-correlated with the assigned signature code of the desired transmitter. In literature (cf. for further reading, such as references [56, 65, 110, 111]), CDMA systems are categorized in synchronous, i.e., employing orthogonal codes, and asynchronous communication, i.e., employing pseudo-random signature codes [110].

In synchronous CDMA each transmitter uses signature code for modulation, that is orthogonal to other signature codes, i.e., all signature vectors are mutually orthogonal. Employing cross-correlation between the orthogonal codes results mathematically to zero, which means the signature codes do not interfere with each other. An application example of synchronous CDMA presents the mobile phone communication using 64 bit Walsh codes to separate maximal 64 users communicating simultaneously (cf. reference [110], and references therein).

Since orthogonal codes are not applicable in scenarios, where radio devices dynamically move, the asynchronous CDMA was developed [110]. It employs pseudo-random binary sequences to create signature codes [110]. In the case of synchronous CDMA the communication fails, because it requires precise coordination, which cannot be established in mobile scenarios. The reason for failing is, that the starting point of decoding

changes whenever, e.g., the mobile devices are moving to other locations. In the asynchronous CDMA approach the employment of the pseudo-random codes is used in the same manner as orthogonal codes are employed. As we mentioned above, an example of pseudo-random sequences represent Gold codes [112], which are statistically low correlated between each other. The overlapping of a large number of pseudo-random codes results mathematically in approximately to a Gaussian noise. When the signals of the radio devices are being received from base station with the same power level, the signal of interest can be extracted, because the other signals appear as noise, that interfere slightly with the signal of interest. In this way, a particular signal with specified pseudo-random code can be retrieved, while signals with different codes encoded, or even same signature code but another timing offset (called multi path interference), appear as noise [110]. Thus, asynchronous CDMA communication can only work, if the signal strength of the radio devices can be controlled, which is usually governed by base station [110].

Considering the utilization of the access channel method CDMA for OE, the employment of the described synchronous and asynchronous CDMA as communication schemes for OE smart labels is, however, in terms of required hardware performance and communication limitations rather challenging to be implemented in polymer electronics. For instance, synchronous CDMA is limited with regard to the number of simultaneously communicating radio devices, being fixed to the number of available orthogonal codes. To this end, a supplementary communication overhead need to be implemented additionally in the OE circuitry, which current polymer electronics is not supporting (cf. discussion in appendix A, and references therein). In the case of asynchronous CDMA the number of active transmitters is not confined, but limited in terms of achieving a desirable Bit Error Rate (BER), since Signal-to-Noise-Ratio (SNR) varies inversely to the number of communicating radio devices. Thus, the advantage of asynchronous over synchronous CDMA is the increased number of active transmitters holding the same mean BER. Furthermore, asynchronous CDMA communication allows transmission to any given time, that is not provided by synchronous CDMA. However, the implementation of asynchronous CDMA into polymer electronics is rather challenging, because the main issue represents the power control of each transmitter (meaning, the reader (base station) needs to receive signals of equal signal strength sent from the transmitters). This, however, increases the hardware complexity and performance requirements for OE smart labels, such that an implementation of it into polymer electronics becomes rather ambitious. Further on, due to the variability in the printing process the variances of the printed electronic components are high (cf. appendix A), such that an attainment of a high fidelity for precise printed circuits indicates an engineering key issue of current PE research [7, 8, 113].

In the light of our review about implementing conventional connection-based communications with Printed Electronics (PE) the realization of IoT remains an open issue, because current state-of-the-art of OE is insufficient to integrate traditional communication strategies into circuitry. However, since conventional connection-based communication schemes are designed to avoid interference and require higher hardware performance than OE is currently supporting, in the following we consider alternative mechanisms of communication, that can be categorized as non-avoiding interference and utilizing of superimposed radio transmission. These kind of communications stands in contrary to the Shannon's principle for conventional communication, that we introduced in the beginning of this chapter describing the background of current IoT and IEs. The motivation/incentive to allow interference, or apply superimposed radio transmission in wireless communications is manifold but mostly to increase the natural communication capacity, being thus the subject to ongoing debate. Therefore, in the following section we pursue to review various approaches applying purposely interference and superimposed radio transmission in their wireless communication design.

## 2.5 Classical Networking and Beyond for IoT

According to our previous conduct we make out that high-priced Things such as TVs, refrigerators, net-books and jewelery can be equipped with conventional Internet technology to become a part of the IoT without to make any noticeable impact on the final price. And, as a desirable outcome of this their value rises up in terms of quality and functionality. However, in the segment for low-priced Things such as yogurts, chocolate bars and fish-sticks (Things that form together by far the major stake of everyday objects) the deployment of Si-based RFID tags and smart sensing devices at item-level is economically not viable (as we worked it out above). Printed electronics offers a possibility to realize the vision of IoT, though, but this technology lacks mostly on achieving the hardware requirements to integrate standard wireless communications efficiently (cf. references [86, 114]). To this end, in the area of deploying wireless sensor networks to monitor any IoT application scenario the employment of conventional communications between IoT nodes is augmenting the issues of data traffic and power consumption: each sensing device requires either a battery or at least a constant source of power such as an electromagnetic RF field, in order to radio its data reliably and individually to a receiver node. The deployment of a battery is not sustainable and environmentally unfriendly [50, 68], despite the fact that improved hardware technology and optimized communications exists such that device lifetime can be prolonged by up to 10 years (cf. s-net<sup>®</sup> technology [115] for realizing energy-saving WSNs). In contrast, the deployment of an electromagnetic RF field to empower battery-free sensing devices

(cf. the WISP node [116], or another RFID-based sensing platform [117]) supports only a short range communication, which restricts the scope to few of possible IoT applications [118]. In addition, the use of wireless power harvesting limits inherently the number of operating IoT nodes that can be empowered simultaneously over the wireless channel (cf. a comprehensive survey about current RF energy harvesting networks given in work [119] discussing state-of-the-art of power harvesting techniques, associated communications and circuits). With respect to applying a communication mechanism further point of issue need to be stressed out: independent of developing versatile and different hard- and software technology appropriately customized for an economically viable IoT scenario the principle of point-to-point communication is almost practiced. In this context, battery-dependent and battery-free sensing platforms continue to be improved technically, but these efforts do not change the fact that conventional communications information-theoretically remains almost the same and hence suboptimal [57]. Furthermore, looking soberly from the view of economical and practical deployments of WSNs employing conventional wireless communications, that have been developed in the last decades, the number of real-world WSN applications is rather low in comparison to potential application scenarios the IoT is posing (cf. a survey and references therein about real deployments of WSNs given by Garcia et al. [120] and Lloret [121]).

### **2.5.1 Design Architectures and Management**

In essence, one can say that the utilization of conventional connection-based wireless communications is a key issue amenable mostly to economic constraints impeding the progress of realizing the IoT vision. However, with approaching the Internet of Things (IoT), the physical world is increasingly penetrated by devices with sensing, computing and communication capabilities [122] enabled by economic viability. The expected impact is enormous [13]. This is reflected, for instance, by the US National Intelligence Council's decision to include the IoT in the list of the six 'disruptive civil technologies' with potential impacts on the US national power [123]. According to an UN report, the IoT will introduce a new era of computing in which humans become the minority of traffic generators and receivers [124]. Objects such as paper documents, clothing, food-packages, furniture, consumer electronics but also animate objects (animals or humans) will be equipped with electronic tags to identify, sense and communicate between objects and environments [125]. Research is currently driven to provide solutions to manage and maintain this huge amount of data and its dissemination [126]. For instance, Ostermaier et al. introduce a real-time IoT search engine [127] and Guinard et al. present a REST-based architecture for the Internet of Things [128]. In the same way that the generated and received traffic will be originated only to a minority by human players, so will the

computational load. Devices in the IoT will be able to cooperate with their neighbors to reach common goals [129]. Unfortunately, the devices in the IoT are predicted to be highly restricted in their computational resources [130]. For economic reasons, the tags that provide the IoT intelligence will be of lowest cost and quality [17]. Possible realizations cover Organic and printed Electronics (OE) as described in the above sections. Due to their simple structure, these sensor types distinguish itself by highly limited computational capabilities and draw on parasitic power sources such as light, temperature or humidity or are powered by external reader systems [119]. This means that, while computational capabilities are restricted, these nodes draw on virtually unlimited energy sources. The IoT will be characterized by a paradigm shift in wireless communication and distributed computation. Unlike in all previous wireless systems, not energy or the amount of communication will be the primary restriction but computational resources. Such situation suggests a collaboration of nodes to reach a common computational goal while exploiting the abandoned restriction in energy. In an IoT it will become possible to trade computational load for communication load.

### **2.5.2 Computation versus Communication**

Traditionally, in classical networks of sensing devices, measurements are forwarded to dedicated sink nodes to achieve a classification, aggregation and interpretation of values. Processing is then conducted by individual nodes in a network [131–133]. Clearly, such a scheme will distribute computational load uneven among network nodes. In particular, in an IoT environment, the tags that constitute the network might be computationally not capable of processing a large number of input values. An approach to economize computation, is to distribute processing load in a way that several nodes collaboratively process data. A single function is then jointly computed by various nodes in a network. Such distribution of processing load has been reported, for instance, for the parallel algorithm to compute a Fast Fourier Transformation (FFT) as presented in work [134]. Further examples for algorithms that are executed in a truly distributed fashion among wireless nodes are MPEG encoding [135], the computation of confidence in mobile agents [136, 137] and also distributed source coding [138].

Recently, there has been a great deal of interest in network coding as another alternative to cooperative data processing in networks of wireless nodes [139–141]. Network coding optimizes routing for multicasting in a network in a way that intermediate nodes send a function of incoming messages, combining rather than sequentially forwarding them.

In all these cases, the data transmission and computation are clearly separated. Although processing load might then be fairly distributed among nodes in the network,

it is not possible to further reduce the computational load of individual nodes when the communication channel is utilized for transmission of data only. This design is fueled by a result of Shannon who showed that separate source and channel code design is asymptotically optimal in a point-to-point setting [64, Theorem 21]. However, although optimal in many cases, separation fails in certain scenarios. For instance, Cover et al. demonstrated that separation is suboptimal for transmitting correlated sources over a MAC [142]. They use source correlations to create channel input probability distributions unavailable to a separation-based scheme. Recently, further authors showed additional efficiency in function processing by effectively executing computation at the time of wireless data transmission on a RF channel (cf. the following section 2.6 reviewing the related work in more detail). These studies were initiated by the pioneering work of Giridhar et al. [143] and Nazer et al. [144] who motivated the computation of mathematical functions at the time of data transmission. Giridhar et al. study the maximum rate at which functions of sensor measurements can be computed and communicated to a sink node. For several function classes and network topologies, they derive bounds on the achievable rates. Also, they mention the possibility to consider communication models in which the collision of data from several nodes contains information. Their study, however, is restricted to the classical case in which collisions are considered as noise. Nazer et al. study the achievable rate for reliably sending arbitrary functions over arbitrary MACs. Their focus is thus shifted from transmitting bits to computing functions jointly by several transmitters.

Recently, Goldenbaum et al. published a set of further results on this transmission scheme [145]. The authors show how the arithmetic mean, the geometric mean, polynomials and other functions can be calculated at the time of transmission on the wireless channel. They utilize superimposition of electromagnetic signals to implement a sum of various input values and implement a pre- and post-processing at transmit and receive nodes, in order to compute more ambitious functions. They further show the computation via SIMO multiple access channels with a similar scheme [146]. Their solution requires accurate estimation of the channel state information at receive nodes, in order to mitigate channel fluctuation. Furthermore, transmit devices are required to achieve identical absolute transmit power. Both these prerequisites are hard to accomplish in real systems, in particular, for resource restricted IoT nodes. Additionally, environmental changes significantly impact channel conditions [147]. A channel-based calculation following the described scheme will severely suffer from such time-dependent fluctuations. In contrast to our work described in this dissertation, Goldenbaum et al. aim to use less wireless resources during computation [148]. Therefore, they still require that considerable computation is conducted at the transmit or receive nodes.

The Internet of Things, however, will feature nodes which are highly limited in their computational resources but potentially draw on virtually unlimited energy sources (e.g., parasitic or externally, reader powered). We will discuss a transmission scheme which achieves to execute addition, multiplication, subtraction and division in one step at the time of transmission on the wireless channel, as well as operations combining these basic functions. Combinations of these functions might require multiple transmissions. This transmission scheme trades computational load for communication load, exploring the relaxed power constraint of IoT nodes.

## 2.6 Beyond the IoT Standard: Function Calculation over Wireless Channels

In the previous section we reported about the classical way of wireless communication, computation and networking used to realize the vision of IoT in combination with OE and viable hardware technology. In addition, we introduced discussing novel approaches, which aim to outperform current bounds of communication complexity commonly determined for WSNs. In the following section we continue reporting and analyzing in more detail the novel approaches, which show solutions beyond the classical way of communication and computation design, representing the related work to this dissertation.

Considering the classical way of communicating and processing of spatially generated and distributed data a common procedure for evaluating, for example, sensor readings from a WSN is first to collect all measurements separately from the sensor nodes transmitted to a sink node (e.g., intermediate receiver node, relay or base station), and then to analyze and process the data centrally in a second step. Hence, the communication (i.e., the transmission of sensory data or function of it) and computation (i.e., evaluating the sensory data) are strictly separated from each other. Based on this processing architecture the resources of WSN, such as power efficiency, network lifetime, communication range, data throughput are optimized. Viewed historically, conventional optimization techniques and approaches can be summarized essentially by doing such as lowering wireless communication, applying data compression, improving WSN routing algorithms and minimizing sampling rates of sensing. Since, optimization is leaning on traditional separation-based communication, hence, consuming mostly the available power resources, thus, the underlying cause of issue can be assigned to be system dependent. Therefore, different forms of data gathering and processing are necessary to be developed, if performance of sensor networks is aimed to be outperformed (cf. survey [53]).

However, before becoming aware of the indicated system dependent issue regarding communication of data within a network and computation of relevant functions at a sink node, Giridhar et al. [63] provided first theoretical results towards describing the communication complexity of collocated and random planar multihop WSNs. In this work, Giridhar et al. [63] provides the meaningful insight of what really matters in operating of WSNs, namely that one is mostly not interested in the identity of a sensor node or the single measurement values of the nodes, but one is rather interested in collecting from a sink node (intermediate node or base station) the outcome of a relevant function of the sensor readings sensed in the WSN. In particular, Giridhar et al. [63] determined the maximal rates for various symmetric functions, such as the subclass of type-sensitive functions (e.g., calculating the mean, mode, median of the collected data of sensor measurements) and subclass of type-threshold functions (e.g., calculating the max, min, or range) to name but a few. Hence, Giridhar et al. provided, i.e., for a mathematical function of interest the maximum rate at which the function of sensor measurements can be computed and communicated to a sink node using the classical way of communication and processing. In our view the most remarkable findings in this work [63] are the acquirement of the limits the conventional communication and processing architecture is indicating, and the fact that for the most WSN tasks the identities and the single measurement values of the sensor nodes are not needed. These, however, inspired researchers (cf. the following subsections) to continue developing of innovative approaches, which can improve and even outperform classically driven WSNs. Since, the classical way of communication and computation is separated from each other, where communication is orthogonalized among the participating nodes in a network, featuring interference-free communication channels, and computation of *desired functions* is organized at central nodes processing the collected data, the novel approaches rather lean towards deploying of non-avoiding, and even embracing [149] the interference. For example, Nazer [57] is talking about exploiting of constructive interference using algebraic structures, Goldenbaum [54] considers interference as inference using analog coding, and Krohn [51, 52] is talking about superimposed radio transmission. However, in all these examples of utilizing the interference the common goal is to enable a concurrent communication and computation of desired functions, such that the limits can be overcome of the conventional connection-based communication and computation paradigm described by Giridhar et al. [63, 143].

Hence, the spawned idea of concurrent transmission and processing data represents a paradigm shift towards merging communication and computation together, in order to improve on the one hand performance parameters of sensor networks, but on the other hand also to establish novel sensor network applications [51, 54, 57]. In the case of wireless communication the underlying topology for a such concurrent processing is

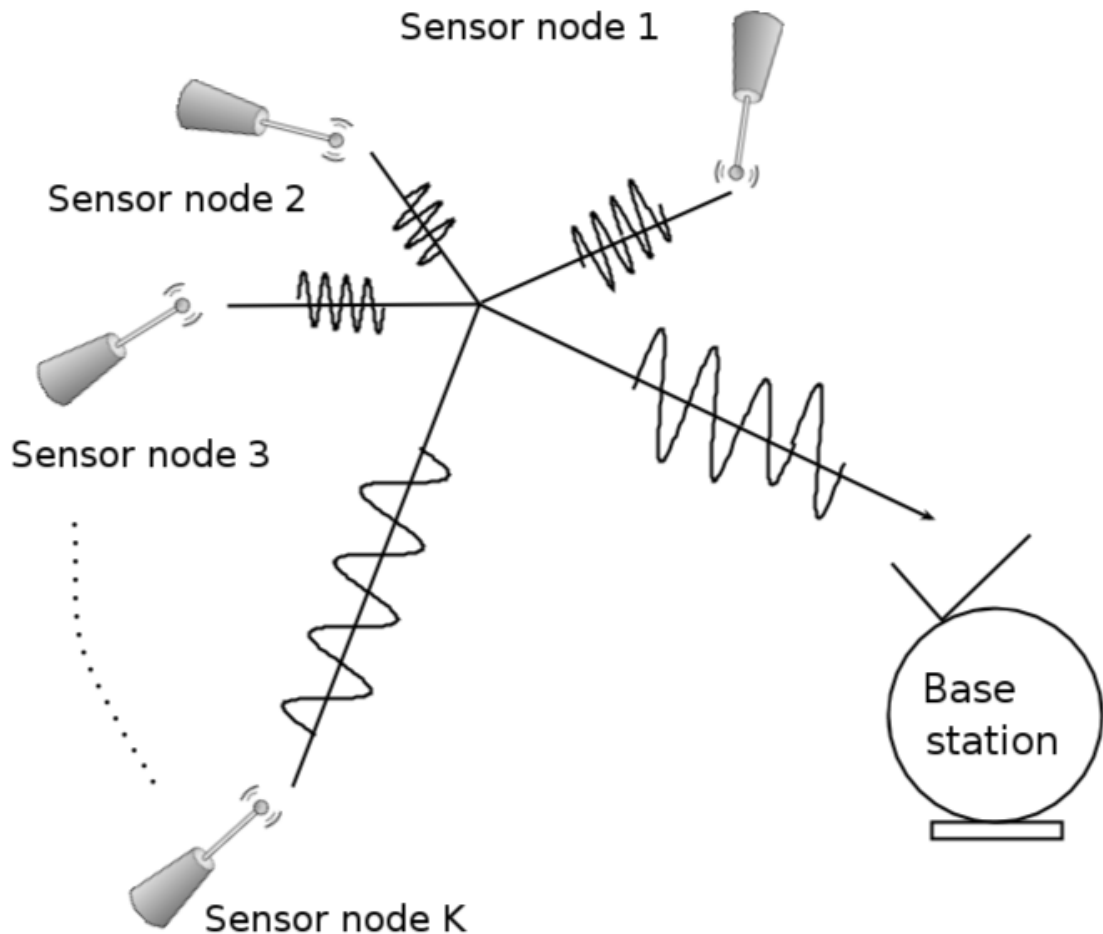


FIGURE 2.2: Illustration of a WSN employing superimposed radio transmission.

illustrated in Figure 2.2, where  $K$  sensor nodes are scattered in a star formation around a base station, i.e., transmitting simultaneously to the fusion center.

The idea of using the wireless channel as a natural analog function computation engine exploiting the superposition property of electromagnetic waves is not new [150, 151], but since then it lacks on practical implementations so far. However, with regard to further review of the related work, in the following we introduce for the sake of better understanding and reflection some formalism describing formally the idea of concurrent transmission and computation of data over the wireless channel, which will help to show what the various approaches have in common, but more importantly how they distinguish in terms of operation, performance and practicality.

In all of the modeled and designed approaches towards simultaneous communication and computation over the wireless channel we realize, that the linear superposition property of electromagnetic waves is used as a mathematical operator to enable a general wireless function computation. This, however, is handled differently in terms of what

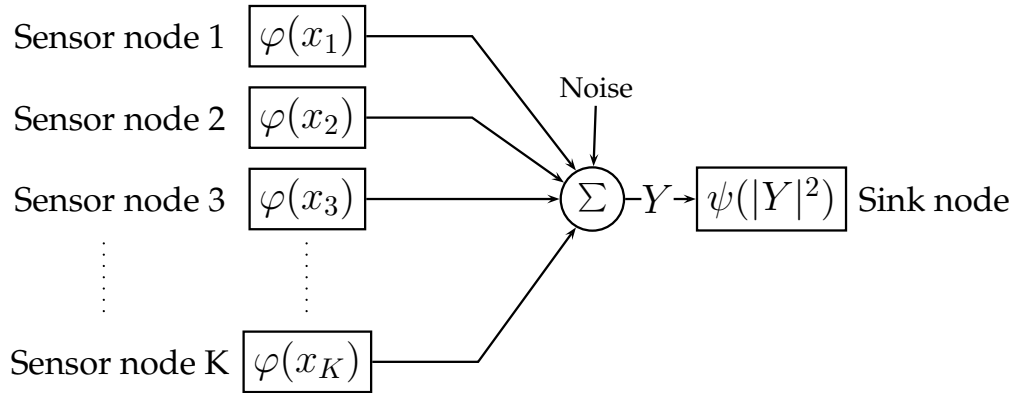


FIGURE 2.3: Function computation using the natural analog wireless channel.

can be theoretically and maximally achieved, and what can be implemented in practice representing with it the main object of research.

The research area comprises collocated WSNs observing, e.g., environments and habitats. For the sake of formality, let a WSN be arranged in the manner as shown in Figure 2.2 consisting by  $K \in \mathbb{N}$  sensor nodes scattered around a sink node. The sensing range of each sensor node is confined by  $\mathcal{X} = [x_{min}, x_{max}] \subset \mathbb{R}$  with  $x \in \mathcal{X}$ ,  $x > 0$  and  $x$  is being the sensing value. Let  $t$  be a discrete time stamp of a measurement, and  $k = 1, 2, \dots, K$  to be the index of the  $k$ -th sensor node. Thus, the vector  $X(t) = (x_1, x_2, \dots, x_K)^T$  represents a snapshot of all measurements captured in a WSN at the time  $t$ . Further, the sensor nodes are created identically and independently distributed from each other observing a physical phenomenon<sup>4</sup>, such as temperature, humidity, light exposure or motion. Hence, the computation function for interpreting sensor readings in  $X(t)$  has the form  $f : \mathcal{X}^K \rightarrow \mathbb{R}$ . Functions of interest are, for example, the calculation of averaged temperature in a WSN at time  $t$ , i.e.,  $f(X(t)) = \frac{1}{K} \sum_{k=1}^K x_k$ . Another example is to detect extrema in a WSN, such as the activation of an alarm if the maximum temperature value exceeds a certain critical threshold. A such maximal sensor value can be extracted by applying  $f(X(t)) = \max\{x_1, x_2, \dots, x_K\} = \lim_{q \rightarrow \infty} \|x\|_q$ , where  $\|x\|_q = \left( \sum_{k=1}^K x_k^q \right)^{\frac{1}{q}}$ .

In order to apply any desired function over the measurements in  $X(t)$  the sensor nodes  $\{1, 2, \dots, K\}$  need to carry out an appropriate preprocessing function  $\varphi(\cdot)$  before transmission. And, at the sink node an appropriate post-processing function  $\psi(\cdot)$  must be chosen in the way, so that the mathematical characteristic of the desired function fits to the superposition property of the physical wireless channel. The mathematical model for calculating a function of interest over the physical wireless channel can be formulated

<sup>4</sup>Depending on the type of sensor the phenomenon being observed can also be biological, chemical or any other form of entity.

as follows

$$f(X(t)) = \psi \left( \left| \sum_{k=1}^K \varphi(x_k) + Noise \right|^2 \right) =: \psi(|Y|^2) \quad (2.1)$$

The variable  $Y$  represents the received signal, which is corrupted with background noise. It poses the superposition of all complex-valued transmitter signals sent simultaneously. Figure 2.3 presents the general form of a function computation in a WSN. In the case of performing merely *addition*  $' + '$  on the RF channel, e.g., to add up all measurements in  $X(t)$ , the preprocessing function for each sensor node is set to  $\varphi(x_k) = x_k$  and, at the sink node the post-processing function is set to  $\psi(|Y|^2) = \frac{1}{c}|Y|^2 - b$ , with  $b, c \in \mathbb{R}$  being constants. To perform multiplication  $' \cdot '$  on the wireless channel the logarithm laws need to be deployed. Here, the preprocessing function for each sensor node is set to  $\varphi(x_k) = \log_a(x_k)$ , where  $a$  denotes an arbitrary base. At the sink node the post-processing function is set to  $\psi(|Y|^2) = a^{\zeta(|Y|^2)}$  to regain the outcome of a multiplication task, whereby  $\zeta(\cdot)$  is being an adjustment, which composition relies on the chosen coding scheme strategy and the computable desired function. Since, the basic mathematical operations  $' + '$  and  $' \cdot '$  can be realized on the wireless channel a set  $\mathcal{F}_d$  of computable functions  $f$  can be built up. The definition of the set  $\mathcal{F}$  is as follows

$$\mathcal{F} = \left\{ f \in \mathcal{F}_d \left| f(X(t)) = \psi \left( \sum_k \varphi_k(x_k(t)) \right) \right. \right\} \quad (2.2)$$

With respect to (2.2) the set  $\mathcal{F}$  can contain all types of functions that can be adjust to the physical characteristic of the wireless channel, such as the arithmetic and geometric mean, weighted sum, calculation of max/min extrema, variance, median or communicating a histogram to name but a few. However, the realm of computable functions is not fixed [152].

Before starting with the discussion about different coding scheme approaches towards implementing a so called CoMAC (cf. Goldenbaum et al. [152]), let define the wireless channel model to be following a flat fading process  $H(\tau)$  afflicted with background and white Gaussian noise  $Noise(\tau)$ , and  $\tau$  is being a variable for denoting continues time. With respect to communication model the superposition of simultaneously transmitted signals  $W_k(\tau)$  sent from  $K$  sensor nodes the channel model is formed as follows

$$(W_1(\tau), W_2(\tau), \dots, W_K(\tau)) \mapsto Y(\tau) := \sum_{k=1}^K H_k(\tau)W_k(\tau) + Noise(\tau) \quad (2.3)$$

Further, we denote  $P \in \mathbb{R}^+$  to be the signal strength, and  $P_{max} \in \mathbb{R}^+$  the peak power constraint of each transmitter node.

Summarizing the modeling of our wireless computation and concurrent transmission engine with multiple senders and one sink node receiving the computation result of a desired function, the enabling of the mathematical operations such as *addition* and *multiplication* with preprocessing and post-processing is sufficiently enough to compute linear and nonlinear functions over the wireless channel (cf. proof by Goldenbaum [54]). In the following we continue reporting on the background, which led to the spawned idea of utilizing the natural structure of wireless channel for concurrent data communication and processing. In addition, we also provide an analysis and classification of the various related work.

### 2.6.1 Linear Network Coding on the Physical Layer

A prequel to the novel paradigm of merging communication and computation over the wireless channel landmarks the work for wired computer networks from Ahlswede [139], who coined the term of *network coding*. In this work [139] Ahlswede et al. are presenting the idea of mixing incoming data packets together on intermediate relay nodes before forwarding them within the network to their destinations. For example, city A and B are connected through a single link over hub-1 and hub-2. Using the classical way of communication, the messages from source nodes in city A or B are first packaged and then consecutively conveyed over the hubs to their destination nodes. However, when many nodes in city A and B try to communicate over the single communication line at the same time, a congestion can occur. With the novel idea of in-network coding [139] the data packets sent out from different source nodes are first mixed together to one single packet at the hubs, such that only the linear combination of the mixed data packets is conveyed over the single link. Once the linear combination is received from hub, then it is used for regaining the original data packets. After the reconstruction process the decoded packages are delivered as usual to their destination nodes.

This principle of communication strategy is also applied for wireless networks [153]. Further, the communication paradigm of network coding designed for wired and wireless networks is primarily laid out to improve overall communication capacity, that is information-theoretically proved [139, 140, 154] showing the multicast capacity. For the interested reader to delve further into an in-depth discussion, a reality-check for wired and wireless network coding is for example provided by Wang et al. [155] and Katti [156], indicating that network coding enables some performance gains despite of some practical issues such as performance loss through scheduling, sensitivity caused by erroneous communication channels, required computational power at the relay nodes to be able to compete with the classical way of communication, and security risks.

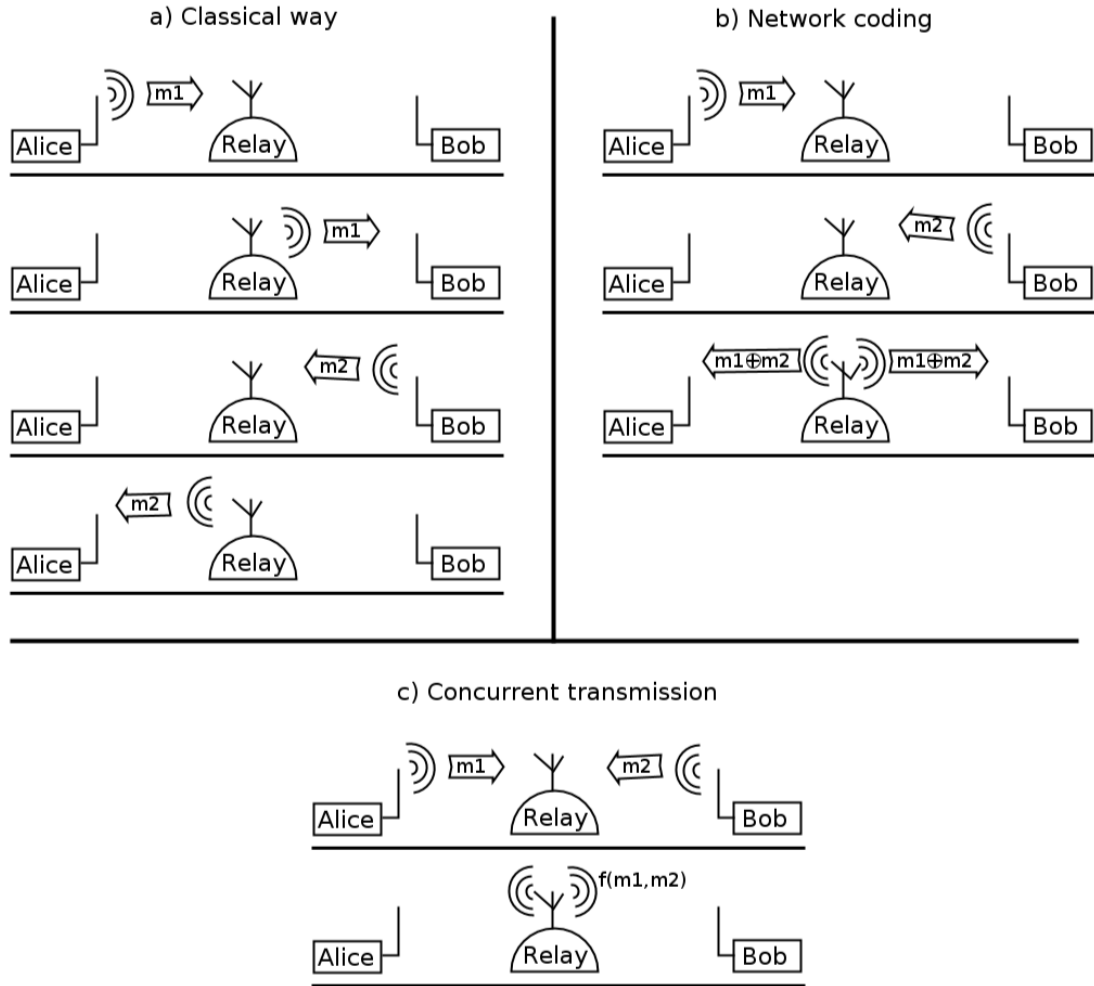


FIGURE 2.4: The subfigures (a), (b) and (c) show three different routing strategies for the two-way relay channel illustrating the evolution of different communication paradigms. The classical way of communication shown in subfigure (a) requires 4 time slots. The use of network coding at relay shown in subfigure (b) reduces communication complexity to 3 time slots. And, letting Alice and Bob transmit their messages simultaneously as shown in subfigure (c), where the relay sends a function of it back to the senders, the communication complexity is even reduced to 2 time slots.

However, the concept of computing functions over the wireless channel, that we introduced earlier, represents a novelty in contrast to network coding and the traditional way of communication, which stands in particular in relation to distributed computation and communication design architectures. For better understanding, differentiating and classification of the various related work, in Figure 2.4 we illustrate the basic ideas of different communicating and computing of messages by means of employing the two-way relay channel model [157].

For instance, in Figure 2.4 (a) we illustrate the classical way of communication, where Alice and Bob require overall 4 time slots to exchange their messages  $m_1$  and  $m_2$ , when communication between them is only possible over the relay station.

In Figure 2.4 (b) we illustrate by means of an implementation of wireless network coding implementing the two-way channel routing [158]<sup>5</sup>. First, Alice sends her message  $m_1$  to relay station, and then Bob sends his message  $m_2$  to the relay station, where the messages  $m_1$  and  $m_2$  are XOR'ed to  $m_1 \oplus m_2$ . Then, the outcome of  $m_1 \oplus m_2$  is transmitted to Alice and Bob in a single hop, where they are finally able to recover the corresponding sent message by XOR'ing it with their own original message. In contrast to the classical way of communication, the network coding strategy requires here only 3 time slots.

In Figure 2.4 (c) we illustrate the strategy of concurrent transmission reducing the overall communication complexity for the two-way relay channel down to 2 time slots: Alice and Bob transmit their messages  $m_1$  and  $m_2$  simultaneously, where afterwards the relay station sends back a function, or just an amplified version of it.

While original network coding [159] and the classical way of communication [55] are sharing the common ground of strictly separating the way of communicating and evaluating data (as illustrated in Figure 2.4 (a) and (b)), in the contrary the state-of-the-art strategies for wireless networks embrace concurrent transmission (as illustrated in Figure 2.4 (c)), and even include at the same time computation of data during the joint wireless transmission [51, 53, 54] exploiting the natural structure of the wireless medium (as illustrated in Figure 2.3).

Considering the related work of network coding [53, 153] the leading motive of developing is to exclusively maximize communication capacity in networks. The aspect of utilizing the wireless MAC for computing linear functions in combination with network coding, as we implied it in Figure 2.4 (c), remains still almost the same motivation of further optimizing the network communication, but the perception of the insight that one can do more over the wireless channel than efficient communication has risen up, when became clear, that theoretically the computation of linear functions such as the modulo-2 adder and real sum is possible to be carried out over the wireless channel [57]. In particular, the area of Wireless Sensor Networks (WSN) becomes a prominent candidate, where the idea of merging computation and communication over the wireless channel can be beneficially exploited [51, 52, 54]. However, the enabling of computation of linear functions over the wireless channel using the concept of network coding on the physical layer is rather more of theoretical construction yet than of practical reality, that can be easily be implemented with real hardware for the real world [51, 54, 149]. On the other hand, the use of a such auxiliary construction integrating wireless network coding with the idea of computing linear functions over the wireless channel, enabled to study the upper bounds

---

<sup>5</sup>The title of the article [158] can be misleading, because the operation XOR is carried out at the relay node, and not over the wireless channel. The senders transmit their data packets sequentially, the routers mix them together before broadcasting the mixed version [158].

of theoretically achievable communication capacity for different wireless network coding strategies [53, 57]. In this information-theoretical analysis provided by Nezer et al. [53, 57], the wireless MAC is either considered to be ideal, i.e., the wireless computation model does not entail noise, or, if Gaussian noise is put into consideration, then it is assumed that simultaneously sent signals are perfectly synchronized at symbol and phase level [57]. However, under the assumption that desired concurrent wireless transmission can be successfully carried out, in this case a substantial speed-up is expected [57].

In order to elucidate the issue of accurate synchronization, for example, in the survey [160] an instructive implementation of the two-way relay channel is given applying the physical layer network coding in combination with Binary Phase Shift Keying (BPSK). The message bits from the two senders are transmitted directly on the wireless channel. The channel gains of the senders are set to be equal and, additive Gaussian noise is expected to be received. After the concurrent transmission the relay acquires a noisy sum of the bits, from which it estimates the modulo-2 sum. Hence, for instance, is supposed that the phase coded bit strings exactly superimpose on the RF channel at the same time, such that the message bits overall fit on top of each other, that is, however, hard to establish in a real system implementation [51, 149].

In the remaining steps of the procedure [53] the Gaussian noise from channel output is removed at the relay, so that the signal values found at the bit positions are mapped to the outcome, creating with it the modulo-2 sum [53]. To achieve a reliable physical layer network coding Nazer et al. suggest to append corresponding end-to-end error correcting codes to the obtained modulo-2 sum, which overall is not going to diminish the gained speed-up [53]. This strategy is conceived for more than two users described for the first time in literature [161–163] in 2006. Since then progression is made by deploying for instance algebraic structures such as nested lattice codes [57] to enable a reliable and more robust concurrent transmission [53] without actually to deal with the real environmental constraints defining the true function of the wireless medium or, to approach the synchronization issue.

In the further elucidation of the works [53, 57], Nazer et al. provide for comparison reasons the performances of the related network coding strategies indicating that nested lattice codes performs best among the other schemes such as the analog and standard wireless network coding (cf. survey [53] for an in-depth analysis, and references therein). In our view the related works of the survey [53] can be categorized to be almost of the kind of being theoretical frameworks implementing the two-way channel model in the manner as we illustrated it in Figure 2.4 (c). The work of Katti et al. [149], however, stands out among the various reported approaches, because it demonstrates its approach

of Analog Network Coding (ANC) in practice, i.e., solving the two-way channel routing in a real system implementation using software-defined radios<sup>6</sup>.

The idea of utilizing Analog Network Coding (ANC) is based on allowing phase coded analog signals to superimpose on the wireless channel [149]. In particular, Minimum Shift Keying modulation (MSK) and a reconstruction framework is employed, enabling with it the concurrent transmission of two senders. According to Katti et al. [149] it solves the two-way relay channel efficiently. After Alice and Bob transmit their MSK encoded signals simultaneously, the relay node amplifies the superimposed signal, and sends it back to Alice and Bob, where it is decoded. Since the message bits are encoded through phase differences, Alice and Bob use their own message to seek in the interfered signal for the respective other message, which is done by reconstructing the phase differences, i.e., solving consecutively equation systems with two unknowns [149]. Synchronization of the concurrent transmission is not required, since a rough overlap of the two simultaneously sent signals is sufficient. In the contrary, the asynchrony is even exploited for the decoding process [149]. In a real deployment using software-defined radios Katti et al. [149] demonstrated the practicality of their ANC approach, indicating that in comparison with the classical way of communication the network capacity is increased by 70 % and, that in comparison with the standard wireless network coding it is improved by 30 %. However, the ANC approach works only for two simultaneously sending senders, that implies time consuming scheduling when more than two senders want to communicate at the same time, diminishing possibly the cost advantage in contrast to standard wireless network coding.

In this subsection we described all kinds of physical layer network coding, covering approaches, that use digital, as well analog network coding strategies. We also described the spawned idea of utilizing the computation of linear functions over the wireless channel to improve network capacity. However, the idea that one can utilize the wireless MAC not only for increasing data throughput within networks, but also for computing mathematical functions in general, in the following we continue to elucidate this new type of approach in more detail, i.e., how it extends the realm of computable linear functions to nonlinear functions, and deals with the synchronization issue.

### 2.6.2 Analog Computing over Wireless Channels

In contrast to our previous elucidation about wireless network coding on the physical layer, arranged to outperform traditional wireless communication and standard network coding by applying, e.g., concurrent transmission, computation codes, analog signals

---

<sup>6</sup>A Software-Defined Radio (SDR) is a radio communication system implemented by means of software on a computer or embedded hardware (cf. Wikipedia entry [164] for more information).

and algebraic structures, in the following we describe a novel approach of analog computing over the wireless channel, targeting to perform WSN task directly on the wireless MAC. Unlike physical layer network coding using algebraic structures, such as the finite field  $\mathbb{F}_q$ , computation coding and lattice codes [57], to enable a function computation over the wireless channel, such as the modulo- $q$  sum and real sum, the novel type of approach [54] provided by Goldenbaum et al. applies directly the analog signal strength to encode, e.g., sensor readings from WSN, such that analog computing can be carried out over the wireless channel. This idea of using the signal strength  $P_k$  to encode sensor values is implemented by mapping the sensing range  $\mathcal{X}$  to the transmission power range of the sensor nodes. Due to the linear superposition principle of electromagnetic waves the addition of amplitudes between simultaneously sent signals is expected. For example, in works [145, 146, 165] Goldenbaum et al. are proposing a such simple analog computation scheme using predetermined power levels  $P_k$  to transmit and compute desired functions over the wireless channel. By means of an example, in Figure 2.5 we illustrate the method from Goldenbaum et al. in a simplified form, showcasing the addition of three signals with different power levels, which results into a superimposed computing indicating the sum. Hence, the maximum amplitude of the received signal carries the outcome of the analog computation. For the sake of simplicity, the signals in the showcase have been set noise-free. According to Goldenbaum et al. [54], in a real scenario for each mathematical function of interest intended to be computed over the wireless channel, an individual error-correcting analysis must be made, and a procedure must be derived for removing the inherent background noise from computation result [54, 152]. So far, for computing the arithmetic mean and geometric mean such error correcting functions exist [54]. In contrast to the physical layer network coding strategy the approach from Goldenbaum et al. requires merely a coarse block synchronization [54]. However, it entails the challenge to estimate properly appropriate power levels for all sent signals culminating at the receiver node. According to approach [54] every sensor node  $1, 2, \dots, K$  generates before transmission a random unit norm transmit sequence  $S_k(t) = (S_{k1}(t), S_{k2}(t), \dots, S_{kM}(t))^T \in \mathbb{C}^M$  with

$$S_{km}(t) = \frac{1}{\sqrt{M}} e^{i\phi_{km}(t)}, k = 1, \dots, K; m = 1, \dots, M$$

and  $\phi_{km}(t)$  is being uniformly and independent identically distributed (i.i.d.) between  $[0, 2\pi)$ . Further on, the sensor nodes require before transmission an instantaneous knowledge about their block fading channel gain  $H_k$ , in order to determine the corresponding transmission power  $P_k$ . In this issue, the fusion center initiates a pilot signal, such that the sensor nodes can estimate their own fading channel coefficient. Then, during transmission the sensor nodes invert their channel gain  $H_k$  and transmit their sequence  $S_k$  (cf. Goldenbaum [54]).

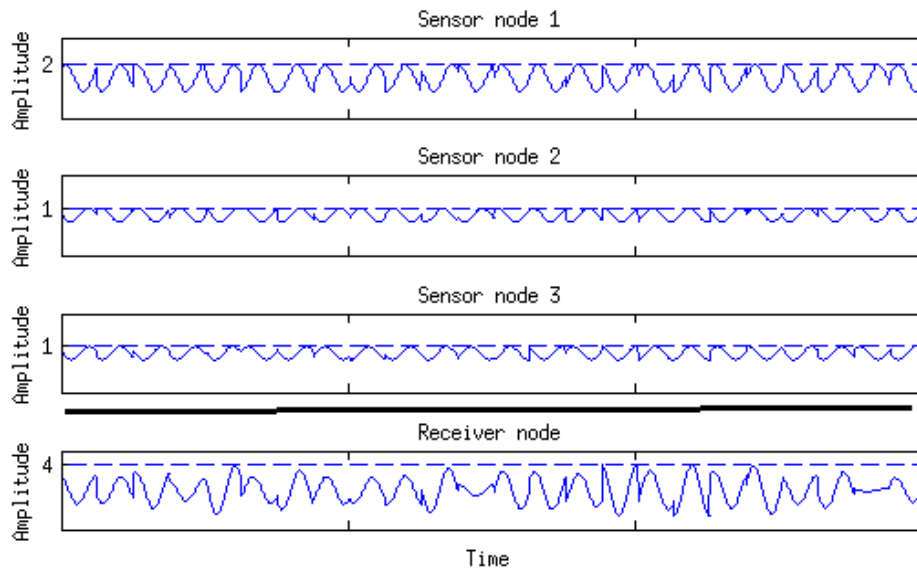


FIGURE 2.5: Showcasing the scheme for analog computation over the wireless channel.

In contrast to physical layer network coding, where constructed computation codes are used to enable concurrent transmission of signals to perform function computation over the MAC, the analog coding scheme from Goldenbaum et al. [54] is based on signal power, which exploits directly the additive superposition property of electromagnetic waves. While physical layer network coding relies on establishing synchronization in signal phase, the approach from Goldenbaum et al. is sensitive to signal power  $P$ , the flat fading channel and background noise. Here, Goldenbaum et al. is providing an analytical error-analysis for some special functions of interest, such as the computation of arithmetic and geometric mean, and customizes corresponding error-correcting rules. But, in our view the analog computation scheme [54] underestimates and neglects the dynamic aspect of radio propagation and the electromagnetic interaction with coincidentally occurring environmental events, such as the sudden start of a rain fall, a truck passes by, an environmental change through vegetation growth, or a simple door opening is changing the signal path of propagation [1, 120, 149, 166], to name but a few. And, when additionally a large-scaled WSN is called to carry out a computation over the wireless channel, dozens of sensor nodes spread in a wide area need to be coordinated and tuned exactly to the fusion center, such that all signal power levels first, represent the sensor readings correctly, and second, convolve to the desired channel output, when transmitted simultaneously. That is, however, in our view a daunting task to be achieved considering the aspiration to built a wireless function calculator, the so called Computational MAC (CoMAC) [54].

The idea of analog computing in WSN using signal power levels has already been tested

experimentally long before the published proposal by Goldenbaum et al., for instance, Krohn and Hermann are reporting in their works [52, 166, pp.73-75] about estimating the number of active sensor nodes in a WSN based on exploiting the superposition principle and the received signal power. In this experiment were up to 5 active sensor nodes (transceiver devices) deployed to transmit in a range of 3 meters a constant burst signal simultaneously. Based on the captured receiver signal the number of participating devices are estimated. The evaluation of the experiment with 2000 trails and different setups has shown, that in principle the number of active sensor nodes can be estimated, but the estimation accuracy drops drastically, as the number of active devices increases. Thus, in our view it is to be expected, that the implementation of Goldenbaum's computation scheme in a real WSN scenario will face severe difficulties, such that computation of functions over the wireless channel cannot be carried out properly, as it will be required.

Reviewing the work from Goldenbaum [54], in our view the merit of this work lies in utilizing the concept of analog computers<sup>7</sup>, which perform computation over the electrical voltage power or nomographically, and the extension of computable functions over the wireless channel, i.e., the computation of linear and nonlinear functions using preprocessing at the sensor nodes and post-processing at the sink node, as we described it above. In addition, Goldenbaum provided the proof, that the linear structure of the wireless channel can be exploited to implement the concept of a fully Computational MAC (CoMAC) [54].

Since the work [54] from Goldenbaum et al. is facing all the practical issues, that also analog computers exhibited before the emergence of digital computers, i.e., low computation accuracy, inflexibility and expensive in implementation, maintenance, as well programming [167]. And, in our view even worse, because the behavior of the wireless medium is changing all the time, that cannot be handled properly [51, 52, 149], in contrast to this approach in the following subsection we present the work from Krohn [52] approaching the idea of superimposed radio transmission through practicability.

### 2.6.3 Jam Signaling

Most of the related work, that we described above, propose rather theoretical frameworks that aim to increase either network capacity or provide efficient computational power for WSNs, than to actually investigating their approaches at bottom-up, i.e., implementing their idea of utilizing concurrent wireless transmission in a real technical system. However, in the following we describe the work from Albert Krohn [51, 52],

---

<sup>7</sup>An introduction about analog computing can be find in textbook [167].

who actually deployed superimposed radio transmission in real, and even more for low resource WSNs. In particular, we are going to describe his approach Synchronous Distributed Jam Signaling (SDJS), that has found use in various WSN scenarios, such as channel access, cooperative transmission, synchronization and data fusion [51, 52]. In a nutshell, the SDJS communication mechanism is primarily designed for low resource wireless sensor networks, that require no complex signal processing, no carrier or phase synchronization. It is based on an ON and OFF keying modulation scheme which uses, i.e., the power of a signal for encoding. As a matter of fact, the low hardware requirements, simplicity and simple design of the communication method from Albert Krohn inspired our research in developing of novel radio transmission schemes using the principle of superimposed information transfer, including our initial work using SDJS to design a minimalistic polymer tag [168]. However, originally, the SDJS communication scheme was introduced in work [1] with some follow-up of contributions, such as the works [52, 169]. It enables within highly mobile and ad hoc wireless networks to estimate the number of active devices in real time. The SDJS mechanism can be described in short as a modulation scheme with superimposing and synchronous burst signaling combined with a statistical evaluation. A further application of the SDJS scheme is described in work [169], where an efficient method is presented for node localization in wireless sensor networks.

In comparison with common radio communication schemes the SDJS operates differently. For instance, data is not encoded and transmitted in the conventional way. But, it communicates information by sending a jam signal over the wireless channel in a randomly drawn time slot. Within the WSN the SDJS method allows to estimate parameters such as the number of present sensor nodes. In parallel, it enables to disseminate the information to all listening devices. For instance, in operation the SDJS communication starts with the broadcast of a start signal transmitting the burst to all participating nodes. After this first step the transceiver nodes occupy within a fixed time frame one slot with sending out a jam signal. Here, each node is choosing a time slot randomly sending in it its jam signal, or tries to detect possible jam signals that were sent from other participating devices. The occurrence of superimposition during jam signaling, i.e., two or more senders jam the same time slot, is not considered as interference, because the SDJS is devised to handle in particular such occurrences. In processing of a concurrent transmission with SDJS each transceiver node keeps two binary vectors. The first vector carries a binary '1' for indicating the time position when to send the jam signal, and '0' for indicating when to listen to the RF channel. And, the second vector is used for recording the entire SDJS communication. It registers a binary '1' on time positions when nodes transmitted or received a jam signal, otherwise a '0' is assigned when no communication took place.



die. In the SDJS approach, however, the issue is discussed in particular of how many hunters have participated at the shooting. The closed form of the mathematical solution for the SDJS issue is based on modeling the maximum likelihood, that a posteriori a number of jammers have in fact jammed a number of time slots out of the time frame [1]. Thus, the solution provides an estimation of the senders, that actually sent a jamming signal, described by confidence interval or point estimation [1].

When we put SDJS in comparison with other approaches of the physical layer network coding and CoMAC, that we described earlier, then we conceive that SDJS utilizes the idea of '*embracing the interference*' differently, i.e., it is restricted to communicate within the communicating users merely by 'Yes/No' messages. This, however, seemingly weakness is powerful, which provides plenty of solutions in terms of resource-restricted sensing devices, minimalistic circuit design, simple communication and computation scheme and reliable superimposed information transfer demonstrated by Krohn et al. [1, 41, 51, 52, 169]. However, despite of its success in various deployments on a real WSN platform [166, 170], it is rather limited in terms of flexibility and computational power, i.e., it is limited in implementing the paradigm of communicating functions over the wireless channel and the concept of a CoMAC. In the following subsection we are going to delve further into the analysis of the state-of-the-art and related work, and elucidate that minimalistic devices with simple communication capabilities in combination with the idea of '*inference*'<sup>8</sup> on the wireless RF channel must not be a contradiction.

#### 2.6.4 Critical Discourse Analysis

In the particular approaches for implementing the ideas of a physical layer network coding and CoMAC, that we described previously, different coding and computation scheme strategies were investigated, which can be roughly assigned in three categories. In the one kind of approaches that follow the assumption, that synchronization issues between communication partners are in principle technically solved and therefore, the superposition of signals at the phase and symbol level is enabled. For instance, specific transmit symbols  $W_k$  sent from adjacent transmitter nodes can overlap in each other, to generate functional code words without leading to an irreparable interference [53]. And, in the second kind of approaches, the practical implementation issues are taken seriously, but rely on exploiting physical quantities for encoding and computation. For instance, the signal power or phase is used to map real values of sensor readings onto signal power levels or phase differences [54, 149], implementing with it the concepts of analog computing [167] or Analog Network Coding (ANC) [156], knowingly to face serious susceptibility to an error-prone channel output. The deployment of multi-antennas to attain accurate

---

<sup>8</sup>Embrace interference to get inference. ☺

Channel State Information (CSI) about the surroundings, and applying specified rules to denoise the channel output from a priori anticipated and modeled computation error (cf. Goldenbaum [54]), does not necessarily guarantee correctly acquired function computation results, because harsh environmental influence and unknown sources of noise generators are leading to one wireless medium, that is rather unpredictable than it can be properly modeled to get a CoMAC [52, 120, 149, 166]. The third kind of approaches are those of which accept only key principles for their construction, if they are implementable from the view of an engineer. For example, Krohn [51, 52] deploys key principles such as the use of a burst signal to jam a time slot, and use of a mathematical framework which guarantees a deterministic output.

In respect to the category of physical layer network coding the objective is primarily to maximize the information flow in sensor networks, in order to outperform traditional wireless communications and standard network coding [53]. However, most of the works, describing different physical layer network coding strategies, report rather about theoretical insights and various frameworks for function type computation via the wireless channel (cf. Nazer et al. [53, 57, 144] and Keller et al. [171]), than to make a reality-check, as it is done for standard wireless network coding<sup>9</sup>, e.g., by Katti et al. [156, 158], which indicates fluctuating performance gain of few percent and several folds between theory and practice.

Taken as a whole, the work from Nazer and Gastpar [57, 144] (known as Computation over Media Access Control (CoMAC), respective, computation coding for sensor networks) is an information theoretical dispute of how the wireless channel can be mostly exploited to communicate of *desired functions* over the physical MAC layer. Their proposal for implementing CoMAC requires a perfect symbol and phase synchronization of signals, that is in practice hard to achieve [51, 52, 149]. However, their work provides key principles in computation coding, distributed computation and coding strategies to analyze the capacity of such networks with a CoMAC. An important result of Nazer et al. [57, 144] yields, that if the linear property of the physical wireless channel matches to a desired mathematical function, then the simultaneous access of sensor nodes, i.e., the concurrent transmission of sensory data and computation can be exploited profitably, i.e., by using the wireless channel as a '*calculator*'. In this case the sink node acquires the outcome of a function computation instantaneously. In relation to the analog CoMAC from Goldenbaum [54], the works from Nazer et al. [53, 57] provide a digital CoMAC, which is limited to the computation of linear functions. However, the implementation of

---

<sup>9</sup>As a reminder, in Figure 2.4 (b) we illustrated by means of the two-way relay example the standard wireless network coding and, in Figure 2.4 (c) we illustrated concurrent transmission, which includes physical layer network coding.

the concept for analog computing over the wireless channel (analog CoMAC) after all, extended the computation capability to nonlinear functions [54, 152].

Considering the various concepts and approaches of the related work with their practical flaws in design and limitation in application to enable a real world CoMAC, is it possible at all to establish a technical system, that is on the one hand robust, accurate and reliable in terms of wireless function computation, and on the other hand, that is powerful as the framework of an analog CoMAC? Our answer is 'Yes', as we will demonstrate it based on our wireless communication and computation schemes, i.e., code-based and time-based Collective Communications, that we are going to describe in chapter 3 and chapter 6. Furthermore, based on the key principles for engineering of low-resource sensing devices with simple communication capability from Albert Krohn [51, 52], it allowed us to develop minimalistic and printable polymer tags (cf. chapter 5), and resource-restricted wireless sensor nodes (cf. chapter 7).

In contrast to the related work, which apply mostly physics to construct coding and computation schemes for building a CoMAC, our mechanisms are derived mathematically, i.e., we use the framework of Vector Symbolic Architecture (VSA) [172] and, exploit stochastic laws with respect to poisson-distributed burst signaling, in order to perform concurrent transmission and function computation over the wireless channel. In addition, our approach allows an ultra light-weighted hardware design, such that resource-limited IoT nodes for application-specific tasks can be implemented straightforward. For instance, in the light of the demand on ultra-low cost devices with simple wireless communication capabilities, in this dissertation some solutions for minimalistic printable polymer tags and resource-restricted IoT sensing devices will be provided.

## 2.7 Summary

In this chapter we provided the background and related work to this dissertation, which comprises the introduction of Intelligent Environments (IE) and its implementation with current Internet of Things (IoT) technologies, as well state-of-the-art wireless communications. In our realization we elucidated the economic issue of Si-based technology being applied in a widespread deployment manner and, in opposition to that, we described practical limitations of current polymer electronics targeting to become economically viable, as well to create new applications in pervasive systems and ubiquitous computing. In our findings we made out that traditional wireless communications may not be suitable for the Internet of Things (IoT) in relation to Printed Electronics (PE), resource-restricted IoT devices, as well as their expected massive amount of deployment in IE. Therefore, we extended our review to current wireless communication research,

which investigates the idea of utilizing superimposed radio transmission, targeting to increase information flow in wireless networks through network coding and computation of functions over the wireless channel. We revealed that most of the related work provide theoretical insights about performance gain with respect to communication and computation capacity, without actually to investigate their frameworks with respect to practicability. However, few works exist that implemented their approach in reality. These, however, are featuring limitations in terms of performance, versatility, flexibility and general applicability.

All in all, we assessed the hardware complexity for printable IoT devices with few hundreds of transistors, that can be manufactured in a mass production, and put this constraint as a rule of thumb for our upcoming work. To this end, we learned the key principles of an engineer to build low-resource sensing devices utilizing the idea of superimposed radio transmission. Further, in our dispute with the related work we learned the concept of Computation over the MAC (CoMAC), describing the tools for enabling the communication and computation of linear and nonlinear functions over the wireless channel.

With the insights and perception we gained in this related work analysis, in the following upcoming work we will make a deep use of it, and come up with solutions that are both, practical and powerful.

## Chapter 3

# Code-Based Collective Communications for Dense Sensing Environments

In the background chapter 2 we stated, that Intelligent Environments (IE) are mostly implemented with RFID and WSN technologies using conventional connection-based communications. However, we also stated, that connection-based communications may impede progress towards Intelligent Environments and the Internet of Things involving massive amounts of RFID labels and sensing devices. In this chapter we start straight away with charting a field of more suitable technologies for communication in IE and IoT, which we call *collective transmission methods*. The idea of collective transmission is to establish communication not between single senders and single receivers but between collectives of senders and receivers, by making use of constructive interference of simultaneously sent signals. In particular, we detail how the collective transmission approach can be realized for a concrete application scenario: item-level tagging using printed organic electronics. We describe an algorithm that can be realized on very simple tags. With a testbed implementation (that we specifically designed to operate in the Low Frequency (LF) domain, and created to foster a development of code-based superimposed radio transmission, cf. chapter 4), we show that the Collective Communications algorithm can realize robust, collective, approximate read-out of more than 20 simultaneously sent signals. The content of this chapter is referring for the most part on our seminal work we published in the scientific contributions [59, 173].

### 3.1 Introduction

To realize the vision of Intelligent Environments (IE) with the Internet of Things (IoT), massive amounts of sensor data need to be processed in a spatially distributed way. Communication in Intelligent Environments is mostly implemented using RFID and WSN technologies with conventional connection-based communications. However, connection-based communications may be unsuitable for IE scenarios involving massive amounts of relatively simple sensing devices. The IoT paradigm implemented conventionally deploys in practice massive amounts of sensors collecting and storing massive amounts of raw sensor and meta data continuously, such that an identification of relevant information and information retrieval, as well a building of context-awareness in IEs represents a challenge [28] leading to scrutinize the system design of conventional IoT itself. The key issues of present-day IoT technologies can be recapped by high communication and computational load, high maintenance costs, resource exhaustive and power hungry devices. The deployment of a battery to empower a device is degrading to the environment despite of a long lifespan a battery-operated device is indicating (cf. our discussion in chapter 2). In the following chapter we are going to point at a spectrum of more suitable technologies for communication in Intelligent Environments and the Internet of Things, which we call *collective transmission methods*. The idea of collective transmission is to establish communication not between single senders and single receivers but between collectives of senders and receivers. We focus our discussion on a simple, yet practically relevant and soon realizable application example from the domain of next generation business process management technologies: item level tagging using extremely low-cost tags implemented with printed organic electronics. In particular, we are going to derive a code-based Collective Communications suitable for dense sensing environments, needed for example in supply chains.

The main part of this chapter is structured as follows. In section 3.2 we introduce the area of supply chain management as a typical application example for dense sensing, identification and tracking of radio tagged commodities, everyday things and items. In section 3.3 we introduce our general approach of Collective Communications for such dense sensing environments, and discuss its potential for wider applicability. In section 3.4, we explore the practical realization of the scenario with our approach. And, with our printed electronics test bed, that we developed to mimic OE smart labels and evaluate devised collective transmission methods, in section 3.5 we present and discuss our experimentally gained evaluation results.

## 3.2 Smart Supply Chain Management: An Example

Store houses, factories, and retail stores are very likely to be among the first Intelligent Environments deploying the concept of Internet of Things. Many business processes can be automated and optimized using item-level tagging [46, 174]. When individual items can be uniquely identified, functions, such as registration of goods received, quality control and in-store processes can be implemented more efficiently:

- **Goods received:** When a pallet with goods arrives, the receiving company usually checks if the right amount and the right goods were delivered. Using item-level tagging, a system can identify which products are packed in a pallet, and compare the quantities and the product identifiers with those in the advanced shipping notification.
- **Quality control:** After checking that a pallet contains the right amount of goods, one checks if the delivered goods fulfill a certain set of quality standards [175]. The data from item-level sensors can be queried to check if for instance a certain temperature threshold is exceeded.
- **In-store processes:** Using item-level tagging, retailers can automatically check whether there are enough goods in the shelves [176]. Also, retailers can check if goods are arranged in a correct way in the shelves, by checking compliance to predefined layout plans, so called planograms [177].

Item-level tagging does not only allow automatization, it also allows more efficient implementation of processes. For instance, the temperature within a pallet with goods may be distributed unevenly during transport and may display different dynamics [178]. Because of that, tagging the complete pallet with only a single smart label captures an incomplete view of the transportation process. As a result, a group of packages in an area that has been over-heated may remain undiscovered if it is far enough from the smart label monitoring the temperature. With item-level tagging this could be avoided, as packages would be monitored individually.

Even though such processes can be efficiently automated and optimized using item-level tagging, item-level data is mostly only needed on a technical level to implement the processes themselves. Many of the processes do not require item-level data but some function computable from item-level data. For instance, for quality control it is in most cases sufficient to know if a pallet is OK or not. If it is, it can be further processed. However, if it does not pass the test, goods might be checked individually before the whole pallet would be sent back.

This scenario makes a strong case for sensing environments using collective communication. Collective communication not only makes the communication process simpler, it also facilitates data processing. This is exemplified using the quality control process:

- **Simpler process:** Using item-level tagging without collective communication involves repeatedly scanning the pallet from different positions, for example with an RFID reader. This is mainly because physical interferences [179] prevent multiple smart labels from being read with one readout. Using collective communication, only one readout is needed, thus making the process simpler and faster to execute.
- **Simpler data processing:** When using item-level tagging without collective communication, the reader device will send the data it gathers to another system where data processing takes place, such as an Enterprise Resource Planning (ERP) system or an Inventory Management System. This system will eliminate duplicate readings and check if the data fulfills predefined standards, for instance, if the temperature of each of the up to 1000 items is below a certain threshold. After that, the system will decide whether the pallet needs further inspection. With collective communication, the aggregated information on the communication channel can be evaluated directly, on the reader itself, to decide if the pallet is OK. Only one reading instead of up to 1000 readings has to be processed.

The vision of item-level tagging comes closer to its realization with organic printed electronics (OE). Organic printed smart labels will be capable of recording sensor data such as temperature, humidity or light exposure. Organic smart label technology promises ultra low-cost massive deployment in industry, food, pharmaceuticals, healthcare and consumer markets, as tags can simply be printed on packages.

Production of organic electronic circuits can be faster, cheaper and simpler than RFID, as industrial standard printers can be used instead of dust-free fabrication facilities needed for silicon-based electronics, allowing massive deployment [37]. However, printed electronics cannot compete in terms of performance, reliability, and size with RFID.

Applications for organic printed smart labels are, for instance, in cost sensitive retail: super markets have on average a shrinkage of 2.77% per year [180]. This is a significant amount as the average profit margin is only 1.10%. The percentage of perishable goods amounts to 30%, causing more than 56% of the entire shrinkage [181] by spoilage. The principal reasons for spoilage are expired products or interrupted cold chains within supply chains from the manufacturer to the retail stores. A key scenario for the first organic printed electronics is therefore temperature monitoring in logistics and supply

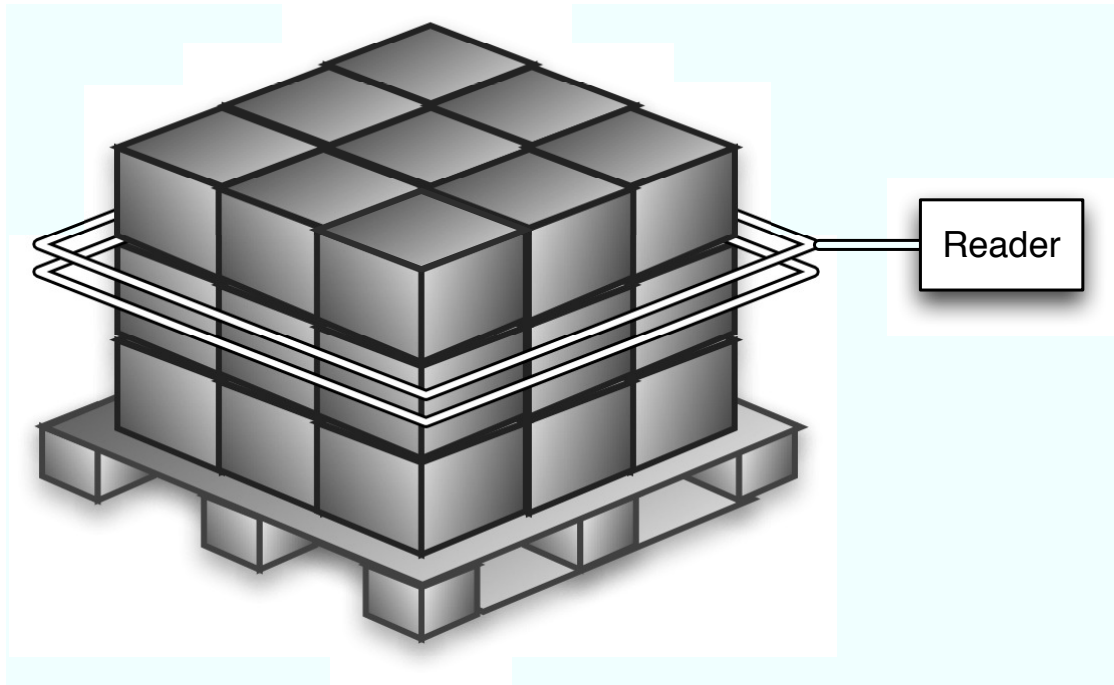


FIGURE 3.1: A typical application scenario for item level tagging in supply chain management: pallets are investigated by a screening device.

chain management, and first destructive binary organic temperature sensors have been developed [78].

In the following, we assume a scenario of a pallet arriving at a storage facility. The pallet contains a large number of items, which are checked for the maximal temperatures measured during transport for quality control. We are interested in two specific tests:

- **binary query:** have any items been exposed to a certain temperature?
- **proportion query:** how many items have been exposed to a given temperature?

In case of cold chains, for instance, a pallet could be rejected if a certain temperature threshold has been exceeded during transport. For some good and if temperatures were not too high, goods could still be sold at a discount, reducing the financial damage. Moreover, these checks would allow the transport company to detect failures of the cooling system in a truck early and avoid successive damaging of goods. 3.1 shows our application scenario for readout of item level tagging in supply chain management. Pallets are investigated by a screening device, which can process the compound signal received from the simultaneously sending tags attached to goods in packages piled up on the pallet.

### 3.3 General Approach

The general problem we study here is how to obtain information from a set of simultaneously sending nodes, in our scenario the tags attached to goods on the pallet. We aim to request from the pallet which proportion of tags measured which values. In principle, this could be done by querying tags individually using any of the well-established protocols. Implementing protocols that assign a distinct channel to each sender however is not feasible in our scenario, since the senders need to be simple and we assume a large number of senders.

For these reasons, we suggest to use novel collective, approximate versions of the traditional multiple access techniques of time division, frequency division, or code division (TDMA, FDMA, CDMA). The SDJS approach of Krohn [1] for counting the number of senders, for instance, can be viewed as a collective, approximate version of TDMA: all tags send a single burst signal in a random time slot of a given base interval and the reader then statistically analyzes from the number of filled time slots, how many tags there might have been. Similar time-slot techniques could be used by the reader to ask the pallet, whether a certain value was measured and even how many tags have measured a certain value.

In a similar way as SDJS but using code division instead of time division, our goal was to develop an algorithm that can statistically analyze the superimposed signals from all tags on the pallet and estimate which proportion of senders sent which value. While time slots and frequencies can encode ranges of values particularly well, our code-based method can be generalized to encode any type of value.

CDMA is based on bit sequences  $c$  that are shared between a sender  $S$  and a receiver  $R$ . A bit sequence  $v$  is sent from  $S$  as  $s = c \oplus v$ , where  $\oplus$  is the bitwise *exclusive or*. The receiver extracts  $v$  from  $s$  by computing  $v = s \oplus c$ . The double application of  $\oplus c$  cancels out  $c$  and  $v$  is regained. Simultaneous connections between a number of senders  $S_i$  and corresponding receivers  $R_i$  can then be achieved: simultaneous transmission yields the superimposed signal as the sum  $s = s_1 + s_2 + \dots + s_n$  of signals  $s_i$  sent, since the amplitudes of synchronized signals of the same frequency are approximately added to each other when the bit sequences  $s_i$  are sent.

The resulting signal  $s$  is *similar* to each of the original signals  $s_i$ , where similarity can be based on various distance metrics on bit sequences  $v, w \in \{0, 1\}^n$ , e.g., on the Hamming distance:

$$d_H(v, w) = \sum_{i=1}^n |v_i - w_i|. \quad (3.1)$$

The similarity can then be defined by choosing a threshold  $T_n$  suitable for the length of the vectors  $n$ . Two bit sequences  $v, w \in \{0, 1\}^n$  are called *similar* if they differ only in a small number  $T_n$  of bits:

$$v \sim w \stackrel{\text{def}}{\Leftrightarrow} d_H(v, w) \leq T_n.$$

A number of pairs of senders and receivers can thus communicate via codes  $c_i$ . If the codes  $c_i$  are chosen so as to be orthogonal ( $d_H(v, w) = 0$ ), or at least sufficiently different ( $d_H(v, w) \ll n$ ) from each other, this entails that we can obtain  $v_i$  from  $s$  by applying  $v'_i = s \oplus c_i$ . The result  $v'_i$  is similar to  $v_i$  so that  $v_i$  can then be regenerated from  $v'_i$ , using error correcting codes. Codes  $c_i$  can be generated so as to be orthogonal, however, sufficiently long random bit sequences, are also suitable: statistical theory suggests that the probability to obtain two random bit sequences of low similarity is higher, the longer the sequences are.

The key properties employed in this encoding are the notions of similarity and difference and of similarity preserving operations and distancing operations: addition is an operation that preserves similarity, whereas  $\oplus$  but also the *circular bitwise shift* are distancing operations, which make their result different from both its operands. CDMA uses the  $\oplus c_i$  encoding to ensure that the signals  $s_i$  sent are sufficiently different, and thus not mixed during simultaneous transmission.

In our scenario, we only need to ensure that different values transmitted can be retrieved from the superimposed signal. Moreover, the individual tags are much too simple and their number  $n$  is too large, as to allow for any complex protocol or encoding mechanism to be implemented. We therefore directly encode numerical values using a single random bit vector  $z_0$  shared by all tags and the receiver. We obtain sufficiently different codes  $z_i$  for numerical values  $i$  by circularly shifting  $z_0$  by the amount of  $i$  bit, since shifting is a distancing operation. In this way, a single bit vector  $z_0 \in \{0, 1\}^n$  can be used to encode  $n$  values.

The received signal  $s = s_1 + s_2 + \dots + s_n$  is then simply a sum of encoded numbers  $z_i$ , directly encoding the multi-set of measured values. If three tags, for instance, send the values  $\{7, 8, 12\}$  the received signal would be  $s = z_7 + z_8 + z_{12}$ . The receiver can now check the similarity between  $s$  and any value  $z_i$  by simply testing  $s \sim z_i$ .

Using this method, we can already resolve the *binary query* outlined in 3.2, to check whether some goods have been exposed to a temperature higher than a given threshold. In many cases, however, an estimation of how many tags sent which of the values is needed (*proportion query*). One way to do this is Least Squares Estimation (LSE), as we will show in more detail in the next section. The algorithm for the reader and tags can then be realized:

1. Tags come initialized with a register  $t$  set to the minimum temperature 0, and transmit code  $z$  set to  $z_0$
2. Each tag measures its environment continuously over a longer duration: if the measured value is  $m > t$ , then
  - (a) it sets  $t := m$ .
  - (b) it shifts the code  $z$  accordingly, that is: set  $z := z_t$ .
3. Reader sends **start** signal to tags.
4. Tags send their respective  $z$ .
5. Reader receives overlaid signal  $s$ :
  - (a) **Binary Query:**
    - i. Set  $S := \emptyset$ .
    - ii. For each possible value  $z_i$ :
      - if  $z_i \sim s$  then  $S := S \cup \{z_i\}$ .
  - (b) **Proportion Query:** For each value  $z \in S$ : use Least Squares Estimation (LSE) to compute proportion of contribution of  $z$ :
    - i. Generate linear equation system for the found values  $z_i \in S$ .
    - ii. Estimate parameters  $a_i$  so that error is minimal.
    - iii. Set  $M := \{(a_i, z_i) | s = \sum_{z_i \in S} a_i * z_i\}$ .
  - (c) **Output:** return  $M$ .

In an actual printed electronics implementation, the register  $t$  and the variable  $z$  of steps 1 and 2 would be combined. It would be possible, for instance, to implement the two steps with a destructive, physical temperature sensor that shifts a start/stop pointer forward along the fixed random vector  $z_0$  in response to higher measured temperatures (3.2). When the readout signal is sent the tag can then respond correctly by sending from start point to end point.

### 3.4 Collective Transmission

We now discuss the details of our implementation of the algorithm. The architecture of our instrumental set-up consists of  $n$  wireless sensor nodes (the tags) and a sink node (the reader) processing the received signal (see Figure 3.3). The data transmission

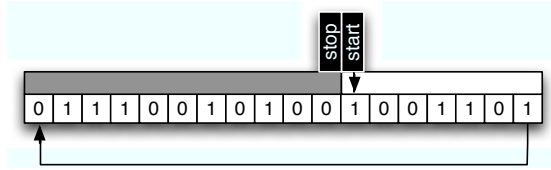


FIGURE 3.2: A model of a simple tag using a destructive, physical temperature sensor (gray and white bar): the start/stop pointer is shifted forward along the fixed random vector  $z_0$  as increasing temperatures permanently alter the material of the sensor (grey). When a readout signal is received the correspondingly shifted vector would be transmitted.

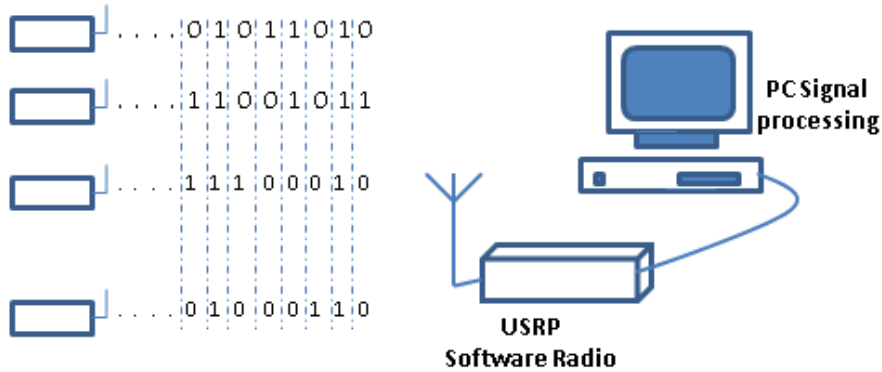


FIGURE 3.3: Principle of collective transmission. Each sensor node reached by an external trigger signal is transmitting its binary sequence at the same time. Based on the different number of '1's in each time slot different maximal amplitudes are generated. On the receiver side, the superimposed binary sequence is captured.

of the sensor nodes is triggered through an external signal (step 3) as in the case of RFID tagging. After initiating the transmission process each node in the sensor field is transmitting its measured sensory value simultaneously. The bit vector encoding a measured value  $v$  to be sent is transmitted in step 4 by a node sending out a sinusoidal signal in a time slot if in the sequence of bits a '1' occurs, otherwise it keeps silent.

In Figure 3.3 a possible scenario is depicted. When two or more nodes are simultaneously transmitting a sinusoidal signal, the signal components interfere on the channel and are received in a superposition by a receiver. Consequently, the amplitude of the superimposed electromagnetic waves is either intensified or becomes less intense.

In Figure 3.4 an example of a superposition between three sine waves is shown. The amplitude strength depends on the number of participating nodes, their individual transmission power, the dominance of the line of sight components to the scattered multi-path signal components and the distance between receiver and sensor nodes. During the transmission of the bit sequences from the  $n$  sensor nodes, the maximum can therefore vary in each time slot making measurement of the strength of the signal difficult. An example for a received raw signal is depicted in Figure 3.5.

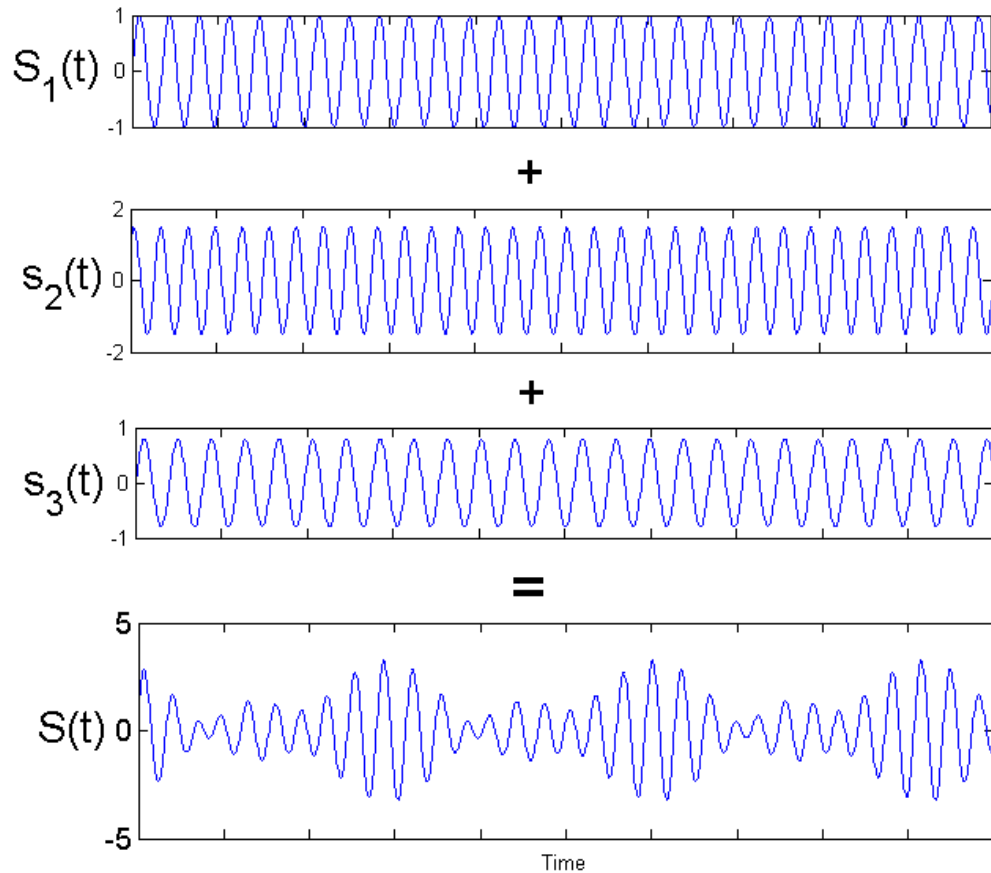


FIGURE 3.4: The superposition principle:  $s(t)$  is a superimposed signal generated by three sine signals  $s_1(t)$ ,  $s_2(t)$  and  $s_3(t)$ . The sine signals are chosen slightly different from each other in frequency, phase and amplitude strength, i.e.,  $f_{s_1} = 16$  Hz,  $f_{s_2} = 18$  Hz and  $f_{s_3} = 20$  Hz. Thus, when two or more waves traverse the same space, the amplitude at each point is the sum of the amplitudes of the individual waves.

By detecting the maximal amplitude in each time slot a vector of maximal amplitudes is created on the receiver side (Figure 3.6, step 5), which is then used to extract the sensory information of the collective information transmission.

For encoding values, we chose a 100-bit-long random vector  $z_0$  in such a way that  $z_i \approx z_j$  for  $i \neq j$ . The vector thus allows robust encoding of 100 values by shifting. Moreover, the relatively long random sequence makes it possible to benefit from statistical methods for robust retrieval of vectors from the superimposed signal. By statistical properties, a noisy version of a random vector may differ in more than a third, and it is still recognizable [172].

The main steps of the algorithm, the binary query (step 5a) and the proportion query (step 5b), have distinct applications. The binary query is a simple and highly reliable method to find out whether a value has been sent at all. The proportion query uses this

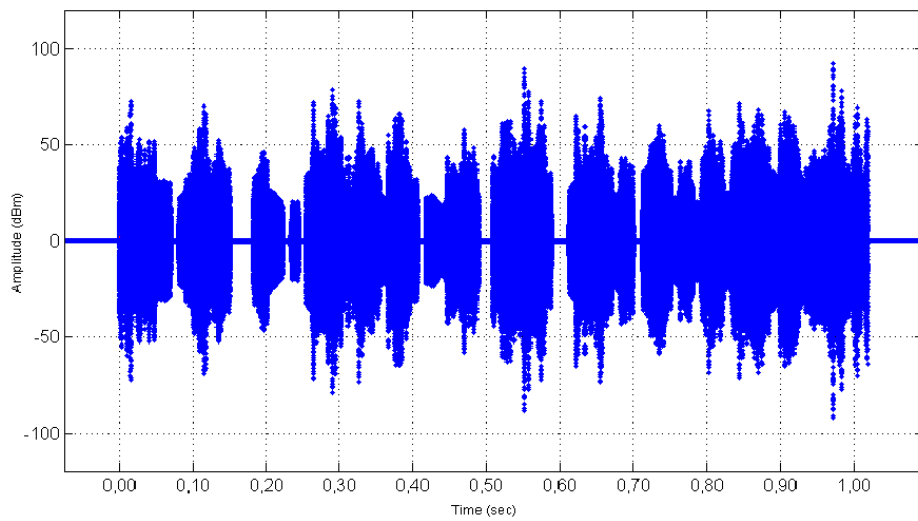


FIGURE 3.5: Raw data of a superimposed signal caused by 21 transducers transmitting different binary sequences simultaneously. The signal length is set to 100 time slots.

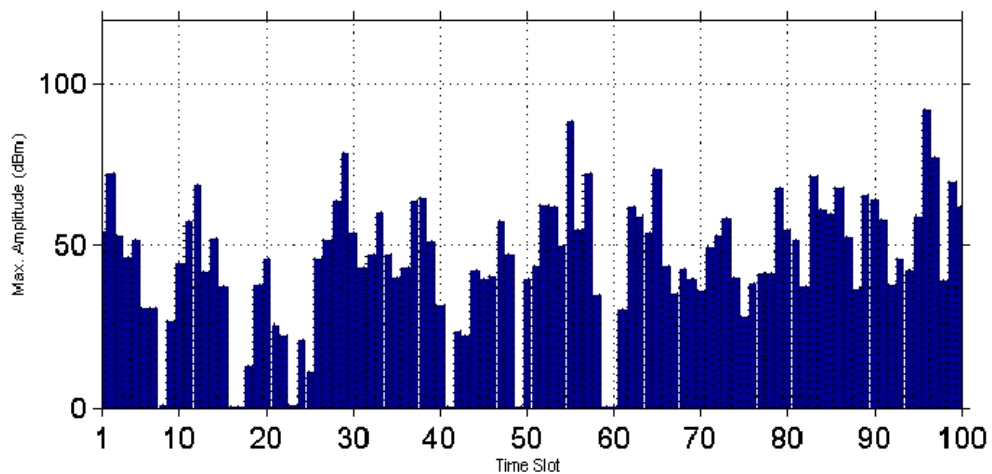


FIGURE 3.6: Quantification of the superimposed signal shown in Figure 3.5. In each time slot the maximal amplitude is detected and visualized by a single bar.

information to additionally compute which percentage of senders have sent a certain value.

### 3.4.1 Binary Query

The advantage of collective information transmission is that we can get sensory information at once in an environmental monitoring application. Often one is not interested in single sensory values, but rather in estimating the state of a sensor field, by detecting

whether or not a certain property is present. The Hamming distance has the property of being suitable to identify vectors contained in a received superimposed signal. For calculating the Hamming distance between two vectors  $v = (v_1, v_2, \dots, v_n), w = (w_1, w_2, \dots, w_n) \in [0, 1]^n \subset \mathbb{R}^n$  equation (3.1) also applies. However, if two vectors are not in the interval  $[0, 1] \subset \mathbb{R}$  they need to be normalized. For measuring the difference between a measured input vector  $v \in \mathbb{R}^n$  and an expected vector  $w \in \mathbb{R}^n$ , we normalize to the maximal amplitudes  $A_v = \max_i v_i$  and  $A_w = \max_i w_i$ , yielding the generalized definition:

$$d_H(v, w) = \sum_{i=1}^n \left| \frac{v_i}{A_v} - \frac{w_i}{A_w} \right|.$$

The similarity can then be defined by

$$v \sim w \stackrel{\text{def}}{\Leftrightarrow} d_H(v, w)/n < T_n,$$

where  $T_n$  is a threshold suitable for the length of the vectors  $n$ .

In practice the usage of the Hamming distance has its limits [172], the Hamming metric is applicable only if small sets of different vectors are added. The more vectors are used to encode entities, the lower the probability of identification. With large sets of different signals, synchronization issues become more critical and noise increases. However, the method still scales with larger numbers of nodes that transmit a small set of values, as in collective transmission. While noise also increases in the case of a large number of nodes, especially due to synchronization issues, values still were still detected reliably in our testbed.

### 3.4.2 Proportion Query

Using binary query alone the following applications can already be realized

- detection of an abnormality, for instance, the pallet containing perished goods,
- detection of the presence of classes  $A, B, C$  indicate temperature intervals, such as  $A = [0\dots 8]^\circ, B = [10\dots 25]^\circ, C = [26\dots 100]^\circ$ .

However, the capabilities of the system can be extended considerably when we can estimate the proportions of the classes  $A, B, C$ , e.g., computing the percentages of senders in the classes as  $A = 30\%, B = 60\%, C = 10\%$ .

To realize the proportion query, a mathematical formalization of the superposition principle combined with the statistical mechanism is required. Thus, the first step is to collect the possible vectors  $s_i$  that can be sent in a matrix  $A$ . Therefore, let

$$A = (s_1 s_2 \cdots s_M) = \begin{pmatrix} 1 & 0 & \cdots & 0 \\ 0 & 1 & \cdots & 1 \\ 1 & 0 & \cdots & 1 \\ \vdots & \vdots & \ddots & \vdots \\ 0 & 1 & \cdots & 0 \end{pmatrix}$$

be an  $N \times M$  matrix that contains the  $M$  vectors  $s_1, s_2, \dots, s_M$  of length  $N$ .

The modeling of superposition is based on a linear system, which is additive and homogeneous. Hence, the physical model is given by the linear system

$$z(a_1 s_1 + a_2 s_2 + a_3 s_3 + \cdots + a_M s_M) = y, \quad (3.2)$$

where the parameters  $a_i \in \mathbb{R}$  indicate the number of sensor nodes that have sent out the binary sequence  $s_i \in \{0, 1\}^N$ . The variable  $y \in \mathbb{R}^N$  contains the recorded  $N$  maximal amplitudes of the  $N$  time slots, cf. Figure 3.6 the received collective information transmission. To adapt the model to the reality numerically, a trade-off is required, which is expressed by  $z \in \mathbb{R}$ .

In the implementation, the first step is to solve the linear system in (3.2) without considering  $z$ , i.e.,

$$\hat{a}_1 s_1 + \hat{a}_2 s_2 + \hat{a}_3 s_3 + \cdots + \hat{a}_M s_M = y. \quad (3.3)$$

In the second step the solution  $\hat{a} = (\hat{a}_1, \dots, \hat{a}_M)^T$  of the linear system and the number of the participating sensor nodes is used to calculate the trade-off  $z$ . The number of the sensor nodes is usually not known. We therefore operate with percentages of senders, and assume the number of sensor nodes  $n$  to be 100 in the following. If the number of senders is known,  $n$  can be set accordingly.

$$z = \frac{n}{\sum_{i=1}^M \hat{a}_i}.$$

Finally, the solution of the parameters  $a = (a_1, \dots, a_M)$  can be estimated as

$$a_i = \hat{a}_i z \text{ for } i = 1, \dots, M.$$

The component  $a_i$  of the solution vector  $a$  then gives the estimated percentage of sensor nodes transmitting the bit sequence  $v_i$ .

Assuming uncorrelated measurements and equal Gaussian error  $\sigma^2$ , the parameters in  $a = (a_1, \dots, a_M)$  can be estimated by using linear least squares estimation. Thus, the

preliminary solution is given by evaluating

$$\hat{a} = (A^T A)^{-1} \cdot (A^T y).$$

Afterwards, the output vector  $\hat{a}$  is used to get the final estimation of  $a$  by applying  $a = z\hat{a}$ , where  $a, \hat{a} \in \mathbb{R}^N$  and  $z \in \mathbb{R}$ , as described above.

## 3.5 Evaluation

### 3.5.1 Organic Electronics Testbed

According to studies on the constraints of printed organic electronics [37, 182], organic electronics will behave and develop very differently from traditional electronics. Thus, for testing purposes, we created thirty transducers on PCB with off-the-shelf components, which conform to the constraints of organic electronics and in this manner mimic their behavior. The operating transmission frequency is set to 135 kHz, because tests have shown that an analog oscillator of the transducer is generating a stable sinusoidal signal in this low frequency domain when using a small number of electronic components. Additionally, it is considered that first working printed circuits will be operating in the lower frequency domain. In chapter 4 we are going to describe the entire experimental platform in detail. In principal, however, our Organic Electronics (OE) testbed consists of the mentioned transducers, a loop antenna operating in the Low Frequency (LF) domain, a  $2D$ -sheet [2, 183–185] for empowering and controlling the transducers, and two Universal Software Radio Peripheral (USRP) devices [186] connected to a PC building together a base station. With respect to the transducer devices, we equipped them with sensors, switches, control lamps, a programmable micro-controller and the ability to receive and transmit wireless signals. To be able to work with the OE reader platform we developed a Software-defined Radio (SDR) running on the PC. We enabled the SDR to be able to initiate a read out of the transducer devices, process superimposed radio transmissions, and visualize results of the readings. In chapter 4 we unveil our printed electronics testbed entirely by describing the buildup and operation of the reader platform, showing schematic and circuit layout of the transducer we are using to mimic envisioned OE smart labels. In addition, in chapter 4 we present fundamental outcomes of basic superimposed broad cast tests.

In relation to evaluate our CC approach described in this chapter, we explicitly chose to mimic a monitoring scenario in which the sensors are observing some environmental parameter, and the base station is reading out the measurements from all sensor devices placed on the  $2D$ -sheet simultaneously. The monitoring of perishable goods in

a cold chain is such an example that we mimic with the OE reader platform. In the following experiments we illustrate the performance and robustness of our code-based CC approach using the OE testbed.

### 3.5.2 Testbed Experiment

#### 3.5.2.1 Experiment Design

To provide proper evaluation results to our CC approach proposed in section 3.4, we setup the transducers to transmit a certain bit sequence corresponding to a certain value. In this way, we conducted the evaluation under realistic and controlled conditions. In the experiment realization we programmed the values into the transducers, but in execution the collective information transmission (step 4 and 5) took place as in the case of a real environmental monitoring scenario. In this way, we arranged several different setups in which the position and vector sent by transducers were varied.

To create the required bit vectors for encoding temperature values, we first generated a 100-bit long equally distributed pseudo-random bit vector. Then the randomly drawn binary vector was circularly bit-wise shifted to encode further values, as described in section 3.3. With respect to circuitry design for organic printed smart labels the circular bit-wise shifting operator was used for testing, as it would be cost-efficient to print tags with only one vector, but synchronization problems could be critical in this case, leading to false values being read.

The choice for using a specific 100-bit long vector was based on preliminary study. Hence, we chose carefully the relatively small bit-length of the vector  $z_0$ . Based on empirical tests, we found out, that the use of higher dimensional binary vectors did not improve or make the performance worse, whereas with the use of lower dimensionality the performance suffers. Moreover, it is possible to encode 100 numerical values using the shifting method with this vector. In our experiments the transducers were placed on the  $2D$ -sheet densely reflecting the intended usage scenario (cf. Figure 3.1).

Through the circular bit-wise shifting operator 100 different temperature classes can be established, however with maximally seven possible different values being used in our instrumental setup, we limited our evaluation to a comparison of only these seven possible classes. We tested all 15 different settings possible. For each setting, ten trials were executed and evaluated. The testing environment was part of the TecO student computing lab, and experiments were conducted during regular usage of the facilities.

### 3.5.2.2 Results

In Table 3.1 we show our evaluation results. The first column describes the setting by chosen values and transducers. For example a setting of 21 describes the trials where all 21 transducers sent the same value and a setting of 9,6,6 means nine transducers sent a value A, six send a value B and the remaining six send a value C. Column two presents the average amount of correctly recognized temperature values using the binary query algorithm exclusively. Column three shows the mean error with respect to the seven possible classes for each set of trials when the proportion query algorithm was applied. When comparing against all 100 possible values (fourth column), the mean error is again considerably lower between 0.01% and 1.16%.

TABLE 3.1: Results

Setting	Binary Query (accuracy)	Proportion Query (mean error per class)	
		7 classes	100 classes
<b>21</b>	88.57%	1.77%	0.0001%
<b>18.3</b>	89.05%	1.70%	0.3963%
<b>15.6</b>	91.90%	1.22%	0.1359%
<b>12.9</b>	97.62%	0.34%	0.0579%
<b>15.3.3</b>	90.00%	1.56%	0.5585%
<b>12.6.3</b>	89.05%	1.63%	0.5199%
<b>9.9.3</b>	89.05%	1.56%	0.3796%
<b>9.6.6</b>	82.38%	2.52%	0.1277%
<b>12.3.3.3</b>	82.86%	2.52%	0.9124%
<b>9.6.3.3</b>	82.38%	2.45%	0.6107%
<b>6.6.6.3</b>	80.95%	2.59%	0.3811%
<b>9.3.3.3.3</b>	80.00%	3.13%	0.6047%
<b>6.6.3.3.3</b>	85.71%	2.11%	0.6991%
<b>6.3.3.3.3.3</b>	80.00%	2.99%	1.1610%
<b>3.3.3.3.3.3.3</b>	79.52%	2.79%	0.9540%

### 3.5.3 Discussion

The experiments suggest, that collective information transmission is possible. The simple algorithm already yields results that would be acceptable for a range of applications, such as estimating whether a pallet has been damaged during transport. For the given number of maximally seven values fixed in the experiments, the simple communication scheme seemingly is robust enough. The different classes of sensory information sent in a collective information transmission are reliably detected, and the number of the senders, which have sent the same sensory information are estimated with an averaged

error of 2.06% in comparison with seven classes. Problems of the deployed testbed are its still low number of senders when compared to the pallet scenario of 1000 tags. Moreover, conditions in the testbed are presumably much better than in a pallet. Different packaging materials and larger distances could increase synchronization problems.

### 3.6 Summary

We outlined a novel approach for communication between large numbers of senders a single receiver. This method of *collective readout* was shown to be a robust, collective, approximate communication method for reading out massive amounts of sensor nodes by combining communication with computation on the channel. We described and tested an implementation to realize collective read-out that can be realized in an efficient manner on very simple tags. The experiments suggest the general feasibility of this mechanism in the economically meaningful scenario of item-level tagging for next-generation business process support.

However, our results have further reaching consequences. While computation on the channel has been advocated previously on theoretical grounds, its practical use for Intelligent Environments and the Internet of Things was so far questionable, as experimental results regarding robustness to noise and inaccurate synchronization under realistic conditions were missing. The implementation of the proposed collective transmission method, however, has shown that statistical methods can be employed to improve tolerance to noise and phase shifts.

The robustness of collective transmission comes from the use of random vector encodings of numerical values. In our example application, collective transmission makes it possible to communicate simultaneously with the complete pallet. Collective transmission does not aim to communicate with individual senders but with the collective. The transmitted signal, the sum of all transmissions, is an approximate representation of a multi-set of values. Future works will further elaborate such construction of representations through collective transmission. A disadvantage of the simple example scenario is its centralized architecture: Intelligent Environments with massive amounts of sensor nodes should not rely on a central processing unit, and instead employ the spatial distribution of nodes. Approaches on distributed representations and computations, such as Vector Symbolic Architectures (VSA) [172], can further guide this work. Collective transmission and read-out could be fundamental building blocks for realizing distributed intelligence.

## Chapter 4

# Experimental Platform for Simultaneous Wireless Transmission

In the previous chapter we presented Collective Communications (CC) for dense sensing environments, that we developed to read-out printable smart RFID labels collectively and simultaneously. To evaluate our CC approach we created a testbed with 30 sensing devices able to mimic behavior of OE smart labels. With regard to low-performing and not yet fully available OE hardware technology, we designed in particular a reader system testbed to accelerate prototyping towards developing high performance wireless communications for OE smart labels. In the following chapter we unveil our OE reader system testbed in detail, and demonstrate its features by means of broadcast tests.

### 4.1 Introduction

Considering the last decades, OE technology is advanced to different levels of matured fabrication processes (see, e.g., OE-A road map [32, 37] or [187]), but it is not yet fully available for mass printing [188] of electronic devices, or to create and print electronic devices with high circuit complexity of high quality and fidelity [182, 189, 190]. However, the implementation of conventional wireless communications requires a high degree of circuit complexity [30], that is not yet implementable using current state-of-the-art OE technology [32, 187, 190]. In order to overcome these technical barriers that OE is featuring, in the previous chapter we presented Collective Communications (CC) developed to read-out printable smart RFID labels of low hardware complexity. To evaluate our CC approach we created a testbed with 30 sensing devices able to mimic behavior of OE

smart labels. With regard to low-performing and not yet fully available OE hardware technology [38, 76, 187, 191], we designed in particular a reader system testbed to accelerate prototyping towards high performance wireless communications for OE. In the following chapter we unveil our OE reader system testbed in detail, and demonstrate its features by means of broadcast tests.

This chapter is structured as follows. In section 4.2 we introduce our composed OE reader platform, and explain its general functioning. We describe in subsection 4.2.1 the hardware setup for the OE testbed, and explain its functionalities in subsection 4.2.2. Thereafter, we reveal in subsection 4.2.3 the schematics of our sensing transducer device, that we created to mimic OE smart labels. In section 4.3 we describe the Software-defined Radio (SDR), that we developed to run the OE testbed. Finally, in section 4.4 we employ our OE reader system testbed to investigate in a pre-study the superimposed radio transmission phenomena, and test in a preliminary work the collective transmission mechanism. Section 4.5 summarizes this chapter.

## 4.2 Reader System Testbed

Based on the key ideas of collective information transmission and superimposed radio transmission [51], in the previous chapter 3 we presented Collective Communication (CC) for reading out of massive amounts of tags deployed, e.g., in a dense sensing environment such as a pallet, where each item may to be labeled by a tag. To evaluate our CC approach, and to study the phenomena of superimposed radio transmission in such dense environment, we created a reader system testbed with 30 Si-based sensing devices able to mimic any kind of envisioned OE smart labels. In the following we unveil our OE testbed in detail.

In our lab we assembled a reader system as a simulation platform for reading OE smart labels in the collective transmission manner. By employing the reader platform for a collective information transmission we achieved a maximal performing capacity of up to 25 smart sensor labels sending their sensory information simultaneously. With regard to the vision of smart sensor labels [82] we created the sensing devices as Si-based transducers, each equipped with a programmable micro-controller, in order to be flexible in emulating any kind of OE smart labels. In particular, we laid out the Si-based transducers to emulate polymer electronics circuitry of few hundreds of electronic components. Based on this setting we enabled rapid adaptation of circuit design for OE smart labels and the development of highly scalable communication schemes for OE smart labels featuring ultra-low hardware complexity. In Figure 4.1 we show our OE reader platform, which consists mainly by one computer, two Universal Software

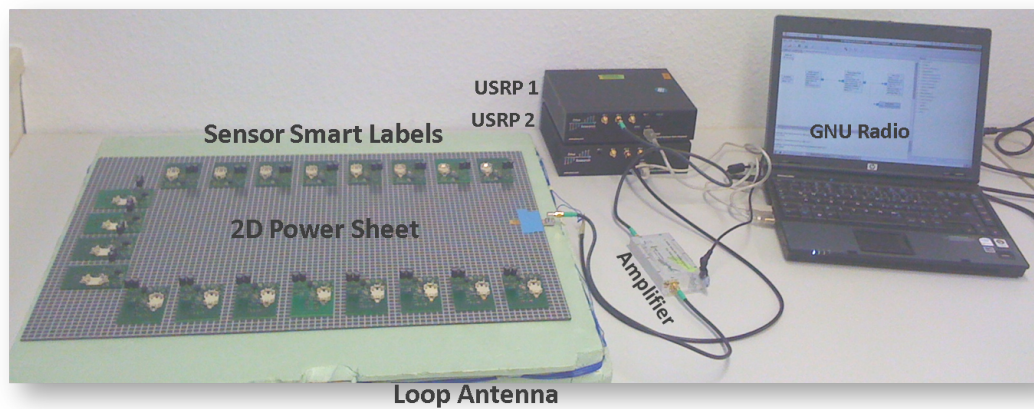


FIGURE 4.1: This figure depicts our OE testbed for reading smart sensing devices, that simulate printed polymer tags.

Peripheral (USRP) devices [186], one 2D power sheet [2] and the Si-based transponders. In the following subsection we continue to describe our OE testbed in more detail.

#### 4.2.1 OE Testbed Setup

Figure 4.1 shows all electronic devices we employed to assemble the OE testbed. The USRP1 device there connects a loop antenna [192] operating in the LF band, and a computer on that a Software-defined Radio (SDR) [193] is running. The USRP2 device connects a 2D power sheet [2] and again the computer. The SDR is managing the reader platform. Both USRP devices realize together a transceiver (base station) designated for initiation and capturing of superimposed information transfer. While the USRP1 device is aligned to capture a superimposed radio transmission using the loop antenna, the USRP2 device is connected over a signal amplifier with the 2D sheet designated to empower the Si-based transponders. Both USRP devices are of the same type, but their functionality is set differently, i.e., while USRP2 is empowering and controlling the 2D power sheet with a 2.4 GHz signal, the USRP1 device is used to receive and relay superimposed radio transmission sent from the Si-based transponders. In general, the 2D power sheet device is designed to enable apart from empowering smart objects on its surface, also to enable communication between them through utilizing exclusively the 2D sheet media [2, 183–185]. However, in our case, we make use of the 2D power sheet device mainly for empowering and activating the Si-based transponders, but not for network communication. In a reading operation all Si-based transducers are sending their signals over the wireless channel simultaneously, whose output is captured by the USRP1 device. The activation procedure and the simultaneous interrogation of the Si-based transponders is as follows.

TABLE 4.1: This Table lists all electronic devices used to assemble the reader hardware infrastructure.

Electronic device	Functionality
Computer	GNU Software-defined Radio (SDR)
USRP2	Provide the 2D power sheet with power supply through 2.4 GHz signal
Amplifier	Boost the 2.4 GHz power signal from USRP2 device to the 2D power sheet
2D power sheet	Hardware platform for wireless empowering and communication of smart devices
USRP1	Receiver device for reading the signals sent by the Si-based transponders
Loop antenna	Designed to receive signal in the Low Frequency (LF) band domain (135 kHz)
Si-based transponder	25 Si-based prototypes designated to emulate polymer tags

1. Activate 2D power sheet to start simultaneous read-out of the transponders by utilizing the SDR (GNU Software Radio)
2. Each tag transmits a binary sequence (message) simultaneously using ON-OFF keying
3. USRP1 device receives the transmission and relays it to the computer for further signal processing and data analysis
4. Extraction of ensemble information

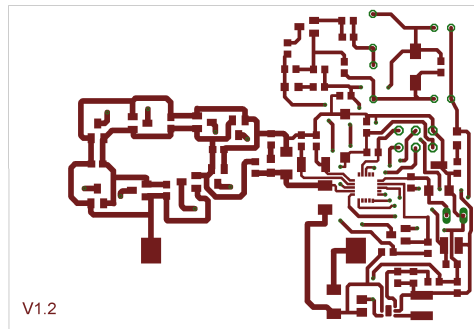
A short description of deployed electronic devices composing our reader platform is provided in Table 4.1.

### 4.2.2 Transducer Device

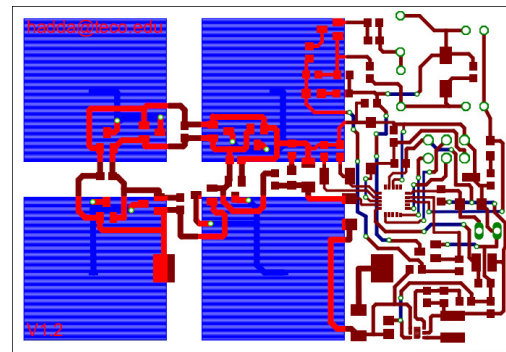
In our purpose to simulate envisioned OE smart labels as close as possible, that integrate the collective communication mechanism, we designed a Si-based transponder to be flexible in adaptation of OE hardware parameters. In a close-up view one of our manufactured Si-based transponder is depicted in Figure 4.2a. Based on programming the on-board Atmel micro-controller [194] integrated on the Si-based transponder, we can simulate different communication schemes. The integrated micro-controller on the Si-based transponder enables rapid prototyping with regard to differently designed collective communications. For instance, it allows to investigate different parameter sets



(A) Si-based transponder, a replacement for an organic and printed transponder.



(B) Top layout.



(C) Bottom layout

FIGURE 4.2: The picture above (A) shows our Si-based transponder device. The circuit layouts below (B,C) depict the top and bottom side of the circuit board. The bottom layout (C) indicates the planar antenna, which harvests the power from 2D power sheet [2]. Circuit design and implementation is made by Ali Hadda [3].

and features, such as coding schemes, carrier frequency, signal length of a bit or transmission range. Hence, we can employ for the circuit design of an OE smart label the best parameter fit. With respect to the development of a holistic smart label circuit, further essential electronic components on the Si-based transponder are considered. For instance, the transmitter unit (transponder coils), the sensor block and the power harvesting unit is to mention. In the following subsection we reveal the schematics of our Si-based transponder prototype.

### 4.2.3 Schematics

A detailed schematic of our Si-based transponder (simulating an organic printed smart label in a phenomenological way) is given in Figure 4.4. It consists basically of the

following circuit components.

1. Atmel ATtiny44A micro-controller [194] (Figure 4.4, C1-C2)
2. Hartley-Oscillator [4] (transmitter unit) (Figure 4.4, B5-C6)
3. Sensor interfaces (sensor block) (Figure 4.4, B3-C3)
4. FM (Frequency Modulation) (Figure 4.4, C5-C6 down)
5. Printed planar antenna (Figure 4.2c) for power harvesting (Figure 4.4, A1-B2)
6. Coin cell connector (Figure 4.4, A4)
7. Control light panel (Figure 4.4, A3,B5 up)

The circuit functionalities of our Si-based transponder are held manifold, in order to be as flexible as possible, so that once developed communications can be transformed easier into organic and printed circuit wiring.

The micro-controller from Atmel [194] is providing the required flexibility. For instance, it controls and manages the transmitter unit, sensor block, FM unit and the control light panel. With regard to printed circuits the micro-controller programming is kept straightforward, so that the implementation of the collective communication into OE can be realized. Upon the electronic board (cf. Figure 4.2b) of the Si-based transponder we established different sensor interfaces in order to have alternatives to integrate various types of sensors, such as temperature, humidity, light or vibration sensors. For the transmitter unit we used a Hartley-Oscillator [4], which consists merely by 2 coils, 1 transistor and 2 capacitors (cf. Figure 4.3). Based on the low hardware complexity of the oscillator we expect that this circuit is printable using OE hardware technology. In Figure 4.3 we show the Hartley-Oscillator circuit [4].

To be able to change transmission frequency, and thus to adapt OE constraints, we integrated a FM unit into the transponder's circuit. Upon the downside of the circuit board we printed a planar antenna (cf. Figure 4.2c) to enable power harvesting from 2D power sheet. The wireless power supply is enabled by the electromagnetic induction between the Si-based transponder devices and the 2D power sheet. The planar antenna itself is connected with the micro-controller and the transmitter unit. The Si-based transponder operates in passive mode fully. However, we integrated in addition a coin cell connector for a battery to maximize the number of operating transducers on the 2D power sheet, and to support operating if necessary. Further, we integrated a control light panel to observe the transponder's reliability performance .

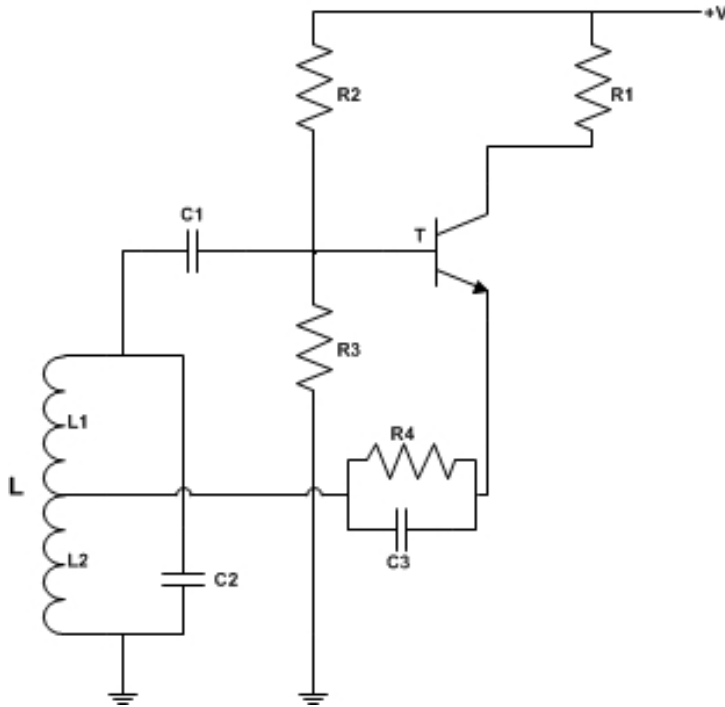


FIGURE 4.3: Shows the Hartley-Oscillator circuit [4] used as signal generator for ON-OFF Keying in our transducer device.

### 4.3 Software-defined Radio (SDR)

In the previous section we described the reader hardware infrastructure of our OE testbed. In the following we describe the software we implemented and applied to run the OE testbed. In order to establish an user interface application for the OE reader system testbed using a Model-View-Controller (MVC) [195], we employed the GNU Radio toolkit [193] to implement a Software-defined Radio (SDR) [164] providing the signal processing, visualization and controlling of the entire reader platform. Based on the GNU Radio Companion (GRC) framework [196] we created a SDR generated here by a GRC flow-graph (cf. Figure 4.5). On the computer the SDR is running in a GRC environment controlling the 2D power sheet over the USRP2 device. As well, the USRP1 device connecting loop antenna and operating as a receiver is integrated and linked within the remaining SDR signal processing blocks. Here, the GNU Radio flow-graph creates overall the composition of all hardware devices building altogether the SDR for the reader system testbed. Considered as a whole, the Software-defined Radio (SDR) consists by several software building blocks combined in a flexible software application. Main building blocks of the SDR are the software devices for the USRP hardware, signal processing blocks such as the band-pass/low-pass filters, signal amplifier, software scope monitor, the data query block, and control unit incorporated in a Graphical User Interface (GUI), controlling and managing the attached hardware devices to the computer station. The software building blocks depicted in the flow-graph are adapted and configured into the GNU Radio Companion (GRC). The flow-graph in

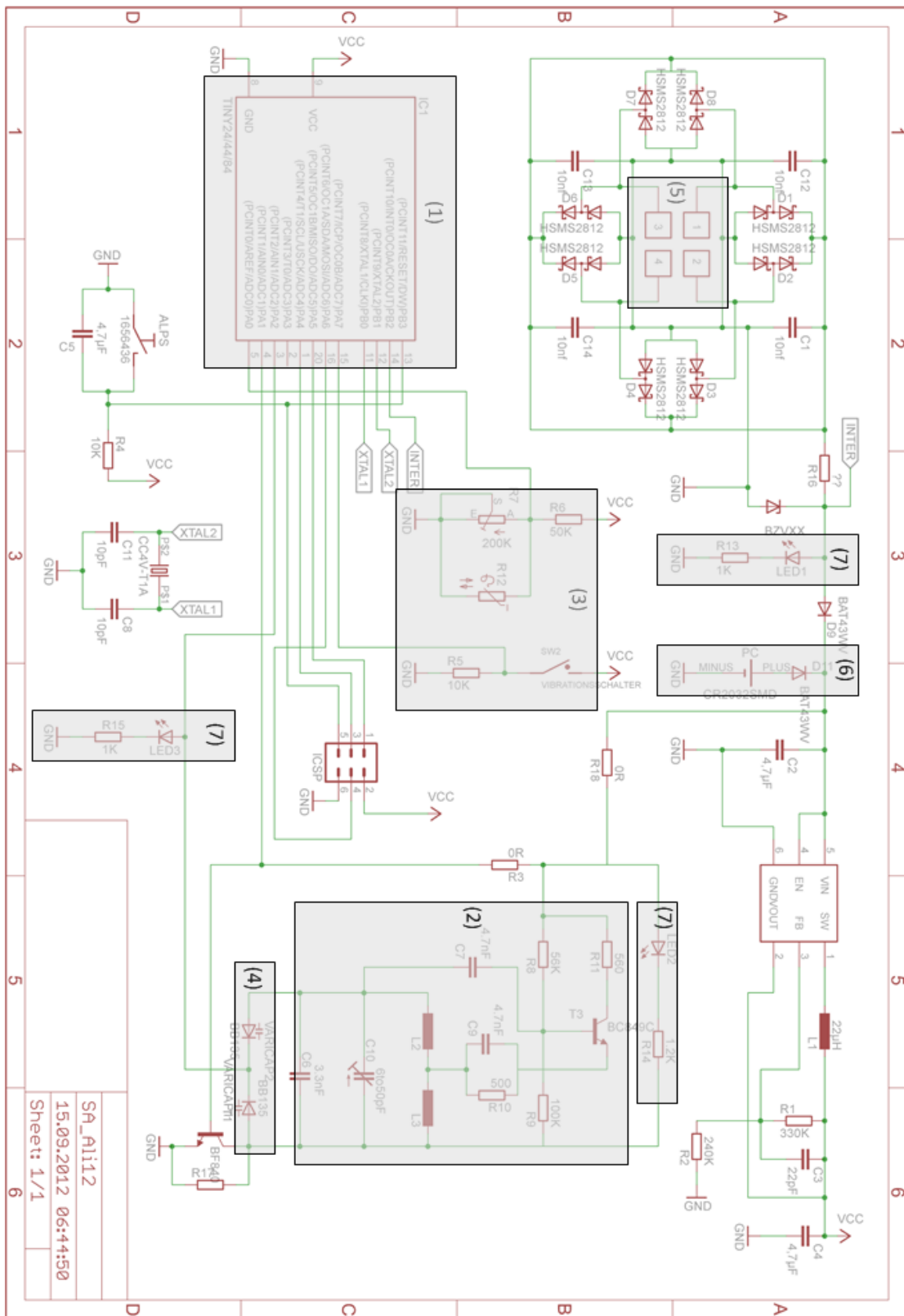


FIGURE 4.4: Schematic of our Si-based transponder.

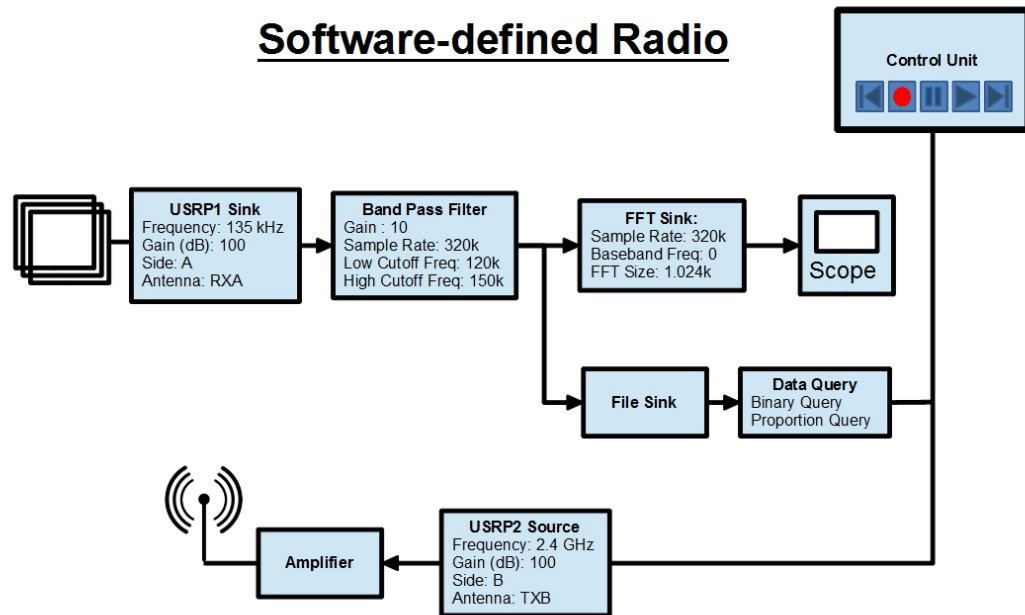


FIGURE 4.5: Shows the flow-graph of the implemented Software-defined Radio (SDR).

Figure 4.5 illustrates an example of a SDR we deploy. It shows all building blocks with their chosen parameter sets. The operation mode of the simultaneous read-out of the Si-based transponders is performed by using the GUI, meaning that activating/deactivating the reader platform, starting/stopping an interrogation, recording/uploading a superimposed radio transmission and data querying can be carried out by request.

## 4.4 Broadcast Tests

Now that we developed the hardware and software for our OE reader system, in the following we present some results of a pre-study investigating the superposition principle of electromagnetic waves. For the pre-study we employed the OE testbed. According to studies on the constraints of printed organic electronics [37, 182], organic electronics will behave and develop very differently from traditional electronics. In our pre-study we employed 30 transducer devices programmed in the manner to conform the constraints of organic electronics. We set the operating transmission frequency to 135 kHz, because tests have shown that an analog oscillator of the transducer is generating a stable sinusoidal signal in this low frequency domain when using a small number of electronic components. Additionally, we consider that first working printed circuits will be operating in the lower frequency domain. To see how the collective transmission of

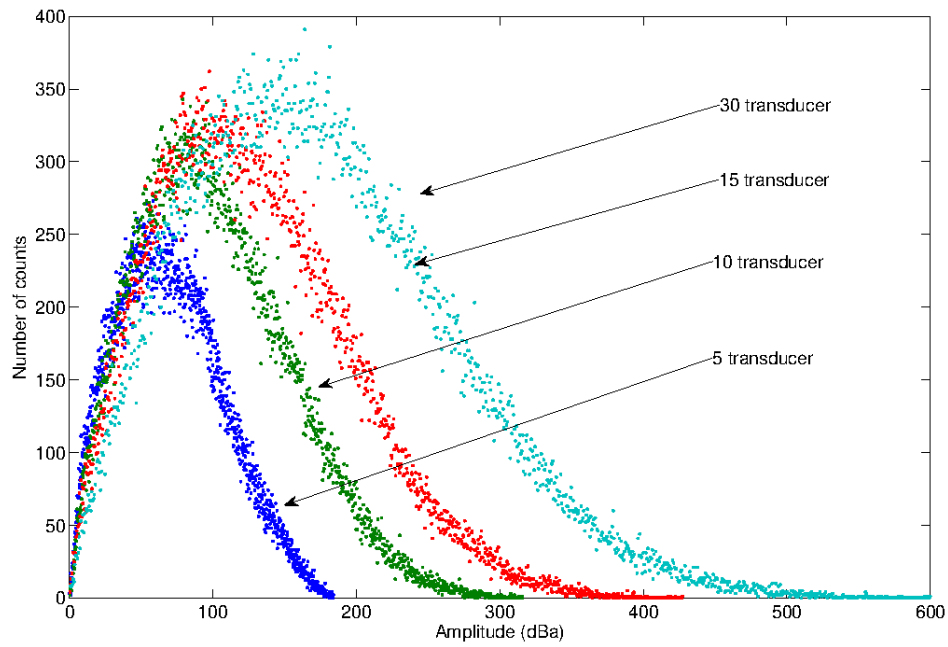


FIGURE 4.6: The four histograms illustrate the distributions of amplitudes which are generated by 5, 10, 15 and 30 transducers sending a sinusoidal signal simultaneously.

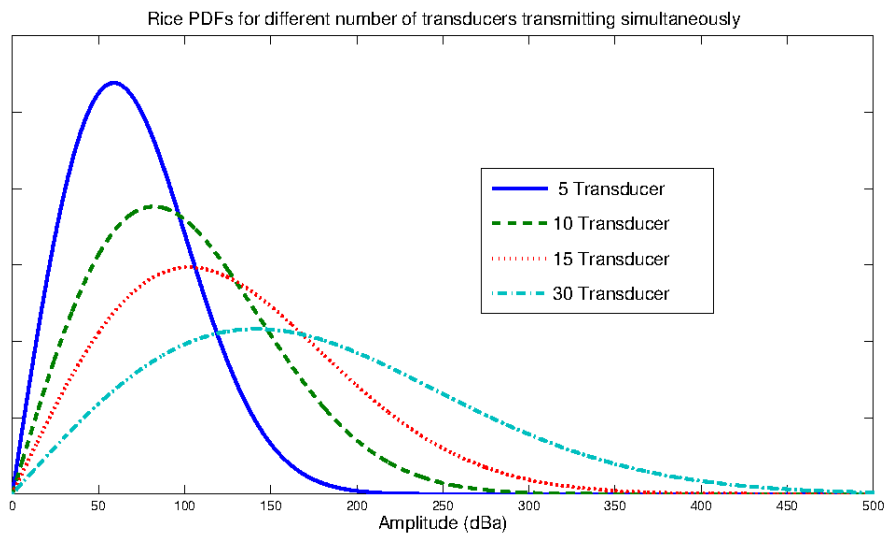


FIGURE 4.7: The four distributions indicate various Rice PDFs obtained by fitting data of 5, 10, 15 and 30 transducers which sent a sinusoidal signal simultaneously.

the transducers behaves under real environmental conditions, we carried out about 360 experiments as follows: by changing the parameters such as the number of transducer transmitting simultaneously and the distance between loop antenna and transducers, we obtained a detailed behavior of the superimposition on the channel. For instance, Figure 4.6 depicts four histograms gained by experiments with 5, 10, 15, and 30 transducers,

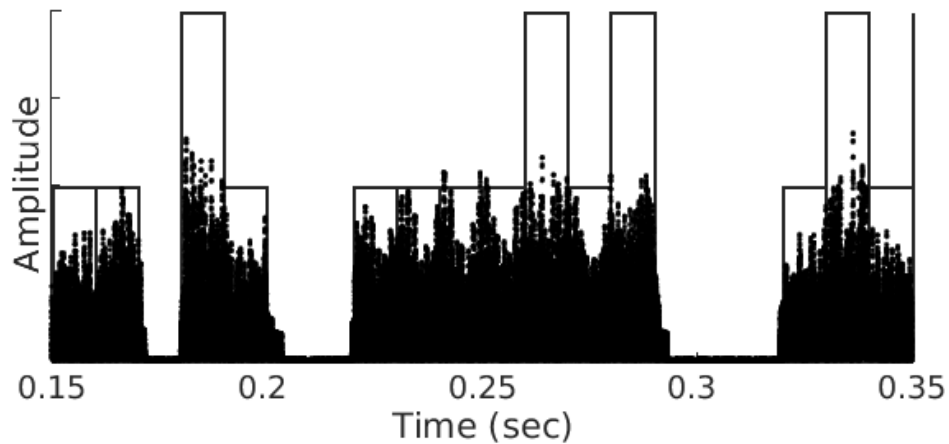


FIGURE 4.8: Raw data of a superimposed signal is shown caused by 12 simultaneously sending transducer devices, whereby 6 of them each sent the same random burst sequence.

respectively. Transducers sent out a sinusoidal signal simultaneously. Here, the positive amplitudes of the superimposed signals are considered. Observe that their histograms resemble a Rician distribution as a Probability Density Function (PDF). Correspondingly, we provided a distribution fit for the four experiments shown in Figure 4.7. The distribution of amplitudes indicates that an amplitude with a high magnitude is a rare event, that is, the exact coincidence of amplitudes from several signals concurring at the same time point is not probable given the hardware. Our testbed thus reflects lack of synchronization in real systems. However, based on an acquired Rician distribution we can extrapolate the sampling to estimate a maximal possible occurring amplitude, even if such event is not yet measured.

In our next broadcast test we programmed the transducer devices to transmit a 100-bit long randomly drawn burst sequence using ON-OFF keying. The duration of a burst signal is set to 10 ms signaling a binary '1'. In case to signal a '0' the transducer holds still for 10 ms, i.e., no burst signal is sent. In Figure 4.8 we show exemplary a partial result of a superimposition of two randomly drawn 100-bit long burst sequences transmitted simultaneously by 12 transducer devices, where 6 of them each transmit one of the predetermined random burst sequence. In this way, we used the OE testbed to evaluate our approach Collective Communication (CC), whose results we reported and discussed in the previous chapter 3. In the particular example shown in Figure 4.8 one can observe how in each time slot the maximal occurring amplitude strengths fluctuate differently from ideal case. However, one can also already observe that the amplitudes stand relatively proportional to each other, such that this behavior indicates a preservation of meaningful information in the superimposed radio signal.

## 4.5 Summary

In this chapter we unveiled our OE reader system testbed in detail, that we used to evaluate our Collective Communication (CC) approach described in the previous chapter. First, we outlined the reader hardware infrastructure of our composed OE testbed, which consists mainly by two USRP devices, one loop antenna, one 2D power sheet from Shinoda labs [197], one computer station and thirty programmable transducer devices with sensing capabilities, building together the experimental reader platform for dense sensing environments. Further, we unveiled the schematics of our programmable and sensing transducer device, which is to be deployed in combination with a 2D power sheet. Second, we described our Software-defined Radio, that we developed to run the OE testbed. And third, we performed broadcast experiments with the OE testbed to investigate in a preliminary work the superimposed radio transmission phenomena. In the next chapter we apply our gained experience for superimposed radio transmission and collective information transmission to develop in particular a printable passive RFID label, which integrates our CC mechanism down to the logic gate level.

## Chapter 5

# An Implementation Example of a Printable Passive Smart Label

In chapter 3 we presented with respect to dense sensing environments and OE our approach for collective communication of sensing (or, any kind of information carrying) smart labels, relying on code-based, wireless and simultaneous superimposed information transfer. And, in chapter 4 we described with regard to the lack of a currently viable OE technology, and the development of Collective Communications, our reader system testbed implementing superimposed radio transmission for up to 30 transducers, that can transmit simultaneously and mimic envisioned OE smart labels. However, state-of-the-art OE allows the printing of simple tags with low hardware complexity, but the printing of RFID chips with large numbers of transistors, that implement an anti-collision RFID protocol, are far away from realization (cf. our review and discussion in chapter 2 and appendix A reporting on state-of-the-art printed RFID). In this chapter we continue to design an OE smart label device based on our Collective Communications, and develop for this purpose one minimalistic, sensor-based and fully functional passive RFID tag implementing the collective transmission scheme (cf. for reference the previous chapter 3). Based on current OE constraints, thus we design and implement in particular a printable passive smart label down to the logic gate level. Further, we integrate a simple global synchronization strategy to ensure simultaneous and collective information transfer from queried passive tags to reader system. To this end, we provide a feasibility assessment towards printing the smart label device with current OE. In conclusion we provide a validation of our proposed OE passive tag reader system by simulating it physically in LTspice.

## 5.1 Introduction

While our work in the previous chapter 3, including chapter 4, prevailed primarily to elaborate and evaluate a simple but yet highly scalable, robust and efficient wireless communication between smart RFID tags and a reader system, that is based on the idea of collective and superimposed information transmission, in the following we pursue to provide to this end a printable circuit device implementing an example of a polymer tag, which integrates our Collective Communications mechanism. The facilitation of a such holistically printed OE smart label is going to enable a wide range of business and scientific applications dealing with sensing, identification and tracking in the area of pervasive and ubiquitous computing (cf. chapter 3). Considering our discussions in the previous chapters, the area of intelligent packaging is one key application for utilizing OE, i.e, the development of organic printed RFID tags (cf. roadmap for OE [37], or consult the related works in chapter 2, and references therein). According to our analysis, OE tags can contain and provide useful information, such as the item identification and sensor readings. In a such application scenario data is generated continuously while items travel through a supply chain, i.e., from manufacturing plant to a final consumer, and enable participants and other stakeholders to improve their business processes, such as quality control, certification, logistics optimization and fraud detection. The implementation of these processes results in cost savings for the producer, suppliers, as well as vendors, and increases product safety for consumers (cf. chapter 3). The potential of printed RFID in logistics and industry is widely acknowledged [37], and its facilitation is promoted by research and industry over the last decades, as we reported in more detail in chapter 2, as well appendix A. However, the performance limits of state-of-the-art OE do not allow yet the implementation of fully-functional and holistically printed RFID fulfilling in particular traditional RFID standards (cf. chapter 2, and appendix A). Instead, rudimentary RFID functionalities and partial protocol generators are successfully implemented in OE. Here, for example, one inductively coupled RFID tag is realized in a p-type organic technology and lithographic printing process operating at 13.56 MHz [74]. Another pioneering OE transponder device realized in complementary organic technology is presented by Blache et al. [198]. Further on, a first demonstration of a bidirectional communication between a polymer tag and reader device implementing a passive envelope-detector is described by Myny et al. [87]. More recently, an improved version of a polymer tag implementing an active envelope-detector is described by Fiore et al. [199, 200]. With respect to state-of-the-art OE hardware performance and its feasibility in terms of printing the polymer tag in high-volumes, in the following we develop an example of a printable passive smart label, which implements our Collective Communications approach in polymer electronics and passive reader-tag-communication (cf. our Collective Communications approach described earlier in chapter 3).

This chapter is structured as follows. In section 5.2 we describe the versatility of our Collective Communications (CC) approach based on an envisioned OE smart label being applicable for various business scenarios. Further, we derive out of it fundamental principles concerning superimposed information transfer, that we use to design the circuitry for our envisioned passive OE smart label. In section 5.3 we design the OE smart label by introducing all its required circuit functions, implementing it to a sensor-based passive tag. To this end, we describe in section 5.4 a global clock synchronization strategy implemented within the proposed passive tag circuitry. The chapter proceeds with a validation of the proposed passive tag by utilizing simulations (section 5.5) and a feasibility assessment (section 5.6) towards printing the smart label device with current OE technology. In section 5.7 we discuss with respect to our proposed minimalistic tag the mass-printing of the device with OE technology, in comparison with a traditional fabrication process utilizing such as a chip foundry. The last section summarizes this chapter.

## 5.2 Collective Communications for Printed Smart Labels

In chapter 3 we introduced and described our Collective Communications approach with all its details. In short, Collective Communications is designed primarily how to obtain information from a set of simultaneously sending nodes, in our application scenario the tags attached to goods on a shelf. We request from the set of items which proportion of tags measured (called proportion query), respective, contain which values (called binary query). In principle, this could be done by querying tags individually using any of the well-established protocols. However, implementing these protocols that assign a distinct channel to each sender is not feasible in our scenario, since the senders need to be simple due to polymer electronics deficiency (cf. appendix A), and we consider large number of senders. In particular, our transmission algorithm is laid out to be on the one hand simple, so that a smart label device can be implemented in polymer electronics, and on the other hand to acquire maximal performance regarding information transfer, scalability and robustness. We achieve these objectives basically by applying the following fundamental principles:

1. All queried tags transmit their stored data simultaneously and start with transmission at the same time
2. A randomly drawn bit sequence encodes a physical entity, such as an identification, sensor value, temperature range, message, etc.

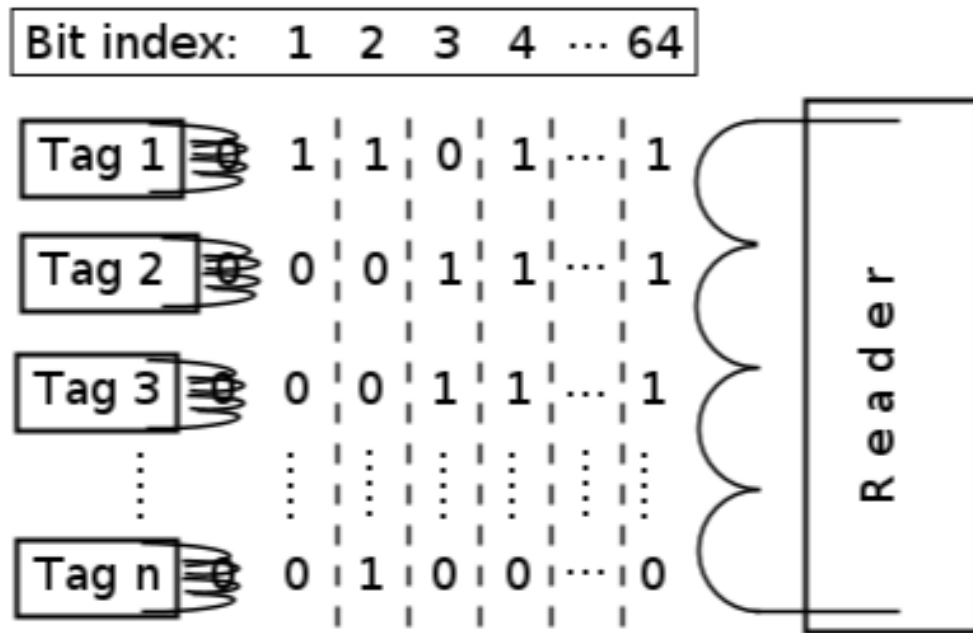


FIGURE 5.1: A passive tag reader system illustrates simultaneous transmission of bit streams sent by a set of 64-bit smart labels.

By applying the rules, the signals sent from tags superimpose on the RF channel. However, the collective and simultaneous transmission mechanism enables to analyze the superimposed signal mathematically at the receiver side, so that the transferred information (e.g, what proportion of senders sent what value) can be extracted.

To show in addition exemplary the versatility of our Collective Communications approach with respect to its manifoldness and possible application scenarios, we envision in the following an OE smart label, that stores aside from a sensed value, a quality grade of a sales item suited to realize intelligent packaging. The smart label we design here can be utilized in such business processes, where it determines a product quality in a bulk reading scenarios, such as the goods inbound processing in a supermarket. For each sales item the quality is determined by the sensor-based smart label attached to the item. In operation the sensor readings are acquired in a single query and interpreted by our algorithm that is specific to product type, e.g., to a quality rating on a scale from 1 to 7. The quality scale, however, can be identical for all product types, i.e., a rating of 1 corresponds to a perished item for both milk packages and tomatoes. Otherwise, no compliance violation is detected, and the goods can be sold. Based on collective and simultaneous querying a single reader device can thus determine the quality ratings of multiple items belonging to different types. The advantage of this approach relies on the use of the same reader hardware infrastructure for multiple smart label application scenarios resulting in saving of setup and maintenance costs.

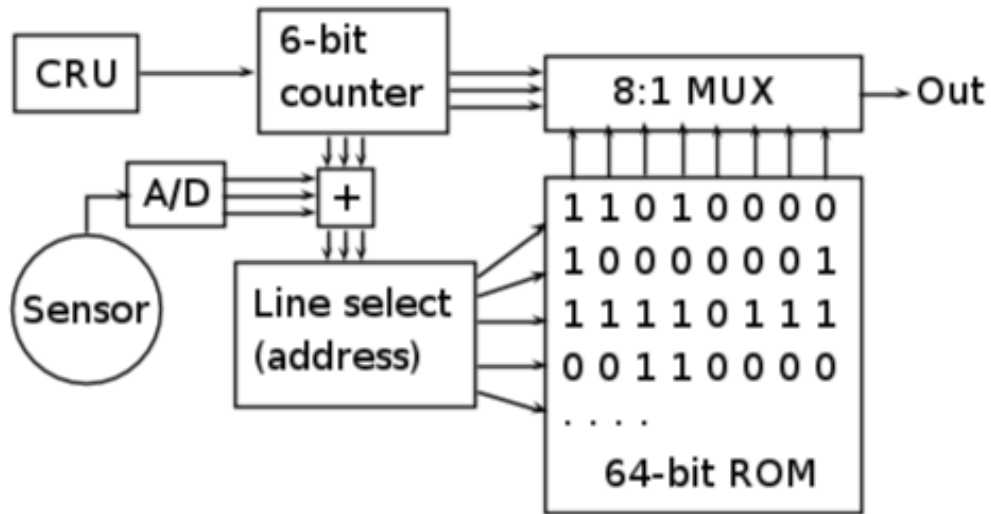


FIGURE 5.2: This block diagram is an example of a circuitry implementing the basic principle of Collective Communications. CRU stands for Clock Recognition Unit, recognizing and conveying externally induced clocking, i.e., by a reader device. The sensor and counter value determine the line select of the ROM, which together enable to output to a sensed value the corresponding bit sequence.

In order to ensure that different values transmitted (such as quality grades and sensor readings) can be retrieved from the superimposed signal, we directly encode the numerical values by using a single random bit vector  $z_0$  shared by all tags and the receiver. We obtain sufficiently different codes  $z_i$  for numerical values  $i$  by circularly shifting  $z_0$  by the amount of  $i$  bit, since shifting is a distancing operation (cf. chapter 3). In this way, a single bit vector  $z_0 \in \{0, 1\}^n$  can be used to encode  $n$  values, and thus save memory capacity on the smart label device. The received signal  $s = s_1 + s_2 + \dots + s_n$  is then simply a sum of encoded numbers  $z_i$ , directly encoding the multi-set of measured values. With respect to our application scenario described above the bit vector  $z_0$  need to be circularly shifted seven times, in order to encode all seven quality grades. Figure 5.1 illustrates a simultaneous bulk reading of a set of tags based on our Collective Communications mechanism: in our application scenario of product quality control all queried tags transmit their 64 bit sequence (generated by the 64 bit vector  $z_0$ ) at the same time. At the receiver side the superimposed signal is interpreted according to our Collective Communications algorithm (cf. chapter 3). In the next section we provide a preliminary draft of a circuit design for our envisioned OE smart label device.

### 5.3 Circuit Design

In the previous section we envisioned an example of an application scenario to utilize Collective Communications, where OE smart labels are determined to retain the quality grade of different types of sales items. The seven grades we predefined can be encoded

by a single 64-bit vector  $z_0$ , which determine the necessary bit-size of our envisioned OE smart label device. In the following we design for our devised application scenario the OE smart label circuitry. Based on our Collective Communications protocol described in chapter 3 the implementation of the smart label device relies merely on features, such as fetching the sensor value, reading and sending out the corresponding bit sequence  $z_i$ . Hence, the necessary building blocks for the circuit device are derived as follows: a sensor unit that consists of one Analog-to-Digital-Converter (ADC) and the sensor itself, a Read-Only-Memory (ROM) building block of fixed length containing a randomly drawn binary sequence, and a circuit logic block enabled to generate the corresponding bit sequence to the sensed value, i.e., by employing the hardwired bit sequence stored in the ROM and carrying out an internal circular shift operation on it. That is, depending on the current state of the counter and sensor value the line select of the ROM is incrementally rearranged, such that it generates for a specific sensor value an unique 64-bit sequence. For the sake of completeness indicating the necessary building blocks for a passive polymer tag (cf. Figure 5.2), the smart label device contains a Clock Recognition Unit (CRU) connecting the counter, which together drive the entire transponder circuit. In operation the CRU extracts and conveys clocking induced externally by a reader device. Further, the transponder circuit consists of a 6-bit counter realized by 6 D-flip-flops, a ROM with 64-bit capacity, and a 3-bit ADC digitizing the sensor value. Since our objective is to create a reader system for passive polymer tags, the smart label circuitry includes in addition a DC rectifier concerning power supply, and a modulator transistor to convey the transponder's binary information to the reader device by deploying inductive coupling. In Figure 5.3 we indicate in connection with the logic circuitry for external signaling (signal generator building block) the modulator transistor by a symbolic on-off switch. Further on, Figure 5.3 shows the schematic of an all-printable and passive polymer tag with its analog and digital electronic components. The principle for collective communications is integrated in the signal generator building block, where a bit sequence out of the ROM is generated according to a sensed value. The binary sequence is controlling the gate of the modulation transistor. For instance, when the modulator transistor is switched on, the transponder circuit draws power from the electromagnetic RF field of the reader. In reverse, when the modulation transistor is switched off, the transponder circuit draws still power from the RF field, but considerably less than it is consuming in the on-state. In this way, the binary information is transferred by means of load modulation to the reader, i.e., by varying the power consumption.

Taking a look back on our smart label circuitry from before, the block diagram in Figure 5.2 illustrates one possible implementation example of our CC, that indicates interacting between participating circuit blocks of a 64-bit polymer tag. However, for

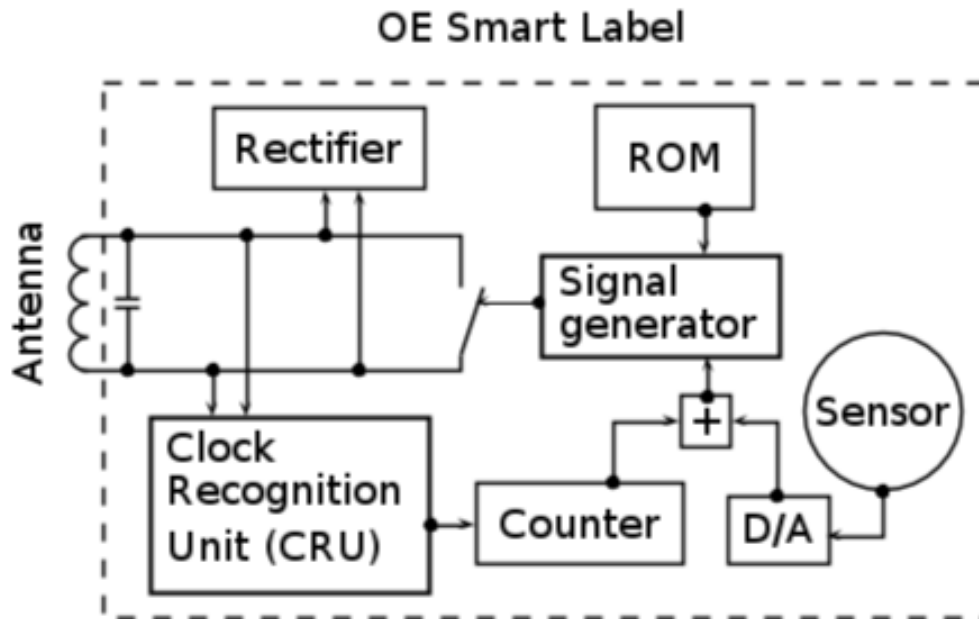


FIGURE 5.3: The circuit block diagram shows the holistic printable passive tag.

particular application scenarios such as sensing, classification, identification and tracking, the circuit design of a smart label can vary. For example, the unique 64-bit sequence for a particular product quality grade can be already printed directly on an OE smart label without to integrate the sensor unit. In this way a sales item of predetermined quality can be beforehand attached with a particular OE smart label reflecting the product quality grade. In this section we illustrated by means of a circuit block diagram an implementation example of our CC turned into an OE smart label circuitry. While most of the circuit blocks shown in Figure 5.2 and Figure 5.3 are self-explanatory, the Clock Recognition Unit (CRU) represents a proprietary solution to the issue of collective synchronization of a set of queried tags in a simultaneous bulk reading, i.e., the CRU enables smart labels to transmit bit-wise simultaneously their binary sequence in time slots provided by a reader (cf. Figure 5.1). In the following section we continue to describe in detail the Clock Recognition Unit (CRU).

## 5.4 Collective Synchronization Strategy

In the previous section we described in essence all needed building blocks for an OE smart label device to implement the protocol mechanism of Collective Communications in a mixed-signal integrated circuitry. While most of the electronic building blocks shown in Figure 5.3 are self-explanatory, the Clock Recognition Unit (CRU) represents a proprietary solution, that we are going to describe in the following in more detail. In principle the CRU, that is responsible to ensure collective synchronization and clocking

among queried tags, can be replaced by any conventional synchronization method, if and only if the OE hardware technology would indicate equal reliability and performance as the Si-based semiconductor electronics, that is mostly not the case, but is rather being hazardous (cf. appendix A reporting on printed RFID, and references therein). The key issue here is, that the switching speed of polymer printed transistors is too low to cope with the reader's generated electromagnetic HF field. Therefore, additional effort in OE system design is needed to cope with current polymer electronics deficiency. In particular, intrinsic variability of the printed electronic components within a circuit device do not always allow predetermined, accurate and reliable electrical behavior, when comparing prints of the same device (cf. appendix A). To overcome these issues such as slow switching polymer printed transistors and hazardous electrical behavior of printed circuits a global synchronization scheme among all queried tags is required, while tags back scatter their binary information at the same time to the reader. It needs to be ensured, that a sent bit information from a tag overlaps approximately with the other sending tags at the same time (cf. Figure 5.1). In a such bulk reading of smart labels in a dense area, i.e., when a set of tags are queried simultaneously, the response of the interrogated tags need to be thus collectively and bit-wise synchronized, but not necessarily phase synchronized as Figure 5.1 might imply<sup>1</sup>. On that issue, we developed for the reader system a collective synchronization method implemented in the transponder circuit. We placed this circuit functionality, as introduced above, in the Clock Recognition Unit (CRU) building block (cf. Figure 5.3). With respect to the polymer electronics constraints and the requirement for collective synchronization and simultaneous read-out of tags, the basis for our solution relies on the key idea of switching on/off the electromagnetic RF field of the reader device coil that empowers the polymer tags. By interrupting the wireless power supply all responsive tags can be instructed simultaneously to either *start with transmitting the first bit of data* or, to *send the next subsequent bit* of their binary information. In Figure 5.4 we illustrated all possible ways of initiating and requesting the next bit read-out showing overall four different ways to start and carrying out a simultaneous data transmission from a set of tags to reader<sup>2</sup>. For instance, all tags can be instructed to start with data transmission by either varying elapsed time of an intermission (i.e., time of no wireless empowering, cf. (a) and (b) in Figure 5.4), or varying the time period for empowering the polymer tags (length of a time slot, cf. (c) and (d) in Figure 5.4). Thus, in order to initiate each tag to start transmission at the same time the signaling from reader can be done

---

<sup>1</sup>In a query all tags transmit simultaneously one bit information per time slot. Figure 5.1 illustrates a such concurrent transmission of bit streams transmitted by several smart labels. Hence, in each synchronized time slot at the current bit index the bit information from all smart labels superimposes as intended on the RF channel generating a specific overlaid signal. At the receiver side (reader device) all superimposed signals generated in the provided time slots are captured and jointly evaluated alongside to our Collective Communication algorithm (cf. mechanism in chapter 3).

<sup>2</sup>In our example of application the transmission of data is based on inductive coupling.

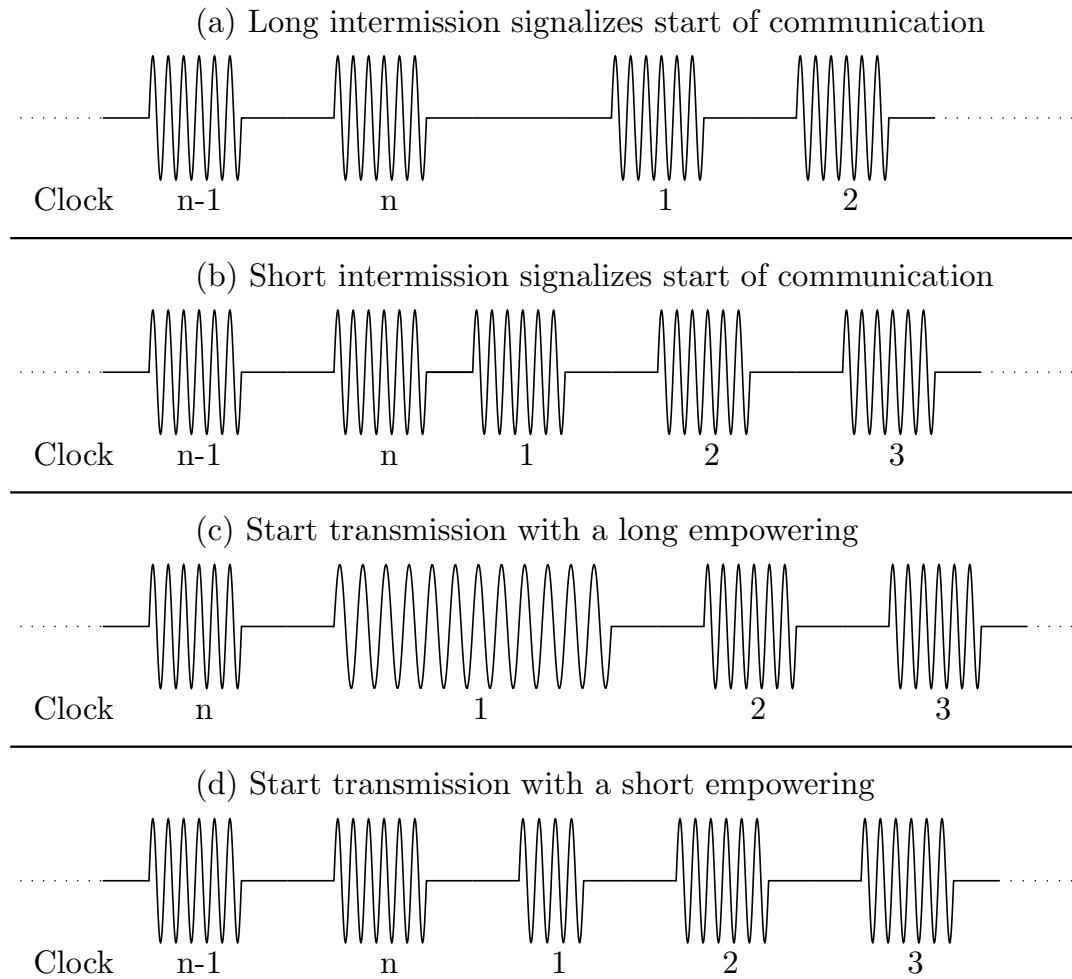


FIGURE 5.4: Four different patterns of reader signaling illustrate four alternatives of commands signaling with respect to a collective and simultaneous communication, when tags have to start and subsequently transmit their data back to the reader device.

either by turning off the reader device coil for a long time period (long intermission) and then start empowering the tags periodically with short intermissions (cf. specifically (a) in Figure 5.4), or begin with transmission by requesting the start bit in a long time slot followed by requesting the subsequent bit stream in regular sized time slots (cf. specifically (c) in Figure 5.4)<sup>3</sup>. Either way, the circuit logic in the CRU building block can be tuned to interpret request orders sent from reader device just based on capacitor discharge behavior and voltage comparator device shown in Figure 5.5. In particular, the circuit logic circuitry for recognizing the externally induced reader signals is connected with the tag rectifier. That is, diodes  $D1$ ,  $D2$ ,  $D3$ ,  $D4$  and capacitor  $C2$  build together conventionally the rectifier for a DC power supply of the tag. The inductor  $L1$  of the tag is the printed antenna, which in combination with capacitor  $C1$  builds together the

<sup>3</sup>The counterparts for (a) and (c) in Figure 5.4 correspond (b) and (d) in Figure 5.4.

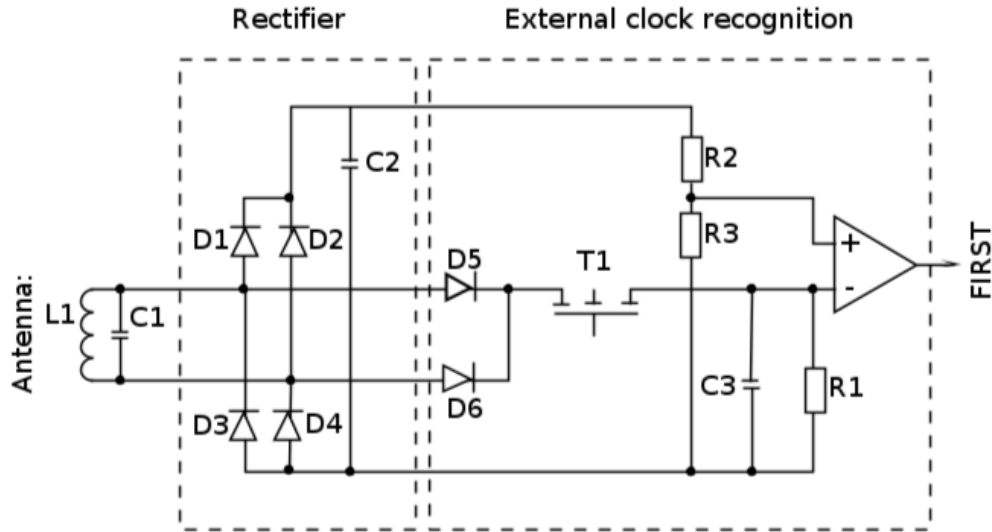


FIGURE 5.5: The schematic shows partially the circuit logic in connection with the tag rectifier for interpreting signaling coming from reader device.

$LC$ -network of the tag. The remaining electronic components in Figure 5.5, such as diodes  $D5$  and  $D6$ , transistor switch  $T1$ , resistors  $R1$ ,  $R2$  and  $R3$ , capacitor  $C3$  and the voltage comparator, build together the circuit function, which recognizes the reader signals depicted in Figure 5.4. In the following we continue to describe in detail, on how we derived and designed the circuit logic for recognizing and interpreting reader signals implemented in the Clock Recognition Unit (CRU).

#### 5.4.1 Synchronized Tags Based on External Clock Recognition

In the previous we introduced primarily our solution on how queried polymer tags can be externally synchronized, namely by switching on and off the electromagnetic RF field of the reader device. Based on a duration of an intermission and the length of time empowering the tags, a tag recognizes situation-dependently when to start and send the next subsequent bit information. The recognition and interpretation of an intermission (duration of no empowering) is implemented in the *external clock recognition* building block shown in Figure 5.5, whereby the whole concept of understanding the reader commands is implemented in the Clock Recognition Unit (CRU) shown in Figure 5.6. In the following we derive our solution with respect to recognition and interpreting of reader's initiated intermissions, enabling with it a synchronization of simultaneously queried tags. In order to implement a such intermission recognition on a tag our approach is based on observing of a capacitor discharge implemented within the circuit logic, which provides the ability to distinguish between a long and short intermission. As long as the tag is not empowered the capacitor discharges exponentially. And, when the tag receives empowering again the current voltage value of the capacitor is compared with an a priori

fixed voltage threshold using a voltage comparator. The outcome of it determines, if the tag's digital counter (cf. CRU in Figure 5.6) needs to be reset or increased by +1. Therewith, the recognition of various reader signals, that we illustrated in Figure 5.4, is implementable at low hardware complexity suitable for OE. In our particular circuit design shown in Figure 5.5 the circuit logic evaluates a reader signal directly at the receiving antenna (inductor  $L1$ ). For the DC power supply of the tag the wireless reader signal is rectified over the diodes  $D1$ ,  $D2$ ,  $D3$ ,  $D4$ , and smoothed over capacitor  $C2$ , supplying the tag with an operational voltage power. In addition, diodes  $D5$  and  $D6$  harvest the wireless power for capacitor  $C3$  when transistor  $T1$  is switched on, charging it at the same voltage level as the operational power supply of the tag. As soon as the tag is not empowered by reader device, capacitor  $C3$  discharges over the resistor  $R1$  exponentially [201]: if in the beginning  $U_0$  denotes the reference of voltage power of  $C3$ , the current state in time is described by

$$U_{C3}(t) = U_0 e^{-\frac{t}{R1 \cdot C3}}. \quad (5.1)$$

Based on elapsed time  $t$  and  $U_{C3}(t) = U_{threshold}$  the recognition of a long and short intermission can be established. In order to fix the voltage value  $U_{threshold}$  for a comparison task in our circuit logic, we utilize in our circuitry a voltage divider using resistor  $R2$  and  $R3$ . Since all circuit parameters, except for  $U_0$ , are fixed, thus the voltage value for  $U_{threshold}$  is only linear dependent by  $U_0$ . In our circuit design thus we apply the ratio of

$$a = \frac{U_{threshold}}{U_0}, \quad (5.2)$$

in order to gain a noncritical and total resistance  $R_{total}$  dividing the voltage value of power supply in the specified ratio, i.e.,

$$R2 = (1 - a)R_{total} \quad (5.3)$$

$$R3 = aR_{total}. \quad (5.4)$$

In operation, when the tag is empowered again after an intermission, the preceding elapsed time of the intermission is accordingly determined by comparing the current voltage value of capacitor  $C3$  with  $U_{threshold}$  using the voltage comparator. Further, transistor  $T1$  is switched off during the evaluation, such that the voltage value of capacitor  $C3$  remains unchanged. When the comparison between  $U_{C3}$  and  $U_{threshold}$  is done, transistor  $T1$  is switched on such that capacitor  $C3$  can be recharged again for a next evaluation round. For further processing of the sent reader signals the output of the voltage comparator is feeding the CRU circuitry shown in Figure 5.6. In the next subsection we continue from this point of view to describe the complete circuitry of the CRU.

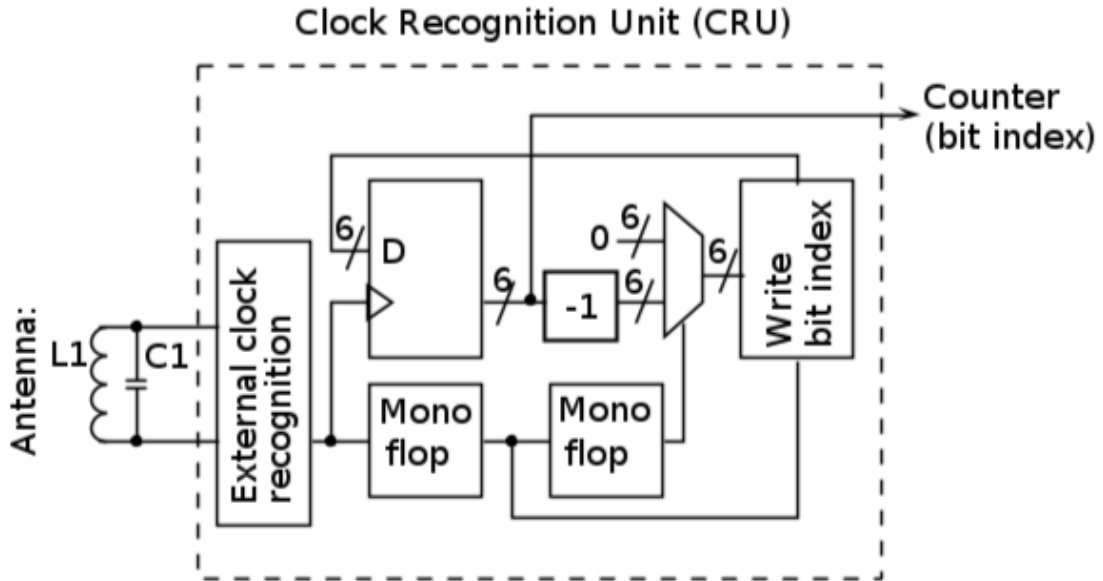


FIGURE 5.6: The schematic presents the Clock Recognition Unit (CRU) consisting mainly by two circuit functionalities, namely by (1) the circuitry for external clock recognition induced by a reader device, and (2) the circuit function for a counter to determine global bit index. The bit index determines and indicates current bit position for all simultaneously queried tags, that need to be send out in the following cycle.

#### 5.4.2 Clock Recognition Unit (CRU)

In the previous subsection we derived in detail the circuit function for the *external clock recognition* shown in Figure 5.5, which represents in our solution an integral building block in the Clock Recognition Unit (CRU) shown in Figure 5.6. In the following we complete our description of the solution towards synchronization of polymer tags, that we integrated in the CRU. While the circuit function in the *external clock recognition* building block is designed to recognize intermissions, that are induced by reader's wireless power discontinuances (cf. Figure 5.4, the circuitry of the CRU shown in Figure 5.6 is determined to provide a clock counter on tag containing the current *bit index* of tag's binary data requested from reader device. In particular the bit index indicates the position within a bit sequence, whose bit information is transmitted to the reader device. In Figure 5.1 we show exemplary a simultaneous readout of several tags transmitting bitwise their 64-bit messages back to the reader. In operation of the tag the internal clock counter, implemented in the CRU, is resetting the bit index to zero, when a reader signal empowers the tag for a long time period (in contrast a short power signal can also be used for resetting, cf. different patterns of reader signaling such as (c) and (d) shown in Figure 5.4). And, the clock counter starts incrementing its value by +1, when the next intermission is registered by the circuit logic. The counter value is preserved temporarily by a memory buffer realized with D-flip-flops represented by *write bit index*

building block shown in Figure 5.6. This type of cache device keeps the storage content even if the polymer tag is not empowered for a short term, i.e., when the reader device initiates an intermission to signalize the next time slot for transmission. Before increasing the bit index an additional memory buffer realized by D-latches stores temporarily the current bit index and induces the bit transmission. After increasing the bit index, it is delayed rewritten in the bit index buffer. Hence, the mono-flops in the circuit block provide the necessary delay for a consecutive and stabilized update, rewriting the content of memory buffer to zero, if a long time period of empowering was received, otherwise current counter value is incremented by +1 and forwarded with regard to further processing outside the CRU. In Figure 5.6 we show the circuitry for the CRU, which implements in particular the recognition and interpreting of reader signaling (c) illustrated in Figure 5.4. In order to implement the recognition and interpreting of reader signaling (d) illustrated in Figure 5.4, the control line for resetting to zero (select line of the multiplexer shown in Figure 5.6) needs to be additionally inverted. Since wireless empowering discontinuances are adopted for synchronization of polymer tags, a reliable source of power supply in a tag poses a critical issue with regard to implementing a functioning passive polymer tag. Therefore, we prefer the implementation of reader signaling according to pattern (c) shown in Figure 5.4. However, the implementation of reader signaling according to pattern (d) shown in Figure 5.4 can also be utilized in a passive reader system. Depending on a circuit technology for polymer electronics and OE the performance of the proposed types of passively operating polymer tags can vary, though. To find out which type of tag is more appropriate for OE and a passive reader system, this issue, however, is within the framework of this thesis out of scope. In the following section we investigate quite the issue of passively transmitted data using superimposed information transfer, that is essential for utilizing Collective Communications (CC) in a passive reader system.

## 5.5 Simulation Results

In this chapter, so far, we created a passively operating polymer tag, which integrates the CC mechanism in its circuitry without to know, if last modulation communication using superimposed information transmission is working at all. In chapter 3 including chapter 4 we proved that our CC approach is efficiently and robustly operating in an active reader system employing ON-OFF Keying (OOK) for the simultaneous and overlaid wireless communication. In the following we analyze in particular the applicability of the CC approach realized in a passive reader system. To do so, in LTspice (a well-known circuit simulator, cf. reference [202]) we established a simulated passive reader system for our analysis, where we placed an antenna coil in the LTspice simulation

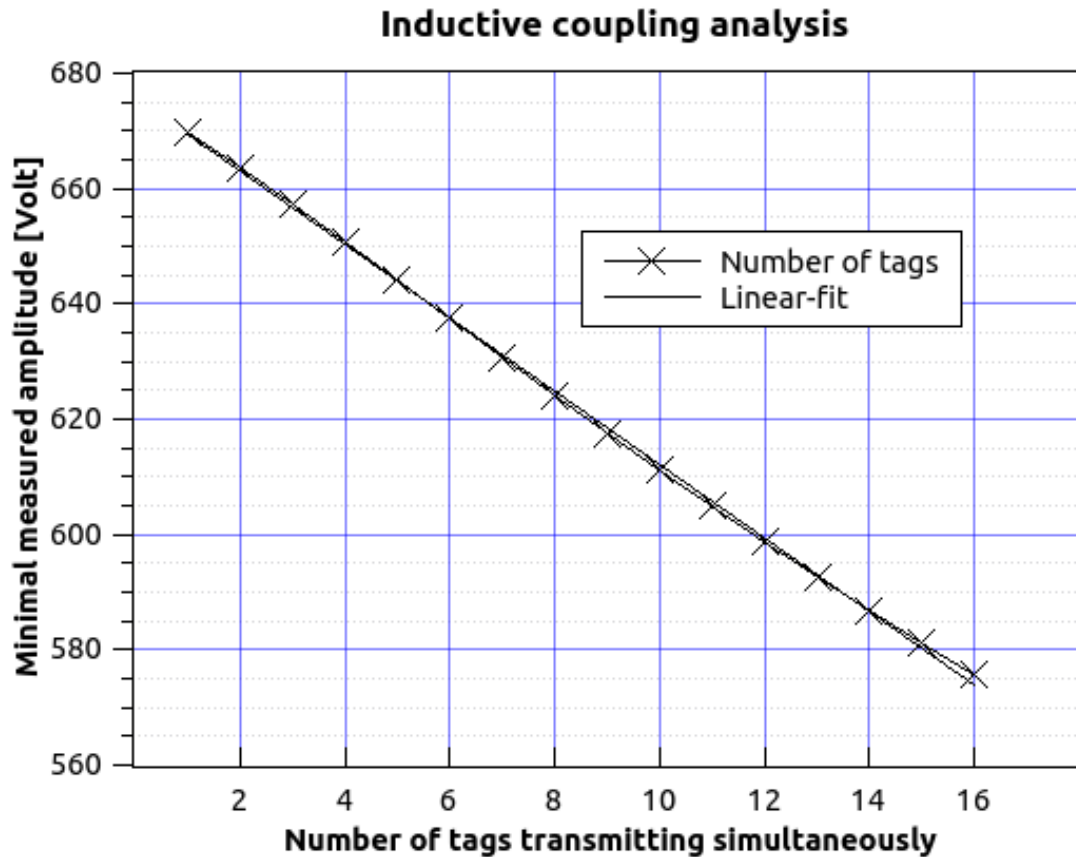


FIGURE 5.7: The overall signal analysis indicates the maximal amplitude difference between different trails with up to 16 simulated passive tags transmitting simultaneously.

environment to mimic a reader device, generating with it an electromagnetic RF field in HF to empower simulated passive transponders. In particular, we enabled with it a wireless empowering of up to 16 simulated passive transponder circuits, that can be arbitrarily placed within the simulation environment by assigning them customized inductive coupling coefficients. Depending on various setups of passively switched on tags the change in the electromagnetic RF field strength, i.e., the amount of drawn energy from the RF field is recorded in time and evaluated at the reader side. With regard to parameterizing the simulation, we chose default parameters from standard RFID reader systems, such as 10 cm in diameter for the reader antenna coil, and 2 cm in diameter for the tag antenna, which conforms to the inductive coupling coefficient of 0.025. The portability of the simulation with respect to polymer electronics is taken for granted, because the key parameter for inductance applies for printed antennas and circuits [203]. In order to simulate different tag positions in relation to the reader antenna, respective, different sizes of tag antennas the coupling coefficient is varied. For the resonant circuit of the reader device generating the 13.56 MHz RF signal the hardware parameters are chosen according to Finkenzeller [30, Chapter 4.1]. The inductance is set by  $2 \mu\text{H}$  with

resistance of  $2.5 \Omega$ . The capacitor is set by  $68.8 \text{ pF}$ . Further on, for the tag coil we chose  $100 \text{ nH}$  and  $0.1 \Omega$ . The results of our signal analysis are shown in Figure 5.7, that indicate the minimal measured amplitude strength for  $n$  simulated passive tags transmitting simultaneously. Therewith, we acquired the maximal amplitude difference distinguishing with it the number of responsive tags. Further on, our simulations show, that the more passive tags response the greater the distinctive features appear among the captured superimposed signals. In essence, the signal strength drop of the electromagnetic RF field behaves proportional to the number of tags drawing simultaneously on the wireless power by last modulation (cf. Figure 5.7). Thus, the analysis of the simulation results suggests, that the deployment of CC in a passive reader system is applicable. Now that we integrated CC in a circuitry on a passively operating transponder circuit, and proved its applicability with respect to a passive reader system, in the following section we continue to investigate the feasibility of our implementation example regarding an OE smart label.

## 5.6 Feasibility Assessment

In the course of implementing the CC mechanism into a passively operating polymer tag and proving its applicability for a passive reader system described above, in the following we provide a feasibility assessment towards printing the implemented example of an OE smart label with current printing technology. A matured and commercially available OE printers for a common customer does not exist yet, but in industry and research exist various and advanced OE technologies promising to become operational in the near future (cf. appendix A). The development of different and versatile printing technologies (such as inkjet, gravure, offset and screen printing), circuit organic technologies (such as unipolar, ambipolar and CMOS-like transistor circuit technology), as well electronic inks (such as carbon nanotubes and pentacene), made in the past a significant progress, but, however, the deployment of these technologies is currently rather confined to the printing of circuit devices at lab-scale (cf. references [7, 8]). The realization of printing electronic devices in mass production at industrial-scale is the major goal, though, representing a key issue of present-day research (cf. appendix A), and references therein). With respect to currently printable smart labels, in chapter 2 we reviewed some essential state-of-the-art works, where all described references indicate a feasibility of printing circuits with low hardware complexity. But, non of them has yet enabled the printing of circuits implementing highly complex functionalities, such as an organic printed RFID chip with large number of transistors. While printing of circuit devices in a lab using for example a vacuum deposition method is achieving a hardware complexity of about 13k transistors [204], approaches deploying mass-printing technologies such as gravure and

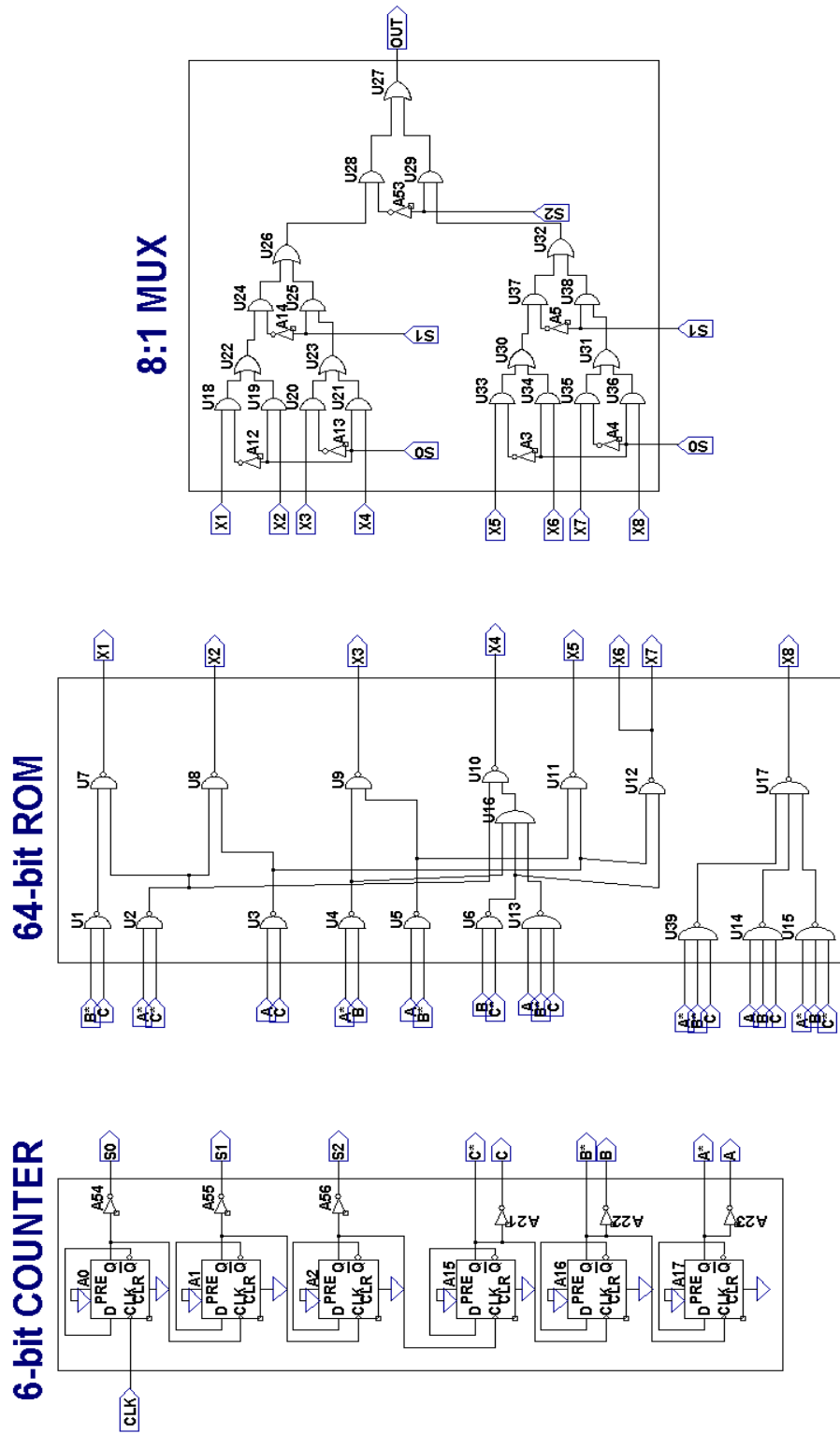


FIGURE 5.8: The schematic of this circuit arrangement implements with respect to our 64-bit polymer tag the remaining part of the tag's circuit logic.

offset printing achieve a much less hardware complexity of functional printed circuit devices (cf. background chapter 2 and appendix A). For example, PolyIC [205] is reporting in this matter on mass-printed circuit devices with a hardware complexity of up to 2k transistors, whereby they also report on challenges experienced in their mass-printing trials to achieve a high yield at all. Apart from considering the hardware complexity, that a mass-printing technology can achieve maximally in combination with a high yield, the print resolution has a major performance impact on either, the functioning of the circuit device and the occupied printed area on a deployed substrate. For instance, mass-printing technologies feature a print resolution of about  $10\ \mu\text{m}$  (cf. appendix A), such that a printing of a traditional RFID chip integrating 72k transistors is, figuratively speaking, occupying at best an area of a 'credit card' size (the printed antenna around is not included into this account) [39]. Either way, to make PE applicable for manifold application scenarios the minimization and optimization of OE circuit design is inherently immanent. Furthermore, one may even have to sacrifice a major part of essential circuit functions to enable an application scenario with OE smart labels at all (e.g., excluding the cryptography functionality and simplifying the communication protocol in a printed RFID circuitry). Further on, printing technologies for PE with a print resolution below  $< 5\ \mu\text{m}$  exist, such as inkjet and screen printing in combination with photolithography (cf. appendix A), but those can be hardly deployed with regard to the demand of enabling mass-printing. However, considering all approaches and encountered issues, hence, we adopt that for a mass production the printing of circuit devices, indicating a hardware complexity with few hundreds of transistors (i.e.,  $< 1\text{k}$  transistors) can be presumed to be viable in the near future.

In respect to our implementation example described above the hardware complexity of our passively operating polymer tag need to be within the constraints the OE is currently indicating. However, as we pointed out in chapter 3, CC mechanism is specifically laid out to enable a minimalistic circuitry, which facilitates intrinsically at the same time maximal possible performance in terms of highly scalable communication, efficiency and robustness. In particular, our CC construction of exploiting concurrent and superimposed information transfer provided primarily to move complexity (hardware, as well software) from tag towards to reader side. In order to determine the hardware complexity of our proposed passive tag, and for the sake of completeness, the remaining part of the circuitry, that we implemented in LTspice, is supplementary shown in Figure 5.8. In this figure we show a 6-bit counter driving the read-out of a hardwired 64 bit sequence, that is partially indicated in Figure 5.2. As can be seen from the circuit block diagram shown in Figure 5.3, the depicted circuits in Figure 5.5, Figure 5.6 and in Figure 5.8, the entire hardware complexity of our tag is reduced to about few hundreds of transistors. More precisely, if we apply an unipolar circuit technology [206, 207] to implement the

circuitry of our tag at the transistor-level, the number of required transistors is estimated with about  $\widetilde{500}$  transistors<sup>4</sup>.

Considering merely the circuit complexity of our tag in relation to some other printed electronic devices manufactured by various research facilities possessing the OE know-how, the fabrication in a clean room of 64-bit ROM devices was already experimentally verified (cf. references [80, 96, 208], or appendix A). The printing of a holistic 4-bit RFID tags employing load modulation for communication is described by reference [205]. In relation to our proposed tag described above, all required circuit functions for it can be printed holistically using a current OE technology. In the following section, we continue discussing about possible technical issues and chances of our proposed example of a passively operating polymer tag integrating the CC mechanism in its circuitry.

## 5.7 Discussion

So far, we implemented an example of a holistically printable polymer tag that is minimalistic without to print it actually with current printing technology, because it requires still at the present miscellaneous and tremendous resources, such that a conducting of this intend with respect to the thesis is out of scope. However, its applicability is indicated with regard to OE as we conducted in the previous section. Hence, the remaining challenges after our implementation example indicate to be manifold, ranging from actually manufacturing the polymer tags, up to designing and producing a reader device specifically tailored for a passive reader system including superimposed information transfer. Thus, the left challenges indicate mainly engineering issues in association with a specific business case, such that we propose in this matter a follow up, where the final issues can be tackled and resolved in a future project combined favorably in a business formation.

Apart from challenges to enable mass-printing at all (cf. appendix A), current OE technologies entail in addition a further basic key issue, namely the printing of hazard-free operating printed circuits ranging in the same hardware complexity as of our proposed passive tag. The development of specific circuit design rules and characterization for a certain OE technology represents in research an own daunting task, that we address this matter to facilities and companies developing specifically PE technology (cf. appendix A). Thus, the development of reliable and ready-to-use OE technology is with regard to this thesis out of scope.

---

<sup>4</sup>Based on how the building blocks for the circuit logic are implemented in OE at transistor-level the count of transistors can vary. The integration of alternative building blocks and further circuit functions such as an Analog-to-Digital Converter (ADC), or by making use of a complementary circuit technology the number of transistors can vary correspondingly.

In relation to our implementation example of a printable passive tag upon some circuit functions need to be especially taken care. For instance, the analog components in the *external clock recognition* building block, such as the voltage comparator and the RC-element for timekeeping (cf. Figure 5.6), need to be printed with high accuracy, in order to diminish unwanted variability in the printing process, so that the circuit characteristic remains consistent. A further elementary issue of OE occurs, where the transmission range regarding polymer-based printed transponders indicates a low modulation index as this was reported by reference [209]. This may, however, constrain the free scalability property of collective communications, i.e., to be able to read-out many tags at once. Further on, in the background chapter 2 we investigated the incentive for developing OE smart labels, and stated that in contrast to the deployment of silicon chips, OE is promising to become in terms of item-level tagging and IoT an economically viable technology. This advantage of OE is justified based on the fact that mass printed OE devices are cost-efficient in contrast to fabricated silicon chips in a foundry used to manufacture the more cost-intensive Si-based electronic devices. With respect to transistor count of a device an OE printed transistor is, however, less cost-efficient than a silicon one on chip. In essence, the price for a single chip is mostly determined by how many chips can be gained out of one silicon wafer in a chip foundry. Here, the price for manufacturing a single wafer is fixed without to consider the number of chips, that can be made out of it. In a hypothetical calculation, Kanellos [25] is reporting, that, in order to make a Si-based RFID technology economically viable, i.e., to make a 1-penny RFID tag, 100,000 tags need to be made out of a single silicon wafer costing about 1,000 dollar. If we take a silicon wafer featuring a diameter of 200 mm, then we get for one chip an area of  $\approx 0.31 \text{ mm}^2$ . Depending on a deployed  $\mu\text{m}$ -technology the maximum available hardware complexity for a circuit area can be determined. In relation to the low hardware complexity of our tag indicating about few hundreds of transistors, hence it is worth to pursue the investigation of utilizing Si-based technology in future work.

## 5.8 Summary

In this chapter we implemented with regard to smart packaging, item level tagging and organic printed smart labels one example of a passively operating polymer tag, which integrates our code-based Collective Communications (CC) mechanism, that we described originally in chapter 3. In particular, we integrated the CC mechanism into the circuitry of a passive tag at logic gate level, and investigated its applicability with respect to a passive reader-tag-communication. For the enabling of simultaneous and superimposed information transmission in a passive reader system, we developed specifically an external and centralized clock synchronization strategy, that we integrated directly into the

front-end of our proposed polymer tag. In a feasibility assessment we determined the hardware complexity of the tag indicating a transistor count of about few hundreds of transistors, being thus appropriate to be printed with present-day printing technology. However, variability in the printing process and low hardware performance of current OE technology constrains its realization, i.e., entailing risks concerning a faulty functioning, and that, despite of the tag's low hardware complexity we achieved in the circuit design. For instance, low communication range and hazard-afflicted circuits, encountered by other organic printed devices with similar hardware complexity (cf. appendix A), can reduce the domain of OE application scenarios. The development of novel conductive inks, improving of circuit design rules with respect to mass-printing and printing technology, promises to resolve these OE issues in the future, though. In our discussion, however, we stated additionally that a pursue of manufacturing the tag with Si-based semiconductor technology in a chip foundry can be worth, since the low hardware complexity of the tag allows a high yield to gain out of a single silicon wafer.

## Chapter 6

# Time-Based Collective Communications for Resource-limited IoT

In chapter 3 we presented the code-based Collective Communications (CC), that we specifically tailored for printable and low-performing RFID smart labels. We utilized simultaneous information transfer and superimposed radio transmission. With regard to low-performing Organic and printed Electronics (OE), in chapter 5 we implemented exemplary a smart RFID label at logic gate level employing the CC concept. In the following chapter we extend and adapt our approach of exploiting the RF channel for simultaneous data transmission and processing to resource-limited Wireless Sensor Networks (WSN). In particular, we are going to utilize the principle of superimposed radio transmission to calculate *desired mathematical functions* on the RF channel, realizing in this way data processing at the time of wireless superimposed transmission.

### 6.1 Introduction

In relation to the Internet of Things (IoT) [9] and its impact on pervasiveness of item-level tagging [45, 161], we presented in the previous chapter 3 our approach of code-based Collective Communications (CC) tailored for printable and low-performing RFID smart labels [59, 173]. The key ideas we utilized for CC are based on simultaneous information transfer and superimposed radio transmission [51, 52]. With regard to low-performing OE [81, 210], in chapter 5 we implemented a smart RFID label at the logic gate level employing the CC approach. In the following chapter we extend our key ideas of exploiting the RF channel for simultaneous data transmission and processing for the development

of resource-limited WSNs [15, 47, 49, 211–213]. In particular, we are going to utilize the principle of superimposed radio transmission to calculate mathematical functions on the RF channel, realizing in this way data processing at the time of wireless superimposed transmission. In contrast to traditional processing of sensory data obtained in a standard WSN [214], our approach of processing data directly over the wireless channel represents a paradigm shift. With respect to the demand of disposable IoT devices [21, 24] and sustainable sensor networks [48] being, e.g., environmental friendly, we expect that future IoT devices are going to be heavily resource limited, possibly parasitic or passive powered nodes [215, 216]. Due to their expected restriction in terms of computational capabilities, we presume that such nodes will be virtually unlimited empowered. In our modeling we exploit this property by trading computational load for communication load. By doing so, we are going to present a communication scheme by which mathematical computations are executed at the time of wireless transmission. This transmission scheme is enabling execution of complex computations by a network of resource restricted, cooperating nodes at a computational load possibly below the operation's computational complexity. In our elaboration, we firstly derive the scheme analytically, then secondly, we explore its feasibility with regard to dense networks deploying mathematical simulations, and thirdly, we demonstrate its practicability in a case study with 15 nodes. In particular, we will show how to calculate *addition, multiplication, subtraction, division*, or any type of mean solely during transmission on the wireless channel by sufficiently encoding values as Poisson distributed burst sequences. Further on, we discuss the partial computation on the wireless channel of other relevant functions.

The following chapter is structured as follows. In section 6.2 we introduce our transmission scheme that enables calculation of mathematical functions on the RF channel. We show how to encode values by Poisson distributed burst sequences, and illustrate the outcome of wireless superimposed computing. Further, in subsection 6.2.1 we discuss implementation of some concrete functions that can be executed completely and partly on the wireless channel. Subsection 6.2.2 describes various mathematical functions being computable over the wireless channel. In section 6.3 we describe a prototypically implemented WSN platform with 15 simple nodes, that we utilized to conduct a case study in our lab, demonstrating the performance of our approach. Section 6.4 summarizes this chapter.

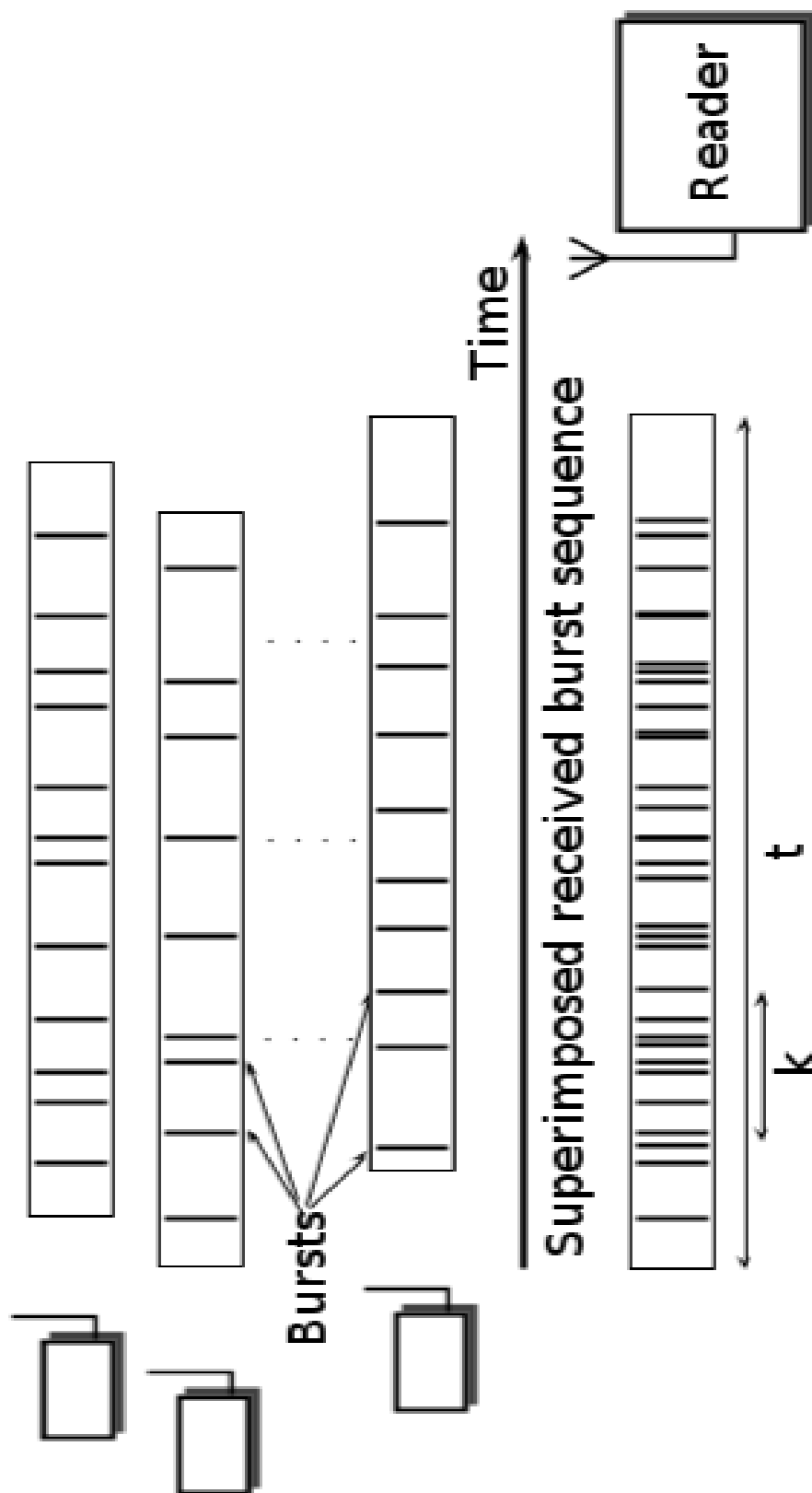


FIGURE 6.1: Burst-sequences encoding the sensor values of the sensor nodes superimpose on the RF channel. The reader device receives the outcome of a function computation.

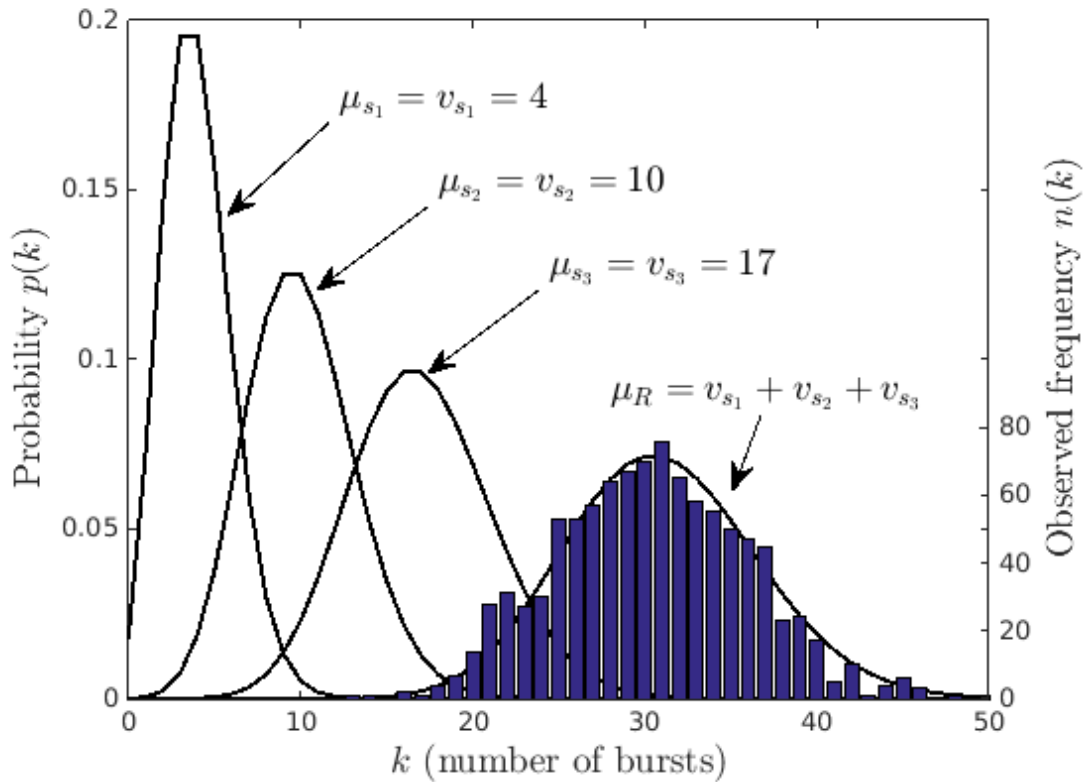


FIGURE 6.2: The sum of Poisson processes with mean value  $\mu_i$  yields again a Poisson distribution with  $\mu = \mu_1 + \mu_2 + \mu_3 + \dots$  and  $p(k; \mu t) = e^{-\mu t} \frac{(\mu t)^k}{k!}$ .

## 6.2 Approach for Function Computation via RF Channel

In chapter 2, where we provided the background and reported on the related works, we discussed thereof various WSN approaches, which utilize the idea of function computation over wireless channels, such that the outcome of it can be communicated to a fusion center. In comparison, we pursue a different approach to calculate basic mathematical functions on the wireless channel. We exploit at the time of simultaneous transmission the robustness of random burst sequences against the collision of individual bursts. We utilize Poisson distributed burst sequences which keep much of their properties when combined. That means, for two sequences encoding the Poisson variables  $\chi_1$  and  $\chi_2$  with means  $\mu_1$  and  $\mu_2$ , their combination  $\chi_1 + \chi_2$  again yields a Poisson distributed variable with mean  $\mu_1 + \mu_2$  [217].

Assume a set of weakly synchronized, distributed IoT nodes  $\mathcal{N}_i; i \in \{1, \dots, n\}$ , each holding a value  $v_i$  which is to be combined during simultaneous wireless transmission, thereby computing a function  $f(v_1, \dots, v_n)$ . In this operation, a receiver obtains the result of  $f(v_1, \dots, v_n)$  rather than the distinct values  $v_i$ . We represent the values  $v_i$  as the mean of a Poisson distribution. To encode this distribution in a transmit sequence, we

choose the following design. Instead of classical transmission protocols we employ burst sequences that constitute a sequence of possible Transmit Intervals ( $\mathcal{TI}$ ) of identical length. In each of these intervals, a transmitter is either silent or transmits a burst. A burst sequence of length  $t$  is divided into  $\kappa t$  sub-sequences of  $\mathcal{TI}$  length  $\frac{1}{\kappa}$ . Each of these subsequences contains with probability  $p_\kappa$  one or more of a finite number of bursts. The Poisson distribution then defines the probability to find  $k$  bursts in this sequence as [218]

$$p(k; \mu t) = e^{-\mu t} \frac{(\mu t)^k}{k!}. \quad (6.1)$$

The parameter  $\mu$  determines the density of bursts within the sequence. The larger  $\mu$  is, the smaller the probability of finding no point. It is also the mean of the distribution. The process of superimposing burst sequences generated by sensor nodes is illustrated in Figure 6.1.

To transmit a value  $v_i$  we define a Poisson process with mean  $\mu = v_i$ . The transmit sequence is then designed such that each of the sub-intervals has the probability  $p(k; \mu t)$  (cf. Equation (6.1)) that it contains exactly  $k$  bursts. To observe the value  $\mu$  at a receiver, we extract the count  $N_i$  of sub-sequences with exactly  $i$  bursts as well as the total number of bursts  $T = \sum_{i=1}^n i \cdot N_i$ . If  $N = \sum_{i=1}^n N_i$  is large, we expect that  $N_k \approx N p(k; \mu t)$  [218]. We can conclude

$$\begin{aligned} T &\approx N (p(1; \mu t) + 2p(2; \mu t) + \dots) \\ &= N e^{-\mu t} \mu t \underbrace{\left( 1 + \frac{\mu t}{1} + \frac{(\mu t)^2}{2!} + \dots \right)}_{\rightarrow e^{\mu t}} \\ &= N \mu t \end{aligned} \quad (6.2)$$

and therefore

$$\mu t \approx \frac{T}{N}. \quad (6.3)$$

A receiver can therefore extract  $\mu$  from a received sequence. Although this process is exhaustive to transmit a single value, due to the properties of the Poisson distribution, it can be used to interpret the superimposition of various such Poisson-distributed burst sequences as the sum of the values  $v_1, \dots, v_n$  they represent.

Figure 6.3 depicts a superimposed burst sequence observed by a receiver device in our case study (see section 6.3).

Observe that burst sequences are not required to be exactly aligned. Since in each sub-sequence of a burst sequence the same probability applies to distribute a number of bursts uniformly, a relative shift of the burst sequences does not change the overall probability in the superimposed sequence.

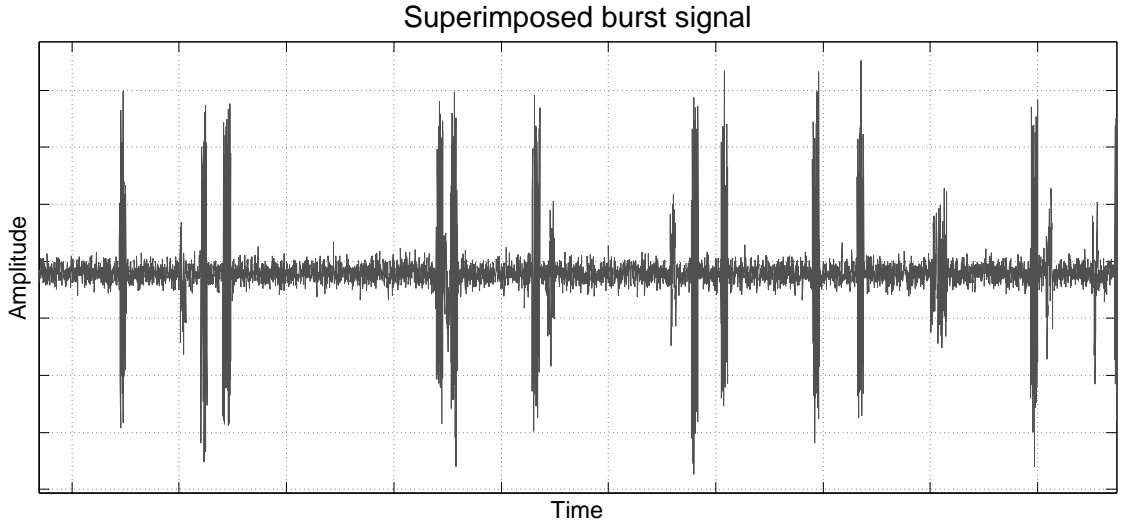


FIGURE 6.3: A burst signal superimposed by 15 transmit nodes as observed by the receiver.

Since a burst sequence is constituted from a concatenation of Poisson distributed sub-sequences, it basically represents a set of  $\kappa t$  random experiments of length  $\frac{1}{\kappa}$ . By relaxing the receiver to consider a superimposition of only  $\kappa t - 2\alpha$  experiments starting after the first  $\alpha$  experiments in the observed superimposition, a misalignment of  $\alpha \cdot \kappa t$  bursts can be compensated. Other issues common in wireless networks regard the identification and counting of nodes, the communication of meta-data (e.g., unit of measure, type of sensor) or the elimination of values from miscalibrated nodes. We can solve the former two issues by adding a preamble that uniquely identifies sensor ID, type or unit of measure. In our earlier work [59, 173], we presented an approach to achieve this in a network of unsynchronized, simultaneously transmitting nodes. Since the channel-based calculation proposed exploits a random process repeated in  $\kappa t$  sub-sequences, we can also identify and eliminate values from a limited number of miscalibrated nodes by having each node transmit only in  $\frac{1}{\epsilon}$  random sub-sequences. A receiver can identify and ignore sub-sequences that deviate from the majority of sequences in its estimation of the superimposed value. Clearly, a collision of bursts will induce a small error. However, when the  $\mathcal{TI} \cdot n \gg T$ , this error is negligible. Provided that the burst sequence is sufficiently sparse, this process can be scaled to an arbitrary number of signals transmitted simultaneously. The computational load at the receiver remains the same regardless of the count of sequences combined, improving in efficiency with increasing count of participants.

## 6.2.1 Basic Operations on the Wireless Channel

In the previous section we theoretically modeled simultaneous communication and processing via RF channel of sensory data observed in a WSN. Thereafter, we outlined its strengths, restrictions and possible drawbacks. In the following we are going to elucidate our approach by exemplifying the proposed coding and transmission scheme for sensor values. Further, we are going to describe basic mathematical operations such as *addition* and *multiplication* to calculate primitive functions on the RF channel, and derive with respect to various WSN application scenarios further essential mathematical functions of interest that can be calculated over the wireless channel efficiently.

### 6.2.1.1 Scenario 1: Counting

As we elaborated in the previous section the coding of a sensor value  $v_i \in \mathbb{R}$  is determined by a random burst sequence following a Poisson distribution with  $p(k; \mu_i) = \frac{\mu_i^k e^{-\mu_i}}{k!}$ . The parameter  $\mu_i$  is set proportionally equal to the sensor value, e.g.,  $\mu_i = v_i$  and  $v_i > 0$ . In case the sensor value  $v_i \leq 0$  the setting of  $\mu_i$  needs an offsetting by a constant  $c$ , i.e.,  $\mu_i = v_i + c > 0$ .

To demonstrate our coding and computation scheme exemplary we show this by implementing a common WSN task: the inquiry for the number of how many sensor nodes are still active in a WSN. According to our approach and its conducting, all active sensor nodes transmit at the same time and simultaneously (triggered by a piloting signal) a constant but the same value (e.g.,  $\mu_{s_i} = v_{s_i} = 1$  coded by random burst sequences) to a base station the reader. Since all simultaneously transmitted burst sequences convolve on the RF channel, and the convolution yields an addition of all bursts, the reader can easily extract the number of active transmitter nodes, namely by applying Equation (6.1), which means the calculation of the average number of bursts occurring in a sub-interval is answering the inquiry. In Figure 6.4 we give an actual example of such inquiry illustrating our approach, where three active sensor nodes  $\{s_1, s_2, s_3\}$  transmit the same value  $v_{s_i} = 1$ . Observe that all random burst sequences indicate a different pattern but represent according to the set Poisson parameter  $\mu_{s_i} = v_{s_i}$  the same constant sensor value. At the receiver side in reader  $\mathcal{R}$  all occurring bursts are subdivided into sub-intervals and counted. Out of it the average of bursts in a sub-interval is derived representing in our example the number of active sensor nodes  $\mu_{\mathcal{R}} = \mu_{s_1} + \mu_{s_2} + \mu_{s_3} \approx 3$ .

Observe that in addition to a random burst sequence the transmission of  $v_{s_i} \in \mathbb{R}$  is further characterized by a fixed time frame of length  $t$  divided into  $\kappa$  sub-intervals, which in turn in practice a sub-interval is divided by the burst signal length.

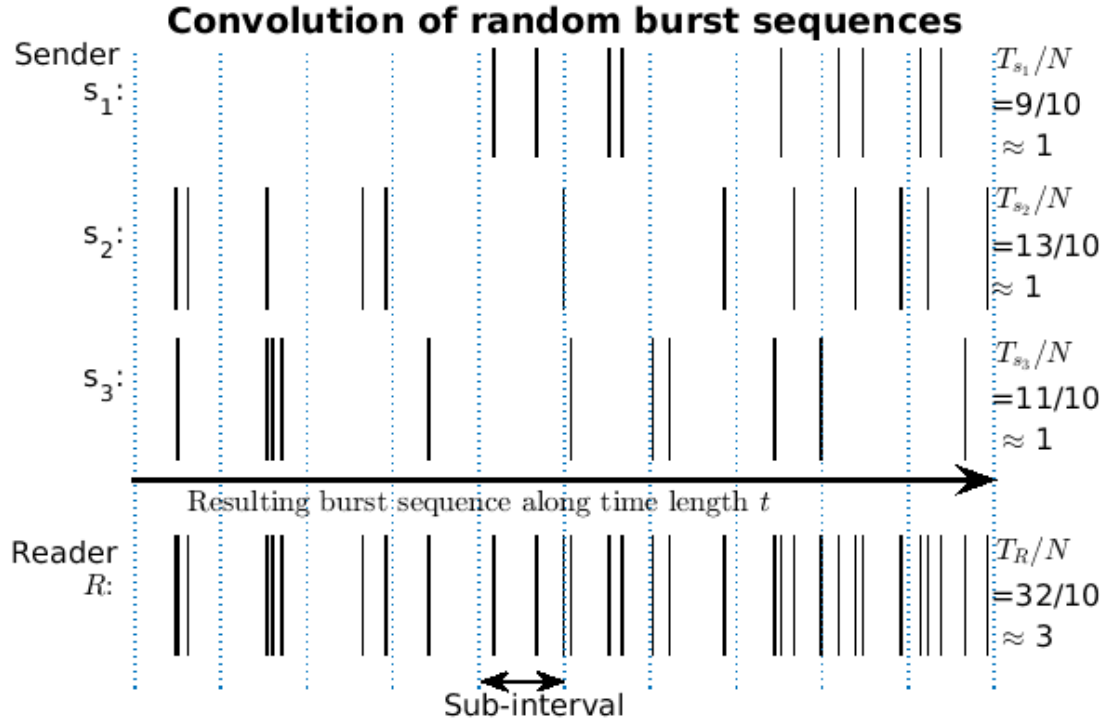


FIGURE 6.4: Three sensor nodes transmit simultaneously random burst sequences encoding a constant value  $\mu_{s_i} = v_{s_i} = 1$ . A reader device captures the superimposition and calculates  $\mu_R \approx 3$ . A short time frame and the collision of bursts observed in second sub-interval the function computation results into a bias calculation of  $\mu_R = \mu_{s_1} + \mu_{s_2} + \mu_{s_3}$ .

Note that the computation of  $T_{s_i}$  the total number of bursts generated in a time frame of length  $t$ , and  $\mu_{s_i}$  require with respect to the computable function further mathematical operations imposing a preprocessing on a sensor node. This, however, is a monotonous process, independent of the actual value encoding, that can be implemented in the transceiver module in hardware, so that it then not induces computational load at the receiver. Depending on the intricacy of function being computable via RF channel, at the receiver side likewise a specific post-processing need to be established in the reader hardware.

In relation to our demonstration example above, however, this requests besides preprocessing and post-processing of further necessary processing steps upon the received burst sequence at the reader device  $\mathcal{R}$ : first, the issue of dealing with the uncertainty of the utilized random process in our encoding scheme inducing a natural statistical error, and second, the systematic error induced by collisions of bursts during simultaneous transmission. In addition, the process of recognizing incoming burst signals correctly is not trivial, such that registered events can become very often indistinguishable for the reader device.

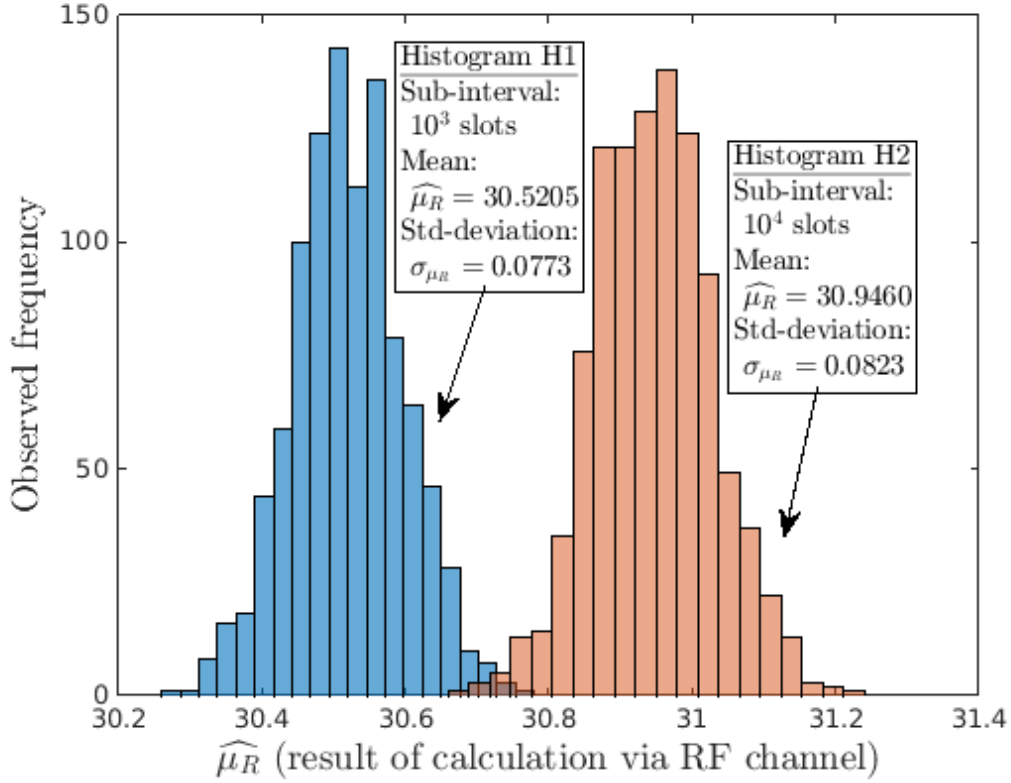


FIGURE 6.5: These two histograms H1 and H2 show the results of 1000 trials each calculating  $v_{s_1} + v_{s_2} + v_{s_3} = 4 + 10 + 17 = 31$  via RF channel. H1 is obtained by using  $10^3$  time slots for a sub-interval and 5000 sub-intervals for a time frame. H2 is obtained by using  $10^4$  time slots for a sub-interval and 5000 sub-intervals for a time frame.

A closer look in Figure 6.4 at the second column (showing the second sub-interval) identifies such an undetected collision leading to a bias of the final calculation result. With regard to the chosen model parameters this illustration depicts a time frame of length  $t = 1000$  time slots corresponding to  $\kappa = 10$  sub-intervals with each of them with 100 time slots. In such time frame a single data point is encoded. An intuition here suggests circumventing an enlargement of the time frame to improve the accuracy of a function calculation. For demonstration purposes we affixed the model parameters as described previously and shown in Figure 6.4. In a practical application scenario the parameters of the calculation model need to be set in the way to fit on the one hand hardware requirements of a sensor node and on the other a desired accuracy of calculation via RF channel.

### 6.2.1.2 Scenario 2: Summation

In our next example we illustrate the addition of three different sensor values  $v_{s_1} = 4$ ,  $v_{s_2} = 10$ ,  $v_{s_3} = 17$  being sensed by three sensor nodes  $\{s_1, s_2, s_3\}$ . In contrast to the

previous example we deploy this time for demonstration purpose different setups to observe the behavior of our approach, such as setting larger sub-interval to avoid collisions over the wireless channel. For instance, in the following we are setting for time frame  $t = 10^6$  and  $\kappa = 10^3$  resulting in a 1000 time slotted sub-interval with overall 1000 sub-intervals. According to our approach the average of the number of bursts occurring in the affixed time frame and sub-interval delivers the summation of the three sensed values  $\mu_{\mathcal{R}} = f(v_{s_1}, v_{s_2}, v_{s_3}) = \mu_{s_1} + \mu_{s_2} + \mu_{s_3} \approx 31$ . The function calculation with this parameter setup is illustrated in Figure 6.2 depicting the burst distributions of the encoded values  $\{v_{s_1}, v_{s_2}, v_{s_3}\}$  and the histogram indicating the outcome of the addition of all three burst sequences over the wireless channel. Since the burst sequences of the sensor nodes follow the Poisson distribution  $p(k; \mu_{s_i})$  and convolve over the wireless channel we fit the resultant theoretical Poisson's Probability Density Function (PDF)  $p(k; \mu_{\mathcal{R}})$  with the observed histogram shown in Figure 6.2. Approximately the PDF fits to the observed histogram, but it shows a noticeable skewness. Further simulation trials with different setups and calculating the same task reveal that the calculation accuracy is more influenced by the chosen length of a sub-interval, than to the choice of a large time frame. The reason for this observation shown in Figure 6.6 lies in the impact of burst collisions: a shorter sub-interval increases the probability for colliding of burst signals that cannot be distinguished from reader device anymore, whereas a larger sub-interval diminishes the number of collisions. Further, using a large time frame  $t$  that consists of a large number of sub-intervals has a scarce influence on the improvement of calculation accuracy, because the collision rate of bursts remains constant over time. The enlargement of a time frame  $t$  reduces the uncertainty of calculation via RF channel, though. For instance, Figure 6.5 shows two histograms H1 and H2 observed by two differently chosen sub-interval length of  $10^3$  and  $10^4$  time slots, with a time frame containing 5000 sub-intervals. The mean values of H1 and H2 that provide the result of calculation task indicate a different absolute distance to the true value describing the systematic error, but entail almost the same standard deviation  $\sigma_{\mu_{\mathcal{R}}}$  describing the statistical error. A series of simulations with varied setups calculating the same mathematical task over the wireless channel are recapped in Figure 6.6. The simulations reveal conclusively that the systematic error remains almost constant independently of a chosen length of time frame  $t$ . In chapter 7 we are going to analyze the calculation error of our approach in detail, and provide a solution with regard to diminish the systematic error drastically. Further, we are going to provide assertions with regard to bound the natural uncertainty, and thus achieve an acceptable calculation accuracy for the most application scenarios.

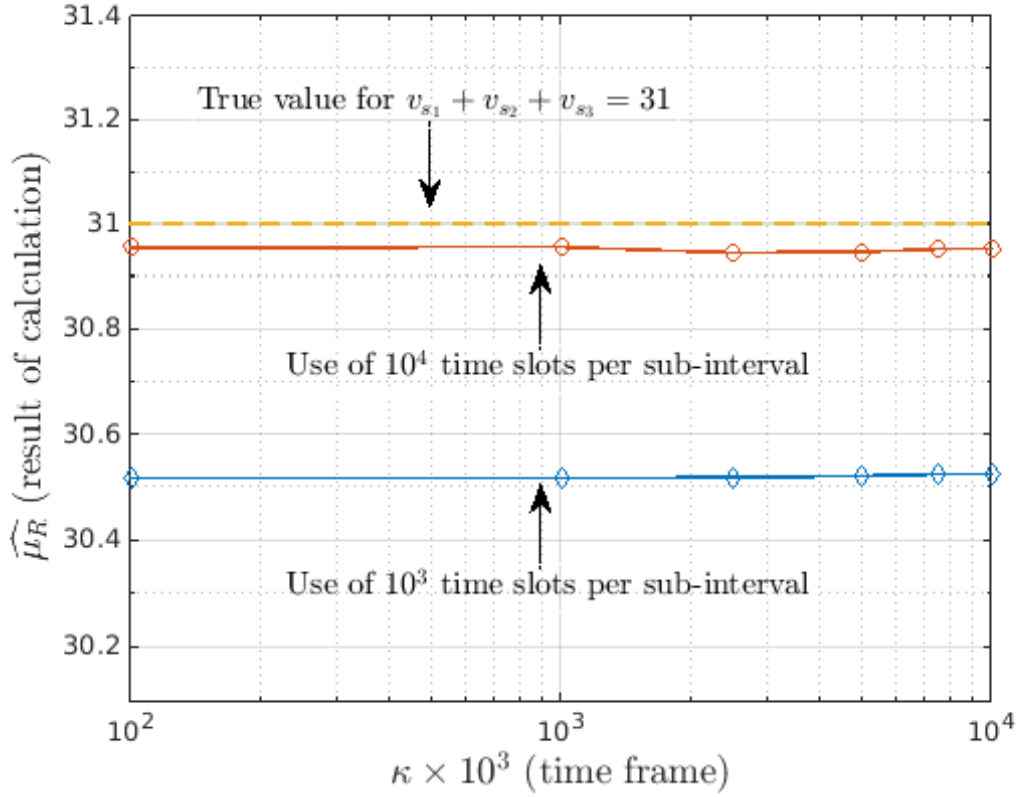


FIGURE 6.6: The function computation over the wireless channel using  $10^4$  time slots per sub-interval shows clearly an improved calculation accuracy in contrast to a chosen sub-interval length of  $10^3$  slots. The use of differently large time frames show scarcely an impact on the calculation accuracy.

Providing the error analysis in chapter 7, in the following we apply in advance its resulting solution to rectify our calculation from previous task by

$$\widehat{\mu}_{R_{new}} = -N \log \left( 1 - \frac{\widehat{\mu}_{R_{old}}}{N} \right) \quad (6.4)$$

The parameter  $N$  in Equation (6.4) denotes the number of time slots within a sub-interval. Exemplary, we show in Figure 6.6 the accuracy improvement for the case  $N = 10^3$ , where the systematic error (as a consequence of applying Formula (6.4)) is almost vanished. In addition to the resultant curve for various time frames we included to the log-log plot point-wise error bars indicating always for 1000 trials the standard deviation of  $1 \sigma$ . This figure illustrates that the effort to reduce the measurement uncertainty growth exponentially. Since in Figure 6.7 the deviation error is hard to distinguish visibly between the true value and the estimation, we show in Figure 6.8 the rectified calculations in a magnified plot. It illustrates that the corrected outcome of our novel estimation now fluctuates around true value indicating seemingly a mere natural statistical error. In the light of developing resource-limited IoT nodes and a desired

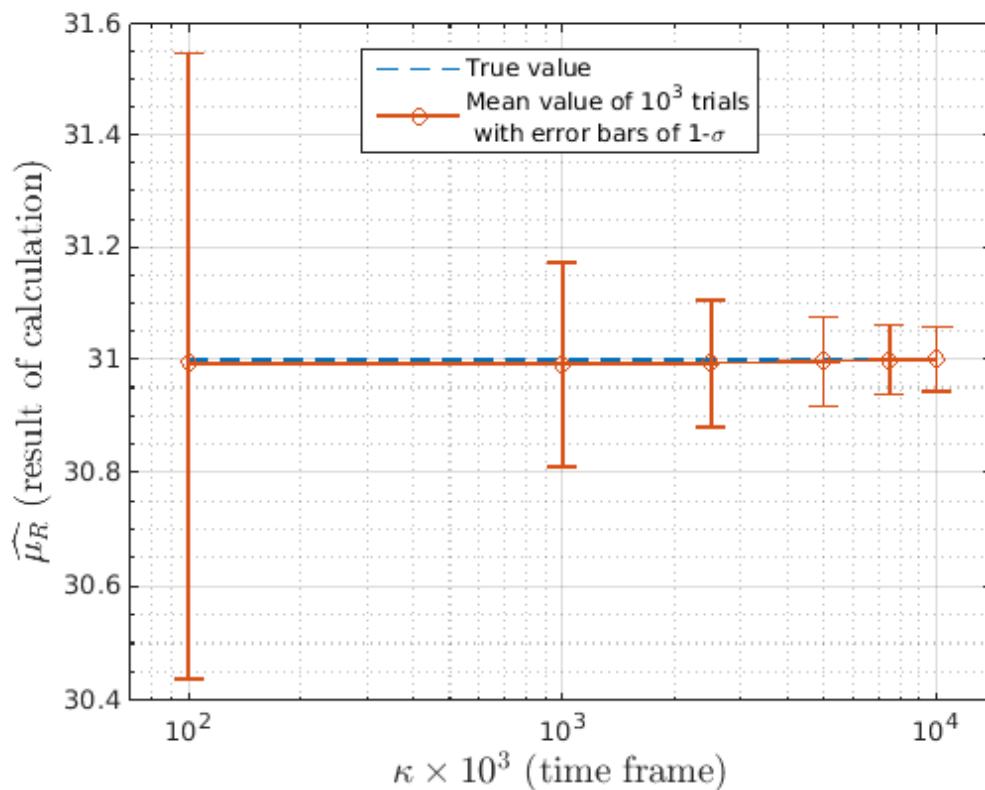


FIGURE 6.7: With respect to a chosen sub-interval length of  $10^3$  slots and the application of equation (6.4) the resulting curve (solid line) shows in comparison to the results in Figure 6.6 a significantly improved calculation accuracy approaching the true value (dashed line). The effort for decreasing the calculation uncertainty is exponential shown by error bars.

calculation accuracy for function computation the model parameters of our approach need to be still chosen wisely.

### 6.2.1.3 Scenario 3: Multiplication

In our next example we demonstrate multiplication of sensor values over the wireless channel, that is tricky to be realized. It requires preprocessing on every sensor node upon the sensed value before transmission, and a post-processing of the received burst sequence at the receiver side holding the outcome of the multiplication task. The solution for this issue relies on using exponentiation and logarithm rules, that allow to transform multiplication into addition over the wireless channel. For instance, on every sensor node  $s_i$  the Poisson's parameter is set to  $\mu_{s_i} = \log_b v_{s_i}$ ,  $b$  denotes an arbitrary base and  $v_{s_i}$  is the sensor value of node  $s_i$ . By transmission every sensor node generates a random burst sequence following Poisson distribution  $p(k; \mu_{s_i})$ . At the receiver side the outcome

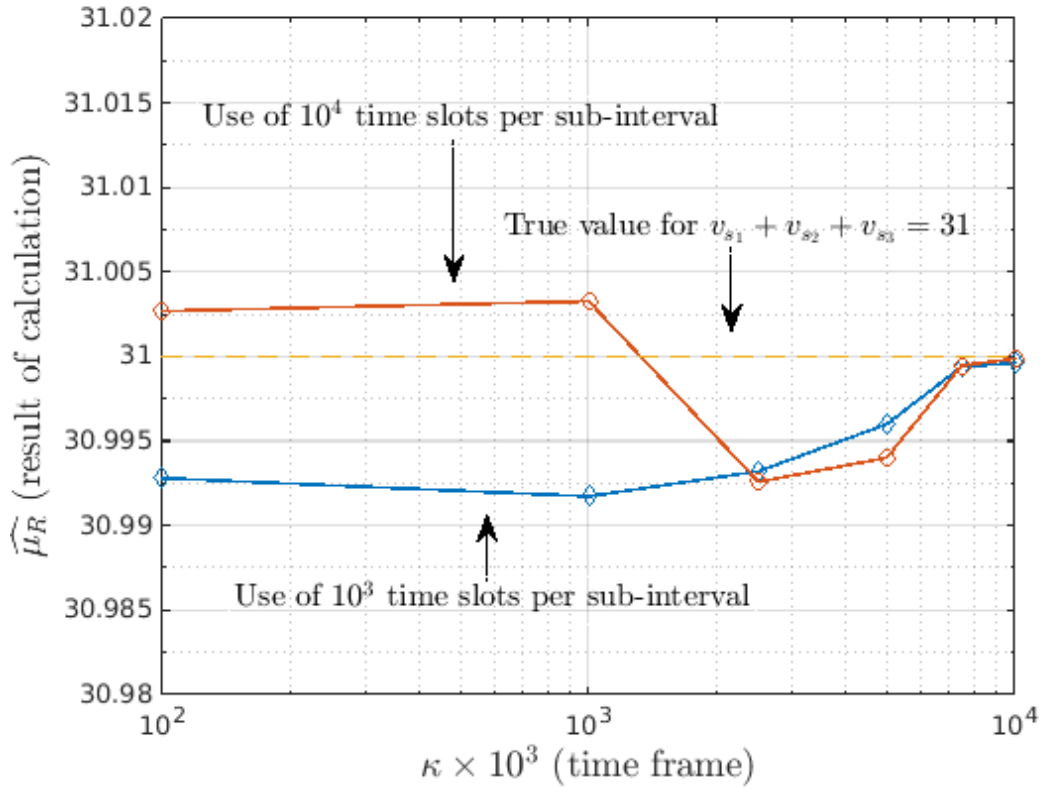


FIGURE 6.8: By applying Eq. 6.4 this plot shows results of rectified calculations for using  $10^3$  and  $10^4$  time slots per sub-interval.

of the multiplication task is regained by empowering  $b$  with the received  $\mu_R$ , i.e.,

$$\begin{aligned} \prod_{i=1}^M v_{s_i} &= b^{(\sum_{i=1}^M \log_b v_{s_i})} \\ &= b^{\mu_R} \end{aligned} \quad (6.5)$$

To elucidate our approach, in the following we exemplify the multiplication operation on the RF channel by multiplying three sensor readings  $v_{s_1} = 2$ ,  $v_{s_2} = 4$ ,  $v_{s_3} = 16$  sensed by three sensor nodes  $\{s_1, s_2, s_3\}$ . Before transmission every sensor node determines its Poisson parameter by setting  $\mu_{s_i} = \log_b v_{s_i}$ . If we use for logarithm base  $b = 2$ , then follows for the sensor nodes  $\{s_1, s_2, s_3\}$  to generate random burst sequences according to  $\mu_{s_1} = \log_2 2 = 1$ ,  $\mu_{s_2} = \log_2 4 = 2$  and  $\mu_{s_3} = \log_2 16 = 4$ . At the receiver side the calculated sum  $\mu_R = \mu_{s_1} + \mu_{s_2} + \mu_{s_3} = 8$  over the channel is used to derive the outcome of the multiplication task, namely, by raising  $b = 2$  to the power  $\mu_R$ , i.e.,  $2^{\mu_R} = 2^8 = 64$ , which answers the multiplication task of  $v_{s_1} \cdot v_{s_2} \cdot v_{s_3} = 2 \cdot 4 \cdot 8 = 64$ .

TABLE 6.1: Elementary functions for data processing over the wireless channel.

Function	
Addition	$\sum_{i=1}^n x_i$
Multiplication	$\prod_{i=1}^n x_i$
Subtraction	$x_i - x_j$
Division	$\frac{x_i}{x_j}$

#### 6.2.1.4 Scenario 4: Division and Subtraction

In the same manner as we realized multiplication and addition via RF channel, we can realize division and subtraction on the wireless channel. In the case of realizing division the fraction is transformed into a multiplication task, e.g.,  $\frac{v_{s1}}{v_{s2}} = v_{s1} \cdot \frac{1}{v_{s2}}$ . The multiplication of  $v_{s1}$  and  $\frac{1}{v_{s2}}$  is carried out in the same way as this is already been described above. In the case of carrying out a subtraction, e.g.,  $v_{s1} - v_{s2}$ , the operational number range need to be shifted into a positive range by a constant  $c$ , such that  $-v_{s2} + c > 0$ . In a post-processing step at the receiver side the shift of the number range need to be undone to acquire finally the correct calculation.

#### 6.2.2 Functions of Interest Calculable on the RF Channel

In the previous section we introduced by means of basic examples practical implementation of calculating mathematical functions over the wireless channel, and described ordinary intrinsic computation issues of our approach. With the basic operations, further relevant mathematical functions can be realized. Table 6.1 lists exemplary primitive functions applying one basic mathematical operation. More convoluted mathematical functions of being of interest in practice are shown in Table 6.2, that are commonly used in data processing. These tables separate between functions solely computable on the wireless channel and such functions that partly require either the computation by the receiving fusion center or transmitting IoT sensor nodes. In particular, the root and the exponentiation are not easily computed over the wireless channel, such that when necessary these operations are left to be computed on the hardware devices itself. The shown tables list a small fraction of functions calculable on the RF channel. A complete set of calculable functions over the wireless channel is not determined yet, and needs further to be investigated theoretically. However, with respect to our approach the shown mathematical functions provide limits and requirements for designing resource-limited

TABLE 6.2: An excerpt of common functions being calculable on the RF channel and applied in data analysis.

Function	
Arithmetic mean	$\bar{x}_A = \frac{1}{n} \sum_{i=1}^n x_i$
Weighted mean	$\bar{x}_W = \frac{1}{\sum_{i=1}^n w_i} \sum_{i=1}^n w_i x_i$
Quadratic mean	$\bar{x}_Q = \sqrt{\frac{1}{n} \sum_{i=1}^n x_i^2}$
Geometric mean	$\bar{x}_G = (\prod_{i=1}^n x_i)^{1/n} = \sqrt[n]{x_1 x_2 \cdots x_n}$
Harmonic mean	$\bar{x}_H = \frac{1}{\frac{1}{n} \sum_{i=1}^n \frac{1}{x_i}}$
$k$ -th moment	$\frac{1}{n} \sum_{i=1}^n X_i^k$
L <sub>1</sub> -norm	$L_1 = \sum_{i=1}^n  x_i $
L <sub><math>k</math></sub> -norm	$L_k = \sqrt[k]{\sum_{i=1}^n  x_i ^k}$
Standard deviation	$\sigma = \sqrt{\frac{1}{n} \sum_{i=1}^n (x_i - \bar{x}_A)^2}$

IoT nodes. In more detail we are going to discuss this issue in chapter 7. Intermediately, in the following section we investigate the calculation error of differently large WSNs applying our data processing architecture.

### 6.3 Case Study

In contrast to our collective data processing architecture calculating mathematical functions over the wireless channel being described above, the classical way of approach is to separate data transmission from data processing in a WSN. From each sensor node first data is aggregated individually in a fusion center, so that in a second step the sensed data is interpreted centrally. For the data analysis software-based processing tools are applied, which we characterize as *off-line* processing of data. In practice, very often simple statistical functions are applied to analyze data, in order to obtain a comprehensive view over an observed environment. In comparison to this, we perform computation over the sensory data directly on the RF channel, such that the receiver node already gets the final or partial outcome of a function calculation. This kind of information processing we characterize as *on-line* processing. In the following we are going to demonstrate our

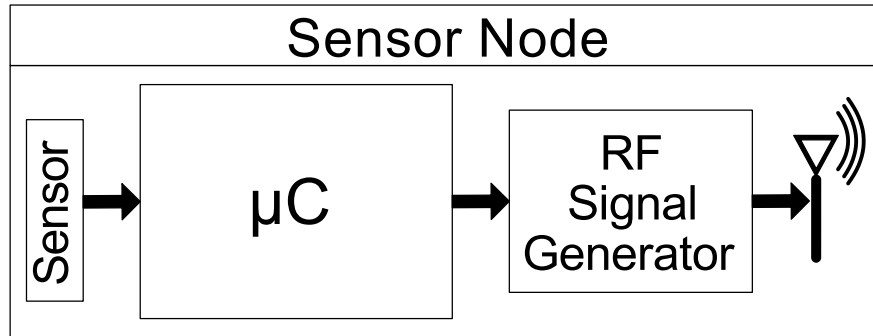


FIGURE 6.9: Block diagram showing our simple sensor node.

approach based on deploying a real wireless sensor network, and put this in comparison with a traditional WSN by conducting a case study.

### 6.3.1 Wireless Sensor Network Platform

To test our approach in practice, we created a wireless sensor network platform with 15 simple nodes and a central receiver, gathering incoming signals. For setting up the experimental WSN platform we deployed the GNU Radio as a receiver device and created to it a Software-defined Radio (SDR), in order to capture burst signals sent from the 15 simple sensor nodes. During transmission of bursts transmitted by the nodes the Software Radio registers all incoming burst signals and computes  $\widehat{\mu}_R$  the averaged number of bursts occurring within a time frame.

With respect to the sensor node hardware we manufactured the transmitter nodes with merely few electronic components, such as a micro-controller, an oscillator device and antenna operating in the 2.4 GHz band. Regarding the micro-controller we used the Arduino Uno board, Revision 3 [219]. With respect to the RF sinusoid signal generator we manufactured it in our lab with off-the-shelf PCB components. To achieve a broadcasting range of Home RF we adapted a standard oscillator circuit [5] to create a transmitter device to our needs (cf. Figure 6.11).

The sensing and managing of data transmission is controlled by the micro-controller unit (cf. Figure 6.9 depicting a block diagram of our simple sensor node). With regard to the transmission scheme we are using simple ON-OFF-Keying, so that the signal generator is switched on/off to transmit or not to transmit a burst. Based on the sensed value each node transmits a Poisson distributed sequence of bursts having the form of a spike train. The burst sequence is generated with the help of an on-board Random Number Generator (RNG) following the Poisson distribution with mean value  $\mu_{s_i}$  initialized with the sensor value  $v_{s_i}$ . The data transmission from the sensor nodes to the sink node is conducted unsynchronized, simultaneously and unidirectional. At

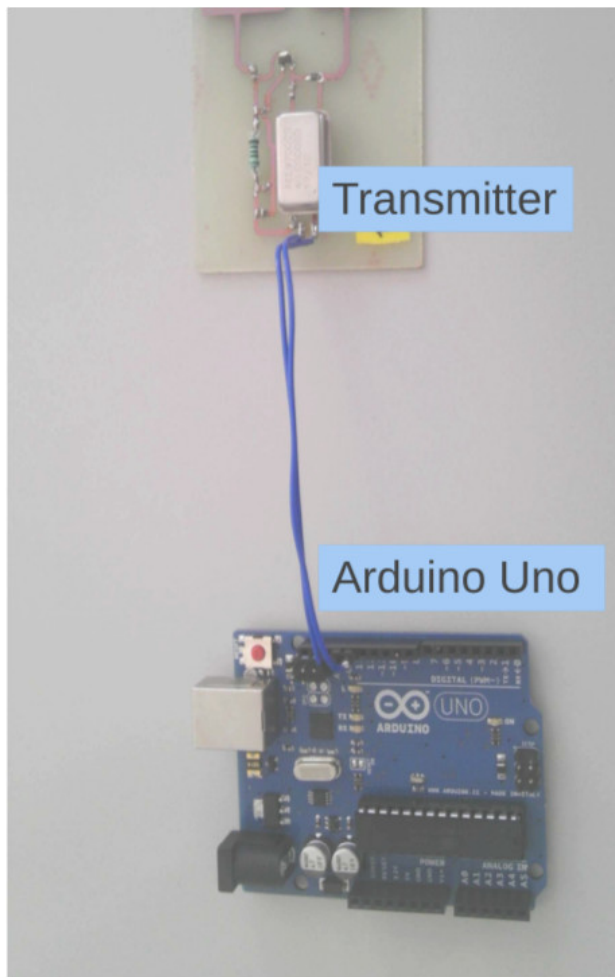


FIGURE 6.10: The sensor node consists of a 2.4 GHz sinusoid signal generator (A) connected to an Arduino Uno micro-controller (B) interfacing with a sensor device.

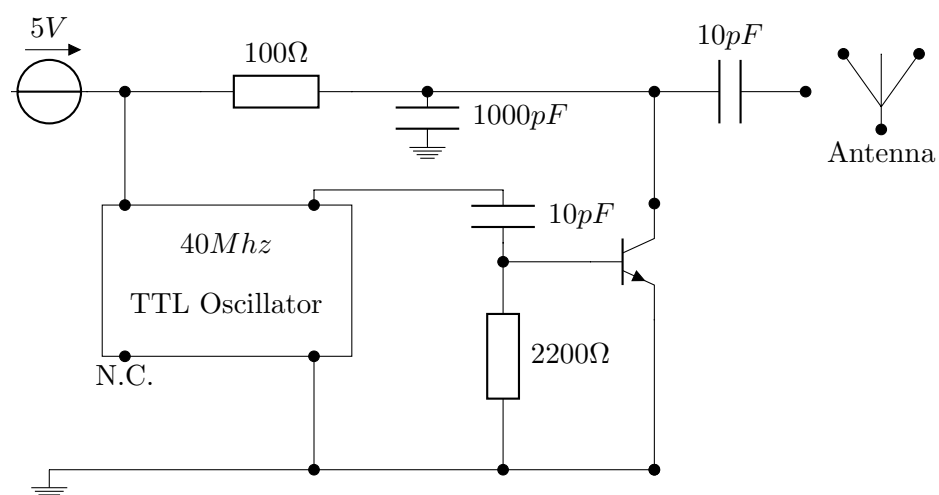


FIGURE 6.11: Schematic of our 2.4 GHz oscillator circuit adapted from John Wright's signal generator [5] by permission.

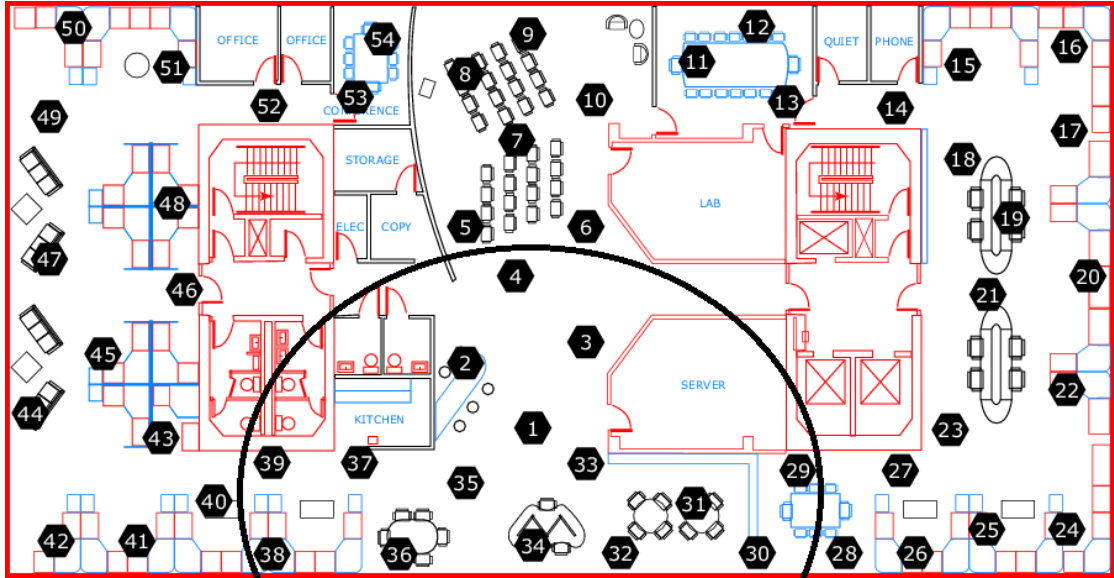


FIGURE 6.12: Wireless sensor network of the Intel Berkeley Lab [6]. The formation of nodes in the encircled area is used to position our 15 nodes in our lab.

the receiver side a Software Radio is processing the incoming signals. From the received superimposed signal the bursts occurring in a time frame are detected and counted to acquire the outcome of a desired function computation. An example of a real captured burst sequence generated by our 15 nodes is depicted in Figure 6.3.

### 6.3.2 Calculation of Mean Temperature Using the WSN Platform

To demonstrate the performance of our approach we used a dataset from the Intel Berkeley Research lab as a benchmark [6]. The dataset was generated by their wireless sensor network and consists of several days readings from sensory data, such as air temperature, humidity, light and voltage.

For our purpose we picked from the dataset a 1-day recording which was generated by 15 sensor nodes (cf. Figure 6.12, nodes we utilized are encircled through an ellipse), and mapped each recorded corresponding time series to one of our sensor nodes. We calculate the average temperature curve obtained during the day. The traditional way to estimate the state of an observed area is primarily to collect data and afterwards to depict in a post processing step the averaged sensory values in a plot. In our case, the sum of the temperature values is derived at the receiver directly due to the superimposition of values. In a  $34\text{ m}^2$  room ( $5.35\text{ m} \cdot 6.35\text{ m}$ ) we scattered our sensor nodes in a similar formation as the nodes are positioned in the Intel lab. In the center of the sensor field we positioned the receiver node. With respect to the deployed hardware of the RF signal generator the transmission time of a burst is set to 25 ms, which is confined by the used electronic components. For the transmission scheme of a sensor value 1000 time slots

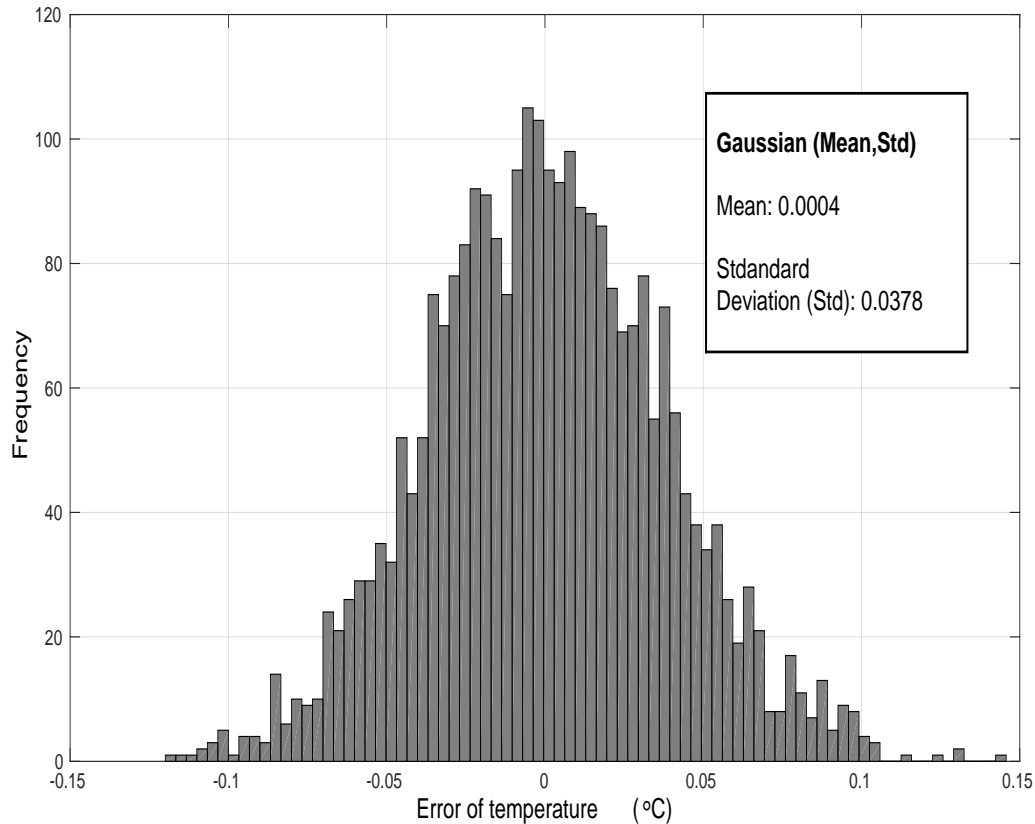


FIGURE 6.13: Deviation error between computation accuracy and the ground truth.

are used, which results in a 25 second long signal. This long signal duration was owing to our prototypical implementation of the sensor nodes. With nodes capable of sending a burst of shorter duration, this time can be significantly reduced.

### 6.3.3 Results

In the experiment we initiated the nodes to transmit the temperature values, whereby the receiver node captured the on-the-channel calculated accumulated temperature value among all 15 sensor nodes and derived the mean through division by 15 (the node count). The resulting temperature curve deviates slightly from the off-line-generated curve (cf. Figure 6.13). To investigate our approach thoroughly we created in addition to the real world experiment simulations applying more time slots to encode a sensor value. The simulations show a higher accuracy the more time slots are used. Figure 6.14 depicts the results for  $10^3$  time slots. Although the estimated curve closely follows the optimum mean calculated for the temperature values off-line, the value deviates slightly. In the case of  $10^6$  time slots the deviation error is approximately 0.04, so that the difference between the original curve and the outcome of our approach is hardly distinguishable (cf. Figure 6.15).

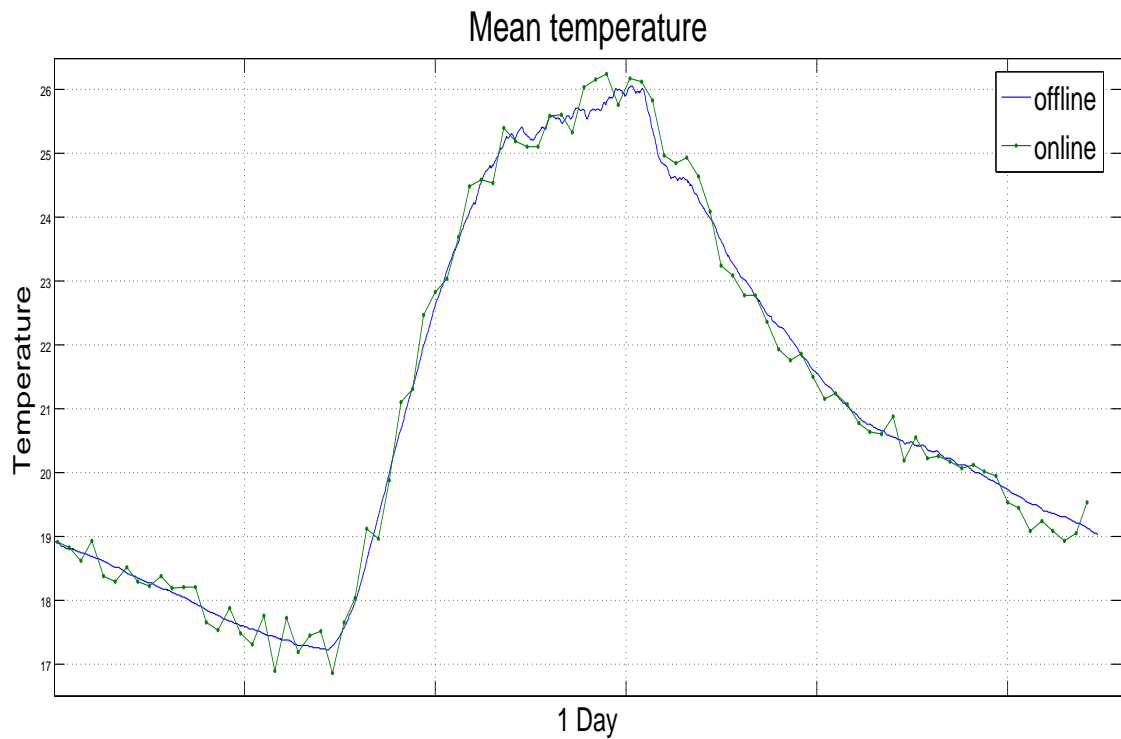


FIGURE 6.14: On-the-channel computed mean temperature of 15 nodes in comparison to the averaged measurement series gained from the Intel lab data when  $10^3$  time slots are used. The standard deviation error is  $\sigma = 0.2293^\circ\text{C}$ .

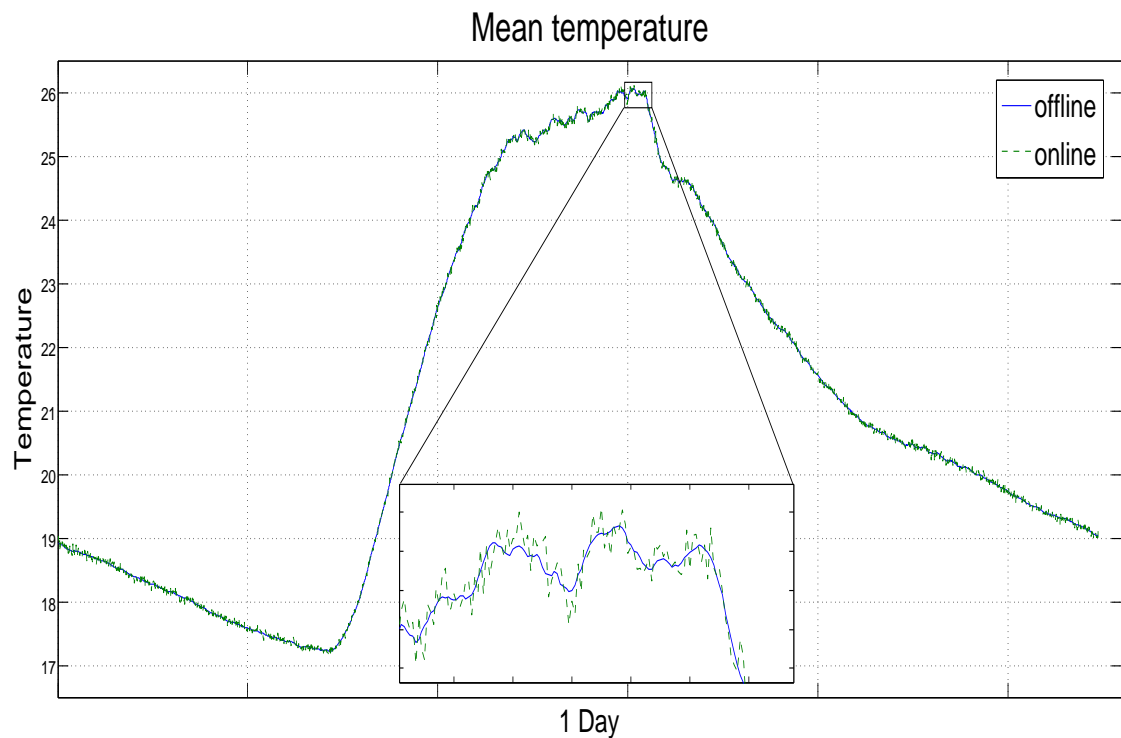


FIGURE 6.15: On-the-channel computed mean temperature of 15 nodes in comparison to the averaged measurement series gained from the Intel lab data when  $10^6$  time slots are used. The standard deviation error is  $\sigma = 0.0378^\circ\text{C}$ .

## 6.4 Summary

In this chapter we introduced an approach for calculating functions of interest on the RF channel, and demonstrated the implicit calculation at the time of simultaneous wireless transmission of Poisson-encoded values. In particular, we developed a simple sensor node capable of sensing and transmitting Poisson-distributed burst sequences and employed 15 nodes in a scenario to simultaneously transmit temperature values to a receiver node. Due to this Poisson distribution of the burst sequences encoding the temperature values, the superimposition observed by the receiver encodes the sum of the temperature values. By dividing this value by the number of transmit nodes, the receiver achieves the mean temperature with small errors enforced by the transmission process. The error can be bounded by increasing the length of the burst sequences, thereby increasing the confidence on the estimated received value. This transmission scheme, that we call time-based Collective Communications (CC), can empower resource restricted IoT nodes to conduct ambitious computation by trading computational load for communication load. In the next chapter we proceed to analyze in detail the systematic error and statistical error of our approach, and derive a solution to minimize the calculation error which emerges during the simultaneous data transmission and data processing over the wireless channel. Further, we are going to elaborate the essentials for designing a circuitry of a resource-limited IoT node, that implements our concept of function calculation on the RF channel.

## Chapter 7

# Analysis of Superimposed Computing and Circuit Design

In the previous chapter we introduced calculation of desired functions on the RF channel for resource-limited WSNs, which we call *wireless superimposed computing*. In the following chapter we derive with respect to the corrupted wireless computing a solution to minimize the calculation error occurring during the simultaneous data transmission and processing over the wireless channel. To this end, we extend our investigation towards designing a resource-limited IoT node in relation to application specific scenarios, and discuss its requirements and implementation issues with respect to current hardware technology.

### 7.1 Introduction

In the last chapter we introduced an approach for wireless superimposed computing and presented a simple sensor network enabled to calculate various desired functions over the RF channel. However, the outcome of the calculation using the RF channel is error corrupted as noticed. With enlarging the time window of radio reception or shortening the burst signal itself we are able to mitigate the error of function computation by brute force at the expense of power and transmission time. These arrangements, however, are not sufficient enough to remove the systematic error efficiently. In this chapter we are going to analyze the error in detail and derive analytically a solution, that rectifies our wireless superimposed computing significantly, such that the previously noticed bias in calculation vanishes. A side benefit of our solution enables in addition to improve transmission time efficacy as well, because it allows to manage the occurring calculation error with desired accuracy.

In relation to application specific scenarios deploying wireless superimposed computing we are going to investigate to this end the hardware design of our approach into resource-limited IoT nodes. With respect to current Organic and printed Electronics (OE) and Si-based CMOS technology, we are going to discuss hardware requirements and implementation issues, such that the development for applications specific IoT sensor networks using our approach can be facilitated.

Before we start with analyzing the calculation error in detail of our approach in section 7.2, we begin in subsection 7.2.1 with characterizing the simultaneous data transmission and processing scheme, pointing out the central properties. After that, we investigate analytically the expected error in subsection 7.2.2, and derive in succeeding a solution to improve computation accuracy. In section 7.3 we provide a thorough evaluation about our wireless superimposed computing approach. In a follow-up, in section 7.4 we turn to circuit design of resource-limited IoT nodes, that integrate our proposed time-based Collective Communications (CC) approach.

## 7.2 Error Analysis of Wireless Superimposed Computing

### 7.2.1 Computation Scheme

In chapter 6 we introduced a communication scheme to realize all four basic mathematical operations (addition, subtraction, multiplication, division) using Poisson-distributed burst-sequences. The scheme is tolerant to weak synchronization of nodes and requires only simple operations by participating nodes. The general principle grounds on the following property: for two random sequences encoding Poisson variables  $\chi_1$  and  $\chi_2$  with means  $\mu_1$  and  $\mu_2$ , their combination  $\chi_1 + \chi_2$  again yields a Poisson distributed variable with mean  $\mu_1 + \mu_2$  [217]. This key idea is used to realize a mathematical operation on the RF channel, for example, to calculate correspondingly  $v_1 + v_2$ , with  $v_1, v_2 \in \mathbb{R}$ , resulting into  $v_1 + v_2 \in \mathbb{R}$ .

We divide a burst sequence of length  $t$  into  $\kappa t$  sub-sequences of length  $\frac{1}{\kappa}$ . Each of these subsequences is generated with the help of a stochastic process following the Poisson distribution  $p(k; \mu_{s_i})$  as described in textbook [218]. The parameter  $\mu_{s_i}$  determines the density of bursts within the sequence generated from transmitter  $s_i$ . The larger  $\mu_{s_i}$  is, the smaller the probability of finding no point. The parameter  $\mu_{s_i}$  denotes the mean of the distribution. Thus, on a transmitter node  $s_i$  we apply a Poisson process with mean  $\mu_{s_i} = v_{s_i}$  to transmit the value  $v_{s_i}$ . In the mode of operation all participating transmitter nodes transmit their burst sequences simultaneously. The receiver  $\mathcal{R}$  captures the superimposed transmission and detects in a time slotted time frame all received bursts.

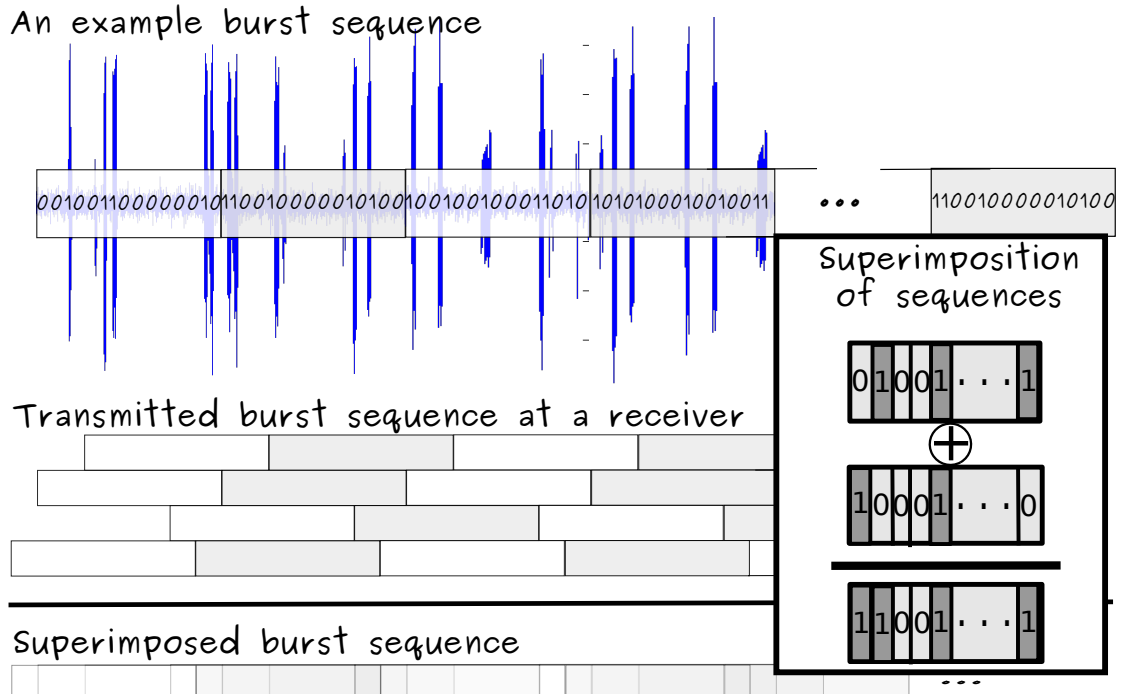


FIGURE 7.1: A sketch of our scheme for the computation of mathematical function via communication channel

To observe the value  $\mu_R$  at the receiver, we extract the count  $N_i$  of sub-sequences with exactly  $i$  bursts as well as the total number of bursts  $T = \sum_{i=1}^n i \cdot N_i$  occurring within a time frame  $t$ . In practice,  $T$  denotes the total number of all counted bursts and  $N = \sum_{i=1}^n N_i$  is the number of all sub-intervals within a time frame  $t$ . Then, the outcome of a function calculation is obtained by

$$\mu_R t \approx \frac{T}{N}. \quad (7.1)$$

Equation (7.1) is true, as long as all sent bursts are captured from receiver  $\mathcal{R}$ , because the received burst sequence again yields a Poisson distribution. The receiver can therefore apply (7.1) to extract  $\mu_R$  from received sequence.

For the calculation of desired functions we utilize superimposed burst sequences from various transmitter nodes. The general mechanism is briefly sketched in Figure 7.1. In the upper-left corner of Figure 7.1 we show a translation of a received burst sequence into a binary sequence indicating for each time slot an occupation by a burst. At the right side of this figure we show exemplarily an addition of two burst sequences. The lower-left side of this figure illustrates superimposition of weakly synchronized burst sequences calculating a function. It means in effect that our approach for data transmission and processing requires no synchronization. This side effect is attributed to our coding scheme. The value  $v_{s_i} \in \mathbb{R}$  is encoded by a mean value of a Poisson distribution  $p(k; \mu_{s_i})$ , but  $v_{s_i}$  is not encoded through a fixed burst sequence. Therefore, our

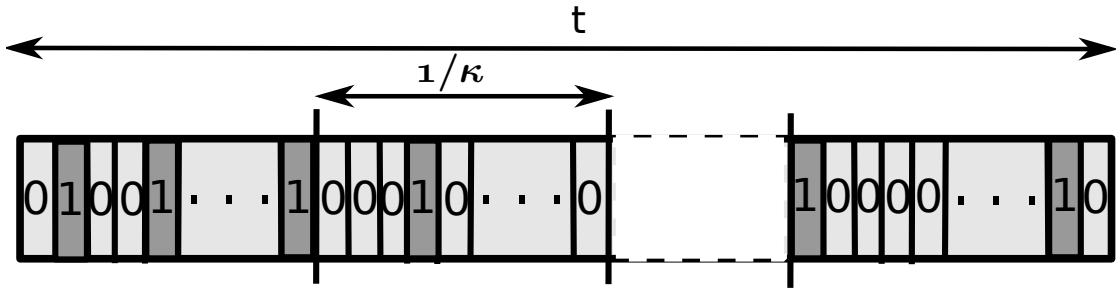


FIGURE 7.2: A binary reception vector of a receiver indicates a bit-sequence representing a concatenated burst sequence

transmission scheme indicates robustness towards inaccurate synchronization in phase, symbol and signal strength level. Since burst sequences are utilized, the exact received power can fluctuate greatly among sequences, provided that the burst sequence received with least power is still significantly above the noise level. Also, burst sequences do not require exact synchronization in transmit phases. In order to understand the impact of inaccurate synchronization on symbol (burst) level, we assume an encoding of a particular value  $v$   $\kappa t$  times in a sequence of length  $t$  that is concatenated from sequences of length  $\frac{1}{\kappa}$  (cf. Figure 7.2). Further, we utilize representations of values as random burst sequences following specified random distributions, which are tolerant for shift and reordering of bursts over a sequence. Furthermore, we implement a value in this manner several times within an overall burst sequence in concatenated sub-sequences. Consequently, taking these two preconditions together, regardless of which distinct  $\frac{1}{\kappa}$  bits from the received sequence are considered by the receiver, they will always encode the same random distribution with about the same properties. Slight variation for a different choice of  $\frac{1}{\kappa}$  bits then result only from possible collisions in burst sequences. Consequently, we can state that sequences do not have to be synchronized on the symbol level.

In the calculation process over the wireless channel burst sequences from various transmit sources arrive overlaid at the receiver. During this process, bursts write though into the received burst sequence. The underlying physical principle for the calculation scheme is therefore the cumulation of bursts in a received sequence. Different functions can be realized by the differing interpretations of these bursts. For instance, the naive implementation of an addition on the wireless channel could simply count the number of bursts in a received sequence, in order to estimate the overall count of bursts in all transmitted sequences.

In doing so, however, it should be noted that our calculation model using the physical channel as a calculator is flawed: the overlay of two or more bursts at the same time in HF band is hard to be distinguished from receiver [52, pp.73-75], leading to an inaccurate calculation of mean value  $\mu_R$ . The occupation of a time slot by two or more bursts

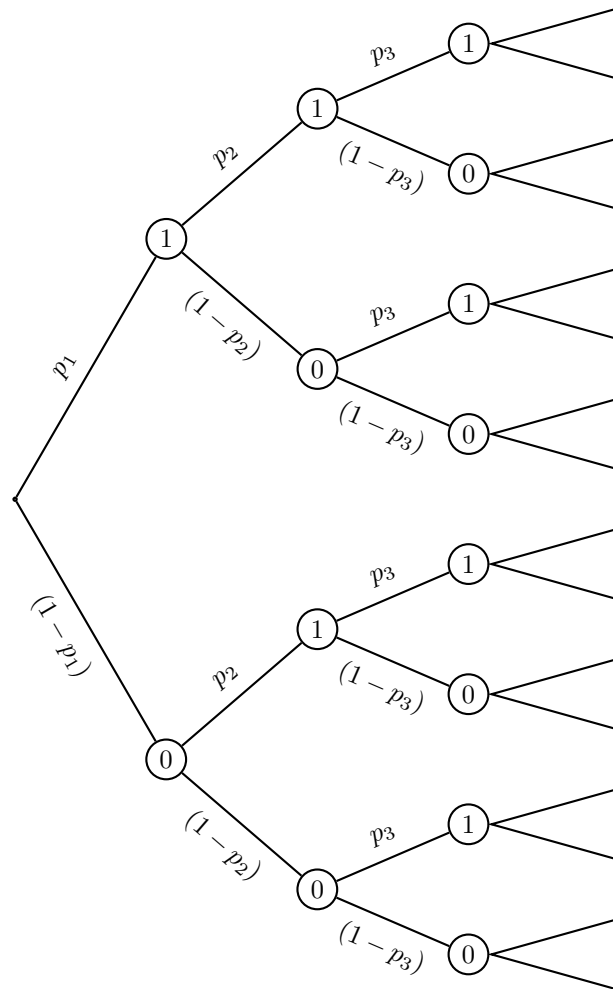


FIGURE 7.3: This probability tree shows all possible combinations of realizations for occurrences of no burst, one burst, or more than one burst in a single time slot. For example, the probability that  $M$  transmitter nodes with transmission rates of  $p_1, p_2, \dots, p_M$  send no burst in the same time slot is  $p(\text{"No burst"}) = (1 - p_1)(1 - p_2) \cdots (1 - p_M)$ .

is in general counted as one burst. In order to mitigate the impact of collisions on the derived value and to achieve better calculation accuracy, we encode a value repeatedly in multiple concatenated and enlarged sub-sequences. The calculation accuracy can also be improved by simply shortening the burst signal itself, because the probability of collision between bursts is automatically reduced. However, these steps for improvement does not change the fact that our computation system remains error-prone. In the following section we investigate in particular the induced error caused by burst collisions.

### 7.2.2 Estimation of Errors Induced by Collisions

The amount of collisions in a received burst sequence impacts the error in the described calculation. With accurate knowledge on the expected amount of collisions it is therefore

possible to correct an error in a calculation on a wireless channel to some extent. As we perceived the issue in our approach that bursts from different transmitter nodes can overlap during transmission without being recognized by a reader  $\mathcal{R}$ , in the following we model this issue by forming a probability tree that provides the probabilities for each possible occurrence of no burst, one burst, or more than one burst in a single time slot<sup>1</sup>. For example, if a WSN consists of  $M$  transmitter nodes, and every node  $s_i$  transmits bursts with a rate  $p_i$ , then the probability for every node transmits a burst at the same time is  $p(\text{"All nodes transmit"}) = p_1 p_2 p_3 \cdots p_M$ . In contrary, the probability for no occurrence of a burst in a time slot is  $p(\text{"No burst"}) = (1 - p_1)(1 - p_2)(1 - p_3) \cdots (1 - p_M)$ . Further possible combinations of realizations are apprehended in the probability tree (cf. Figure 7.3). From the viewpoint of a reader  $\mathcal{R}$  only the realization of  $p(\text{"No burst"})$  is for certain to be recognized correctly. If in case an event is detected, then the reader  $\mathcal{R}$  is not able to distinguish for certainty between one or more bursts that can occur in a single time slot. However, if we observe occurring events over an affixed time frame, then we can conclude statistically about the real number of occurring bursts, though. In doing, we slice an observation time into  $N$  time slots, whereby time length of a time slot corresponds to burst signal length. The detection of an event in a time slot represents a Bernoulli process. By considering a fixed number of  $N$  Bernoulli trials we can describe this process by a binomial distribution  $b(N, p)$ , where  $p$  denotes the probability for observing an event in a time slot. Here, we are allowed to assume to observe a binomial process despite of expecting a Poisson process.

*Proof.* We assume a reader  $\mathcal{R}$  is receiving events of bursts following a Poisson distribution  $p(\mu; k) = \frac{\mu^k e^{-\mu}}{k!}$  originating from sources that generate those Poisson distributed events. Due to limitations of reader device  $\mathcal{R}$  an affixed observation time is sliced into  $N$  time slots, such that for a high number of  $N$  slots and a small probability  $p(\text{"Burst occurs"})$ ,

---

<sup>1</sup>For the sake of simplicity we abusively use the lowercased  $p(\cdot)$  to represent either, the probability  $p(\text{"Event"})$  for the occurrence of an event with rate  $p$ , and the Poisson probability density function  $p(\mu; k)$  with parameter  $\mu$  the mean value of events and  $k$  the number of events.

we can state  $\mu = N \cdot p$ . Now, we can replace  $\mu$  and conclude

$$\begin{aligned}
 \frac{(Np)^k e^{-Np}}{k!} &= \frac{(Np)^k}{k!} \left[ 1 \cdot \left(1 - \frac{1}{N}\right) \left(1 - \frac{2}{N}\right) \cdots \left(1 - \frac{k-1}{N}\right) \frac{\left(1 - \frac{Np}{N}\right)^N}{\left(1 - \frac{Np}{N}\right)^k} \right] \\
 &= \frac{(Np)^k}{k!} \left[ 1 \cdot \left(1 - \frac{1}{N}\right) \left(1 - \frac{2}{N}\right) \cdots \left(1 - \frac{k-1}{N}\right) \right] (1-p)^{N-k} \\
 &= \frac{N^k}{k!} \left[ \frac{N}{N} \left(\frac{N-1}{N}\right) \left(\frac{N-2}{N}\right) \cdots \left(\frac{N-k+1}{N}\right) \right] p^k (1-p)^{N-k} \\
 &= \frac{N(N-1)(N-2) \cdots (N-k+1)}{k!} p^k (1-p)^{N-k} \\
 &= \frac{N!}{k!(N-k)!} p^k (1-p)^{N-k} \\
 &= \binom{N}{k} p^k (1-p)^{N-k}
 \end{aligned}$$

Thus, proof is provided that reader  $\mathcal{R}$  is observing a binomial random process.  $\square$

Now that we obtained a binomial distribution for observing events in a time slotted window, we can apply the expectation value  $E(X) = Np$ , with  $X \sim b(N, p)$ . Hence, we are obtaining the greatest lower-bound  $\mu_{lower}$  to observe the true mean value  $\mu_{true}$  of a superimposed burst sequence following a Poisson distribution. To acquire the least upper-bound value  $\mu_{upper}$  for receiving bursts, we apply the realization of  $p$  ("No burst in  $N$  slots")  $= (1-p)^N$ , and conclude

$$\begin{aligned}
 (1-p)^N &= \frac{(\mu_{upper})^0 e^{-\mu_{upper}}}{0!} = e^{-\mu_{upper}} \\
 \Rightarrow N \log(1-p) &= -\mu_{upper} \\
 \Rightarrow \mu_{upper} &= -N \log(1-p)
 \end{aligned} \tag{7.2}$$

Finally, we determined the greatest lower-bound value  $\mu_{lower}$  and the least upper-bound value  $\mu_{upper}$  for bounding the searched true mean value  $\mu_{true}$  by

$$Np \leq \mu_{true} \leq -N \log(1-p). \tag{7.3}$$

For point estimation we use the least upper-bound value. However, since in practice the systematic error is not fully removed because of other additional systematic errors, we use a modified version of Equation (7.3), namely

$$\mu_R = -(N - \Delta_1) \log(1-p) + \Delta_2, \tag{7.4}$$

where  $\Delta_1$  and  $\Delta_2$  represent calibration parameters mitigating further systematic errors, such as the influence of inaccurate clocks of transmitter devices, utilizing pseudo-random

number generators, or jamming transmitters. The calibration parameters  $\Delta_1$  and  $\Delta_2$  can be determined by simple testing the entire WSN. For example, the counting task of active transmitter nodes in a WSN can be used to perform a proper calibration. However, since this issue is more hardware-dependent, and in relation to approach independent, for further analysis we continue to use only Equation (7.3).

### 7.3 Simulations

In the previous section we investigated analytically the systematic error of our approach induced in particular by collisions of bursts, and derived a solution eliminating almost the calculation error from function computation over wireless channel. Further, we gained insights about our coding scheme setting appropriate parameters for randomly drawn burst sequences. In the following we perform empirical experiments to test our derived solution, and extend investigation towards deploying differently large WSNs. In particular, we are going to test behavior of our computation model being deployed in small and large WSNs. For testing we employ and conduct Matlab-based simulations, in order to estimate calculation error experienced during calculating mathematical functions at the time of transmission on the wireless channel. In our investigation, we are simulating up to 50 IoT nodes being randomly (uniformly distributed) placed in a  $30\text{ m} \times 30\text{ m}$  environment with the receiver located 3 m above the center of this square.

The phase offset of the received dominant signal component from each transmitter is calculated according to the transmission distance in a direct line of sight. For a signal wavelength of  $\lambda$  and a transmit power of  $P_{tx}$  over a distance  $d$ , path loss is calculated by the Friis equation  $P_{tx} \left(\frac{\lambda}{2\pi d}\right)^2 G_{tx} G_{rx}$  with antenna gain for the transmitter and the receiver as  $G_{rx} = G_{tx} = 0$  dB. Burst signals  $m_i(t)$  are transmitted at 2.4 GHz with transmit power  $P_{tx} = 1$  mW. All received signals are then summed up to achieve the superimposed signal. Finally, a noise sequence is added to estimate the signal at the receiver. We utilize ambient white Gaussian noise (AWGN) at  $-103$  dBm as proposed by reference [220]. With regard to further considerations about the propagation of electromagnetic waves and the proposed collective data processing architecture, we introduce the following formalism: by simultaneously transmitting values  $v_{s_i}$  from  $n$  transmitter nodes over the wireless channel, a receiver is observing a superimposition

$$\zeta_{\text{rec}}(t) = \Re \left[ \left( e^{j2\pi f_c t} \sum_{i=1}^n v_{s_i} \text{RSS}_i e^{j\gamma_i} \right) + \zeta_{\text{noise}}(t) \right] \quad (7.5)$$

of these values.

In Equation (7.5),  $f_c$  represents a common transmit frequency,  $RSS_i$  and  $\gamma_i$  the received signal strength and relative phase shift of a signal component transmitted by node  $s_i$  and  $\zeta_{\text{noise}}(t)$  the noise signal. We understand the simultaneous transmission over a wireless channel as the execution of a function  $y = f(v_{s_1}, \dots, v_{s_n})$  with the transmitted values  $v_{s_i}$  as input parameters and the reception  $\zeta_{\text{rec}}(t)$  as the output  $y$  of the function.

### 7.3.1 Experiment 1: Error Tracking

To get started with exploring limits and behavior of our solution improving computation accuracy of wireless superimposed computing (cf. Equation (7.4)), we begin first with a calculation of an arbitrarily chosen mathematical task. For instance, we setup a WSN with 5 sensor nodes in our simulator to calculate a mathematical function of the form  $f(v_{s_1}, v_{s_2}, v_{s_3}, v_{s_4}, v_{s_5}) = v_{s_1} + v_{s_2} + v_{s_3} + v_{s_4} + v_{s_5}$ . In particular, we let  $f(10, 5, 3, 2, 1) = 21$  to be calculated 10 000 times on the RF channel employing thereby different coding scheme parameters. To investigate the impact of differently chosen sub-intervals, namely  $10^2$  and  $10^3$  time slots, we chose for  $\kappa = 1000$ , resulting into time frames of lengths  $t_1 = 10^5$  and  $t_2 = 10^6$  time slots. With regard to the parameters of Equation 7.4, we set  $\Delta_1 = 0$ , and  $\Delta_2 = 0$ , in order to investigate the occurring error induced by burst collisions. In Figure 7.4 we show our simulation results obtained by calculating the chosen mathematical task. The upper Plot 7.4 (a) depicts absolute errors of  $|21 - \bar{\mu}_R|$ , where  $\bar{\mu}_R$  is mean of calculation trials. For a distinct and complementary representation we provide in the lower Plot 7.4 (b) nonlinear fits to simulation results. The results indicate a steady reduction of calculation error tending to zero line the more trials are performed and put into the reckoning. Since the log-log plots in Figure 7.4 exhibit straight falling lines on the long run, we presume that an exponential effort is needed to achieve a steady improvement. Furthermore, the straight falling of the calculation error indicates a mere statistical error to be remained, appearing that the induced error by collisions of bursts over the wireless channel is of no more existence to be. The choice for using a time frame with  $10^3$  slots/sub-interval seams to provide in tendency a better performance in contrast to the choice of a time frame with  $10^2$  slots/sub-interval, but not in general.

### 7.3.2 Experiment 2: Computation Accuracy

In the following experiment we extend our investigation towards calculating the same mathematical function as before, but deploy this time different sets of 5-tuples to observe behavior of our computation model at the broader level. With regard to issue we created a data set of 5-tuples, whose inset  $v_{s_1}, v_{s_2}, v_{s_3}, v_{s_4}, v_{s_5} \in [1, 20]$  in  $f(\cdot)$  yields

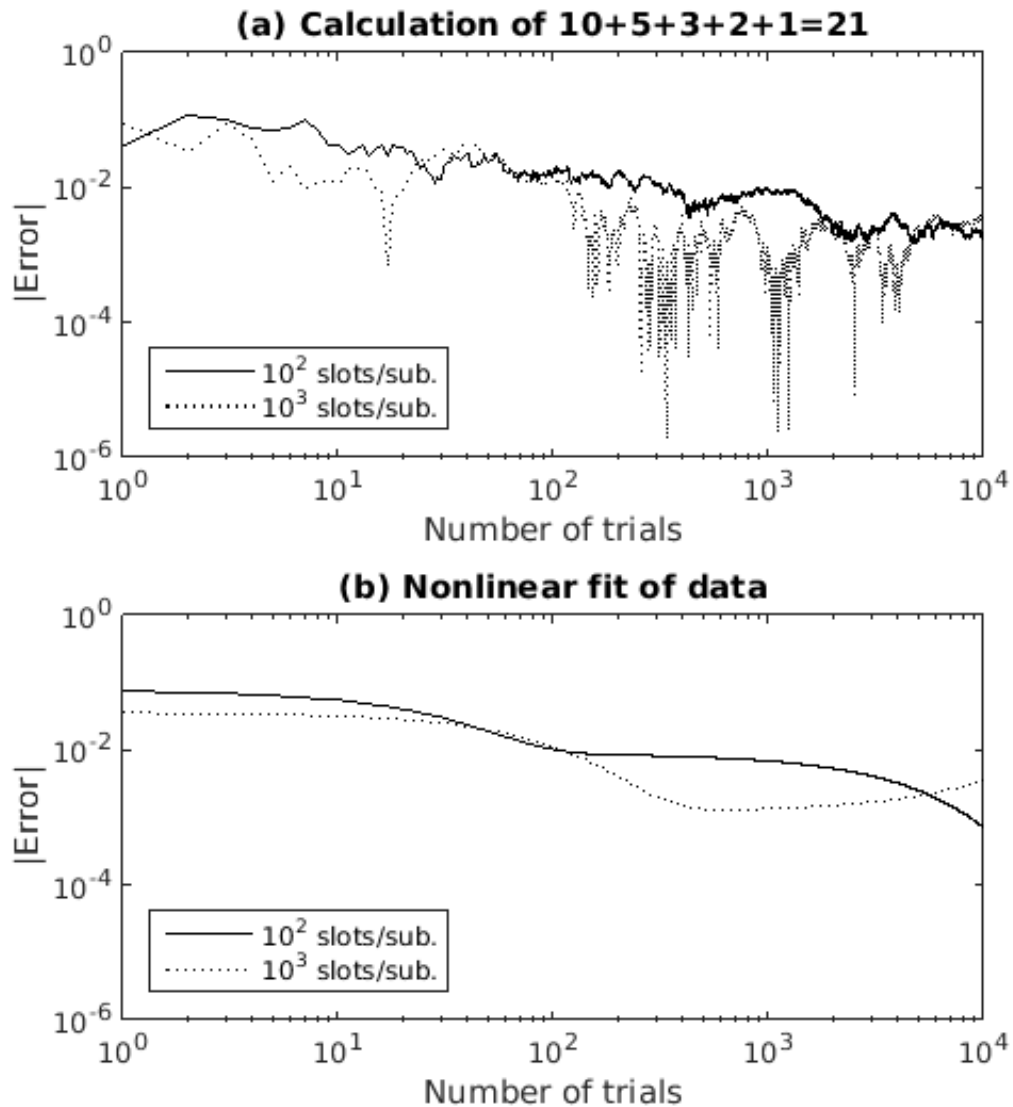


FIGURE 7.4: Plot (a) shows averaged values of absolute calculation error of calculating the mathematical task  $10 + 5 + 3 + 2 + 1 = 21$  over wireless channel using different sub-interval lengths. Plot (b) shows nonlinear fits to data presented in plot (a).

$y \in \{5, 6, 7, \dots, 98, 99, 100\}$ . To avoid bias in data we created for each  $y$  the most variety of 5-tuples, i.e., for each  $y$  we assigned 1000 most variable insets resulting into  $95 \times 1000$  calculation trials. The results of this investigation are given in Figure 7.5. The left column of subplots renders the calculation error for using  $10^2$  time slots/sub-interval, and the right column describes the same for using  $10^3$  slots/sub-interval. The subplots (a) and (b) each depict all occurring calculation errors experienced during calculating the 95 000 trials. Subplots (c) and (d) provide some statistical descriptors about the endogenous calculation error. For instance, for all 95 sets, with each set of 1000 trials

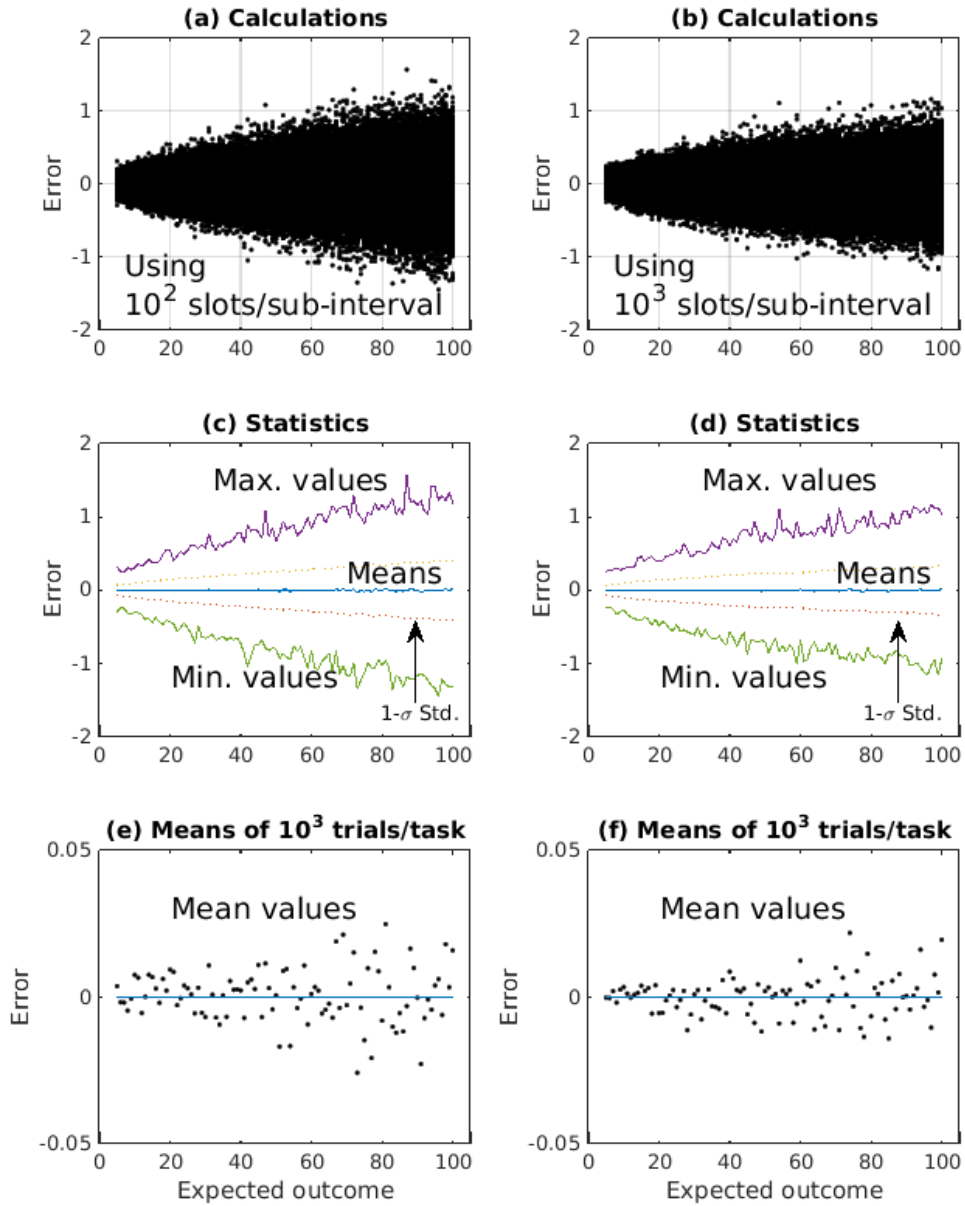


FIGURE 7.5: The subplots here show simulation results of wireless superimposed computing performed by a WSN with 5 sensor nodes. The left and right column present statistics for the calculation error experienced during calculating  $95 \times 1000$  mathematical tasks such as  $v_{s_1} + v_{s_2} + v_{s_3} + v_{s_4} + v_{s_5}$ , and  $v_{s_1}, v_{s_2}, v_{s_3}, v_{s_4}, v_{s_5} \in [1, 20]$ .

assigned to a certain  $y$ , their maximum, minimum, mean and  $1 \sigma$  standard deviation error is acquired. In subplots (e) and (f) we show the mean values in a zoom mode, which present their fluctuation in a visible range. According to the results in Figure 7.5 we can determine that in comparison the use of a coding scheme with  $10^3$  slots/sub-interval provides in relation to calculation error a better performance. This can be inferred visually by comparing all subplots together. Further, the calculation error is distributed symmetrically around the zero line, such that we can assume here to observe only an error caused by stochastic processes. Further on, we can state by considering the subplots a steady rise of calculation error, that we attribute to be owing to our coding scheme: the higher the value  $v_{s_i}$  is need to be encoded by a random burst sequence, the more entropy is loaded into a burst sequence leading proportionally to a higher statistical fluctuation. Considering subplot (c) and (d) we can register a drastic reduction of calculation error by taking the mean of trials. For instance, we sustain for using a coding scheme with  $10^2$  slots/sub-interval an inaccuracy of computation, that is conservatively considered, less than  $< 0.0258$ , when taking 1000 trials in a row. In case of using  $10^3$  slots/sub-interval we obtain an inaccuracy less than  $< 0.0219$ . The comparison of mean values depicted in subplots (e) and (f) indicates in tendency a better computation accuracy when using  $10^3$  slots/sub-interval.

### 7.3.3 Experiment 3: Large-scaled WSN

In the previous experiments we investigated behavior of wireless superimposed computing based on a WSN with 5 sensor nodes and using Equation (7.4) for error rectifying. In the following we investigate our solution for rectifying wireless superimposed computing in relation to larger WSNs with different sizes. In particular, we investigate WSNs with sizes of 10, 20, 30, 40, and 50 sensor nodes. Corresponding to size of a WSN with  $n$  nodes, we are calculating mathematical functions on the RF channel that have the form  $f(v_{s_1}, \dots, v_{s_n}) = v_{s_1} + \dots + v_{s_n} = y$ .

In a simulation of wireless superimposed computing we initialize first each sensor node with a prior drawn value  $v_{s_i}$  from  $\mathcal{X} = [1, 20]$ , so that in a second step, all sensor nodes generate correspondingly, and transmit simultaneously a random burst sequence. Since in simulations input and output of the mathematical tasks are a priori known, we can finally observe the calculation error for various configurations and differently large WSNs. In the simulations we incorporate asynchronous transmission of burst sequences to reflect real world characteristics of weak synchronization among nodes and distinct signal propagation times imposed by nature. The receiver counts incoming bursts and estimates the resulting  $\widehat{\mu}_R$  value as a result of addition of individual  $v_{s_i}$ -values. After taking the mean, outcome  $\widehat{\mu}_R$  is corrected at the receiver side by applying Equation (7.4).

TABLE 7.1: Errors experienced by calculation of valued during simultaneous transmission ( $t = 10^6$  and  $\kappa = 10^3$ )

	10 nodes	20 nodes	30 nodes	40 nodes	50 nodes
mean err.	0.2726	0.3673	0.4868	0.5777	0.6825
std-dev.	0.2143	0.2666	0.3625	0.4265	0.5114
max err.	1.1638	1.7065	2.0060	2.2395	2.7971
median err.	0.2266	0.3113	0.4123	0.4966	0.5677

To experience the calculation error of our solution with regard to various configurations and different WSN sizes, we simulate calculation on the RF channel for each mentioned WSN size calculating 1000 different mathematical tasks. In order to create manifold tasks we used randomly drawn values  $v_{s_i} \in [1, 20]$ . For every calculated task over the wireless channel we measure the absolute error to the ground truth. The investigation is in fact based on calculating a linear function  $f(\cdot)$ , but we take the simulation results for granted to be valid as well for other forms of mathematical functions, because the physical RF channel remains invariant regardless of the used encoding scheme and type of function.

In Table 7.1, 7.2, 7.3 and 7.4 we show some conspicuous simulation results. Further, in the excerpts we provide some statistics to the experienced calculation error. For instance, Table 7.1 depicts our results for network sizes of up to 50 nodes, employing a time frame of  $t = 10^6$  slots fixed by employing a sub-interval length of  $10^3$  and  $\kappa = 10^3$ . The parameter  $\kappa$  denotes divisor of time frame  $t$  indicating the number of sub-intervals within  $t$ . In Figure 7.6 we compiled those simulation results together gained by using explicitly a sub-interval length of  $10^3$  in all simulated WSNs and configurations. Hence, we observe that the mean error for all calculated tasks is rising linearly, when the number of sensor nodes in a WSN increases as well linearly. And, the larger a time frame  $t$  for encoding is used the smaller the resulting calculation error. Here, we achieve approximately each time an improvement of computation accuracy by a factor of  $3\times$ , whenever the length of time frame is proportionally enlarged by factor  $10\times$ . This assessment, however, is useful allowing to trade computation accuracy with constraints of a hardware technology. That means, that the calculation error is manageable and allows to define hardware requirements for future WSN application scenarios.

In further simulations we observe that the mean error is rising for using a time frame of  $10^6$  slots and a sub-interval of  $10^4$  slots (cf. Table 7.3), but we obtain an improvement in comparison to the results in Table 7.1, when we instead employ a time frame of length  $10^7$  and sub-interval of  $10^4$  (cf. Table 7.2). In particular, the use of a larger sub-interval but the same  $\kappa$  indicates a distinct better computation accuracy, when it is deployed for larger WSNs. We assume that a sub-interval length has a varying

TABLE 7.2: Errors experienced by calculation of valued during simultaneous transmission ( $t = 10^7$  and  $\kappa = 10^4$ )

	10 nodes	20 nodes	30 nodes	40 nodes	50 nodes
mean err.	0.0857	0.1227	0.1558	0.1844	0.2083
std-dev.	0.0642	0.0933	0.1156	0.1404	0.1626
max err.	0.3370	0.5338	0.6389	0.7878	0.9667
median err.	0.0717	0.1014	0.1323	0.1523	0.1729

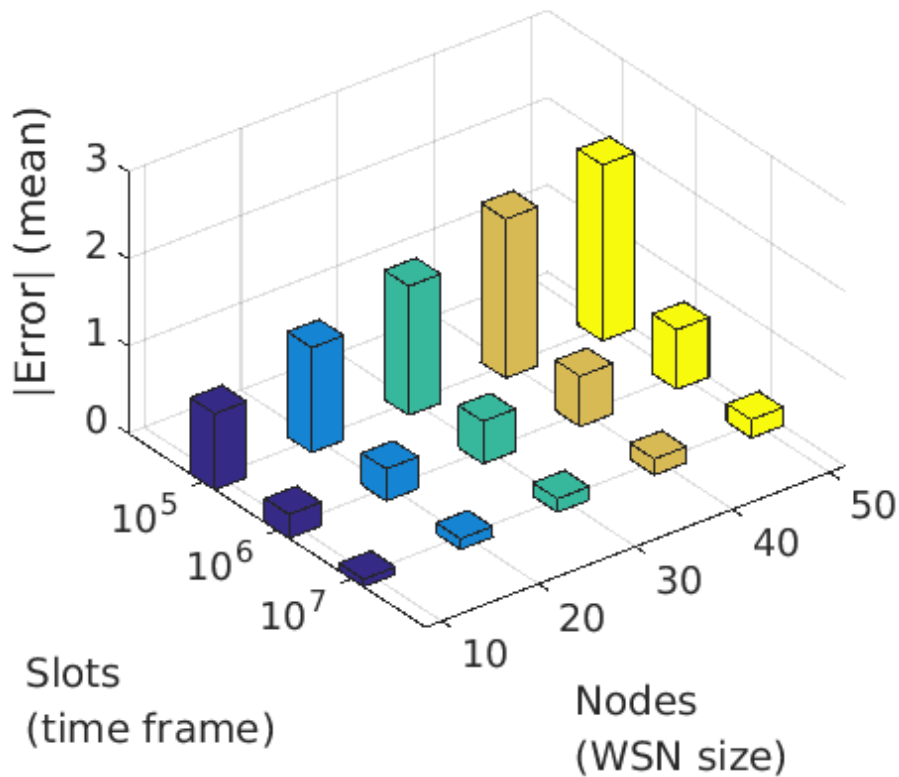


FIGURE 7.6: The 3D bar-chart presents error mean of wireless superimposed computing for various WSN sizes and different lengths of time frame experienced each time by calculating 1000 mathematical tasks.

TABLE 7.3: Errors experienced by calculation of valued during simultaneous transmission ( $t = 10^6$  and  $\kappa = 10^2$ )

	10 nodes	20 nodes	30 nodes	40 nodes	50 nodes
mean err.	0.8096	1.1558	1.4036	1.7522	1.9854
std-dev.	0.6235	0.8965	1.0789	1.2983	1.5007
max err.	3.9657	4.8954	7.3358	6.8628	9.5549
median err.	0.6828	0.9831	1.1777	1.5058	1.7066

TABLE 7.4: Errors experienced by calculation of valued during simultaneous transmission ( $t = 10^7$  and  $\kappa = 10^3$ )

	10 nodes	20 nodes	30 nodes	40 nodes	50 nodes
mean err.	0.2585	0.3681	0.4610	0.5139	0.5978
std-dev.	0.2015	0.2727	0.3499	0.3937	0.4556
max err.	1.1140	1.4718	1.7643	2.2535	2.9150
median err.	0.2197	0.3140	0.3945	0.4149	0.5084

impact on calculation accuracy, when the number of bursts therein is varying differently strong. But, we notice that a larger time frame  $t$  with smaller sub-interval length has a greater impact on the computation accuracy. However, we infer that the choice for a sub-interval length depends on the fixed operating number range. In our experiment we used to operate in range  $\mathcal{Y} = [10, 1000]$  (e.g., imagine that 50 sensor nodes are sending value  $v_{s_i} = 20$ , and all these values sum up on the RF channel). It seems that our choice for a sub-interval length of  $10^3$  is just sufficient to cover up the operating number range  $\mathcal{Y}$ , since the choice for a sub-interval length of  $10^4$  did not improve greatly. In addition, the simulation results indicate strongly, that the induced error by burst collisions is vanished, since we use our solution (cf. Equation 7.4) to correct wireless superimposed computing. Therefore, we conclude that a larger sub-interval length does not provide an improvement in computation accuracy automatically, but a larger time frame is always providing a better accuracy.

Thus, we can state that by increasing the count of sub-intervals (i.e., enlarging time frame) by either increasing  $t$  or decreasing the signal burst length, the error can be arbitrarily decreased at the expense of increased transmission time. To get practical experience for the configuration we utilized, the transmission time with  $t = 10^6$  at 2.4 GHz is about 10 ms with a burst length of  $0.01 \mu\text{s}$ . When we exemplarily increase the count of sub-sequences to  $t = 10^7$ , this induces a 100 ms transmission time resulting to performance as depicted in Table 7.2 and Table 7.4.

For setting appropriate parameters for our approach of wireless superimposed computing, we derive from simulations as a rule of thumb, that

- increasing the number of sub-intervals at the same sub-interval length increases calculation accuracy, whereas
- increasing only the sub-interval, or shortening the burst signal itself, does not necessarily improve the accuracy, and
- increasing the number of sub-intervals by dividing the same transmission time  $t$  with a greater  $\kappa$  increases calculation accuracy, as long as the sub-interval length fits to operating number range.

## 7.4 Design of a Resource-limited Sensor Node

In chapter 6.3 we described a WSN platform with 15 simple sensor nodes, that implements our approach of wireless superimposed computing. We created prototypically sensor nodes with off-the-shelf PCB electronic components deploying a commercially available micro-controller [219]. In a case study we demonstrated our approach of function calculation on the RF channel. However, the high power supply of the prototype with 5 Volts and slow burst signal generation makes it necessary to design a resource-limited IoT sensor node from scratch. A possible technique to this issue can be the utilization of a customized Application Specific Integrated Circuit design (ASIC) with integrating mixed-signal circuits [71]. However, as part of this thesis in the following we discuss practical implementation issues towards a resource-limited IoT node using traditional Si-based CMOS technology, and the emerging organic and printed electronics.

In the light of developing ultra-low cost sensing devices, such as smart labels based on organic and printed electronics [75], and on other hand sensor-based RFID networks [87] produced in traditional Si-based technology, the circuit design of such devices requires, due to manufacturing costs and low power constraints, complete simpleness and extreme low hardware complexity. For instance, organic electronics (OE) has the potential to become easy to manufacture and low-cost technology, enabling item-level tagging. But, on the other hand, the surface occupation to integrate sufficient number of transistors to realize a digital circuitry is too high, so that current state-of-the-art OE is not able to realize IoT sensor nodes with standard communication protocols. While future technological advances might mitigate these hindrances, another motivation to consider highly resource restricted nodes is to enable self-contained wireless sensor networks relying entirely on power harvesting techniques [221]. An alternative, until OE becomes more mature, is indicated by deploying Si-based CMOS hardware technology, which commonly known provides high performance in terms of transmission range, carrier frequency generating, computational power, clocking frequency and surface consumption. However, the production costs for these devices are higher. To mitigate manufacturing cost, in the meantime one can assemble a hybrid technology between Si-based technology and OE [222].

The system architecture of the proposed resource-limited IoT node is shown in Figure 7.7, consisting essentially of an integrated circuit (IC) and three external components, such as the power harvesting unit, the sensor interface and the printed antenna on the circuit board. The circuit layout inside the IC is partitioned into several circuit functions such as the ring oscillator providing the synchronous system clock, the demodulator and modulator responsible for the external communication, and the control logic unit realizing the operating system of the sensor node.



### 7.4.3 Random Burst Sequence Generation

As we pointed out a RNG is needed to generate Poisson-distributed burst sequences coding the sensory information. To enable transmission of random bursts following a specific Poisson distribution, i.e., to enable a hardware device to do so, we exploit the relationship between a Poisson and exponential distribution:

*If a Poisson process generates the number of occurrences of events per time interval, then the lengths of time between two occurrences describe an exponential process [223, Chap. I.4].*

This means with regard to our application scenario, that if  $\mu$  denotes averaged number of bursts within a fixed time window  $\Delta w$ , and  $\mu$  is expectation value of a Poisson distribution, then the averaged waiting time  $\lambda$  between two occurring bursts results in  $\lambda = \Delta w/\mu$ , denoting expectation value of an exponential distribution. Hence, we utilize this relation to synthesize the circuit functionality that produces time points for burst transmissions. In order to generate exponentially distributed random lengths of time, assigning them to as waiting times between two bursts, we employ the Inverse Transform Method (ITM) (cf. reference [224, pp. 41-42] or textbook [225, Chap. 5.3]), that transforms random numbers from an uniform distribution into another requested distribution. For instance, if  $u \in U(0, 1)$  is uniformly distributed, and  $F$  denotes the Cumulative Distribution Function (CDF) of a requested Probability Density Function (PDF), then, we can obtain the random number  $z$  following a requested distribution by  $z = F^{-1}(u)$ . Thus, following the ITM, we proceed with  $u \in U(0, 1)$  and  $F(t) = 1 - e^{-\lambda t}$  is being CDF of exponential PDF  $f_\lambda(t) = \lambda e^{-\lambda t}$ ,  $t \geq 0$ , and conclude  $u = 1 - e^{-\lambda t} \Rightarrow \lambda t = -\log(1 - u) \Rightarrow t = -\log(u)/\lambda$  obtaining  $t = F^{-1}(u)$ . Note, that  $u \in U(0, 1) \Leftrightarrow 1 - u \in U(0, 1)$ . Out of reference [225, pp. 164].

With the result of using ITM, we can now formulate the procedure for generating Poisson-distributed burst sequences as follows.

1.  $N$  : number of time slots within a time interval;  
 $t_i$  :  $i$ -th time point;  
 $\lambda$  : parameter of exponential distribution  $f_\lambda(t) = \lambda e^{-\lambda t}$ , for  $t \geq 0$
2. Draw a random number from an uniform distribution  $u_j \in U(0, 1)$
3. Calculate next time point for sending a burst by  $t_i = t_{i-1} - N \log(u_j)/\lambda$
4. Transmit a burst at time point  $t_i$
5. Go back to step 2.

As we can observe in the procedure the essential hardware synthesis relies on implementing building blocks for a RNG generating uniformly distributed random numbers, and a logarithm function to attain exponential deviates.

With respect to numerical precision and internal processing on-chip the choice for embedding a True Random Number Generator (TRNG) [226] can be seen as best utilizing, e.g., a physical phenomenon such as atmospheric noise [227], but a technical implementation of a TRNG into hardware can be difficult and costly [228]. Further, the random number generation of such TRNG can be at low rate [229], power inefficient [230] and susceptible to outside influences [231] such as an unnatural environmental change by hostile attacks. The relative high power consumption [230, 232] dissents additionally the objective of designing a resource-limited IoT node.

As an alternative for embedding a RNG into our envisioned resource-limited IoT node we can use a Pseudo-Random Number Generator (PRNG) [233] producing random numbers based on a deterministic algorithm. Hence, we have for our disposal a wide range of PRNG algorithms [225, Chap. 5][234], that can be categorized mainly by Linear Congruential Generators (LCG), Lagged Fibonacci (LFG) and Feedback Shift Register Generators (FSRG).

#### 7.4.4 Circuit Core Design

With respect to circuit design of an IoT sensor node featuring ultra-low hardware complexity, simple PRNG algorithms are preferable to be considered, when putting power supply, area occupation on-chip, speedup and efficiency of random number generation into account, because their implementation leads presumably to simple hardware circuitry. Therefore, in the following we focus on pointing out implementation issues of PRNGs, that can help, and be crucial by designing a resource-limited IoT node for a specific application scenario. First, we begin with implementing a common LCG algorithm, following by a LFG random generator, and finalizing discussion with a FSRG. Second, we investigate in addition solutions for implementing logarithm computation on-chip, that we use to transform uniformly distributed random numbers into exponential deviates.

The most obviously simple LCG algorithm is originating by Lehmer [235] commonly generalized to recurrence equation [236]

$$x_j = (a \cdot x_{j-1} + c) \bmod m, \quad (7.6)$$

featuring three integer constants, namely, multiplier  $a$ , increment  $c$ , and modulus  $m$ . By initializing the recurrence relation (7.6) with seed  $x_0$  of type integer, pseudo-random numbers  $x_1, x_2, \dots$  of type integer are generated deterministically between 0 and  $m - 1$ . To produce pseudo-random numbers of type real,  $u_j = x_j/m$  is calculated. The outcome of  $x_j = 0$  is rejected, such that  $u_j \in U(0, 1)$ . Depending on chosen parameters  $a$ ,  $c$  and  $m$  the recurrence equation (7.6) fabricates different pseudo-random sequences. Based on Hull-Dobell Theorem [237][238, pp. 86] LCG parameters are chosen along complying with following conditions [225, pp. 156][239, pp. 17-19][236]

1.  $c \neq 0$ ,
2. Offset  $c$  and modulus  $m$  have no common divisor,
3.  $a$  and  $c$  are relatively prime,
4.  $(a - 1)$  is divisible by all prime factors of  $m$ ,
5.  $(a - 1)$  is divisible by 4, if  $m$  is divisible by 4.

Thus, if, and only if LCG parameters hold these requirements (Hull-Dobell Theorem [237] or, cf. textbook [238, pp. 86]), then the LCG produces pseudo-random numbers with full period by  $m$ . For example, if we choose for our envisioned IoT node an 8-bit processor unit, then we can set by default  $a = 17$ ,  $c = 5$ , and  $m = 2^8$ . Checking all parameters with above listed requirements – we attain that all conditions are holding: (1)  $c = 5 \neq 0$ ; (2)  $c = 5$  and  $m = 2^8$  have no common divisor; (3)  $a = 17$  and  $c = 5$  are relatively prime; (4) all prime factors of  $m = 2^8$  is 2, and  $a - 1 = 16$  is divisible by 2; (5)  $a - 1 = 16$  is divisible by 4, and  $m = 256$  is divisible by 4.

For implementing the LCG into our 8-bit IoT node at hardware level we need just to deploy an 8-bit shift register with doing operations of shifts to multiply and additions [238, pp. 86-88]. For example, when we initialize register  $R = [b_7b_6b_5b_4b_3b_2b_1b_0]_2$  with start value  $R \leftarrow x_0 = [00001111]_2 = 15_{10}$ , and carry out  $x_1 = (17 \cdot 15 + 5) = 260_{10}$ , we sustain an overflow  $R = [1\ 00000100]_2$ . However, since the leftmost bit is truncated automatically by the 8-bit register, we obtain instantly modulo calculation by  $m = 2^8$  resulting into  $R \leftarrow x_1 = [00000100]_2 = 4_{10}$ . Further, we obtain even more by doing nothing: the content of register  $R$  can be interpreted as outcome of  $u_j = x_j/m$  by setting at the leftmost bit a binary point resulting to  $u_j = (0.00000100)_2 = (4/256)_{10} = 0.015625_{10}$ . By using a parallel multiplier [240] in combination with register  $R$  and an adder, the multiplication and addition of  $R \leftarrow a \cdot R + c$  can be accomplished in few clock cycles. Further, if we beforehand store  $\log(u_j)$  for each  $x_j$  in a Look-Up Table (LUT), then the remaining calculation of  $N \log(u_j)/\lambda$  is straightforward. However, in case the word size

of our processor unit is greater than 8-bit or, computation on-chip need to be performed with a higher precision, explicit computation of  $\log(u_j)$  is inevitable, because storing  $2^b$  values in a LUT, by  $b \gg 8$ , is in terms of allocatable memory impractical.

Therefore, alternative techniques implementing the log-function on-chip need to be considered. For example, a technique that uses small LUT along with linear function interpolating between table values [241] can be deployed. Similar techniques based on using ROMs are described by references [242, 243]. An overview about differences in using LUT-based techniques is given by reference [244]. The works [245–247] use multipliers for logarithm computation instead. Further on, in work [248] a method for variable precision logarithm is described using polynomial approximation. Other methodologies that approximate  $\log()$  are the Coordinate Rotation Digital Computer (CORDIC) algorithm [249–252] converging digit-by-digit iteratively and Parabolic Synthesis (PS) [253–255] deploying parabolic functions for approximation.

Taken as a whole, we described so far all elementary circuit functions needed to create an IoT sensor node, that in turn realizes our approach of data processing on the RF channel. In the following we investigate further optimization issues regarding sensor node circuitry.

As we mentioned above, different types of RNGs exist generating uniformly distributed pseudo-random numbers. Hence, we can replace the LCG in our circuit design by deploying a LFG function (producing lagged Fibonacci sequences). An interpretation of an additive LFG expressed in a recurrence relation [256][225, pp. 158] represents

$$u_n = (u_{n-j} + u_{n-k}) \bmod 1 \quad 0 < j < k, \quad (7.7)$$

with  $j = 24$ ,  $k = 55$ , and  $x \bmod 1 = x - \text{int}(x)$ . The maximum period of this generator is estimated by  $(2^k - 1)2^{M-1}$  [256], where  $M$  denotes word size of used microprocessor. An advantage of LFG over LCG is its period that can become much more larger [228, pp. 15-16]. Consequently, more variability in computing the exponential deviates is expected, which makes it less susceptible to cause systematic errors. However, disadvantage of LFG is its overhead to include sufficient randomness in the process of random number generation [256][225, pp. 158-159]. For example, randomness is increased when during random number generation thereof partial sequences are rejected periodically [257, 258]. This is, however, in terms of speed inefficient. The additional overhead, which is needed to be implemented in circuitry, raises disadvantageously the hardware complexity.

The third category of PRNG we take into consideration is based on a shift register using linear feedback function to generate inside uniformly distributed pseudo-random numbers [259], that we abbreviate with FSRG. The FSRG begins with initializing the

register with a bit string of same size. After that the bit stream inside is shifted bit-wise in one direction, e.g., to the left. The output bit resulting from shift operation and a number of fetched bits, tapped from predetermined positions within register, are inputted in a linear feedback function, whose outcome is sequentially fed back to shift register - in our example - at the rightmost bit position. The implementation of the linear feedback function into hardware is based on using a single or a series of interconnected *exclusive-or* (XOR) gates (cf. references [259, 260] or an example of a hardware implementation [261]). For theoretical background regarding concept of FSRG see for example [262, 263], textbook [234, Chap. 1.6] and references therein).

For our study we consider in particular the class of Generalized Linear Feedback Shift Register (GLFSR) pseudo-random number generators initially introduced by Lewis and Payne [264]. The GLFSR algorithm is based on Tausworthe's method [262] operating mathematically in Galois Field  $GF(2)$ . It uses, algebraically speaking, a ring structure of polynomials, i.e.,  $\mathbb{Z}_2[x]/f(x)$ , with  $f(x)$  being an irreducible polynomial. In particular, a GLFSR generator employs an irreducible polynomial of form  $f(x) = x^p + x^{p-q} + 1$  called primitive trinomial. Instances of such primitive polynomials found in  $GF(2)$  are gathered, e.g., in works [264–268]. Hence, a chosen trinomial of degree  $p$  for hardware implementation determines size of shift register  $R(p, q)$  and linear feedback function. For example, if we choose trinomial  $f(x) = x^{31} + x^3 + 1$ , then we need a shift register  $R(31, 28) = [b_{31}b_{30}b_{29}b_{28} \dots b_3b_2b_1]$ , with  $\{p = 31, q = 28\}$  denoting tapping bit positions, that are connected with the linear feedback function. Since we deploy here a two tap shift register the linear feedback function consists of a single XOR gate, whose output is reconnected with shift register  $R(p, q)$  as described earlier. The operation mode of GLFSR generator can be expressed by the following recurrence relation

$$\begin{aligned} b_i &\equiv (b_{i-p} + b_{i-p+q}) \pmod{2} \\ \Leftrightarrow b_i &\equiv b_{i-p} \oplus b_{i-p+q}. \end{aligned} \tag{7.8}$$

Based on applying the recurrence relation (7.8) we obtain a randomly appearing bit stream. Thereof, pseudo-random numbers are created by decimating the generated bit stream into  $l$ -wide sized binary numbers, where  $l \leq p$ . The GLFSR algorithm produces pseudo-random numbers with a period of  $2^p - 1$ , when, e.g., the initialization strategy by Collings and Hembree [269] is employed. This method performs preprocessing on Tausworthe's sequence, where a table of  $p \times l$  bits is laid out. In our case, if we choose to work with 16-bit processing, then we need to allocate  $31 \times 16 = 496$  bits of memory. Once the GLFSR table is established the pseudo-random numbers are generated efficiently through bitwise shifting.

Summarizing our study about designing circuit core of our envisioned IoT sensor node, we introduced implementation of our burst sequence generation method at hardware level, and investigated various techniques to implement elementary circuit functions such as random number generation and logarithm computation on-chip. With respect to generators of random numbers utilized for controlling random burst transmissions, we realized that a Linear Congruential Generator (LCG) is easy to be implemented in hardware, and efficient in operation, but lacks of having a desirable large period. Lagged Fibonacci Generators (LFG) provide a large period in random number generation, but they lack of being efficient. Generalized Linear Feedback Shift Register (GLFSR) generators, on the other hand, are efficient and can have a very large period for the price of allocating memory in kilobyte range. However, memory allocation and length of period are scalable. With respect to implement  $\log()$  function, various techniques exist, such that a specific method can be chosen to fit fixed hardware requirements.

#### **7.4.5 Computation on the RF Channel**

In our design of a resource-limited IoT node presented above we provided all necessary circuit blocks to create finally a sensor node at hardware level integrating our approach of data processing on the RF channel. In the following we continue to provide an overall functioning of a sensor network deploying our type of IoT node, and complete with it the system description.

The regular procedure for calculating a desired mathematical function on the wireless channel, such as calculating the mean temperature value in a scattered sensor network, is initiated at the base station by broadcasting a request command to all sensor nodes. Consequently, all sensor nodes are transmitting their random burst sequence approximately at the same time. Additional synchronization is not required for the wireless calculation. However, by expanding the length of the burst sequence or of the bursts itself the tolerance for inaccurate synchronization is increased. At the base station the superimposed burst sequence is evaluated by counting the occurred bursts in a fixed time frame. Based on the mean value of the obtained histogram the final outcome of the calculated function on the RF-channel is acquired.

### **7.5 Summary**

In this chapter we analyzed analytically our wireless superimposed computing approach in detail, and derived a solution to deal with systematic and statistical calculation errors efficiently. In particular, we achieved to remove the induced error caused by burst

collisions, and to manage statistical fluctuations. In practice we obtain all along approximately a  $3\times$  better computation accuracy, whenever we employ our solution for error correction and the enlargement of time window for radio reception by factor  $10\times$ . Thus, we can now arbitrarily minimize the error of wireless superimposed computing at the expense of transmission time. To this end, we discussed the hardware design for resource-limited IoT sensor nodes implementing our approach of wireless superimposed computing. In particular, we elaborated hardware constraints needed to implement our approach into circuitry with different hardware technologies, and provided a circuit design for a resource-limited IoT node at the function blocks level. Vital circuit block functions are discussed in detail. The way for implementing the circuitry into an Application Specific Integrated Circuit (ASIC) is facilitated. In the next chapter we summarize our achievements worked out in this thesis, and provide a final conclusion and outlook about Collective Communications (CC), printable RFID smart labels using collective transmission and resource-limited IoT sensor networks employing our wireless superimposed computing approach.

## Chapter 8

# Conclusion and Outlook

In this final chapter, we summarize and discuss our achievements, provide a conclusion, outline main limitations, and sketch promising directions for future work.

### 8.1 Conclusion

The main issues for realizing the IoT are to obtain ultra-low cost RFID and sensing technology with respect to item-level tagging, resource-limited WSN and high communication load. Organic and printed Electronics (OE) has the potential to enable IoT, but indicates serious limitations with respect to evolving to high-performance electronics technology.

In this thesis we investigated the exploitation of superimposed radio transmission to achieve highly scalable and robust communications for minimalistic OE smart labels. In addition, we utilized the superimposed radio transmission to obtain resource-limited WSNs. With regard to low-cost RFID technology we developed code-based Collective Communications (CC) tailored specifically for obtaining minimalistic OE smart labels. The approach is based on collaborative and simultaneous transmission of data encoded with randomly drawn burst sequences of fixed length. Based on statistic laws and the superposition principle of electromagnetic waves we enabled the communication of so called ensemble information, meaning the concurrent bulk reading of sensed values, ranges, quality rating, identifiers (IDs), or any other conceivable entity. With 21 testing transducers on a small-scale reader platform mimicking OE smart labels, we investigated the performance of our approach proving the scalability property and reliability. The evaluation of our code-based CC method shows a robust, collective, approximate communication method suitable for reading massive amounts of sensor labels. Through the

simplified communication scheme a minimalistic circuit design for OE smart labels was achieved. The experiments suggest a general feasibility of this mechanism in the economically meaningful scenario of item-level tagging for next-generation business process support.

An issue of our testbed presents the low number of senders when compared to a pallet scenario of 1000 tags. Moreover, conditions in the testbed are presumably much better than in a pallet: different packaging materials and larger distances could decrease the readability of the tags. However, this addresses an engineering challenge, where a reader platform need to be specifically designed for a particular application scenario. For example, one can think of a smart shelf where a loop antenna is surrounding the bottom shelf embracing all products in short distance.

To reveal the hardware complexity of such proposed minimalistic OE smart label, we implemented the code-based CC mechanism into an all-printable 64-bit passive RFID label down to the logic gate level. Based on current stage of OE, we provided a feasibility assessment, that indicates the printing of the proposed smart RFID label is in principle with present-day printing technology possible, but entails risks, such as low communication range and hazard-afflicted circuits that have been encountered by organic printed devices with similar hardware complexity. The causes for it were led back in the used conductive inks and fluctuations at the printing process. Hence, the specified hardware parameters may vary drastically, so that the printed polymer tags may exhibit unexpected and consequently unwanted behavior. However, the feasibility of printing our smart label circuit has been thankfully confirmed by the project partner PolyIC.

For obtaining resource-limited WSNs we developed time-based CC, which utilizes as well the idea of superimposed radio transmission in combination with the concept of function computation over the wireless channel. In particular, we applied in this respect superimposed radio transmission to obtain the computation of desired functions, i.e., to carry out processing of sensed data directly on the RF channel, such that the receiver node acquires the result of a computation automatically, rather than receiving in traditional way the single sensor values sent from the sensor nodes individually. For processing of the sensor values over the wireless channel, we employed essentially Poisson-distributed burst sequences. For proving our approach in a real scenario, we created for this matter a WSN with 15 simple nodes, that we deployed in a case study, where it calculated the mean temperature with a negligible inaccuracy at the time of transmission. In our analysis we determined all possible stochastic and systematic errors of our time-based CC approach, and found out that they are completely removable. First, the computation error can be arbitrarily minimized at the cost of increasing the length of the burst

sequences, which implies an increased power consumption, and, shortening the burst itself. Second, in post-processing the systematic error is completely removable.

For employing our time-based CC with respect to other WSWN application scenarios, we elaborated some circuit design recommendations offering a minimalistic circuit design for a desired mixed-signal ASIC device.

With respect to computational power on the RF channel, time-based CC enables the computation of linear and nonlinear functions. This transmission scheme, as it became apparent, can empower resource restricted IoT nodes to conduct ambitious computation by trading computational load for communication load.

## 8.2 Future Work

The investigation and exploitation of the superimposed radio transmission in this thesis yields practical solutions, strategies and methods for the area of RFID and WSN technology, which identifies following features, such as

- collective, unidirectional and simultaneous transmission of ensemble information containing data of a group of senders to a fusion center,
- real time output,
- approximate recovery of information out of the superimposed radio transmission,
- light-weighted circuit design for IoT electronic devices.

The proposed communication schemes in both areas are based on the same principles, such as using randomly drawn burst sequences and overlaying of signals on the RF channel, but distinguishes in data coding and interpreting the outcome of a superimposition. While code-based CC method (cf. chapter 3 and 5) recovers sent data, the computation mechanism based on time-based CC in chapter 6 and 7 performs data processing on the RF channel. For future work these methods can be combined to one methodology, in order to achieve better access to superimposed radio transmission, and thus better understanding about superimposed coding. Further on, since mathematical computation is enabled on the RF channel one can extend this idea to develop algorithms running on the RF channel, and in comparison to conventional processing improve their computational complexity.

Following the results of the thesis the next steps can be the economical exploitation of the proposed approaches. With regard to OE smart labels employing code-based CC one

can create an application-dependent tag-reader-system deployed for example in product quality rating. With regard to resource-limited WSN implemented with time-based CC one can, for example, design and manufacture wireless sensor nodes specifically for production lines in factories, or environmental monitoring in supermarkets to monitor freshness of vegetables and fruits.

# Appendix A

## Printed RFID in a Nutshell

### A.1 Introduction

The prospect of low-cost and flexible organic printed RFID tags for item-level tagging using conventional printing technology for their fabrication, the development of printed RFID is one of the driving forces in industry and research to realize the vision of Printed Electronics (PE) [37, 38]. In the last decade several global players<sup>1</sup> such as the companies Kovio, Thinfilm Electronics and PolyIC, and research facilities such as the Fraunhofer, IMEC and Sunchon University, have been working with others of industry and academia in various projects, advancing steadily the technology for printed RFID. To report on such undertakings, for example, the project PRISMA (PRInted SMARt labels, 2007–2009) marks the first use of printed radio chips embodied in electronic tickets, being tested in public fields, such as the issuance of more than 400 printed electronic tickets on the international OEC-2007 conference, and at another event (the Mediatech trade fair, 2008) even 4000 admission tickets have been handed out [34]. In a following project named ORICLA (2010–2012), funded by the European Union within the Seventh Framework Programme (EU FP7), the involved companies and research institutes worked together to overcome the performance limitations of organic and printed RFID by developing hybrid organic-oxide complementary thin-film technology for an all-printable RFID system on foil [270]. With combining organic and novel oxide semiconductor materials, to create complementary thin-film technology, the ORICLA partners enabled in this venture for the first time bi-directional communication between a printed tag and reader-device, communications in Ultra High Frequency (UHF) band, large memory on chip to contain the EPC code of 128 bits, and a rectifier circuit working at UHF. At

---

<sup>1</sup>A list of involved companies and research institutes developing OE can be found, e.g., at the yearly occurring LOPEC exhibition, an international trade fair and conference for printed electronics, being held in Munich, Germany. See <http://www.lopec.com>.

the homepage of the project ORICLA a publication list about their achievements is available [271].

In consideration of the demand for ultra-low cost electronics, and the prospect of novel applications and markets in pervasive computing utilizing Organic Electronics (OE), the German Federal Ministry of Education and Research initiated project Polytos (2009–2013) to promote the printing technology for producing polymer-only tags in large-scale. The objective of this research project targeted to develop printed organic circuits with integrated sensors capable of recording data, such as temperature, humidity or light exposure. The incentive was the deployment of these types of printed organic circuits for item-level tagging in logistics and supply chain scenarios, which can be used as organic printed smart labels in the future. In terms of providing the technology for mass-printing, as well as the communications and business software for organic and printed smart labels, the project partners were collaborating substantially in two groups: a hardware group (developing fundamentals of mass-printing technology, semiconductor materials, sensors, design rules for logic circuits) and, software group (developing the application side for business software and smart label scenarios). In this project we were as subcontractor within the software group developing highly scalable communication protocols for minimalistic printed passive smart labels, i.e., that are capable to read out sensory information from densely shelved items within a short time frame. Some of our contributed solutions and scientific publications to this project are partly reproduced in this dissertation.

A similar undertaking to project Polytos to enable a technological platform for producing ultra-low cost printed smart tags with sensors is called PROLOG (P<sub>R</sub>inted Organic LOGic circuits for low-cost smart tags, 01/10/2012–31/03/2015) [33]. In contrast to Polytos the objective of project PROLOG was the development of actively driven printed smart tags integrating a printed logic circuit which allows to interface with printed memory, display and a battery. With regard to circuit design the project PROLOG brought out of two transistor technologies, namely the circuit design with OTFTs (Organic Thin-Film Transistors) and OECTs (Organic Electrochemical Transistors). Based on these transistor technologies basic circuit functions such as a voltage pump for a tag, sense amplifier, display driver and memory readout are implemented [33].

For information about further projects and undertakings in the area of Printed Electronics (PE) dealing in particular with smart packaging, we refer to the OPE journal (cf. references [73, 272]). In the remaining part of this appendix we continue to introduce basic fundamentals of PE. For instance, in section A.2 we provide some foundations of PE circuit design, which aim to provide the reader with awareness of challenges that current PE is facing. Further on, in section A.3 we report on state-of-the-art of PE,

which in particular relate to some aspects of printed RFID. In the last section A.4 we introduce some commonly deployed mass-printing technologies with performance parameters, indicating with it the gap of feasibility between manufacturing of OE at lab and industrial-scale.

## A.2 Some Printed Electronics Foundations

In the previous section we introduced some key projects advancing the PE printing technology over the last decade dedicated in particular in the area of printed RFID. As we mentioned above, in the project Polytos our role in the software group was to develop primarily highly scalable communications for minimalistic and performance limited printed smart tags with integrated sensors, whereby we partly reproduce some of our solutions in this dissertation. Further, as one can already identify from above various technologies and methods are in the process of developing efficient and robust circuit design, printing techniques and electronic inks. However, while our work in the development of communication mechanisms for performance limited printed smart tags can be understood as a software solution for PE issues, the counterpart represents the steady efforts in improving the PE printing technology itself. Exemplary, in relation to the project Polytos in the hardware group the research foci were the development of novel materials for conductive inks and substrates, characterization of electronic components and automated design rules for printing circuits, as well as manufacturing processes regarding mass-production [273]. From various fields of expertise, engineers, material scientists, chemists and physicists have been working together interdisciplinary, in order to advance OE<sup>2</sup> for the packaging industry. The subject matter of research is to bring up all required technical building blocks to complete an entire value chain for producing intelligent and flexible printed devices with an integrated sensor in industrial-scale. Initialized by investigating and developing of novel printing methods, semiconductor materials and high-speed Roll-to-Roll (R2R) printers, the hardware group tested and refined their methods towards printing basic electronic structures, such as transistors, diodes, capacitors, or an irreversible binary temperature sensor [78, 191, 273].

Based on optimizing in particular the hardware parameters for printing OFETs (Organic Field-Effect Transistors) the findings and experiences of various approaches are discussed, and exchanged among the project members [273]. With regard to improving the hardware performance of printed transistors, the project partners applied novel

---

<sup>2</sup>Organic and printed Electronics (OE) describes printed devices produced by using polymer-based electronic inks, and Printed Electronics (PE) is a general term for including printed devices manufactured with inorganic semiconductor materials.

semiconductor polymers and manufacturing processes. However, the optimization process can be essentially described in relation to modeling a high-performance organic printed transistor by applying the framework for conventional transistors [274]. Hence, the guidelines for OFETs are specified by setting the operating frequency  $f$  and the electro mobility  $\mu$  for semiconductor materials. For instance, to operate in HF range (13.56 MHz) demands a very low channel length by  $\sim 14 \mu\text{m}$  and a carrier charge mobility of  $10 \text{ cm}^2\text{V}^{-1}\text{s}^{-1}$ . The Equation A.1 below enables optimizing transistor maximum switching frequency  $f$  along the channel, by varying the mobility  $\mu$ , gate voltage  $V_{GS}$  and channel length  $L$ :

$$2\pi f = \frac{\mu \times (V_{GS} - V_{th})}{L^2} \quad (\text{A.1})$$

The measure of transistor switching speed is given by the ratio of transconductance  $g_m$  to input capacitance  $C_g$  as follows:

$$\frac{g_m}{C_g} = \frac{\mu}{L^2} (V_{GS} - V_{th})$$

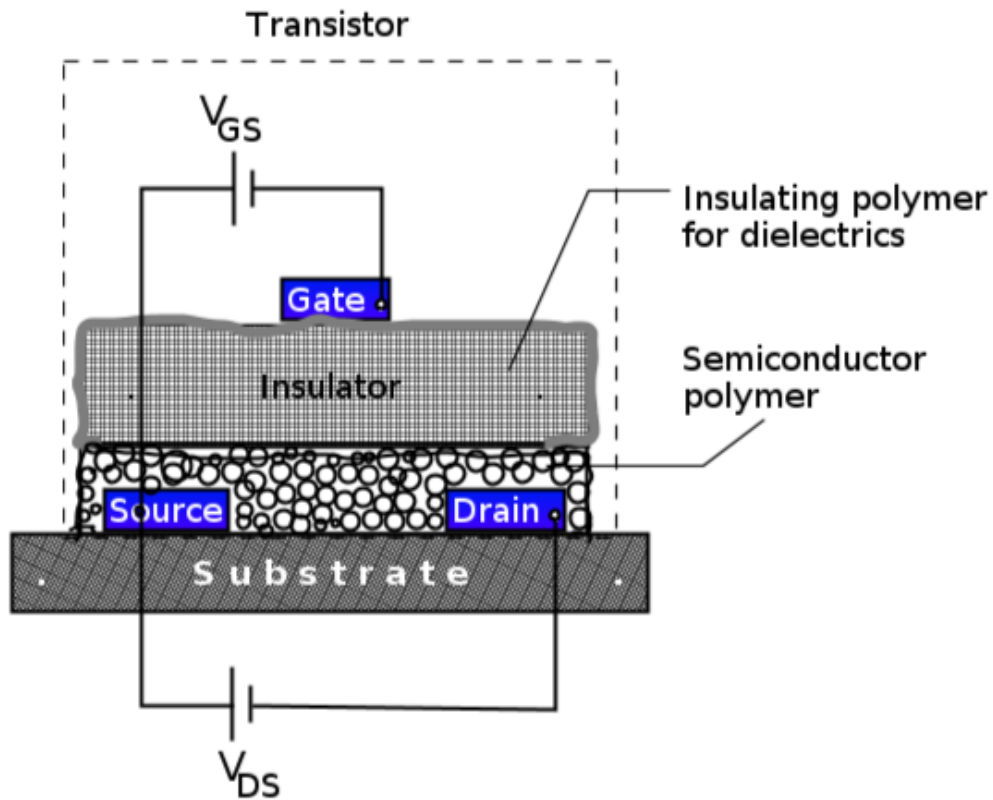


FIGURE A.1: Depicted is an organic transistor printed on a plastic substrate. The source and drain are separated by a semiconductor polymer. An insulating polymer forms the dielectric layer between gate and the other layers.

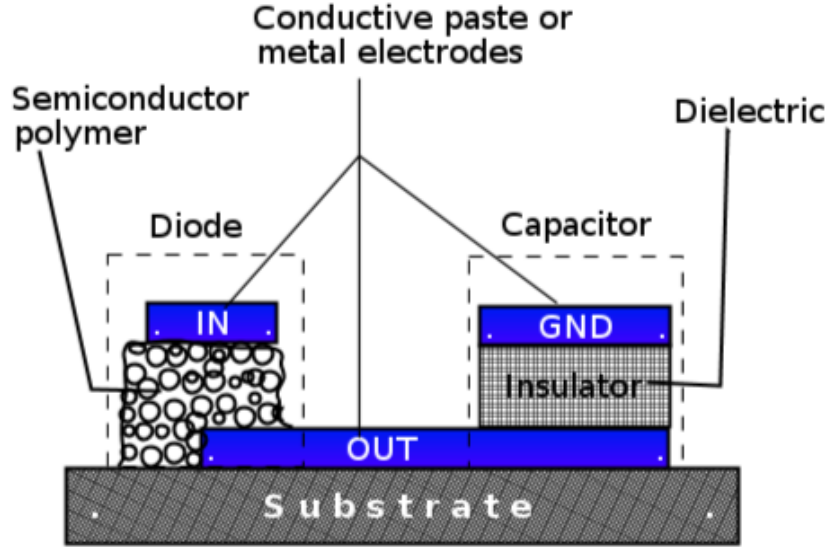


FIGURE A.2: The diode (left) and capacitor (right) together form a half-wave rectifier with a reservoir capacitor.

$$C_{ox} = \frac{C_g}{W \times L}$$

The parameter  $V_{th}$  denotes the threshold voltage,  $C_{ox}$  specifies the oxide capacitance, and  $W$  is the channel width.

In order to acquire an optimized printed circuit device the optimizing process needs to consider all occurring hardware parameters at the same time [79]. Apart from considering the electro mobility of semiconductor polymers and the behavior of single printed transistors, it is additionally necessary to determine the geometry of the printed circuit, i.e., the layer thickness has an affect on the electrical system of a printed device [8, 79]. Thus, simulators for OE are deployed to estimate the electrical functionality of an devised circuit design (cf. references [191, 275]). Regarding device manufacturing, rapid prototyping of novel circuit concepts with adapted transistor channel length and width is used. The basic structure of an organic and printed transistor is exemplary illustrated in Figure A.1, depicting a multilayer printing of several functional materials, such as plastic foil as substrate carrier, metal electrodes for source (S), drain (D) and gate (G), and using semiconductor, as well insulating polymers for dielectrics. Figure A.2 depicts further printed electronic components, such as a diode and a capacitor, together building a simple half-way rectifier with a reservoir capacitor (cf. Figure A.3). With respect to OE smart label design, the rectifier device represents an essential electronic building block, that is used to empower a passive RFID label by scavenging the energy from an electromagnetic RF field. An early implementation example of such a rectifier device in a printed passive RFID tag is reported by Henning Rost and Wolfgang Mildner [79].

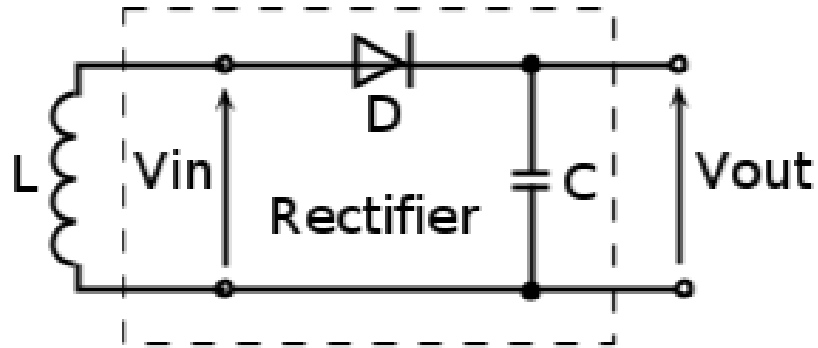


FIGURE A.3: Half-wave rectifier circuit with a reservoir capacitor.

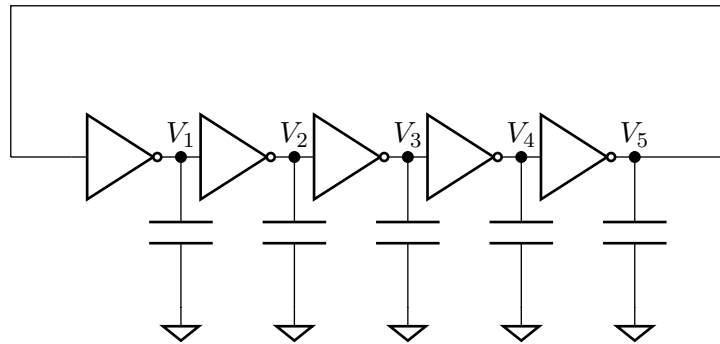


FIGURE A.4: Circuit diagram of a 5-stage ring oscillator realized with five logic inverter gates. The capacitor between two inverter gates serves to delay the input signal of the following inverter.

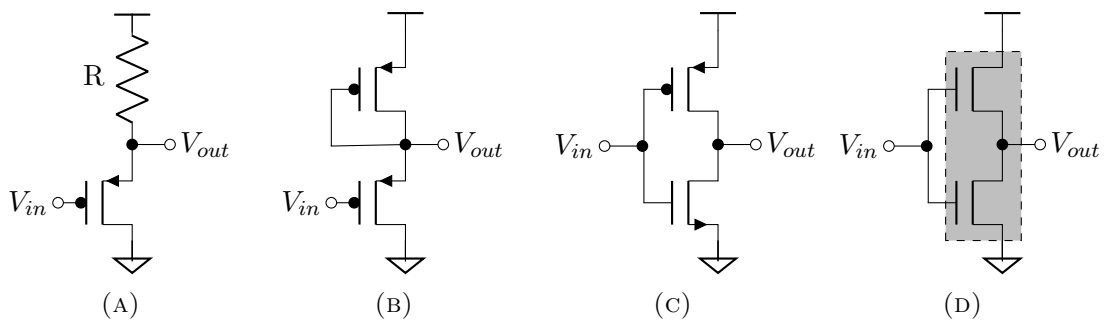


FIGURE A.5: The circuit diagrams (A), ..., (D) illustrate four different architectures realizing the logic inverter gate 'NOT'. The configurations (A) and (B) are characterized as unipolar, that are realized with p-only semiconductor material, whereby (A) is an inverter with load resistor, and (B) integrates a depletion load transistor. The configurations (C) and (D) are denoted as complementary CMOS-like inverter architectures. A distinctive feature indicates configuration (D), because its complementary circuit architecture is realized by a single ambipolar semiconductor material underlaid with a grayed out rectangle in subfigure (D).

An intricately and more sophisticated electronic component on a printed RFID tag represents the Integrated logic Circuit (IC), which is electrically connected and empowered by the rectifier circuit (cf. Myny et al. [87]). The IC realizes a Finite State Machine (FSM), responsible to process from outside incoming messages, read out of memory banks, convert analogue-to-digital sensor values, and generate coded messages for wireless communication purposes [30]. To implement all these functionalities the integration of various basic digital circuit functions such as logic gates, a counter, a shift register, a ring oscillator, a line select driver to address the memory, an adder, or an Analog-to-Digital (ADC) converter is required. In all these circuit functions being used to compose the IC, however, the most basic and elementary function represents the logic inverter gate 'NOT' negating a digital input signal (cf. reference [276]). Based on the electrical behavior of such an inverter circuitry the construction of further and more sophisticated circuit functions and logic gates (e.g., gates carrying out the logic function 'NAND' and 'XOR') is approached and straightforwardly realized [276]. However, the complexity of an organic circuit design can additionally rise, when different semiconductor and printable material are applied [8, 79, 81]. In Figure A.5 we show by means of examples (A), ..., (D), four different design architectures implementing the same logic inverter function with either unipolar or ambipolar transistor technology. Depending on the semiconductor material one of the four design architectures is chosen, i.e., if p-type and n-type semiconductors show the same transistor characteristics, then inverter architecture (C) is chosen, else one of the others is used [8]. In case p-type only semiconductor is used to print circuit devices, the architectures (A) and (B) are taken [8]. More recently, ambipolar semiconductor material is developed showing the same properties of p- and n-type MOSFET<sup>3</sup> in a single semiconductor material (cf. illustration in Figure A.5d)<sup>4</sup>. For more information about printed circuit design and operation of unipolar and CMOS-like complementary logic we confer to Baeg et al. [8], and references therein.

In PE circuit design another vital electronic component represents the ring oscillator composed of an odd number of logic inverters, that are chained and connected in a ring, such that the output signal of a previous logic inverter gate is feeding the subsequent inverter (cf. reference [277]). An example of a 5-stage ring oscillator is depicted in Figure A.4. Based on negating the digital logic voltage signal in each stage, the odd number of inverters and a delay of forwarding the input signal to the next inverter (by switching a capacitor between two inverter gates), an oscillation with frequency  $f$  is generated, that is used to clock for example the IC of an OE smart tag. If  $n$  denotes the number of inverter gates, and  $\tau$  determines the propagation delay between two stages,

---

<sup>3</sup>MOSFET: Metal Oxide Semiconductor Field-Effect Transistor.

<sup>4</sup>Technical terms such as 'CMOS-like' and 'pseudo-CMOS' for complementary circuit technology have the same meaning.

then the achievable circuit speed is calculated by [276, Chapter 11]:

$$f = \frac{1}{2n\tau} \tag{A.2}$$

In this respect, it is to be noted that, in the ring oscillator the subsequent inverter gate is negating only its logic state, if the load capacitor beforehand obtains first the switching voltage input signal. The circuit speed of an IC is, therefore, additionally to the carrier charge mobility  $\mu$  of each applied semiconductor, and the geometrical shape (Width  $W$  and Length  $L$ ) of the printed transistors, also dependent on the chosen capacitance of the load capacitors for the ring oscillator. In PE, boosting the circuit speed is thus more than a simple optimization problem, because simply increasing the supply voltage  $V_{DD}$ , changing the electro mobility  $\mu$ , or widening and reducing the transistor shape, can cause unexpected electrical behavior leading to undesired results [8, 79, 81]. In particular, the low resolution and natural limited printing process (e.g., the overlap of a transistor's printed gate over a source/drain structure) cause an unwanted parasitic capacitance, aggravating the performance loss in relation to circuit speed and power consumption. However, the printing of basic electronic components such as logic circuits and ring oscillators allows to test and improve deployed printing techniques and developed design rules for printing electronic devices [7, 8]. In the following section, we continue to report on PE at a broader level, i.e., we are going to present some state-of-the-art works, being related to a certain extent to printed RFID.

### **A.3 Some Review on RFID-Related Printed Electronics**

In the previous section we introduced PE at the level of a printed transistor and basic circuit logic. In the continuation of describing printed RFID in a nutshell, in the following we extend our view on reporting on some state-of-the-art works, which allow to provide a glance in what current PE is capable of. Therefore, in respect to the outcomes of the research projects we introduced in the beginning of this appendix, and the achievements of other related PE research, i.e., the development of PE devices and hardware technology relating to printed RFID, in particular we are going to outline various accomplishments of printed circuit functions, that are often used as building blocks in creating of more sophisticated printed applications such as an OE smart label.

To note in advance, however, in all PE undertakings, it has to be pointed out, that current state-of-the-art works, aiming to implement PE devices such as printed smart labels, smart objects, RFID, memory and display, are primarily oriented by implementing basic circuit functionalities, that perform tasks such as sensing environment, conversion and analyzing of data, storing, displaying and transmitting of collected data. Some of these

TABLE A.1: Printed devices:state of the art.

Printed device	Technology	TFT count	Reference	Year
Ring oscillator	p-type	5	[75]	2010
	Complementary	10	[278]	2011
	p-type	> 5	[279]	2016
Shift register and line select driver	Complementary	864	[280]	2000
	p-only	1888	[281]	2004
	p-only	4000	[282]	2005
	p-only	13440	[204]	2014
Rectifier	Complementary	1216	[283]	2014
	p-type	–	[79]	2008
	Complementary	–	[87]	2012
	Complementary	–	[284]	2012
	Complementary	–	[285]	2012
ADC	Complementary	–	[199]	2014
	p-only	53	[286]	2010
	p-only	70	[287]	2011
	p-only	NA	[288]	2013
DAC	p-only	106	[289]	2013
	Complementary	22	[290]	2010
Microprocessor	p-only	129	[291]	2012
	Complementary	3381	[292]	2012
Memory	Complementary	3504	[38]	2014
	p-type	NA	[293]	2010
	p-type	128	[294]	2012
	p-type	16	[295]	2013
	p-type	NA	[296]	2015

circuit functions are already implemented in OE, but others need to be accomplished yet (cf. OE roadmap [32]). Further, in PE research specific basic digital circuit functions such as a ring oscillator and shift register are implemented by manifold PE approaches (cf. by means of Table A.1) applying various functional electronic inks in combination with different printing techniques on different substrate carriers with proprietary design rules and distinctive electrical characteristics [7, 8], resulting if compared to each other in a complex PE assessment. To make this issue more clear, e.g., very often inorganic electronic inks indicate with respect to electro mobility a superiority in comparison with p-type only organic semiconductors, but they also require in the processing flow unwanted high temperatures [283], leading with respect to the printed application to become in the end of a value chain cost-inefficient. Another typical example represents manufacturing of printed devices, e.g., an inkjet printer has a high printing resolution and registration capability, but low throughput in comparison with other printing techniques (cf. references [7, 8]). Therefore, our collection of PE scientific works in Table A.1

presents a variety of different PE approaches, that needs to be considered as an excerpt of state-of-the-art research and intermediate development step towards fully-functional and flexible PE. With respect to printed RFID, a further intention of our collection by Table A.1 is to enlist common electronic components of an OE smart label, that indicates in addition to the electronic components corresponding hardware complexities and feasibility in PE. However, in chapter 2, which provides the background and related works for this dissertation, we refer there to our report introducing already some holistic and fully-functional implementations of printed RFID tags manufactured by various research groups. In this appendix, however, we focus on in more detail to provide PE research results of single state-of-the-art printed electronic devices, as being enlisted in Table A.1.

To begin with, in designing and testing PE digital circuitry, a printed ring oscillator circuit represents a typical electronic component, that is often used to benchmark own PE approach [205]. For instance, switching speed and the regeneration capability of printed transistors is acquired by testing the printed circuit device, which allows to evaluate a devised PE semiconductor technology. For example, Jung et al. [75] implements an all-printed and Roll-to-Roll (R2R) printable 1-bit operating RF tag on plastic foil, within implementing a p-type, 5-stage ring oscillator using carbon nanotubes as active semiconductor material for the OTFTs. At a DC supply voltage of 10 V (rectified by RF tag itself) an oscillation frequency of  $f_{osc} = 60$  Hz is achieved (and, at a direct supply voltage of 12 V an oscillation frequency of  $f_{osc} = 67.4$  Hz is observed). Distinctly improved clocking frequency for a 5-stage ring oscillator is achieved by developing a complementary organic semiconductor technology, e.g., Kitamura et al. [278] describes a complementary 5-stage ring oscillator circuit realized with p-type (pentacene) and n-type ( $C_{60}$ ) TFTs, achieving an oscillation frequency of up to 200 kHz with increasing the supply voltage steadily. However, the use of photolithography for creating channel lengths of source/drain structures below  $5 \mu\text{m}$ , and dry plasma-etching process in combination with p-type only and hybrid semiconductor materials, led recently to achieve speeds above 100 kHz for unipolar organic ring oscillators (cf. Watson et al. [279], and references therein). In particular, Watson et al. [279] presents an unipolar, 5-stage ring oscillator operating routinely in 250 – 350 kHz range, and at best even  $> 500$  kHz.

However, while a ring oscillator is mostly used for clocking the Integrated Circuit (IC), a shift register attains manifold application in circuit design. In particular, in this dissertation we employ the shift register as a *central processing component*, that we apply once as a code generator in our OE smart label circuit design (cf. chapter 5), and use it in another application scenario as a pseudo-random number generator to encode sensed data designing with it a resource limited sensor node (cf. chapter 7). In PE research and industry the use of a shift register is destined mostly for realizing driver electronics

of matrix arrays in display, sensor and memory application [281, 297, 298]. Looking in PE history, the implementation of printed shift registers and line select drivers is mostly based on p-type transistor technology (cf. Table A.1), indicating to some degree of OE maturity, which can be underlined by a 240-stage printed shift register realized with more than thirteen thousand transistors [204]. However, since recently developed n-type semiconductor materials indicate stability the development of complementary organic technology is making progress (cf. Sahel Abdinia’s PhD thesis [283] and Book [299], respectively). With balancing the electro mobilities between p-type organic TFTs and n-type oxide TFTs using solution-processed metal-oxide semi-conductors, an appropriate complementary circuit technology for creating of printed applications with higher hardware complexity is enabled [283, 300]. For example, Myny et al. [38, 301] uses this technology to improve hardware performance of an earlier developed p-type-based printed rudimentary microprocessor [292]. And, by using the same complementary hybrid organic-oxide technology (transistor channel lengths  $\geq 2 \mu\text{m}$ ), for the first time in printed RFID a bidirectional wireless communication between RFID reader device and a printed tag is demonstrated (cf. Myny et al. [87]). In particular, the adaptation of transistor’s speed with the reader HF signal, in which reader’s clock and data is transmitted to the tag, it enabled primarily this accomplishment. In comparison, the deployment of p-type only circuit technology in printed RFID [74, 79, 86, 96] allows so far an unidirectional communication (tag-talks-first principle), owing essentially to the transistor’s parameters of low hole mobility and inadequately large featured channel lengths.

In the continuation of developing printed RFID with complementary logic circuitry, the work by Fiore et al. [199, 200] marks current state-of-the-art for printed RFID in organic complementary TFT technology. The passive RFID tag is printed on a flexible plastic foil with more than 250 transistors, tuned to operate in HF band, bounding a separately R2R printed planar near-field antenna (reading distance there is specified by 2 – 5 cm) [200]. Further on, since scavenging of wireless power represents an essential building block in printed RFID, and for the sake of completion, in Table A.1 we gathered, apart from above mentioned wireless power scavengers, further state-of-the-art works, which implement in their printed RFID front-end an OE rectifier circuit.

With regard to an envisioned OE smart sensing label, as we are pursuing it in this dissertation, further electronic elements need to be considered, such as printable Analogue-to-Digital (ADC) and Digital-to-Analogue (DAC) converters (cf. Table A.1). For converting of an analogue signal into a digital representation, and converse, various organic ADC and DAC approaches exist, which currently allow a digital resolution of up to 6 bits (cf. references [286–288], and references [290, 291]). For instance, reference [286] employs a Successive-Approximation-Register (SAR), reference [287] applies a  $\Delta\Sigma$  structure, and reference [288] uses an architecture of a Voltage-Controlled Oscillator (VCO), achieving

a 6 bit data conversion. In converse, organic DACs with 6 bit resolution exist in p-type only circuit technology [291], as well as in complementary organic technology [290].

Apart from digital signal converters for smart sensing, another essential building block for OE smart labels represents storing and reading out of digital information such as the device identification, sensory data, machine instructions and look-up tables (cf. references, which report on various types of printed memory listed in Table A.1). The OE research, hence, focuses on developing of organic nonvolatile memory for a wide range of printed applications [293–296]. In particular, implemented examples of nonvolatile printed memory, using a single organic transistor structure, are described in references [295, 302, 303]. Thereof, it can be distinguished in types of ferroelectric nonvolatile memory [293, 296], and printed ROM array using 'anti-fuse' capacitors [295]. While ferroelectric nonvolatile memory rely on cost-intensive fabrication processes to create stable floating gate transistors enabling with it long retention time, on the other hand the use of anti-fuse capacitors in combination with p-type transistors consummate disproportionately large printing area (e.g., the hardware implementation reported in reference [295] requires an area of  $70.6 \text{ mm}^2$  to store 16 bits). However, the state-of-the-art for nonvolatile printed memory represents an intermediate evolutionary step, showing feasibility and capabilities of prototypically tested current PE technologies.

Summarizing this section, we dealt with describing state-of-the-art of elementary PE circuitry relating to printed RFID building blocks, that show in essence single cutting-edge solutions for various OE circuit functionalities such as printed ring oscillators, shift registers, RFID front-ends, digital signal converters, and memory. Considering the level of maximum possible hardware complexity for PE, for p-type only circuit technology we acquire the most achievable transistor count for a printed device with more than thirteen thousand transistors, whereby state-of-the-art complementary organic technology yields printed devices of several hundreds of OTFTs, but maximal just over one thousand transistors (cf. Table A.1). However, in terms of mass-printing of OE in high-volumes and low-cost fabrication the reported high performance of state-of-the-art PE need to be put in perspective, because the manufacturing thus far mostly takes place at lab-scale using inkjet or screen printing in combination with clean-room processes such as photolithography and vacuum-deposition, which allow to create OE circuits of high performance transistor structures below  $5 \mu\text{m}$ . In comparison with employing exclusively fully-printed and mass-printing processes such as flexography and gravure printing (posing least feature sizes  $\geq 10 \mu\text{m}$ ), the performance achievement is rather low [7, 8, 304], such that an advancing from lab to industrial-scale poses a technical key issue. While efforts exist to promote inkjet and screen printing for industrial manufacturing of PE (cf. research reports by reference [73]), the advancement of mass-printing techniques such

as flexography and gravure printing remains inevitable, because a such vision of item-level tagging and IoT succumbs to economic constraints [24, 25, 72, 182]. Therefore, in the next section we continue to report in more detail on mass-printing technologies.

#### A.4 Some Mass-Printing Techniques for Printed Electronics

In the previous section we provided a glance in what is brought out the most of current OE research relating to printed RFID, and determined thereby the level of feasible OE hardware complexity. Further, we realized that maximum possible achieved high performance for OE is mostly attributed to the result of combining clean-room manufacturing processes such as photolithography and vacuum-deposition, with high precision performing printing techniques such as inkjet and screen printing. However, these kind of OE manufacturing is scarcely applicable for a low-cost mass-production. While inkjet and screen printing are primarily applicable for high precision work and manufacturing of small quantities, to the contrary, for mass-printing scenarios of OE applications it is relying on Roll-to-Roll (R2R) printing strategies such as flexography, offset lithography, and gravure printing, originating from mass-printing methods for fabrication of graphics art [8]. In respect to the high volume production strategies, therefore, in the following we focus on describing R2R-based printing machines in more detail, which use preferably cost-efficient organic conductive inks and plastic foils as substrate carriers.

To begin with, the mass-printing method based on *flexography* is illustrated in Figure A.6. It shows schematically the R2R printing principle. The process is direct, where a flexible relief plate transfers an image onto a substrate. The printing plate is mounted on a cylinder, and applies ink from a metering roller. The surface of the ink roller is tainted with regular sized cells and shape. Based on the image resolution and the ink film thickness, the number of cells per centimeter varies. A doctor blade removes the excess of ink from the metering roller surface, leaving the cells filled with the needed amount. The flexographic process is able to print on a wide range of substrates, such as paper, corrugated cardboard, flexible and rigid polymers, metal, or glass. The printing speed is about 3 – 10 m/s.

Another mass-production method with higher throughput is based on *gravure printing* illustrated in Figure A.7. The printing process applies an engraved cylinder and high pressure to transfer an image to substrate. For engraving the cylinder, which is steel-based and covered with a thick layer of copper, an electrochemical process is used. The engraving of the cells onto the cylinder results into varied width and depth. During the

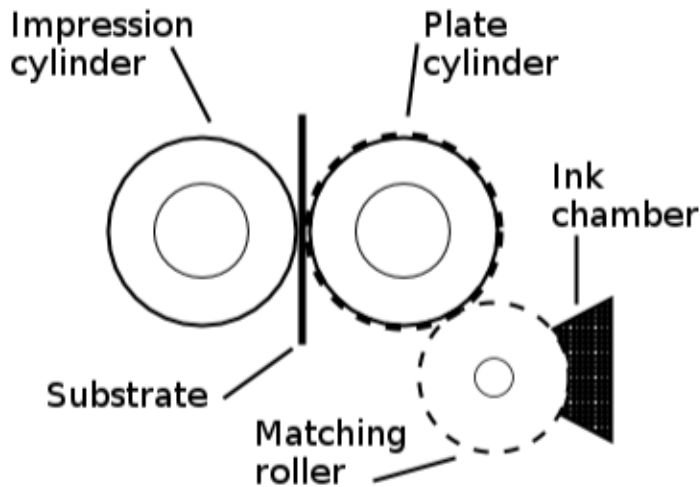


FIGURE A.6: Flexography.

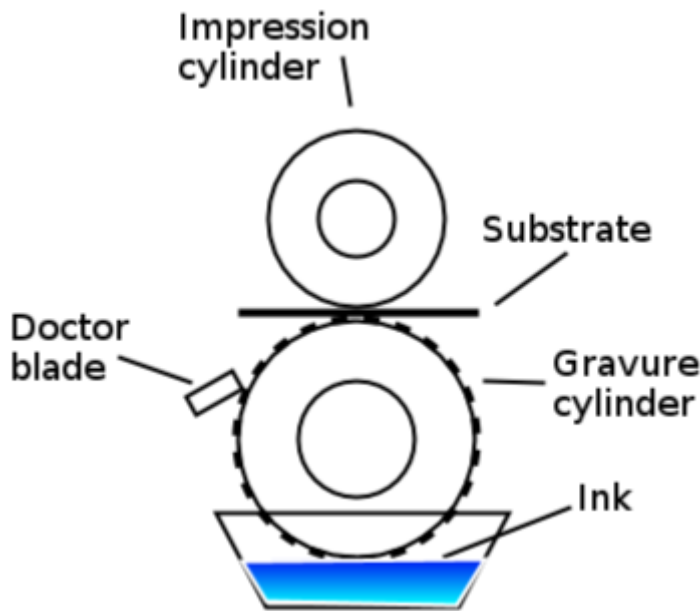


FIGURE A.7: Gravure printing.

printing process the gravure cylinder dives and rotates in an ink reservoir. By using a doctor blade the excess of the ink is removed. The remaining ink in the cylinder cells is transferred to the substrate with the help of an impression cylinder. The speed of the R2R gravure printing amounts to 10 – 16 m/s.

A further applied R2R printing method is based on *offset lithography* illustrated in Figure A.8. This printing technique is well known, and widely used for high volume, low cost and high quality graphical printing, e.g., it is used to print newspapers, magazines, books, or packaging material. In respect to print OE, it is applied to fabricate electronic circuit devices in large-scale. Offset printing represents an indirect lithographic process.

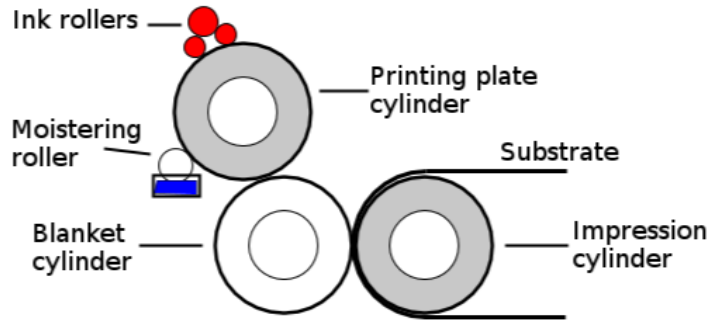


FIGURE A.8: Offset lithography.

In the printing process, the plate cylinder is moisturized by a dampening solution consisting mostly of water. The areas of the image are not moisturized, whereas non-image areas are covered generously with dampening solution. When the plate cylinder is inked, then the ink only spreads on the image areas, where no moisture is located. During this operation the image is transferred onto an intermediate cylinder plate named blanket, which in turn transfers the image onto the substrate. Roll-to-roll printer machines, that realize offset lithography, achieve a printing speed of 8 – 15 m/s. The resolution of minimal printed structures is  $> 10 \mu\text{m}$ , which also applies to the above described flexography and gravure printing.

## A.5 Some Technical Key Issues in Printed Electronics

In our study above about Printed Electronics (PE) for printed RFID we determined several technical key issues in manufacturing and functioning of OE devices. For instance, we identified key issues such as

- (i) the mass-printing challenge of OE with transistor density resolution below  $10 \mu\text{m}$ ,
- (ii) the lack of carrier charge mobilities for p-type semiconductor inks greater than  $\mu_{FET} = 1 \text{ cm}^2\text{V}^{-1}\text{s}^{-1}$ ,
- (iii) relative high power supply voltages  $V_{DD}$  and variability in transistor characteristics behavior for unipolar printed circuit devices,
- (iv) degradation of deployed semiconductor materials indicating short live spans of printed devices,
- (v) parasitic capacitance behavior of printed transistors inducing high power consumption and limiting transistor's speed, as well as maximum possible printed hardware complexity.

Even though, clean-room methods for PE are deployed, such as photolithography, to realize printed circuits with feature sizes below  $5\ \mu\text{m}$  (even printed circuits in submicron resolution is obtained [305] using silicon stencil masks), and solution-processed electronic inks with high field-effect mobilities  $\geq 10\ \text{cm}^2\text{V}^{-1}\text{s}^{-1}$  are developed [306, 307], and high-precision inkjet printing is engineered [308] reducing almost gate overlap with parasitic capacitance behavior, that improve on the whole performance of OE substantially, however, the vision of low-cost and mass-printable OE is with it leveraged, because these manufacturing processes and electronic inks are cost-inefficient, lowering economically speaking the number of viable printed applications drastically. In case of item-level tagging and IoT the development of low-cost and mass-printable smart label front-ends implementing HF rectification, as well as low-voltage driven printed circuits, is inevitable [284, 285]. Considering exemplary performance parameters of gravure printing [8], the mass-printing of OE devices with up to two thousand transistors is possible [81], but indicates thus far unacceptable yield of fabricated devices, whereby printed circuits with hardware complexity of about two hundred of transistors indicate in terms of mass-printing an acceptable yield (cf. references [81, 191]). Considering the last decade of OE development, all in all, a substantial progress is made in hardware performance and manufacturing of reliable and robust printed devices (cf. Table A.1). However, the state-of-the-art accomplishments made in a laboratory need yet to be transferred at industrial-scale. And still, the level of current maximal achievable circuit speed and hardware complexity need to be raised up, such that a printed RFID application performing an industrial standard can be attained (cf. discussion in chapter 2).

# Bibliography

- [1] Albert Krohn, Michael Beigl, and Sabin Wendhack. SDJS: Efficient statistics for wireless networks. In *Proceedings of the 12th IEEE International Conference on Network Protocols*, pages 262–270, 2004.
- [2] Akihito Noda and Hiroyuki Shinoda. Power transmission coupler for low leakage 2D-communication sheet. pages 24–30, 2009. URL <http://dl.acm.org/citation.cfm?id=1802340.1802345>.
- [3] Ali Hadda. Hardware-Entwurf und Implementierung eines Sensor Smart Labels für hochskalierbare Kommunikationsprotokolle. Studienarbeit, Karlsruhe Institute of Technology (KIT), 2012.
- [4] Hartley oscillator. Wikipedia. URL [https://en.wikipedia.org/wiki/Hartley\\_oscillator](https://en.wikipedia.org/wiki/Hartley_oscillator).
- [5] John Wright. 2400 MHz test oscillator (simple signal generator), May 2001. URL <http://www.g4dmf.co.uk/2400/2400.html>.
- [6] Intel lab data, April 2004. URL <http://db.csail.mit.edu/labdata/labdata.html>.
- [7] Saumen Mandal and Yong-Young Noh. Printed organic thin-film transistor-based integrated circuits. *Semiconductor Science and Technology*, 30(6):064003, 2015. URL <http://stacks.iop.org/0268-1242/30/i=6/a=064003>.
- [8] Kang-Jun Baeg, Mario Caironi, and Yong-Young Noh. Toward printed integrated circuits based on unipolar or ambipolar polymer semiconductors. *Advanced Materials*, 25(31):4210–4244, 2013. ISSN 1521-4095. doi: 10.1002/adma.201205361. URL <http://dx.doi.org/10.1002/adma.201205361>.
- [9] Jayavardhana Gubbi, Rajkumar Buyya, Slaven Marusic, and Marimuthu Palaniswami. Internet of Things (IoT): A vision, architectural elements, and future directions. *Future Generation Computer Systems*, 29(7):1645–1660, 2013. ISSN 0167-739X. doi: 10.1016/j.future.2013.01.010. URL <http://>

- [www.sciencedirect.com/science/article/pii/S0167739X13000241](http://www.sciencedirect.com/science/article/pii/S0167739X13000241). Including Special sections: Cyber-enabled Distributed Computing for Ubiquitous Cloud and Network Services - Cloud Computing and Scientific Applications Big Data, Scalable Analytics, and Beyond.
- [10] A. Al-Fuqaha, M. Guizani, M. Mohammadi, M. Aledhari, and M. Ayyash. Internet of Things: A survey on enabling technologies, protocols, and applications. *IEEE Communications Surveys Tutorials*, 17(4):2347–2376, Fourthquarter 2015. ISSN 1553-877X. doi: 10.1109/COMST.2015.2444095.
- [11] Omar Said and Mehedi Masud. Towards Internet of Things: Survey and future vision. *International Journal of Computer Networks (IJCN)*, 5(1):1–17, April 2013.
- [12] S. H. Shah and I. Yaqoob. A survey: Internet of Things (IoT) technologies, applications and challenges. In *2016 IEEE Smart Energy Grid Engineering (SEGE)*, pages 381–385, August 2016. doi: 10.1109/SEGE.2016.7589556.
- [13] The internet of things: Impact and applications in the high-tech industry. *Cognizant 20-20 Insights*, March 2015.
- [14] Juan C. Augusto, Vic Callaghan, Diane Cook, Achilles Kameas, and Ichiro Satoh. Intelligent environments: A manifesto. *Human-centric Computing and Information Sciences*, 3(1):12, 2013. ISSN 2192-1962. doi: 10.1186/2192-1962-3-12. URL <http://dx.doi.org/10.1186/2192-1962-3-12>.
- [15] Elhadi Shakshuki, Ansar Yasar, Xenofon Fafoutis, Thomas Srensen, and Jan Madsen. The 5th international conference on ambient systems, networks and technologies (ANT-2014), the 4th international conference on sustainable energy information technology (SEIT-2014) energy harvesting - wireless sensor networks for indoors applications using IEEE 802.11. *Procedia Computer Science*, 32:991–996, 2014. ISSN 1877-0509. doi: 10.1016/j.procs.2014.05.523. URL <http://www.sciencedirect.com/science/article/pii/S1877050914007236>.
- [16] Christoph Michael Goebel. *The Value of Item-Level RFID in the Supply Chain*. PhD thesis, Humboldt-Universität zu Berlin, 2009.
- [17] Edmund W. Schuster, Stuart J. Allen, and David L. Brock. *Global RFID - The Value of the EPCglobal Network for Supply Chain Management*. Springer Science & Business Media, 2007.
- [18] Christian Decker, Martin Berchtold, Leonardo Weiss F. Chaves, Michael Beigl, Daniel Rohr, Till Riedel, Monty Buster, Thomas Herzog, and Daniel Herzog. Cost-benefit model for smart items in the supply chain. The Internet of Things, 2008.

- [19] Ali Dada and Frédéric Thiesse. Sensor applications in the supply chain: The example of quality-based issuing of perishables. In *The Internet of Things*, Zürich, 2008.
- [20] Amit Shukla, Prasad Deshpande, and Jeffrey F. Naughton. Materialized view selection for multidimensional datasets. In *Proceedings of VLDB'98*, 1998.
- [21] Carrie MacGillivray. Opportunity beyond the IoT: Printed electronics and smart systems. *IDC OPINION*, September 2014.
- [22] Peter Harrop. RFID in the supply chain. Website, June 2006. URL <http://www.chainlinkresearch.com/research/detail.cfm?guid=A4CODE5E-B30F-4223-323E-18BD1CF6D547>.
- [23] RFID vs Barcodes: Advantages and disadvantages comparison. Website, May 2012. URL [http://www.aalhysterforklifts.com.au/index.php/about/blog-post/rfid\\_vs\\_barcodes\\_advantages\\_and\\_disadvantages\\_comparison](http://www.aalhysterforklifts.com.au/index.php/about/blog-post/rfid_vs_barcodes_advantages_and_disadvantages_comparison).
- [24] Woodrow Hartzog and Evan Selinger. The internet of heirlooms and disposable things. *Journal of Law & Technology*, 2016. URL <http://scholarship.law.unc.edu/ncjolt/vol117/iss4/2>.
- [25] Michael Kanellos. The 1 cent RFID tag getting close to reality. Website. URL <https://www.cnet.com/news/the-1-cent-rfid-tag-getting-close-to-reality/>.
- [26] Bill C. Hardgrave, Matthew Waller, and Robert Miller. RFID's Impact on Out of Stocks: A Sales Velocity Analysis. Technical report, University of Arkansas, 2006.
- [27] Min Chen, Shiwen Mao, and Yunhao Liu. Big Data: A survey. *Mob. Netw. Appl.*, 19(2):171–209, April 2014. ISSN 1383-469X. doi: 10.1007/s11036-013-0489-0. URL <http://dx.doi.org/10.1007/s11036-013-0489-0>.
- [28] C. Perera, A. Zaslavsky, P. Christen, and D. Georgakopoulos. Context aware computing for the Internet of Things: A survey. *IEEE Communications Surveys Tutorials*, 16(1):414–454, First 2014. ISSN 1553-877X. doi: 10.1109/SURV.2013.042313.00197.
- [29] Yongrui Qin, Quan Z. Sheng, Nickolas J. G. Falkner, Schahram Dustdar, Hua Wang, and Athanasios V. Vasilakos. When things matter: A survey on data-centric Internet of Things. *Journal of Network and Computer Applications*, 64: 137–153, April 2016. ISSN 10848045. doi: 10.1016/j.jnca.2015.12.016. URL <http://dx.doi.org/10.1016/j.jnca.2015.12.016>.

- [30] Klaus Finkenzerler and Dörte Müller. *RFID Handbook: Fundamentals and Applications in Contactless Smart Cards, Radio Frequency Identification and Near-Field Communication*. John Wiley & Sons, 2010.
- [31] EPC tag data standards, version 1.3. In *EPCglobal Inc, Standard*, 2006.
- [32] Organic Electronics Association. OE-A organic and printed electronics - applications, technologies and suppliers. *White Paper*, (5th), 2014.
- [33] ERA-LEARN 2020. PPrinted Organic LOGic circuits for low-cost smart tags. Website. URL <https://www.era-learn.eu/network-information/networks/eurostars/eighth-eurostars-cut-off-01-march-2012-20h00-c-e-t/printed-organic-logic-circuits-for-low-cost-smart-tags>.
- [34] PolyIC. PRISMA: First use of printed radio chips realized in public field tests - results within the framework of the funded project PRISMA Printed Smart Labels. Website, April 2010. URL [http://www.polyic.com/press-news-events/prtest/details-tt-news.html?tx\\_ttnews%5Btt\\_news%5D=124&cHash=3e04b7b1795f05a4ab07951f53b9361a](http://www.polyic.com/press-news-events/prtest/details-tt-news.html?tx_ttnews%5Btt_news%5D=124&cHash=3e04b7b1795f05a4ab07951f53b9361a).
- [35] Eugenio Cantatore, editor. *Applications of Organic and Printed Electronics - A Technology-Enabled Revolution*. Springer, 2013.
- [36] Katsuaki Suganuma. *Introduction to Printed Electronics*. Springer Briefs in Electrical and Computer Engineering, 2014.
- [37] Organic Electronics Association. OE-A roadmap for organic and printed electronics. *White Paper*, 2008.
- [38] Kris Myny, Steve Smout, Maarten Rockelé, Ajay Bhoolokam, Tung Huei Ke, Soeren Steudel, Brian Cobb, Aashini Gulati, Francisco Gonzalez Rodriguez, Koji Obata, Marko Marinkovic, Duy-Vu Pham, Arne Hoppe, Gerwin H. Gelinck, Jan Genoe, Wim Dehaene, and Paul Heremans. A thin-film microprocessor with inkjet print-programmable memory. Technical report, December 2014.
- [39] Peter Harrop. Printed RFID in 2010. Website, January 2010. URL <http://www.piworld.com/article/outlook-printed-rfid-technology-printed-electronics-2010-pi-watch/>.
- [40] Bharatendu Srivastava. Critical management issues for implementing RFID in supply chain management. *International Journal of Manufacturing Technology and Management*, 21:289–307, 2010. doi: 10.1504/IJMTM.2010.035437. URL <http://www.inderscienceonline.com/doi/abs/10.1504/IJMTM.2010.035437>.

- [41] Albert Krohn, Tobias Zimmer, Michael Beigl, and Christian Decker. Collaborative sensing in a retail store using synchronous distributed jam signalling. In *International Conference on Pervasive Computing*, pages 237–245. Springer Verlag, 2005.
- [42] Bill C. Hardgrave, Matthew Waller, and Robert Miller. RFID’s impact on out of stocks: A sales velocity analysis. Technical report, University of Arkansas, 2006.
- [43] K. Myny, S. Van Winckel, S. Steudel, P. Vicca, S. De Jonge, M.J. Beenhakkers, C.W. Sele, N.A.J. van Aerle, G.H. Gelinck, J. Genoe, and P. Heremans. An inductively-coupled 64b organic rfid tag operating at 13.56mhz with a data rate of 787b/s. In *Solid-State Circuits Conference, 2008. ISSCC 2008. Digest of Technical Papers. IEEE International*, 2008. doi: 10.1109/ISSCC.2008.4523171.
- [44] Leonardo Weiss Ferreira Chaves and Florian Kerschbaum. Security and privacy in Track & Trace infrastructures. In Duarte Boua and Amaro Gafagno, editors, *Agent-Based Computing*. Nova Science Publishers, 2010. ISBN 978-1-60876-684-0.
- [45] Leonardo Weiss Ferreira Chaves and Christian Decker. A survey on organic smart labels for the Internet-of-Things. In *Proceedings of the INSS’10*, 2010.
- [46] Leonardo Weiss Ferreira Chaves and Zoltán Nochtá. Printed organic smart labels: Breakthrough towards the Internet of Things? In Damith C. Ranasinghe, Quan Z. Sheng, and Sherali Zeadally, editors, *Unique Radio Innovation for the 21st Century*. Springer, 2010. ISBN 978-3-642-03461-9.
- [47] Junaid Ahmed Khan, Hassaan Khaliq Qureshi, and Adnan Iqbal. Energy management in wireless sensor networks: A survey. HAL archives-ouvertes, January 2014. URL <http://www.sciencedirect.com/science/article/pii/S0045790614001773>.
- [48] Z. G. Wan, Y. K. Tan, and C. Yuen. Review on energy harvesting and energy management for sustainable wireless sensor networks. In *2011 IEEE 13th International Conference on Communication Technology (ICCT)*, pages 362–367, September 2011. doi: 10.1109/ICCT.2011.6157897.
- [49] W. K. G. Seah, Z. A. Eu, and H. P. Tan. Wireless sensor networks powered by ambient energy harvesting (WSN-HEAP) - survey and challenges. In *1st International Conference on Wireless Communication, Vehicular Technology, Information Theory and Aerospace Electronic Systems Technology (Wireless VITAE)*, pages 1–5, May 2009. doi: 10.1109/WIRELESSVITAE.2009.5172411.
- [50] Yen Kheng Tan and Sanjib Kumar Panda. *Sustainable Wireless Sensor Networks*, chapter Review of Energy Harvesting Technologies for Sustainable WSN, pages 15–43. [www.intechopen.com](http://www.intechopen.com), 2010. URL <https://www.intechopen.com>.

- [//www.intechopen.com/books/sustainable-wireless-sensor-networks/review-of-energy-harvesting-technologies-for-sustainable-wsn](http://www.intechopen.com/books/sustainable-wireless-sensor-networks/review-of-energy-harvesting-technologies-for-sustainable-wsn).
- [51] Albert Krohn. *PhD Thesis Abstract: Superimposed Radio Signals for Wireless Sensor Networks*. PhD thesis, Telecooperation Office (TecO), Universität Karlsruhe, 2007. URL <https://www.teco.edu/~krohn/doctoral.pdf>.
- [52] Albert Krohn. *Überlagerte Funksignale in drahtlosen Sensornetzwerken*. PhD thesis, Karl-Friedrich-Gauss-Fakultät für Mathematik und Informatik der Technischen Universität Carolo-Wilhelmina zu Braunschweig, TU Braunschweig, 2007.
- [53] B. Nazer and M. Gastpar. Reliable physical layer network coding. *Proceedings of the IEEE*, 99(3):438–460, March 2011. ISSN 0018-9219. doi: 10.1109/JPROC.2010.2094170.
- [54] Mario Goldenbaum. *Computation of Real-Valued Functions Over the Channel in Wireless Sensor Networks*. Dissertation, Technische Universität München, München, 2014.
- [55] Andrew Tanenbaum. *Computer Networks*. Prentice Hall Professional Technical Reference, 4th edition, 2002. ISBN 0130661023.
- [56] William Stallings. *Wireless Communications & Networks (2nd Edition)*. Prentice-Hall, Inc., Upper Saddle River, NJ, USA, 2004. ISBN 0131918354.
- [57] Bobak Anthony Nazer. *Exploiting Interference Through Algebraic Structure*. PhD thesis, Electrical Engineering and Computer Sciences, University of California at Berkeley, December 2009.
- [58] Predrag Jakimovski, Ali Hadda, Michael Zangl, and Nina Oertel. Fully functional passive RFID tag with integrated sensor for item level tagging based on collective communications and organic printed electronics. In *ICWMC 2014, The Tenth International Conference on Wireless and Mobile Communications*, June 2014.
- [59] Predrag Jakimovski, Hedda R. Schmidtke, Stephan Sigg, Leonardo Weiss, Ferreira Chaves, and Michael Beigl. Collective communication for dense sensing environments. *Journal of Ambient Intelligence and Smart Environments (JAISE)*, 2012.
- [60] Mark Weiser. The computer for the 21st century. *Scientific American*, 265(3):66–75, September 1991.
- [61] Mininath R. Bendre and Vijaya R. Thool. Analytics, challenges and applications in big data environment: A survey. *Journal of Management Analytics*, 3(3):206–239, 2016. doi: 10.1080/23270012.2016.1186578. URL <http://dx.doi.org/10.1080/23270012.2016.1186578>.

- [62] Amruta S. Pattanshetti and N. D. Kale. A survey on big-data gathering using mobile collector in densely deployed wireless sensor network. *International Journal of Engineering Research & Technology*, 3(12), December 2014. URL <http://www.ijert.org>.
- [63] A. Giridhar and P. R. Kumar. Computing and communicating functions over sensor networks. *IEEE Journal on Selected Areas in Communications*, 23(4):755–764, April 2005. ISSN 0733-8716. doi: 10.1109/JSAC.2005.843543.
- [64] C. E. Shannon. A mathematical theory of communication. *Bell Syst. Tech. Journal*, 27:379–423, 1948.
- [65] Andrea Goldsmith. *Wireless Communications*. Cambridge University Press, 2005.
- [66] Bojkovic Zoran, Bakmaz Bojan, and Bakmaz Modrag. Recent trends in emerging technologies toward 5G networks. *Advances in Circuits, Systems, Signal Processing and Telecommunications*, pages 137–143, 2015.
- [67] Claire Goursaud and Jean-Marie Gorce. Dedicated networks for IoT : PHY / MAC state of the art and challenges. *EAI endorsed transactions on Internet of Things*, October 2015. doi: 10.4108/eai.26-10-2015.150597. URL <https://hal.archives-ouvertes.fr/hal-01231221>.
- [68] Wenqi Guo and William M. Healy. Power supply issues in battery reliant wireless sensor networks: A review. *International Journal of Intelligent Control and Systems*, 19(1):15–23, March 2014.
- [69] E. Gaura, L. Girod, J. Brusey, M. Allen, and G. Challen. *Wireless Sensor Networks - Deployments and Design Frameworks*. Springer, 2010.
- [70] Moore’s law. Wikipedia, 2017. URL [https://en.wikipedia.org/wiki/Moore's\\_law](https://en.wikipedia.org/wiki/Moore's_law).
- [71] Keith Barr. *ASIC Design in the Silicon Sandbox: A Complete Guide to Building Mixed-Signal Integrated Circuits*. McGraw-Hill Education, 2007.
- [72] On a roll. Website, July 2016. URL <http://www.economist.com/news/science-and-technology/21702741-printing-conventional-rotary-presses-will-create-cheaper-electronics>.
- [73] Deutscher Fachverlag GmbH. OPE journal no 18. Online, March 2017. URL <http://www.ope-journal.com>.

- [74] K. Myny, S. Van Winckel, S. Steudel, P. Vicca, S. De Jonge, M. J. Beenhakkers, C. W. Sele, N. A. J. M. Van Aerle, G. H. Gelinck, J. Genoe, and P. Heremans. An inductively-coupled 64b organic RFID tag operating at 13.56MHz with a data rate of 787b/s. In *IEEE International Solid-State Circuits Conference (ISSCC 2008) - Digest of Technical Papers*, pages 290–614, 2008. doi: 10.1109/ISSCC.2008.4523171.
- [75] Minhun Jung, Jaeyoung Kim, Jinsoo Noh, Namsoo Lim, Chaemin Lim, Gwangyong Lee, Junseok Kim, Hwiwon Kang, Kyunghwan Jung, A. D. Leonard, J. M. Tour, and Gyoujin Cho. All-printed and roll-to-roll-printable 13.56-MHz-operated 1-bit RF tag on plastic foils. *IEEE Transactions on Electron Devices*, 57(3):571–580, 2010. ISSN 0018-9383. doi: 10.1109/TED.2009.2039541.
- [76] Peter Harrop. Sunchon University printed transistors, October 2011. URL <http://www.printedelectronicsworld.com/print-articles.asp?articleids=2664>.
- [77] Henning Rost. Printed electronic circuits: Off the reel. *Kunststoffe International*, 2007.
- [78] PolyIC. Website. URL <http://www.polyic.com>.
- [79] Henning Rost and Wolfgang Mildner. On the way to printed electronics. *Kunststoffe International*, June 2008.
- [80] A. Ullmann, M. Böhm, J. Krumm, and W. Fix. Polymer multi-bit RFID transponder. In *ICOE*, 2007.
- [81] Wolfgang Clemens, Jürgen Krumm, and Robert Blache. *Applications of Organic and Printed Electronics Integrated Circuits and Systems*, chapter Printed RFID and Smart Objects for New High Volume Applications, pages 115–132. Springer, 2f013.
- [82] Thinfilm builds first stand-alone sensor system in printed electronics. Website, October 2013. URL <http://thinfilm.no/2013/10/16/stand-alone-system/>.
- [83] Paul. Printable smart labels warn when the milks gone bad. Website, October 2013. URL <https://securityledger.com/2013/10/printable-smart-labels-warn-when-the-milks-gone-bad/>.
- [84] Matthew Bright. Printed electronics embed intelligence - everywhere. Website, 2015. URL <http://embedded-computing.com/articles/printed-intelligence-everywhere/>.

- [85] Inc. Kovio. Kovio NFC Barcode, March 2013. URL <http://www.thinfilm.no/wp-content/uploads/2014/01/Thin-Film-Electronics-ASA-Kovio-NFC-Encore-Platform-Product-requirement-document.pdf>.
- [86] K. Myny, M. J. Beenhakkers, N. A. J. M. Van Aerle, G. H. Gelinck, J. Genoe, W. Dehaene, and P. Heremans. A 128b organic RFID transponder chip, including Manchester encoding and ALOHA anti-collision protocol, operating with a data rate of 1529b/s. In *IEEE International Solid-State Circuits Conference (ISSCC 2009) - Digest of Technical Papers*, pages 206–207, 2009. doi: 10.1109/ISSCC.2009.4977380.
- [87] Kris Myny, Maarten Rockele, Adrian Chasin, Duy-Vu Pham, Jürgen Steiger, Silviu Botnaras, Dennis Weber, Bernhard Herold, Jürgen Ficker, Bas van der Putten, Gerwin H. Gelinck, Jan Genoe, Wim Dehaene, and Paul Heremans. Bidirectional communication in an HF hybrid organic/solution-processed metal-oxide RFID tag. In *2012 IEEE International Solid-State Circuits Conference Digest of Technical Papers (ISSCC)*, pages 312–314, February 2012.
- [88] B. K. Charlotte Kjellander, Wiljan T. T. Smaal, Kris Myny, Jan Genoe, Wim Dehaene, Paul Heremans, and Gerwin H. Gelinck. Optimized circuit design for flexible 8-bit RFID transponders with active layer of ink-jet printed small molecule semiconductors. *Organic Electronics*, 14(3):768–774, 2013. ISSN 1566-1199. doi: 10.1016/j.orgel.2012.12.027. URL <http://www.sciencedirect.com/science/article/pii/S1566119912005770>.
- [89] Yang Byung-Do, Oh Jae-Mun, Kang Hyeong-Ju, Park Sang-Hee, Hwang Chi-Sun, Ryu Min Ki, and Pi Jae-Eun. A transparent logic circuit for RFID tag in a-IGZO TFT technology. *ETRI Journal*, 4(4), August 2013. doi: 10.4218/etrij.13.1912.0004. URL <http://dx.doi.org/10.4218/etrij.13.1912.0004>.
- [90] Smart label sensors - cost-effective electronic monitors as thin as a chemistry-based label. Website. URL <http://thinfilm.no/products-sensor-platform/>.
- [91] Botao Shao, Qiang Chen, Yasar Amin, Ran Liu, and Li-Rong Zheng. Chipless RFID tags fabricated by fully printing of metallic inks. *Annals of Telecommunications*, 68(7-8):401–413, 2013. ISSN 0003-4347. doi: 10.1007/s12243-013-0378-3. URL <http://dx.doi.org/10.1007/s12243-013-0378-3>.
- [92] Botao Shao. *Fully Printed Chipless RFID Tags towards Item-Level Tracking Applications*. PhD thesis, Information and Communication Technology (ICT), 2014.
- [93] Mary Catherine O’Connor. Kovio unveils printed-silicon HF RFID, chip tag. Website, October 2008. URL <http://www.rfidjournal.com/articles/view?4389>.

- [94] Lori Shen. Kovio and Nissan chemical ramp up production of silicon ink for RF products and displays. Website, February 2010. URL <http://www.pangaeaventures.com/news/item/1-kovio-and-nissan-chemical-ramp-up-production-of-silicon-ink-for-rf-products-and-displays>.
- [95] Hanne Degans. European project reaches milestone bidirectional communication for thin-film RFIDs, enabling item-level RFID tags. Website, February 2012. URL [http://registrations.leuvenmindgate.be/event/36/1960/European\\_project\\_reaches\\_milestone\\_bidirectional\\_communication\\_for\\_thin-/](http://registrations.leuvenmindgate.be/event/36/1960/European_project_reaches_milestone_bidirectional_communication_for_thin-/).
- [96] Kris Myny, Soeren Steudel, Peter Vicca, Monique J. Beenhakkers, Nick A. J. M. van Aerle, Gerwin H. Gelinck, Jan Genoe, Wim Dehaene, and Paul Heremans. Plastic circuits and tags for 13.56 MHz radio-frequency communication. *Solid-State Electronics*, 53:1220–1226, 2009.
- [97] Bettina Koch. Indium, Selenium, Tellurium and Gallium - rare metals from the glass sandwich. Website, 2016. URL <http://www.invest-in-saxony-anhalt.com/report-invest/newsletter-iisa/2016/06/technology-PV-scrap-recycling>.
- [98] Stevan Preradovic and Nemai Karmakar. Fully printable chipless RFID tag. In Stevan Preradovic, editor, *Advanced Radio Frequency Identification Design and Applications*, 2011. doi: 10.5772/14555. URL <http://www.intechopen.com/books/advanced-radio-frequency-identification-design-and-applications/fully-printable-chipless-rfid-tag>.
- [99] Mohammadali Forouzandeh and Nemai Chandra Karmakar. Chipless RFID tags and sensors: A review on time-domain techniques. *Wireless Power Transfer*, 2(2): 62–77, 2015. doi: 10.1017/wpt.2015.10.
- [100] M. A. Islam and N. C. Karmakar. A novel compact printable dual-polarized chipless RFID system. *IEEE Transactions on Microwave Theory and Techniques*, 60(7):2142–2151, 2012. ISSN 0018-9480. doi: 10.1109/TMTT.2012.2195021.
- [101] Daniel M. Dobkin. *The RF in RFID: Passive UHF RFID in Practice*. Newnes, Newton, MA, USA, 2007. ISBN 0750682094, 9780750682091.
- [102] H. Martn, E. S. Milln, P. Peris-Lopez, and J. E. Tapiador. Efficient ASIC implementation and analysis of two EPC-C1G2 RFID authentication protocols. *IEEE Sensors Journal*, 13(10):3537–3547, October 2013. ISSN 1530-437X. doi: 10.1109/JSEN.2013.2270404.
- [103] Gate equivalent. Wikipedia. URL [https://en.wikipedia.org/wiki/Gate\\_equivalent](https://en.wikipedia.org/wiki/Gate_equivalent).

- [104] Y. J. Huang, W. C. Lin, and H. L. Li. Efficient implementation of RFID mutual authentication protocol. *IEEE Transactions on Industrial Electronics*, 59(12): 4784–4791, December 2012. ISSN 0278-0046. doi: 10.1109/TIE.2011.2178215.
- [105] H. Reinisch, M. Wiessflecker, S. Gruber, H. Unterassinger, G. Hofer, M. Klamminger, W. Pribyl, and G. Holweg. A multifrequency passive sensing tag with on-chip temperature sensor and off-chip sensor interface using EPC HF and UHF RFID technology. *IEEE Journal of Solid-State Circuits*, 46(12):3075–3088, December 2011. ISSN 0018-9200. doi: 10.1109/JSSC.2011.2167548.
- [106] EPC Gen2. Website, 2017. URL <http://www.nxp.com/>.
- [107] Time-division multiple access. Wikipedia. URL [https://en.wikipedia.org/wiki/Time-division\\_multiple\\_access](https://en.wikipedia.org/wiki/Time-division_multiple_access).
- [108] Frequency-division multiple access. Wikipedia. URL [https://en.wikipedia.org/wiki/Frequency-division\\_multiple\\_access](https://en.wikipedia.org/wiki/Frequency-division_multiple_access).
- [109] Electronic oscillator. Wikipedia. URL [https://en.wikipedia.org/wiki/Electronic\\_oscillator](https://en.wikipedia.org/wiki/Electronic_oscillator).
- [110] Code-division multiple access. Wikipedia. URL [https://en.wikipedia.org/wiki/Code-division\\_multiple\\_access](https://en.wikipedia.org/wiki/Code-division_multiple_access).
- [111] David Tse and Pramod Viswanath. *Fundamentals of Wireless Communication*. Cambridge University Press, 2005. ISBN 0521845270.
- [112] Gold code. Wikipedia. URL [https://en.wikipedia.org/wiki/Gold\\_code](https://en.wikipedia.org/wiki/Gold_code).
- [113] S. Khan, L. Lorenzelli, and R. S. Dahiya. Technologies for printing sensors and electronics over large flexible substrates: A review. *IEEE Sensors Journal*, 15(6): 3164–3185, June 2015. ISSN 1530-437X. doi: 10.1109/JSEN.2014.2375203.
- [114] K. X. Myny, S. Steudel, S. Smout, P. Vicca, F. Furthner, B. van der Putten, A. K. Tripathi, G. H. Gelinck, Jan Genoe, Wim Dehaene, and Paul Heremans. Organic RFID transponder chip with data rate compatible with electronic product coding. *Elsevier Science*, 2010. ISSN 1566-1199.
- [115] s-net technology for extremely power-efficient wireless sensor networks. Website. URL <https://www.iis.fraunhofer.de/en/ff/kom/tech/drahtlose-kommunikation/sn.html>. [www.s-net-info.com](http://www.s-net-info.com).
- [116] A. P. Sample, D. J. Yeager, P. S. Powlledge, A. V. Mamishev, and J. R. Smith. Design of an RFID-based battery-free programmable sensing platform. *IEEE Transactions on Instrumentation and Measurement*, 57(11):2608–2615, November 2008. ISSN 0018-9456. doi: 10.1109/TIM.2008.925019.

- [117] Percy S., Knight C., Cooray F, and Smart K. Supplying the power requirements to a sensor network using radio frequency power transfer. *Sensors (Basel, Switzerland)*, (12(7)):8571–8585, 2012. doi: 10.3390/s120708571.
- [118] WISP (Wireless Identification and Sensing Platform). Website. URL <http://sensor.cs.washington.edu/WISP.html>.
- [119] Xiao Lu, Ping Wang, Dusit Niyato, Dong In Kim, and Zhu Han. Wireless networks with RF energy harvesting: A contemporary survey. *CoRR*, abs/1406.6470, 2014. URL <http://arxiv.org/abs/1406.6470>.
- [120] Miguel Garcia, Diana Bri, Ra Sendra, and Jaime Lloret. Practical deployments of wireless sensor networks: A survey. *Int. J. Adv. Netw. Serv*, pages 136–178, 2010.
- [121] Jaime Lloret. Introduction to practical deployments on wireless sensor networks: A survey. *Int. J. Adv. Netw. Serv*, 2010.
- [122] S. Sarma, D.L. Brock, and K. Ashton. The networked physical world, proposals for engineering the next generation of computing, commerce and automatic-identification, 2000. Auto-ID Center White Paper.
- [123] National Intelligence Council. Disruptive civil technologies – six technologies with potential impacts on US interests out to 2025 – conferences report. Technical report, US National Intelligence Council, April 2008. URL [http://www.dni.gov/nic/NIC\\$\\_\\$home.html](http://www.dni.gov/nic/NIC$_$home.html).
- [124] M. Botterman. Internet of Things: An early reality of the future internet. Technical report, For the European Commission Information Society and Media Directorate General, Networked Enterprise and RFID Unit – D4, May 2009.
- [125] S. Haller. The things in the Internet of Things. In *Proceedings of the Internet of Things Conference*, 2010.
- [126] Fahim Kawsar, Gerd Kortuem, and Bashar Altakrouri. Supporting interaction with the Internet of Things across objects, time and space. In *Proceedings of the Internet of Things Conference*, 2010.
- [127] Benedikt Ostermaier, Kay Rmer, Friedemann Mattern, Michael Fahrmaier, and Wolfgang Kellerer. A real-time search engine for the Web of Things. In *Proceedings of the Internet of Things Conference*, 2010.
- [128] Dominique Guinard, Vlad Trifa, and Erik Wilde. A resource oriented architecture for the Web of Things. In *Proceedings of the Internet of Things Conference*, 2010.

- [129] D. Giusto, A. Iera, G. Morabito, and L. Atzori, editors. *The Internet of Things*. Springer, 2010.
- [130] Luigi Atzori, Antonio Iera, and Giacomo Morabito. The Internet of Things: A survey. *Elsevier Computer Networks*, 4247, May 2010.
- [131] Guanling Chen, Ming Li, and David Kotz. Design and implementation of a large-scale context fusion network. In *Proceedings of the First Annual International Conference on Mobile and Ubiquitous Systems: Networking and Services (MobiQ-uitous'04)*, 2004.
- [132] Guanling Chen, Ming Li, and David Kotz. Data-centric middleware for context-aware Pervasive Computing. *Pervasive and Mobile Computing*, 4(2):216–253, April 2008. ISSN 1574-1192.
- [133] Guanling Chen. *Solar: Building A Context Fusion Network for Pervasive Computing*. PhD thesis, Hanover, New Hampshire, 2004.
- [134] C. F. Chiasserini and R. R. Rao. On the concept of distributed digital signal processing in wireless sensor networks. In *Proceedings of the IEEE Military Communication Conference (MILCOM)*, 2002.
- [135] M. Goel and T. Imielinski. Prediction-based monitoring in sensor networks: Taking lessons from MPEG. *ACM SIGCOMM Computer Communication Review*, 31(5):82–98, 2001.
- [136] L. Prasad, S. S. Iyengar, and R. L. Rao. Fault-tolerant sensor integration using multiresolution decomposition. *Physical Review E*, 49(4):3452–3461, 1994.
- [137] H. Qi, Y. Xu, and X. Wang. Mobile-agent-based collaborative signal and information processing in sensor networks. *Proceedings of the IEEE*, 91(8):1172–1183, 2003.
- [138] Holger Karl and A. Willig. *Protocols and Architectures for Wireless Sensor Networks*. Wiley, May 2005.
- [139] R. Ahlswede, Ning Cai, S. Y. R. Li, and R. W. Yeung. Network information flow. *IEEE Transactions on Information Theory*, 46(4):1204–1216, July 2000. ISSN 0018-9448. doi: 10.1109/18.850663.
- [140] S. Y. R. Li, R. W. Yeung, and Ning Cai. Linear network coding. *IEEE Transactions on Information Theory*, 49(2):371–381, February 2003. ISSN 0018-9448. doi: 10.1109/TIT.2002.807285.

- [141] Tracey Ho, R. Koetter, M. Medard, D. R. Karger, and M. Effros. The benefits of coding over routing in a randomized setting. In *Proceedings of IEEE International Symposium on Information Theory*, pages 442–ff, June 2003. doi: 10.1109/ISIT.2003.1228459.
- [142] T. Cover, A. El Gamal, and M. Salehi. Multiple access channels with arbitrarily correlated sources. *IEEE Transactions on Information Theory*, IT-26(6):648–657, 1980.
- [143] A. Giridhar and P. R. Kumar. Toward a theory of in-network computation in wireless sensor networks. *IEEE Communications Magazine*, 44(4):98–107, April 2006. ISSN 0163-6804. doi: 10.1109/MCOM.2006.1632656.
- [144] B. Nazer and M. Gastpar. Computation over multiple-access channels. *IEEE Transactions on Information Theory*, 53(10):3498–3516, October 2007. ISSN 0018-9448. doi: 10.1109/TIT.2007.904785.
- [145] Mario Goldenbaum, Slawomir Stanczak, and Michal Kaliszan. On function computation via wireless sensor multiple-access channels. In *IEEE Wireless Communications and Networking Conference (WCNC '09)*, Budapest, Hungary, April 2009.
- [146] Mario Goldenbaum and Slawomir Stanczak. Computing functions via SIMO multiple-access channels: How much channel knowledge is needed? In *Proceedings of the IEEE International Conference on Acoustics, Speech and Signal Processing (ICASSP '10)*, pages 3394–3397, Dallas, USA, March 2010.
- [147] Markus Reschke, Johannes Starosta, Sebastian Schwarzl, and Stephan Sigg. Situation awareness based on channel measurements. In *Proceedings of the fourth Conference on Context Awareness for Proactive Systems (CAPS)*, 2011.
- [148] S. Stanczak, M. Wiczanowski, and H. Boche. Distributed utility-based power control: Objectives and algorithms. *IEEE Transactions on Signal Processing*, 55(10):5058–5068, October 2007.
- [149] Sachin Katti, Shyamnath Gollakota, and Dina Katabi. Embracing wireless interference: Analog network coding. In *SIGCOMM*, 2007.
- [150] J. Körner and K. Marton. How to encode the modulo-two sum of binary sources (corresp.). *IEEE Transactions on Information Theory*, 25(2):219–221, March 1979. ISSN 0018-9448. doi: 10.1109/TIT.1979.1056022.
- [151] R. Ahlswede and Han Te. On source coding with side information via a multiple-access channel and related problems in multi-user information theory. *IEEE Transactions on Information Theory*, 29(3):396–412, 1983.

- [152] Mario Goldenbaum and Slawomir Stanczak. Robust analog function computation via wireless multiple-access channels. *CoRR*, abs/1210.2967, 2012. URL <http://arxiv.org/abs/1210.2967>.
- [153] Takahiro Matsuda, Taku Noguchi, and Tetsuya Takine. Survey of network coding and its applications. *IEICE Transactions on Communications*, E94.B(3):698–717, 2011. doi: 10.1587/transcom.E94.B.698.
- [154] R. Koetter and M. Medard. An algebraic approach to network coding. *IEEE/ACM Transactions on Networking*, 11(5):782–795, October 2003. ISSN 1063-6692. doi: 10.1109/TNET.2003.818197.
- [155] M. Wang and B. Li. Lava: A reality check of network coding in peer-to-peer live streaming. In *IEEE INFOCOM 2007 - 26th IEEE International Conference on Computer Communications*, pages 1082–1090, May 2007. doi: 10.1109/INFCOM.2007.130.
- [156] Sachin Rajsekhar Katti. *Network Coded Wireless Architecture*. PhD thesis, Department of Electrical Engineering and Computer Science, Massachusetts Institute of Technology, 2008.
- [157] Yunnan Wu, Philip A. Chou, and Sun-Yuan Kung. Information exchange in wireless networks with network coding and physical-layer broadcast. Technical report, Microsoft Research, Redmond, WA, August 2004.
- [158] S. Katti, H. Rahul, W. Hu, D. Katabi, M. Medard, and J. Crowcroft. XORs in the air: Practical wireless network coding. *IEEE/ACM Transactions on Networking*, 16(3):497–510, June 2008. ISSN 1063-6692. doi: 10.1109/TNET.2008.923722.
- [159] Christina Fragouli and Emina Soljanin. Network coding fundamentals. In *FOUNDATIONS AND TRENDS IN NETWORKING*, 2007.
- [160] B. Nazer and M. Gastpar. Compute-and-forward: Harnessing interference through structured codes. *IEEE Transactions on Information Theory*, 57(10):6463–6486, October 2011. ISSN 0018-9448. doi: 10.1109/TIT.2011.2165816.
- [161] Shengli Zhang, Soung Chang Liew, and Patrick P. Lam. Hot topic: Physical-layer network coding. In *Proceedings of the 12th Annual International Conference on Mobile Computing and Networking*, MobiCom '06, pages 358–365, New York, NY, USA, 2006. ACM. ISBN 1-59593-286-0. doi: 10.1145/1161089.1161129. URL <http://doi.acm.org/10.1145/1161089.1161129>.
- [162] P. Popovski and H. Yomo. The anti-packets can increase the achievable throughput of a wireless multi-hop network. In *2006 IEEE International Conference*

- on Communications*, volume 9, pages 3885–3890, June 2006. doi: 10.1109/ICC.2006.255688.
- [163] B. Nazer and M. Gastpar. Computing over multiple-access channels with connections to wireless network coding. In *2006 IEEE International Symposium on Information Theory*, pages 1354–1358, July 2006. doi: 10.1109/ISIT.2006.262047.
- [164] Software-defined radio. Wikipedia. URL [https://en.wikipedia.org/wiki/Software-defined\\_radio](https://en.wikipedia.org/wiki/Software-defined_radio).
- [165] Mario Goldenbaum and Slawomir Stanczak. Computing the geometric mean over multiple-access channels: Error analysis and comparisons. In *Proceedings of the 43rd Asilomar Conference on Signals, Systems and Computers*, Monterey, USA, November 2009.
- [166] Markus Hermann. Evaluierung der Empfangsleistungen von überlagerten Funksignale. Master thesis, Universität Karlsruhe, TecO, 2005.
- [167] Bernd Ulmann. *Analog Computing*. De Gruyter Oldenburg, 1 edition, June 2013.
- [168] Predrag Jakimovski, Till Riedel, Ali Hadda, and Michael Beigl. Design of a printed organic RFID circuit with an integrated sensor for smart labels. In *International Multi-Conference on Systems, Signals Devices (SSD)*, pages 1–6, March 2012. doi: 10.1109/SSD.2012.6197986.
- [169] Albert Krohn, Mike Hazas, and Michael Beigl. Removing systematic error in node localisation using scalable data fusion. In *Fourth European conference on Wireless Sensor Networks*, pages 341–356, 2007.
- [170] The particle computer company. Website. URL <http://particle.teco.edu/>.
- [171] L. Keller, N. Karamchandani, and C. Fragouli. Function computation over linear channels. In *IEEE International Symposium on Network Coding (NetCod)*, pages 1–6, June 2010. doi: 10.1109/NETCOD.2010.5487679.
- [172] Pentti Kanerva. Hyperdimensional computing: An introduction to computing in distributed representation with high-dimensional random vectors. *Cognitive Computation*, pages 139–159, 2009. URL <http://dx.doi.org/10.1007/s12559-009-9009-8>.
- [173] Predrag Jakimovski, Florian Becker, Stephan Sigg, Hedda R. Schmidtke, and Michael Beigl. Collective communication for dense sensing environments. In *7th IEEE International Conference on Intelligent Environments (IE)*, pages 157–164, 2011. (\*\*Best paper\*\*).

- [174] Christian Decker, Martin Berchtold, Leonardo Weiss Ferreira Chaves, Michael Beigl, Daniel Röhr, Till Riedel, Monty Beuster, Thomas Herzog, and Daniel Herzig. Cost-benefit model for smart items in the supply chain. In *Proceedings of the Internet of Things'08*, 2008.
- [175] Leonardo Weiss Ferreira Chaves and Florian Kerschbaum. Industrial privacy in RFID-based batch recalls. In *Proceedings of the International Workshop on Security and Privacy in Enterprise Computing InSPEC'08*, 2008.
- [176] Leonardo Weiss Ferreira Chaves, Erik Buchmann, and Klemens Böhm. Tagmark: Reliable estimations of RFID tags for business processes. In *Proceedings of the KDD'08*, 2008.
- [177] Leonardo Weiss Ferreira Chaves, Erik Buchmann, and Klemens Böhm. RPCV: RFID planogram compliance verification. In *Proceedings of the ICDE'10*, 2010.
- [178] R. Jedermann, L. Ruiz-Garcia, and W. Lang. Spatial temperature profiling by semi-passive RFID loggers for perishable food transportation. *Computers and Electronics in Agriculture*, 2009.
- [179] C. Floerkemeier and M. Lampe. Issues with RFID usage in Ubiquitous Computing applications. In *Proceedings of Pervasive'04*, 2004.
- [180] Larry Miller and Janet Allen. National supermarket shrink report. Technical report, National Supermarket Research Group, 2005. URL [http://www.securestoreadvantage.com/pdfs/Supermarket\\_Survey\\_Executive\\_Summary.pdf](http://www.securestoreadvantage.com/pdfs/Supermarket_Survey_Executive_Summary.pdf).
- [181] Paul Beswick, Mathew Isotta, and Stefan Winter. A retailer's recipe for fresher food and far less shrink. In *Oliver Wyman Journal Issue 24*, pages 47–53, 2008.
- [182] Vivek Subramanian, Josephine B. Chang, Alejandro de la Fuente Vornbrock, Daniel C. Huang, Lakshmi Jagannathan, Fank Liao, Brain Mattis, Steven Molesa, David R. Redinger, Daniel Soltman, Steven K. Volkman, and Qintao Zhang. Printed electronics for low-cost electronic systems: Technology status and application development. In *38th European Solid-State Device Research Conference (ESSDERC)*, pages 17–24, 2008.
- [183] Takashi Matsuda, Toshifumi Oota, Youiti Kado, and Bing Zhang. An efficient wireless power transmission system using phase control of input electrode array for two-dimensional communication. pages 610–615, 2011. URL <http://ieeexplore.ieee.org/stamp/stamp.jsp?tp=&arnumber=5745887>.

- [184] Akihito Noda and Hiroyuki Shinoda. Selective wireless power transmission through 2D waveguide sheet using strong electromagnetic confinement by choke-enclosed resonant coupler. pages 178–181, 2011. URL <http://ieeexplore.ieee.org/stamp/stamp.jsp?tp=&arnumber=5725464>.
- [185] Hiroyuki Shinoda, Yasutoshi Makino, and Naoshi Yamahira. Surface sensor network using inductive signal transmission layer. pages 201–206, 2007. URL <http://ieeexplore.ieee.org/stamp/stamp.jsp?tp=&arnumber=4297420>.
- [186] Ettus Research. Website. URL <http://www.ettus.com/products>.
- [187] Zheng Cui. *Printed Electronics - Materials, Technologies and Applications*. Wiley, 2016.
- [188] G. C. Schmidt, M. Bellmann, B. Meier, M. Hamsch, K. Reuter, H. Kempa, and A.C. Hübler. Modified mass printing technique for the realization of source/drain electrodes with high resolution. *Organic Electronics*, 11(10):1683–1687, 2010. ISSN 1566-1199. doi: 10.1016/j.orgel.2010.07.018. URL <http://www.sciencedirect.com/science/article/pii/S156611991000248X>.
- [189] Organic Electronics Association. OE-A toolbox catalogue for organic and printed electronics. *White Paper*, 2015/2016.
- [190] Eugenio Cantatore. Applications of organic and printed electronics: A technology-enabled revolution. Boston: Springer, 2013. URL <http://dx.doi.org/10.1007/978-1-4614-3160-2>.
- [191] R. Ganesan, J. Krumm, S. Pankalla, K. Ludwig, and M. Glesner. Design of an organic electronic label on a flexible substrate for temperature sensing. In *Proceedings of the ESSCIRC*, pages 423–426, September 2013. doi: 10.1109/ESSCIRC.2013.6649163.
- [192] Loop antenna. Wikipedia. URL [https://en.wikipedia.org/wiki/Loop\\_antenna](https://en.wikipedia.org/wiki/Loop_antenna).
- [193] GNU Radio. URL <http://gnuradio.org/redmine/projects/gnuradio/wiki>.
- [194] Atmel. *ATtiny44A Datasheet*. Atmel Corporation., 2012. URL <http://www.atmel.com/Images/doc8183.pdf>.
- [195] ModelAndViewController. Wikipedia. URL <https://en.wikipedia.org/wiki/Model%E2%80%93view%E2%80%93controller>.
- [196] GNU Radio Companion. Website. URL <http://gnuradio.org/redmine/projects/gnuradio/wiki/GNURadioCompanion>.

- [197] Shinoda Laboratory. Website. URL <http://www.ks.c.titech.ac.jp/english/index.html>.
- [198] R. Blache, J. Krumm, and W. Fix. Organic CMOS circuits for RFID applications. In *2009 IEEE International Solid-State Circuits Conference Digest of Technical Papers (ISSCC)*, pages 208–210, February 2009.
- [199] V. Fiore, E. Ragonese, S. Abdinia, S. Jacob, I. Chartier, R. Coppard, A. van Roermund, E. Cantatore, and G. Palmisano. A 13.56 MHz RFID tag with active envelope detection in an organic complementary TFT technology. In *2014 IEEE International Solid-State Circuits Conference Digest of Technical Papers (ISSCC)*, pages 492–493, February 2014. doi: 10.1109/ISSCC.2014.6757526.
- [200] V. Fiore, P. Battiato, S. Abdinia, S. Jacobs, I. Chartier, R. Coppard, G. Klink, E. Cantatore, E. Ragonese, and G. Palmisano. An integrated 13.56 MHz RFID tag in a printed organic complementary TFT technology on flexible substrate. *IEEE Transactions on Circuits and Systems*, 62(6):1668–1677, June 2015. ISSN 1549-8328. doi: 10.1109/TCSI.2015.2415175.
- [201] RC circuit. Wikipedia, . URL [https://en.wikipedia.org/wiki/RC\\_circuit](https://en.wikipedia.org/wiki/RC_circuit).
- [202] LTspice IV. Website, 2013. URL <http://www.linear.com/designtools/software/>. [Software; Version 4.19i].
- [203] Frank Lahner and Peter Thamm. *Gedruckte Polymer-RFID-Transponder*, chapter Lesegerät für gedruckte RFID-Tags. Jan Marco Leimeister and Helmut Krcmar, 2009.
- [204] D. Raiteri, P. van Lieshout, A. van Roermund, and E. Cantatore. Positive-feedback level shifter logic for large-area electronics. *IEEE Journal of Solid-State Circuits*, 49(2):524–535, February 2014. ISSN 0018-9200. doi: 10.1109/JSSC.2013.2295980.
- [205] Jürgen Krumm and Wolfgang Clemens. Printed Electronics – First circuits, products, and roadmap. In *AACD Workshop*, pages 333–346, 2010.
- [206] S. Shen, R. Tinivella, M. Pirola, G. Ghione, and V. Camarchia. SPICE library for low-cost RFID applications based on pentacene organic FET. In *2010 6th International Conference on Wireless Communications Networking and Mobile Computing (WiCOM)*, pages 1–4, September 2010. doi: 10.1109/WICOM.2010.5601134.
- [207] Riccardo Tinivella, Vittorio Camarchia, Marco Pirola, Shu Shen, and Giovanni Ghione. Simulation and design of OFET RFIDs through an analog/digital physics-based library. *Organic Electronics*, 12(8):1328–1335, 2011. ISSN 1566-1199. doi: 10.1016/j.orgel.2011.03.047. URL <http://www.sciencedirect.com/science/article/pii/S1566119911001571>.

- [208] E. Cantatore, T. C. T. Geuns, G.H. Gelinck, E. van Veenendaal, A. F. A. Gruijthuijsen, L. Schrijnemakers, S. Drews, and Dago M. De Leeuw. A 13.56 MHz RFID system based on organic transponders. *IEEE Journal of Solid-State Circuits*, 42(1):84–92, 2007. ISSN 0018-9200. doi: 10.1109/JSSC.2006.886556.
- [209] Markus Böhm. *A System Study for RFID, Transponders Based on Polymer Semiconductors*. Cuvillier Verlag, 2007.
- [210] Stephan Kirchmeyer. The OE-A roadmap for organic and printed electronics: Creating a guidepost to complex interlinked technologies, applications and markets. IOPScience, March 2016. URL <http://iopscience.iop.org/2053-1613/3/1/010301>.
- [211] Gongbo Zhou, Linghua Huang, Wei Li, and Zhencai Zhu. Harvesting ambient environmental energy for wireless sensor networks: A survey. *Journal of Sensors*, 2014.
- [212] P. P. Yupapin, Sommai Pivsa-Art, H. Ohgaki, and Prusayon Nintanavongsa. 11th Eco-energy and materials science and engineering (11th EMSES) a survey on RF energy harvesting: Circuits and protocols. *Energy Procedia*, 56: 414–422, 2014. ISSN 1876-6102. doi: 10.1016/j.egypro.2014.07.174. URL <http://www.sciencedirect.com/science/article/pii/S1876610214010364>.
- [213] Silvia Santini. *Adaptive Sensor Selection Algorithms for Wireless Sensor Networks*. PhD thesis, ETH Zürich, October 2009.
- [214] Wireless sensor network. Wikipedia, . URL [https://en.wikipedia.org/wiki/Wireless\\_sensor\\_network](https://en.wikipedia.org/wiki/Wireless_sensor_network).
- [215] T. Le, K. Mayaram, and T. Fiez. Efficient far-field radio frequency energy harvesting for passively powered sensor networks. *IEEE Journal of Solid-State Circuits*, 43(5):1287–1302, May 2008. ISSN 0018-9200. doi: 10.1109/JSSC.2008.920318.
- [216] Aaron N. Parks, Alanson P. Sample, Yi Zhao, and Joshua R. Smith. *A Wireless Sensing Platform Utilizing Ambient RF Energy*, pages 127–129. 2013. ISBN 9781467329309. doi: 10.1109/WiSNet.2013.6488656.
- [217] M. D. Springer. *The Algebra of Random Variables*. Wiley Series in Probability and Mathematical Statistics. Springer, 1979.
- [218] W. Feller. *An Introduction to Probability Theory and its Applications*, volume 1. Wiley, 1968.
- [219] Arduino UNO board. URL <http://arduino.cc/en/Main/arduinoBoardUno>.

- [220] 3GPP. 3rd generation partnership project; technical specification group radio access networks; 3G Home NodeB study item technical report (release 8). Technical Report 3GPP TR 25.820 V8.0.0 (2008-03), March 2008.
- [221] S. Sudevalayam and P. Kulkarni. Energy harvesting sensor nodes: Survey and implications. *IEEE Communications Surveys Tutorials*, 13(3):443–461, Quarter 2011. doi: 10.1109/SURV.2011.060710.00094.
- [222] Arne Casteleyn. *Healthcare & Well-being*, chapter Smart Label Monitors Temperature of a Cold Chain, page 37. OPE journal, 2015.
- [223] W. Feller. *An Introduction to Probability Theory and its Applications*, volume 2. Wiley, 1968.
- [224] Glen Cowan. *Statistical Data Analysis*. Clarendon Press, 1998.
- [225] Volker Blobel and Erich Lohmann. *Statistische und Numerische Methoden der Datenanalyse*. Teubner Verlag, 1998.
- [226] Mario Stipčević and Çetin Kaya Koç. *Open Problems in Mathematics and Computational Science - True Random Number Generators*, chapter 12, pages 275–315. Springer International Publishing, 2014.
- [227] Website. URL <https://www.random.org/>.
- [228] David DiCarlo. *Random Number Generation: Types and Techniques*. Senior thesis, Liberty University, 2012.
- [229] Louise Foley. Analysis of an on-line random number generator. Technical report, The Distributed Systems Group, Computer Science Department, Trinity College Dublin (TCD), 2001.
- [230] W. T. Holman, J. A. Connelly, and A. B. Dowlatabadi. An integrated analog/digital random noise source. *IEEE Transactions on Circuits and Systems I: Fundamental Theory and Applications*, 44(6):521–528, June 1997. ISSN 1057-7122. doi: 10.1109/81.586025.
- [231] B. Sunar, W. J. Martin, and D. R. Stinson. A provably secure true random number generator with built-in tolerance to active attacks. *IEEE Transactions on Computers*, 56(1):109–119, January 2007. ISSN 0018-9340. doi: 10.1109/TC.2007.250627.
- [232] G. Evans, J. Goes, A. Steiger-Garcia, M. D. Ortigueira, N. Paulino, and J. S. Lopes. Low-voltage low-power CMOS analogue circuits for Gaussian and uniform noise generation. In *Proceedings of the 2003 International Symposium*

- on *Circuits and Systems (ISCAS)*, volume 1, pages 145–148, May 2003. doi: 10.1109/ISCAS.2003.1205521.
- [233] Pseudorandom number generator. Wikipedia. URL [https://en.wikipedia.org/wiki/Pseudorandom\\_number\\_generator](https://en.wikipedia.org/wiki/Pseudorandom_number_generator).
- [234] James E. Gentle. *Random Number Generation and Monte Carlo Methods*. Springer, second edition, 2004.
- [235] D. H. Lehmer. Random number generation on the BRL high-speed computing machines. *Mathematical Reviews*, 15:559–559, 1954. ISSN 0025-5629.
- [236] Linear congruential generator. Wikipedia. URL [https://en.wikipedia.org/wiki/Linear\\_congruential\\_generator](https://en.wikipedia.org/wiki/Linear_congruential_generator).
- [237] T. E. Hull and A. R. Dobell. Random number generators. *Society for Industrial and Applied Mathematics Review*, 4(3):230–254, July 1962. ISSN 0036-1445 (print), 1095-7200 (electronic). doi: 10.1137/1004061. URL <http://link.aip.org/link/?SIR/4/230/1>; [https://dspace.library.uvic.ca:8443/bitstream/handle/1828/3142/Random\\_Number\\_Generators.pdf?sequence=3](https://dspace.library.uvic.ca:8443/bitstream/handle/1828/3142/Random_Number_Generators.pdf?sequence=3).
- [238] Frank L. Severance. *System Modeling and Simulation*. John Wiley & Sons, Ltd, 2001.
- [239] Donald E. Knuth. *Seminumerical Algorithms*, volume 2 of *The Art of Computer Programming*. Addison-Wesley, second edition, May 2014.
- [240] Jean-Michel Muller. *Elementary Functions: Algorithms and Implementation*. Birkhäuser Boston, second edition, 2006.
- [241] S. Paul, N. Jayakumar, and S. P. Khatri. A fast hardware approach for approximate, efficient logarithm and antilogarithm computations. *IEEE Transactions on Very Large Scale Integration (VLSI) Systems*, 17(2):269–277, February 2009. ISSN 1063-8210. doi: 10.1109/TVLSI.2008.2003481.
- [242] D. M. Lewis and L. K. Yu. Algorithm design for a 30-bit integrated logarithmic processor. In *Proceedings of the 9th Symposium on Computer Arithmetic*, pages 192–199, September 1989. doi: 10.1109/ARITH.1989.72826.
- [243] F. J. Taylor, R. Gill, J. Joseph, and J. Radke. A 20 bit logarithmic number system processor. *IEEE Transactions on Computers*, 37(2):190–200, February 1988. ISSN 0018-9340. doi: 10.1109/12.2148.
- [244] M. Arnold, T. Bailey, and J. Cowles. Error analysis of the Kmetz/Maenner algorithm. *Journal of VLSI signal processing systems for signal, image and video*

- technology*, 33(1):37–53, 2003. ISSN 0922-5773. doi: 10.1023/A:1021189701352. URL <http://dx.doi.org/10.1023/A:1021189701352>.
- [245] J. N. Coleman, E. I. Chester, C. I. Softley, and J. Kadlec. Arithmetic on the European logarithmic microprocessor. *IEEE Transactions on Computers*, 49(7):702–715, July 2000. ISSN 0018-9340. doi: 10.1109/12.863040.
- [246] D. M. Lewis. Interleaved memory function interpolators with application to an accurate LNS arithmetic unit. *IEEE Transactions on Computers*, 43(8):974–982, August 1994. ISSN 0018-9340. doi: 10.1109/12.295859.
- [247] D. M. Lewis. 114 MFLOPS logarithmic number system arithmetic unit for DSP applications. *IEEE Journal of Solid-State Circuits*, 30(12):1547–1553, December 1995. ISSN 0018-9200. doi: 10.1109/4.482205.
- [248] J. Hormigo, J. Villalba, and M. J. Schulte. A hardware algorithm for variable-precision logarithm. In *Proceedings of IEEE International Conference on Application-Specific Systems, Architectures, and Processors*, pages 215–224, 2000. doi: 10.1109/ASAP.2000.862392.
- [249] CORDIC. Wikipedia. URL <https://en.wikipedia.org/wiki/CORDIC>.
- [250] J. E. Volder. The CORDIC trigonometric computing technique. *IRE Transactions on Electronic Computers*, EC-8(3):330–334, 1959. doi: 10.1109/TEC.1959.5222693. URL [http://www.jacques-laporte.org/Volder\\_CORDIC.pdf](http://www.jacques-laporte.org/Volder_CORDIC.pdf).
- [251] A. Boudabous, F. Ghozzi, M. W. Kharrat, and N. Masmoudi. Implementation of hyperbolic functions using CORDIC algorithm. In *ICM 2004 Proceedings of the 16th International Conference on Microelectronics*, pages 738–741, December 2004. doi: 10.1109/ICM.2004.1434772.
- [252] Jack E. Volder. The birth of CORDIC. *J. VLSI Signal Process. Syst.*, 25(2):101–105, June 2000. ISSN 0922-5773. doi: 10.1023/A:1008110704586. URL <http://dx.doi.org/10.1023/A:1008110704586>.
- [253] E. Hertz and P. Nilsson. A methodology for parabolic synthesis of unary functions for hardware implementation. In *2nd International Conference on Signals, Circuits and Systems*, pages 1–6, November 2008. doi: 10.1109/ICSCS.2008.4746866.
- [254] E. Hertz and P. Nilsson. Parabolic synthesis methodology implemented on the sine function. In *2009 IEEE International Symposium on Circuits and Systems*, pages 253–256, May 2009. doi: 10.1109/ISCAS.2009.5117733.

- [255] Jingou Lai. Hardware implementation of the logarithm function using improved parabolic synthesis. Master thesis, The Department of Electrical and Information Technology, Lund University, 2013.
- [256] Lagged Fibonacci generator. Wikipedia. URL [https://en.wikipedia.org/wiki/Lagged\\_Fibonacci\\_generator](https://en.wikipedia.org/wiki/Lagged_Fibonacci_generator).
- [257] Martin Luescher. A portable high-quality random number generator for lattice field theory simulations. *Computer Physics Communications*, 79:100–110, preprint DESY 93–133, 1994.
- [258] F. James. RANLUX:a Fortran implementation of the high-quality pseudorandom number generator of Lüscher. *Computer Physics Communications*, 79(1):111–114, February 1994.
- [259] Linear-feedback shift register. Wikipedia, . URL [https://en.wikipedia.org/wiki/Linear-feedback\\_shift\\_register](https://en.wikipedia.org/wiki/Linear-feedback_shift_register).
- [260] Linear feedback shift registers. Website, . URL [http://www.newwaveinstruments.com/resources/articles/m\\_sequence\\_linear\\_feedback\\_shift\\_register\\_lfsr.htm](http://www.newwaveinstruments.com/resources/articles/m_sequence_linear_feedback_shift_register_lfsr.htm).
- [261] Javad Frounchi, Mohammad Hossein Zarifi, and Aanz Asgari Far. Design and analysis of random number generator for implementation of genetic algorithms using FPGA. In *5th International Conference on Electrical and Electronics Engineering*, 2007.
- [262] It. C. Tausworthe. Random numbers generated by linear recurrence modulo two. *Math. Comp.*, (19):201–209, 1965.
- [263] Solomon W. Golomb. *Shift Register Sequences*. Aegean Park Press, Laguna Hills, CA, USA, second edition, 1982.
- [264] T. G. Lewis and W. H. Payne. Generalized feedback shift register pseudorandom number algorithm. *J. ACM*, 20(3):456–468, July 1973. ISSN 0004-5411. doi: 10.1145/321765.321777. URL <http://doi.acm.org/10.1145/321765.321777>.
- [265] Florent Chabaud. Polynomials over Galois fields. Website, 2000. URL <http://fchabaud.free.fr/English/default.php?COUNT=1&FILE0=Poly>.
- [266] Neal Zierler and John Brillhart. On primitive trinomials (mod 2). *Information and Control*, 13(6):541 – 554, 1968. ISSN 0019-9958. doi: [http://dx.doi.org/10.1016/S0019-9958\(68\)90973-X](http://dx.doi.org/10.1016/S0019-9958(68)90973-X). URL <http://www.sciencedirect.com/science/article/pii/S001999586890973X>.

- [267] Neal Zierler and John Brillhart. On primitive trinomials (mod 2), II. *Information and Control*, 14(6):566–569, 1969. ISSN 0019-9958. doi: 10.1016/S0019-9958(69)90356-8. URL <http://www.sciencedirect.com/science/article/pii/S0019995869903568>.
- [268] A. C. Arvillias and D. G. Maritsas. Partitioning the period of a class of m-sequences and application to pseudorandom number generation. *J. ACM*, 25(4): 675–686, October 1978. ISSN 0004-5411. doi: 10.1145/322092.322106. URL <http://doi.acm.org/10.1145/322092.322106>.
- [269] Bruce Jay Collings and G. Barry Hembree. Initializing generalized feedback shift register pseudorandom number generators. *J. ACM*, 33(4):706–711, August 1986. ISSN 0004-5411. doi: 10.1145/6490.6493. URL <http://doi.acm.org/10.1145/6490.6493>.
- [270] ORICLA. Towards Electronic Product Coding with RFID tags based on hybrid organic-oxide complementary thin-film technology. Website, 2009. URL <https://projects.imec.be/oricla/node/1>.
- [271] Publications of project towards Electronic Product Coding with RFID tags based on hybrid organic-oxide complementary thin-film technology (ORICLA - FP7-ICT-2009-4). Website. URL [https://www.openaire.eu/openaire?format=raw&projectId=corda\\_:::6bf81c0d08f96fd9a18549232e3f1fdc&size=17&view=publications](https://www.openaire.eu/openaire?format=raw&projectId=corda_:::6bf81c0d08f96fd9a18549232e3f1fdc&size=17&view=publications).
- [272] Ben Hofmann. Organic and printed electronics in packaging. *OPE journal*, issue 2, 2013.
- [273] Research projects - Printed Organic Circuits and Chips (POLYTOS). Website. URL <https://www.innovationlab.de/en/research/research-projects/>.
- [274] Arjuna Marzuki, Zaliman Sauli, and Ali Yeon Shakaff. Advances in RFID components design: Integrated circuits. In Cristina Turcu, editor, *Development and Implementation of RFID Technology*. InTech, 2009. doi: 10.5772/6524. URL [https://www.intechopen.com/books/development\\_and\\_implementation\\_of\\_rfid\\_technology/advances\\_in\\_rfid\\_components\\_design\\_\\_integrated\\_circuits](https://www.intechopen.com/books/development_and_implementation_of_rfid_technology/advances_in_rfid_components_design__integrated_circuits).
- [275] S. Pankalla, R. Ganesan, D. Spiehl, H. M. Sauer, E. Dösam, and M. Glesner. Mass characterisation of organic transistors and Monte-Carlo circuit simulation. *Organic Electronics*, 14(2):676–681, 2013. doi: 10.1016/j.orgel.2012.11.033. URL <http://www.sciencedirect.com/science/article/pii/S1566119912005496>.
- [276] R. Jacob Baker. *CMOS: Circuit Design, Layout, and Simulation*. Wiley-IEEE Press, 3rd edition, October 2010.

- [277] Ring oscillator. Wikipedia, 2017. URL [https://en.wikipedia.org/wiki/Ring\\_oscillator](https://en.wikipedia.org/wiki/Ring_oscillator).
- [278] Masatoshi Kitamura, Yasutaka Kuzumoto, Shigeru Aomori, and Yasuhiko Arakawa. High-frequency organic complementary ring oscillator operating up to 200 kHz. *Applied Physics Express*, 4(5):051601, April 2011. URL <http://stacks.iop.org/1882-0786/4/i=5/a=051601>.
- [279] Watson C. P., Brown B. A., Carter J., Morgan J., and Taylor D. M. Organic ring oscillators with sub-200 ns stage delay based on a solution-processed p-type semiconductor blend. *Adv. Electron. Mater.*, 2, 2016. doi: 10.1002/aelm.201500322.
- [280] B. Crone, A. Dodabalapur, Y.-Y. Lin, R. W. Filas, Z. Bao, A. LaDuca, R. Sarpeshkar, H. E. Katz, and W. Li. Large-scale complementary integrated circuits based on organic transistors. *Nature*, 403:521–523, February 2000. doi: 10.1038/35000530.
- [281] Gerwin H. Gelinck, H. Edzer A. Huitema, Erik van Veenendaal, Eugenio Cantatore, Laurens Schrijnemakers, Jan B. P. H. van der Putten, Tom C. T. Geuns, Monique Beenhakkers, Jacobus B. Giesbers, Bart-Hendrik Huisman, Eduard J. Meijer, Estrella Mena Benito, Fred J. Touwslager, Albert W. Marsman, Bas J. E. van Rens, and Dago M. de Leeuw. Flexible active-matrix displays and shift registers based on solution-processed organic transistors. *Nature Materials*, 3: 106–110, January 2004. doi: 10.1038/nmat1061.
- [282] P. van Lieshout, E. van Veenendaal, L. Schrijnemakers, G. Gelinck, F. Touwslager, and E. Huitema. A flexible  $240 \times 320$ -pixel display with integrated row drivers manufactured in organic electronics. In *2005 IEEE International Digest of Technical Papers, Solid-State Circuits Conference (ISSCC)*, volume 1, pages 578–618, February 2005. doi: 10.1109/ISSCC.2005.1494127.
- [283] Sahel Abdinia. *Circuit Design in Complementary Organic Technologies*. PhD thesis, Technische Universiteit Eindhoven, 2014.
- [284] H. Klauk. Organic thin-film transistors for flexible displays and circuits. In *70th Device Research Conference*, pages 237–238, June 2012. doi: 10.1109/DRC.2012.6256946.
- [285] H. Klauk. Organic complementary circuits – scaling towards low voltage and submicron channel length. In *2012 Proceedings of the European Solid-State Device Research Conference (ESSDERC)*, pages 41–45, September 2012. doi: 10.1109/ESSDERC.2012.6343329.

- [286] W. Xiong, U. Zschieschang, H. Klauk, and B. Murmann. A 3V 6b successive-approximation ADC using complementary organic thin-film transistors on glass. In *2010 IEEE International Solid-State Circuits Conference (ISSCC)*, pages 134–135, February 2010. doi: 10.1109/ISSCC.2010.5434017.
- [287] H. Marien, M. S. J. Steyaert, E. van Veenendaal, and P. Heremans. A fully integrated  $\Delta\Sigma$  ADC in organic thin-film transistor technology on flexible plastic foil. *IEEE Journal of Solid-State Circuits*, 46(1):276–284, January 2011. ISSN 0018-9200. doi: 10.1109/JSSC.2010.2073230.
- [288] D. Raiteri, P. van Lieshout, A. van Roermund, and E. Cantatore. An organic VCO-based ADC for quasi-static signals achieving 1LSB INL at 6b resolution. In *2013 IEEE International Solid-State Circuits Conference Digest of Technical Papers*, pages 108–109, February 2013. doi: 10.1109/ISSCC.2013.6487658.
- [289] Ramkumar Ganesan, Jürgen Krumm, Klaus Ludwig, and Manfred Glesner. Investigation of voltage-controlled oscillator circuits using organic thin-film transistors (OTFT) for use in VCO-based analog-to-digital converters. *Solid-State Electronics*, 93(0):8–14, 2014. ISSN 0038-1101. doi: 10.1016/j.sse.2013.12.002. URL <http://www.sciencedirect.com/science/article/pii/S003811011300350X>.
- [290] W. Xiong, Y. Guo, U. Zschieschang, H. Klauk, and B. Murmann. A 3-V, 6-bit C-2C digital-to-analog converter using complementary organic thin-film transistors on glass. *IEEE Journal of Solid-State Circuits*, 45(7):1380–1388, July 2010. ISSN 0018-9200. doi: 10.1109/JSSC.2010.2048083.
- [291] T. Zaki, F. Ante, U. Zschieschang, J. Butschke, F. Letzkus, H. Richter, H. Klauk, and J. N. Burghartz. A 3.3V 6-bit 100 kS/s current-steering digital-to-analog converter using organic p-type thin-film transistors on glass. *IEEE Journal of Solid-State Circuits*, 47(1):292–300, January 2012. ISSN 0018-9200. doi: 10.1109/JSSC.2011.2170639.
- [292] K. Myny, E. van Veenendaal, G. H. Gelinck, J. Genoe, W. Dehaene, and P. Heremans. An 8-bit, 40-instructions-per-second organic microprocessor on plastic foil. *IEEE Journal of Solid-State Circuits*, 47(1):284–291, January 2012. ISSN 0018-9200. doi: 10.1109/JSSC.2011.2170635.
- [293] Sung-Min Yoon, Shinhyuk Yang, Chunwon Byun, Sang-Hee K. Park, Doo-Hee Cho, Soon-Won Jung, Oh-Sang Kwon, and Chi-Sun Hwang. Fully transparent non-volatile memory thin-film transistors using an organic ferroelectric and oxide semiconductor below 200 °C. *Advanced Functional Materials*, 20(6):921–926, 2010. ISSN 1616-3028. doi: 10.1002/adfm.200902095. URL <http://dx.doi.org/10.1002/adfm.200902095>.

- [294] Kang-Jun Baeg, Dongyoon Khim, Juhwan Kim, Byung-Do Yang, Minji Kang, Soon-Won Jung, In-Kyu You, Dong-Yu Kim, and Yong-Young Noh. High-performance top-gated organic field-effect transistor memory using electrets for monolithic printed flexible NAND flash memory. *Advanced Functional Materials*, 22(14):2915–2926, 2012. ISSN 1616-3028. doi: 10.1002/adfm.201200290. URL <http://dx.doi.org/10.1002/adfm.201200290>.
- [295] Byung-Do Yang, Jae-Mun Oh, Hyeong-Ju Kang, Soon-Won Jung, Yong Suk Yang, and In-Kyu You. Printed organic one-time programmable ROM array using anti-fuse capacitor. *ETRI Journal*, 35(4):594–602, August 2013. doi: 10.4218/etrij.13.1912.0010.
- [296] Soon-Won Jung, Jeong-Seon Choi, Jae Bon Koo, Chan Woo Park, Bock Soon Na, Ji-Young Oh, Sang Chul Lim, Sang Seok Lee, Hye Yong Chu, and Sung-Min Yoon. Flexible nonvolatile organic ferroelectric memory transistors fabricated on polydimethylsiloxane elastomer. *Organic Electronics*, 16:46–53, 2015. ISSN 1566-1199. doi: 10.1016/j.orgel.2014.08.051. URL <http://www.sciencedirect.com/science/article/pii/S1566119914003796>.
- [297] D. E. Schwartz and T. N. Ng. Comparison of static and dynamic printed organic shift registers. *IEEE Electron Device Letters*, 34(2):271–273, February 2013. ISSN 0741-3106. doi: 10.1109/LED.2012.2233709.
- [298] Tse Nga Ng, David E. Schwartz, Leah L. Lavery, Gregory L. Whiting, Beverly Russo, Brent Krusor, Janos Veres, Per Bröms, Lars Herlogsson, Naveed Alam Olle Hagel, Jakob Nilsson, and Christer Karlsson. Scalable printed electronics: An organic decoder addressing ferroelectric non-volatile memory. *Scientific Reports*, 2(585), August 2012. doi: 10.1038/srep00585.
- [299] Sahel Abdinia, Arthur H. M. van Roermund, and Eugenio Cantatore. *Design of Organic Complementary Circuits and Systems on Foil*. Springer-Verlag GmbH, 2015.
- [300] Maarten Rockelé, Duy-Vu Pham, Arne Hoppe, Jürgen Steiger, Silviu Botnarus, Manoj Nag, Soeren Steudel, Kris Myny, Sarah Schols, Robert Müller, Bas van der Putten, Jan Genoe, and Paul Heremans. Low-temperature and scalable complementary thin-film technology based on solution-processed metal oxide n-TFTs and pentacene p-TFTs. *Organic Electronics*, 12(11):1909–1913, 2011. doi: 10.1016/j.orgel.2011.08.009. URL <http://www.sciencedirect.com/science/article/pii/S1566119911002850>.
- [301] K. Myny, S. Smout, M. Rockel, A. Bhoelokam, T. H. Ke, S. Steudel, K. Obata, M. Marinkovic, D. V. Pham, A. Hoppe, A. Gulati, F. G. Rodriguez, B. Cobb,

- G. H. Gelinck, J. Genoe, W. Dehaene, and P. Heremans. 8 b Thin-film microprocessor using a hybrid oxide-organic complementary technology with inkjet-printed P2ROM memory. In *2014 IEEE International Solid-State Circuits Conference Digest of Technical Papers (ISSCC)*, pages 486–487, February 2014. doi: 10.1109/ISSCC.2014.6757523.
- [302] Gerwin Gelinck, Paul Heremans, Kazumasa Nomoto, and Thomas D. Anthopoulos. Organic transistors in optical displays and microelectronic applications. *Advanced Materials*, 22(34):3778–3798, 2010. ISSN 1521-4095. doi: 10.1002/adma.200903559. URL <http://dx.doi.org/10.1002/adma.200903559>.
- [303] Paul Heremans, Gerwin H. Gelinck, Robert Müller, Kang-Jun Baeg, Dong-Yu Kim, and Yong-Young Noh. Polymer and organic nonvolatile memory devices. *Chemistry of Materials*, 23(3):341–358, 2011. doi: 10.1021/cm102006v. URL <http://dx.doi.org/10.1021/cm102006v>.
- [304] M. Guerin, A. Daami, S. Jacob, E. Bergeret, E. Benevent, P. Pannier, and R. Coppard. High-gain fully printed organic complementary circuits on flexible plastic foils. *IEEE Transactions on Electron Devices*, 58(10):3587–3593, October 2011. ISSN 0018-9383. doi: 10.1109/TED.2011.2162071.
- [305] F. Ante, F. Letzkus, J. Butschke, U. Zschieschang, K. Kern, J. N. Burghartz, and H. Klauk. Submicron low-voltage organic transistors and circuits enabled by high-resolution silicon stencil masks. In *2010 International Electron Devices Meeting*, pages 516–519, December 2010. doi: 10.1109/IEDM.2010.5703409.
- [306] C. Y. Wei, S. H. Kuo, W. C. Huang, Y. M. Hung, C. K. Yang, F. Adriyanto, and Y. H. Wang. High-performance pentacene-based thin-film transistors and inverters with solution-processed barium titanate insulators. *IEEE Transactions on Electron Devices*, 59(2):477–484, February 2012. ISSN 0018-9383. doi: 10.1109/TED.2011.2174459.
- [307] Jinhua Li, Jun Du, Jianbin Xu, Helen L. W. Chan, and Feng Yan. The influence of gate dielectrics on a high-mobility n-type conjugated polymer in organic thin-film transistors. *Applied Physics Letters*, 100(3):033301.1–033301.4, 2012. doi: 10.1063/1.3678196. URL <http://dx.doi.org/10.1063/1.3678196>.
- [308] Huai-Yuan Tseng and Vivek Subramanian. All inkjet-printed, fully self-aligned transistors for low-cost circuit applications. *Organic Electronics*, 12(2):249–256, 2011. ISSN 1566-1199. doi: 10.1016/j.orgel.2010.11.013. URL <http://www.sciencedirect.com/science/article/pii/S156611991000371X>.